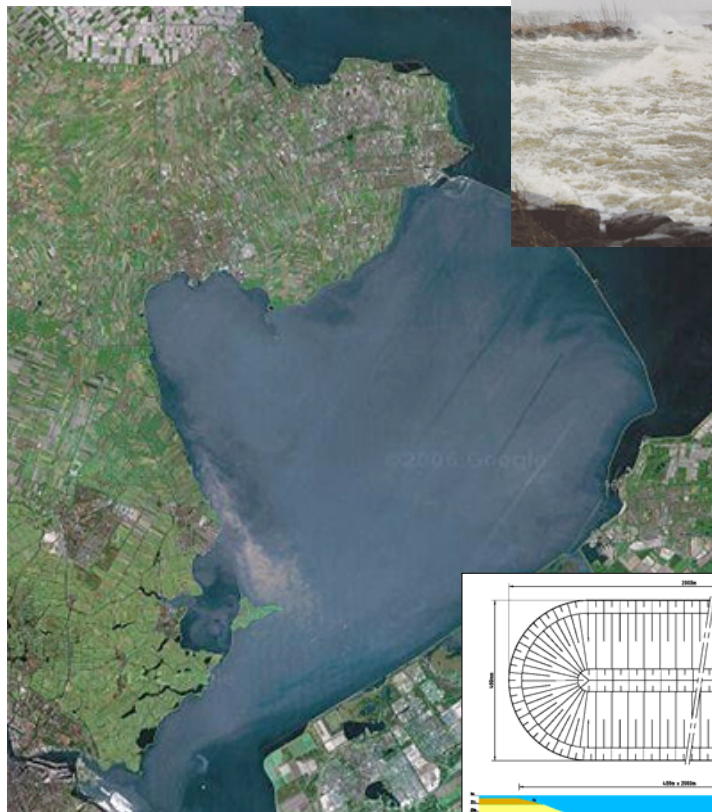


MSc Thesis

Mud dynamics in the Markermeer

Silt traps as a mitigation measure for turbidity

Thomas Vijverberg
May 2008



Mud dynamics in the Markermeer

Silt traps as a mitigation measure for turbidity

MSc Thesis

Thomas Vijverberg

Delft University of Technology
Faculty of Civil Engineering and Geosciences
Department of Hydraulic Engineering

Graduation committee:

Prof. dr. ir. M.J.F. Stive	Professor Coastal Engineering Delft University of Technology
Dr. ir. J.C. Winterwerp	Associate professor Delft University of Technology / Deltares
Dr. ir. S.G.J. Aarninkhof	Senior project engineer Royal Boskalis Westminster nv (Hydronamic)
Drs. M.W.M. Kuiper	Senior researcher/consultant WL Delft Hydraulics / Deltares
Dhr. H. Drost	Rijkswaterstaat, Waterdienst

Preface

This report is the final task for my Master Study Hydraulic Engineering at Delft University of Technology. While completing this report I will finish my fantastic study time in Delft.

About 9 months ago I started this exiting MSc Thesis Study about a very beautiful area in the Netherlands, which I know very well: The Markermeer. Born close to the lake I played a 'home match' in the study of the mud dynamics in the lake and the effectiveness of silt traps. Although I got prescience about the lake, I could not finish this study all by myself. In this preface I want to thank all the people who cooperated in this project, gave advice or supported me in the previous months.

First of all, my graduation committee: Han, Marcel, Maarten, Hans and especially Stefan, who was not only my first supervisor. He was also a 'colleague' at Boskalis Hydronamic, with whom I have been working together for more than a year, starting with my internship in February 2007. In this period I learned a lot about the practical work in the civil engineering business, thanks for that!

Many thanks to the measurement team of the field campaign: Bas and Joop, the measurement specialists at Delft Hydraulics. Fishermans Meindert and Jan, who were the captains of the measurement vessel. But most of all: Klaas Pieter, Lara, Philipi, Rose and Heleen. Sailing out on the Markermeer with such an international team was something I could not think about it before. We had a lot of fun!

Also thanks to the Delft Hydraulics specialists: Gerben de Boer, Bas van Maaren, Thijs van Kessel and Andre van der Westhuysen. By using their advice, the modelling part of the study became a success.

Thanks to all the other colleague graduation students, for making fun during the sometimes boring moments behind the computer. From Boskalis: Merijn, Gerben and Stefanie. From Delft Hydraulics: Noud, Claartje, Johan, Anton, Laura, Robert, Gao, Marieke, Renske and John. Special thanks to Stephan. I know him from my first hours in Delft, became my friend, team mate, rowing mate and finally our study time ends in the same office room in Papendrecht. Many thanks for all the advice! In the end, I also learned a lot about toe structures of breakwaters!

Thanks to my parents and sister for support during the years I studied in Delft. For being always interested on what I was working on, although it was sometimes hard to understand.

And finally last, but not least, Eva. Not only for the advice about the text, but most of all for cheering me up and supporting me in the last months. For the interest in my work and for the fun we have in our new city, Utrecht. It is always a pleasure to come home after a day of hard work.

Enjoy reading this report!

Thomas Vijverberg
May 2008

Summary

The Markermeer is an important fresh water lake in the centre of the Netherlands. Because of its variety of functions (main functions: safety, fresh water supply and ecology) and total scale of the lake, it is a unique area in Europe. The lake is an official European wetland and is part of the Habitat and Bird regulation.

Over the years several problems have arrived in the Markermeer, which affect appropriate functioning of the lake. One of these problems is the decreasing ecological value (water quality) of the lake. This decrease in water quality is caused by a high turbidity of the water in the lake. Large amounts of mud sediment are suspended in the water column, even during normal conditions. This high turbidity has a large impact on the ecosystem, which is indicated in a decreasing population of the 'Driehoeks' mussel and diversity of birds.

Rijkswaterstaat set up a study about several measures to decrease the high turbidity and improve the water quality of the lake. One of those measures is a deep silt trap, to catch the suspended sediment. Although some previous studies are carried out on the sediment behaviour in the Markermeer, the exact functioning of a silt trap is unknown. This MSc study focused on the mud dynamics in the Markermeer and the effects of a silt trap as a solution for the turbidity problem. Main question in this study is:

Is a silt trap an effective measure to improve the water quality in the Markermeer?

Boskalis has some experiences with dredging deep sand pits in the Markermeer. Sedimentation rates in those pits were observed very high. Higher than expected from only settling of sediment from the water column. Other mechanisms might also be responsible for the infill of the silt trap. It is hypothesized that two mechanisms are responsible for the infill of the silt trap:

- Settling of sediment from the water column
- Density currents near the bed

Density currents can be generated if a high sediment concentration layer exists near the lake bed and a density difference is present between two locations in the lake (for example near a silt trap). However, the knowledge of the mud behaviour in the Markermeer is insufficient to determine if density currents can exist. In this study this question is answered first. After that, the study shifted to the effects of a silt trap on the sediment behaviour.

To determine if density currents can occur in the Markermeer a better understanding of the near bed mud dynamics is needed. Previous model studies of the Markermeer were carried out in 2D, so all hydrodynamic and sediment transport processes are simulated as depth average values. These models assume a uniform distribution of suspended sediment over the water column. This year, Deltares (WL Delft Hydraulics) set up a 3D mud model of the Markermeer. The model is developed to assess the effect of several measures for the turbidity problem on the total scale of the lake. The effect of density currents is not taken into account in that model. For this MSc study the Deltares model is further developed into a 3D online sediment transport model, to simulate density currents and assess the effects of a silt trap.

Markermeer mud is characterized by the presence of two fractions: a fine and a coarse fraction. A similar sediment schematization is also applied in the model.

The fine fraction has a very low settling velocity and the sediment is uniformly distributed in the water column during most of the time. This fraction can only settle if wind speed drops to 1 or 2 Bft (all hydrodynamic and sediment transport processes are completely driven by the wind). If this occurs a very thin mud layer is generated on the lake bed. This layer is considered as the fluffy layer. This layer is very mobile and can rapidly resuspend from the shallow lake bed. This fine fraction is the main cause of the turbidity problem.

The coarse fraction has a high settling velocity and is suspended in the water column if wind speed 5 Bft. and higher occurs. In storm periods the sediment concentration of this fraction can be 100 – 150 mg/l.

To assess if density currents can occur in the Markermeer, special measurements were carried out during the field measurement campaign in autumn 2007. The measurements focus on the near bed sediment concentration. The occurrence of a higher concentration layer near the bed is an indication for the existence of density currents. Measurements confirm the presence of a layer with high sediment concentration near the bed:

- Turbidity measurements with an Optical Back Scatter (OBS) show higher concentrations near the bed; up to a factor 2 higher than in the water column
- Echo sounding measurements indicate a soft mud layer near the bed with an average thickness of 10 cm. The density of that soft mud layer is not known
- Sediment concentration measurements with the Argus Surface Monitor (ASM) show very high concentrations (700-800 mg/l) in the lower 20 cm of the water column, during times of increasing and decreasing wind speeds

The Markermeer model developed for this study is calibrated against measured data: wave height in the centre of the lake and sediment concentration near the bed (ASM data). The model results show good agreement with the field data. The high sediment concentration layer is also observed in the model results.

In the model density currents are observed near the silt trap edge. The flow velocity due to density currents is in the order of 2 to 5 cm/s. Comparing to the wind driven flow velocities in the lake (0.10 to 0.20 m/s) this is an increase of about 25 to 50 %. Density currents become significantly large (velocity is more than 2 cm/s) if the sediment concentration near the bed increases to 1 g/l. Significant density currents can only be generated if mild wind conditions occur for at least one day after a storm. Field measurements with the ASM showed sediment concentrations up to 800 mg/l, which is in the same order as the 1 g/l to get a significant density current. So, density currents can exist in the Markermeer.

The dominant mechanism that fills the silt trap differs for the two sediment fractions. The model shows a different behaviour for both fractions.

For the fine fraction advection and settling of sediment is dominant. The sedimentation rate of this fine fraction in the silt trap is small, about 5 to 10 % of the sedimentation rate of the coarse fraction. About 1 % of the total amount of fine material in the lake will accumulate in the trap each year.

For the coarse fraction both mechanisms occur, although the settling process is of major importance. 80 % of the total amount of coarse sediment accumulated in the silt trap is due to settling, 20 % due to density currents.

With the model, a study is carried out to the optimal orientation (parallel or perpendicular) of the silt trap to the main flow direction. Main goal of the silt trap is to reduce the sediment concentration and consequently improve water quality. A reduction in sediment concentration is achieved by two processes:

- Direct effect of reducing the concentration in the water column above and just near the trap.
- Accumulation of sediment in the trap reduces the total amount of sediment in the water column. Fine sediment accumulates in deep pits and is no longer available for resuspension

In both orientations a silt trap causes a reduction in concentration and an accumulation of sediment. However, a silt trap orientated perpendicular to the main flow direction has a higher efficiency. In the parallel case the trap attracts flow and causes an increase in flow velocity and turbulence intensity. This yields an increase of sediment in suspension which decrease the generation of density currents.

Overall it can be concluded that a silt trap can be used as a mitigation measure for turbidity and improve the water quality.

Although a silt trap will have a positive effect on the local scale, a silt trap alone will not work on the scale of the Markermeer. This is attributed to the enormous amount of fine sediment available and the extremely slow settling speed. The effect of the silt trap can be increased if it is combined with other measures to mitigate the turbidity problem.

All conclusions are based on results of the model, which is set up especially for this study. In general, models are just a schematization of reality. Also the silt trap model has its shortcomings. Some basic processes in cohesive sediments are not included and it is recommended that further research should be carried out on the effect of these processes on the efficiency of a silt trap:

- Erosion and sedimentation are not included in the model. As a consequence, in the model all sediment is kept in the water column. So including erosion and sedimentation will be a first improvement of the model. (Lab) measurements should give an indication of the erosion and sedimentation parameters.
- Also the exact erosion areas in the lake should be determined, together with the total erosion flux (production of mud sediment). If the total production of mud sediment is higher than the removal of sediment by the silt traps, the total amount of sediment in the water column increases: in that case silt traps are not a solution to the turbidity problem.
- Flocculation can be an important mechanism that influences the efficiency of the silt trap. The existence of flocculation of the sediment in the Markermeer is not proved. First a study about flocculation behaviour in the lake should be carried out. After that the influence of flocculation on the efficiency of the silt trap can be investigated.
- Consolidation of the bed inside or just outside the silt trap can affect the sediment behaviour near the trap. In the model this is not taken into account. (Lab) research should be carried out to the consolidation behaviour of the Markermeer mud.

In this MSc study it is assumed that water quality is governed by turbidity (sediment concentration) only. This is not true in reality. Water quality is a complex ecological value, determined by many other parameters besides sediment concentration (for example algae growth, light penetration and nutrients). Those parameters should be included in the future models as well.

The application of state-of-the-art 3D mud models, in this study as well as the Deltares study has contributed importantly to our understanding of the Markermeer mud dynamics. Realization of a pilot silt trap in the Markermeer would be a prerequisite for future developments, including improved insight in silt traps efficiency, validation of basic model processes and the development of an integral ecological model for the Markermeer.

Table of Contents

Preface	v
Summary	vii
Table of Contents	xi
List of figures	1
List of tables	3
List of symbols	5
1 Introduction and problem analysis	7
1.1 Problem description	7
1.2 Hypothesis	9
1.3 Objective of the study	10
1.4 Set up of the report	12
Part I: Mud dynamics in the Markermeer	13
2 The Markermeer, a general description	15
2.1 History	15
2.2 Topography	15
2.3 Water depth and water balance	16
2.4 Geology and sediment characteristics	17
2.5 Wind climate	19
3 Large scale processes in the Markermeer	21
3.1 Hydrodynamics	21
3.2 Sediment transport processes in cohesive sediments	26
3.3 Morphological processes	33
4 Field Measurements	37
4.1 Spatially distributed sediment and water column data	37
4.2 Echo sounding	40
4.3 Cesium measurements	43
4.4 Argus Surface Monitor (ASM)	45
4.5 Overall observations	48
4.6 Conclusion	49
5 Large scale Delft3D model	51
5.1 Markermeer model WL Delft Hydraulics	51
5.2 General lay out of the model	53
5.3 Calibration	61
5.4 Results	65
5.5 Conclusion	67
Part II: Silt traps as a mitigation measure for turbidity	69
6 Processes in and around a silt trap	71
6.1 Hydrodynamics	71
6.2 Sediment transport processes	76
7 Delft3D model of the silt trap	81
7.1 General lay out	81

7.2	Alternative scenarios	85
7.3	Results.....	87
Part III: In summary		97
8	Conclusions, discussion and recommendations	99
8.1	Conclusions	99
8.2	Discussion.....	103
8.3	Recommendations	107
References		111
Appendices		113
Appendix A: Field measurements		115
A-1:	Turbidity measurements	115
A-2:	Echo soundings	117
A-3:	Cesium measurements.....	119
A-4:	Argus Surface Monitor	121
Appendix B: Large scale Delft3D model		127
B-1:	Other model settings	127
B-2:	Calibration results	129
B-2:	Results	133
Appendix C: Delft3D model of the silt trap.....		135
C-1:	Observation points and cross sections	135
C-2:	Validation	137
C-3:	Comparison to theory	138
C-4:	Results	141

List of figures

Figure 1.1: Overview of the total IJsselmeer area.....	7
Figure 1.2: Satellite image of the Markermeer, which illustrates the turbidity problem.....	9
Figure 1.3: Two general mechanisms to fill a silt trap with sediment.....	10
Figure 1.4: Schedule of the water quality problem.....	11
Figure 2.1: Topographic overview of the Markermeer.....	15
Figure 2.2: Depth profile in the Markermeer.....	16
Figure 2.3: Water balance of the Markermeer in the year 1988.....	17
Figure 2.4: Geological profile of the Markermeer, cross section west to east.....	17
Figure 2.5: Sediment composition of the top layer of the bed.....	18
Figure 2.6: Location of the IJsselmeer deposits and its thickness.....	18
Figure 2.7: Behaviour of the IJsselmeer deposit layer, years 1958-1994.....	19
Figure 2.8: Wind rose Schiphol.....	20
Figure 2.9: Wind speed and percentage of occurrence for different directions.....	20
Figure 2.10: Seasonal variations of the wind speed and direction, location Schiphol.....	20
Figure 3.1: Schematic situation of wind setup in a lake.....	21
Figure 3.2: Water level and velocity profile due to wind forcing.....	21
Figure 3.3: Horizontal velocity (m/s) in the upper layer in the vertical, wind SW.....	23
Figure 3.4: Horizontal velocity (m/s) in the lowest layer in the vertical, wind SW.....	23
Figure 3.5: Schematic situation of wave growth in limited water depth.....	24
Figure 3.6: Wave growth curves. Dimensionless H_s and T_p as a function of fetch F	24
Figure 3.7: Computed significant wave heights (m) in the lake, during 2 wind directions.	26
Figure 3.8: Processes of cohesive sediments.....	26
Figure 3.9: Classification of grain sizes for different standards.....	27
Figure 3.10: Triangular classification diagram according to NEN 5104.....	27
Figure 3.11: Three different types of clay minerals, microscopic picture.....	28
Figure 3.12: Typical three layer system of mud sediment.....	28
Figure 3.13: Mud floc taken from the Merwede.....	31
Figure 3.14: Large scale morphological behaviour of mud, conceptual model.....	34
Figure 3.15: Conceptual lay out of the bed in the Markermeer.....	35
Figure 4.1: Measurement locations of the field campaign.....	38
Figure 4.2: Van Veen Grab. Used for taking bed samples.....	38
Figure 4.3: CTD, OBS and Chlorophyll sensors.....	38
Figure 4.4: Brown fluffy layer (few mm's thick) on top of the grey mud layer.....	39
Figure 4.5: Locations where the fluffy layer is found (yellow) and where not (blue).....	39
Figure 4.6: Sediment concentration profiles measured by the OBS sensor.....	40
Figure 4.7: Principle of the working of an echo sounder and the transducer in practice.....	41
Figure 4.8: Echo sounder data, location 12 on 26 th of November.....	41
Figure 4.9: Echo sounder data, location 14 on 23 th of November.....	41
Figure 4.10: Histogram of the thickness of the soft mud layer.....	42
Figure 4.11: Schematic distribution of Cesium in a core.....	43
Figure 4.12: Beeker sampler and core in practice.....	43
Figure 4.13: Typical cesium profile. 86' layer is located between 25 – 50 cm.....	44
Figure 4.14: Locations where Beeker samples have been taken during the campaign.....	44
Figure 4.15: Argus Surface Monitor, schematic (left), in reality (mid) and EMC (right).....	46
Figure 4.16: ASM result 4 th of December 2007 22:10.....	48
Figure 4.17: ASM result 7 th of December 2007 6:50.....	48
Figure 5.1: Schematic set up of the Delft3D modelling software.....	53
Figure 5.2: Overview of the modelling domain.....	54
Figure 5.3: FLOW and WAVE grid of the model.....	55
Figure 5.4: Bathymetry of the Lake as implemented in the model.....	55
Figure 5.5: Differences between 2DH and 3D modelling in velocity profile.....	56
Figure 5.6: Schematic picture of sigma-layers (left) and z-layers (right).....	56
Figure 5.7: Initial sediment concentration profile.....	58

Figure 5.8: Nautical definition wind direction.....	59
Figure 5.9: Wind speed during modelling period, measured in Berkhout.....	59
Figure 5.10: Time series of significant wave height.....	63
Figure 5.11: Time series of sediment concentration averaged over upper 10 cm of ASM. ..	65
Figure 5.12: Sediment concentration of both fractions, 7 Dec. 3h00.....	66
Figure 5.13: Sediment concentration of both fractions, 12 Dec. 12h00.....	66
Figure 6.1: Definition of flow angles.....	72
Figure 6.2: Flow parallel to the silt trap.....	72
Figure 6.3: Flow profiles near the silt trap (perpendicular case).....	73
Figure 6.4: Refraction of the streamlines in case of a flow with oblique inlet angle.....	74
Figure 6.5: Flow pattern near a silt trap with wind driven flow.....	75
Figure 6.6: Wave direction near a channel or silt trap.....	76
Figure 6.7: Schematic picture of a density current near a silt trap.....	78
Figure 6.8: Velocity of the density current as a function of the sediment concentration....	79
Figure 7.1: Design of the silt trap in the report 'Transparante Markermeren'	81
Figure 7.2: Location of the silt trap in the bathymetry of the Delft3D model.....	81
Figure 7.3: Location of the silt trap, parallel.....	82
Figure 7.4: Grid of the silt trap model, parallel. Refinement in the silt trap area.....	82
Figure 7.5: Part of the vertical grid near the silt trap.....	83
Figure 7.6: Bathymetry of the silt trap model.....	83
Figure 7.7: Two alternative orientations of the silt trap, parallel and perpendicular.....	87
Figure 7.8: Depth average flow velocity situation silt trap parallel, 7-12 12h00.....	87
Figure 7.9: Schematic situation of refraction pattern of waves near a silt trap.....	88
Figure 7.10: Velocity and sediment concentration profile on the 3 th of December 0h10... ..	89
Figure 7.11: Direction of positive transport through the cross sections.....	91
Figure 7.12: Cumulative Total Transport in trap Mud 2, upper 3 m of the water column..	93
Figure 7.13: Average sediment concentration Mud 2.....	93
Figure 7.14: Sediment concentration Mud 2, longitudinal cross section over trap.....	94
Figure 8.1: Explanation of the model effects.....	106

List of tables

Table 3.1: Wind setup and resulting flow velocity and bed shear stress for several wind speeds in the Markermeer.....	22
Table 3.2: Wave height, period and length for several wind speeds in the Markermeer....	25
Table 3.3: Density ranges of consolidated mud for several stages.....	33
Table 3.4: Critical shear stress for erosion in the Ketelmeer.....	33
Table 5.1: Characteristics of the two sediment fractions.....	57
Table 5.2: Settings of some calibration runs for the Markermeer model.....	64
Table 7.1: Height of the vertical layers ($k = 1$ top layer, $k = 20$ lowest layer) as a percentage of water depth.....	82
Table 7.2: Schedule of the different alternative simulations of the silt trap model and the different settings.....	85
Table A.1: Results of analysis of calibration samples of the OBS.....	115
Table A.2: Results of echo sounding measurements.....	117
Table A.3: Results of the cesium measurements.....	120
Table A.4: Results of analysis of calibration samples for the ASM.....	121

List of symbols

<u>Symbol</u>	<u>Unit</u>	<u>Description</u>
A	m ²	Area
C	m ^{1/2} /s	Chezy friction coefficient
C _d	-	Wind drag coefficient
CFL	-	Courant number
D	m	Diameter of a mud floc
D _p	m	Diameter of a mud particle
D ₅₀	m	Diameter of a mud floc (50 % percentile)
F	m	Fetch of the wind
H _s	m	Significant wave height
H _{m0}	m	Zero order wave height
L	m	Wave length
R	-	Correlation coefficient
S	-	Salinity
S _{tot}	m ³ /s	Total sediment transport
T	s	Wave period
T _{peak}	s	Peak wave period
U	m/s	Mean flow velocity
U ₁₀	m/s	Wind speed at the height of 10 m
c	kg/m ³	Sediment concentration
C _{gel}	kg/m ³	Gelling concentration, reference density hindered settling
d	m	Thickness of the soft mud layer
g	m/s ²	Gravitational acceleration (9.81 m/s ²)
h	m	Water depth
i	-	Water level gradient
k	-	Number of vertical layer in the model grid
p	N/m ²	Pressure
t	s	Time
u	m/s	Flow velocity (x direction)
\hat{u}_b	m/s	Amplitude of orbital velocity near the bed
u*	m/s	Shear velocity
v	m/s	Flow velocity (y direction)
w _s	m/s	Settling velocity of sediment
w _{s,r}	m/s	Settling velocity of a single mud particle
x	m	Horizontal coordinate
y	m	Horizontal coordinate
z	m	Vertical coordinate
Γ _T	m ² /s	Eddy diffusivity
Δt	s	Time step of the model
Δx	m	Spatial step of the model
α	-	Angle between main flow velocity and trap orientation
β	-	Rouse number

κ	-	Von Karman coefficient (0.4)
ν	m^2/s	Kinematic viscosity (10^{-6})
ρ	kg/m^3	Density
ρ_{air}	kg/m^3	Density of air ($1.0 \text{ kg}/\text{m}^3$)
ρ_w	kg/m^3	Density of water ($1000 \text{ kg}/\text{m}^3$)
ρ_s	kg/m^3	Specific density of sediment ($2650 \text{ kg}/\text{m}^3$)
σ	-	Standard deviation
σ_T	-	Prandtl Smidt number (0.7)
τ_b	N/m^2	Bed shear stress
$\tau_{c,e}$	N/m^2	Critical shear stress for erosion
$\tau_{c, sed} / \tau_d$	N/m^2	Critical shear stress for sedimentation
τ_{wind}	N/m^2	Wind shear stress on the water surface
ν_v	m^2/s	Vertical eddy viscosity

1 Introduction and problem analysis

1.1 Problem description

The Markermeer is an important fresh water lake in the centre of the Netherlands. It is part of the total IJsselmeer area (Figure 1.1), which consists of the Markermeer and the IJsselmeer. Principal functions of the two lakes are safety, fresh water supply and ecology, but also user functions like: transport, fishing, (water) recreation, energy supply and sand mining.



Figure 1.1: Overview of the total IJsselmeer area, consisting of the IJsselmeer and Markermeer. (www.wikipedia.nl)

For *safety* (flood defence) the lakes are important areas. The Afsluitdijk and Houtribdijk were built to protect the low country for flooding. Both lakes (IJsselmeer and Markermeer) are used as a reservoir to store fresh water from, for example, the river IJssel during times of high water levels. The water level in the lakes is regulated on the basis of a strict water level policy. The lakes are also an important link in the fresh *water management* of the Netherlands. In dry periods the northern parts of the country take fresh water from the lake for drinking water, agriculture and nature.

Another important aspect of the lakes is the great *ecological value* for birds, because of its food supply, shallow water and calm climate. Therefore the IJsselmeer area is an official European wetland and is part of the Habitat and Bird regulation, which implies that degradation of the ecological value of the lakes should be prevented.

Overall, the Markermeer is a unique area in Europe, both in variety of functions, as well as the scale of the lake.

Over the years, several problems have arrived in the Markermeer, which affect appropriate functioning of the lake (Ministerie van V & W, 2007):

- Safety is no longer guaranteed because of the too low crest heights of the dikes. Due to climate change (global warming), the sea level will rise. Expected values of sea level rise are 15 till 35 cm in the year 2050, with a maximum of 85 cm in 2100. Discharge of water from the lakes through sluices to the Waddensea is driven by a water level difference. If the sea level rises, the water level in the Markermeer will have to rise as well, to maintain this water level difference. Land subsidence of the surrounding polders (and dikes) will enhance the problem with an expected 50 cm in the year 2050.
- Spatial pressure on the area will increase, because of population growth and changing demands. Extra space is needed for living, mobility and recreation. Especially for cities like Amsterdam and Almere this will give problems. Extending these cities into the Markermeer is a solution for the problem, but will affect the functions of the lake.

- The ecological value (water quality) of the lake is decreasing. High turbidity of water in the lake is one of the causes. Due to the construction of the Afsluitdijk and Houtribdijk natural flushing of the lake stopped. During storm events large amounts of sediments (mud and organic material) are suspended into the water column. Because of the closure of the Markermeer this sediment remains in the system. The amount of sediment in the water is even enlarged by erosion of the peat layers in the west part of the lake. As a result the turbidity in the lake increases; light penetration decreases. Even during normal conditions the lake is much more turbid than for example the IJsselmeer. This high turbidity has large negative impacts on the ecosystem, which is indicated in a decreasing population of the 'Driehoeks' mussel (Riza, 2003) or decreasing diversity of birds.

To solve these problems, large scale rearrangement projects will be carried out in the Markermeer in the coming years, which will thoroughly renew the appearance of the lake.

This study will focus on the third problem of the Markermeer: the turbidity problem and will be part of a large Rijkswaterstaat project. One of the aims of that project is to give an answer to the following question (Ministerie van V & W, 2007):

What are the characteristics of the mud behaviour in the Markermeer and what is the effectivity of the several solutions to the turbidity problem?

In this Rijkswaterstaat project several organizations will cooperate:

The national government is the main stakeholder and funds the project. RIZA (Institute for fresh water and waste water management, part of Ministry of transport and water management, nowadays part of Deltares) together with Rijkswaterstaat IJsselmeergebied are responsible for the execution of the project.

Before the rearrangement projects can be designed and carried out, a better understanding of the mud dynamics in the Markermeer is needed to assess the efficiency of the projects.

The availability of an accurate numerical model is a prerequisite to do so.

Modelling research on the sediment behaviour in the Markermeer started in the early 1990's. Vlag (1992) developed a 1D model for resuspension and sedimentation of mud, with an application to the Markermeer. Processes like erosion/resuspension, sedimentation and consolidation of the sediment are included in the model. The model gave good results for three distinctive locations in the lake. However horizontal transport can not be simulated with the model and also flocculation processes are neglected. Therefore the model can not be used as an integral model for mud dynamics across the Markermeer.

Van Duin (1992) developed a 2D model called STRESS-2D for sediment transport, resuspension and sedimentation in shallow lakes. The model is set up for lakes in the IJsselmeer area. The model uses the hydrodynamic model WAQUA with extensions for resuspension and sedimentation and is coupled to models for simulating light attenuation by suspended solids and algal growth. The large scale suspended sediments concentration patterns in the model show good agreements with measurements. The results of the algal growth model are not satisfying. This model can not be used for local assessments of the detailed processes, for example processes near a silt trap. 3D processes which occur near a trap are not taken into account in this model.

The importance of 3D processes is confirmed by Royal Haskoning and WL Delft Hydraulics (2006). Royal Haskoning and WL Delft Hydraulics (2006) carried out a study to identify the knowledge gaps in our understanding of the Markermeer mud dynamics. In addition they address possible solutions to the turbidity problem. Some of these solutions are:

- Deep silt traps to catch the sediment.
- Artificial islands to split up the Markermeer in compartments.
- Marsh development on the shores.
- Detached breakwaters in front of the shores.
- Covering of mud layers with sand, to reduce the erosion of mud (source term).

However only a rough analysis is carried out on these solutions. The study also leaves some questions unanswered about the mud behaviour in the Markermeer. Especially the role of organic material in the mud and detailed 3D effects are not taken into account.

For this reason Deltares is requested to build a 3D mud model of the Markermeer to carry out research on the mud behaviour in the Markermeer and to determine the effect of several solution alternatives on the water quality of the lake. This is the first time that a 3D model is set up for the Markermeer. WL Delft Hydraulics (2007a) describes the results of the set up and calibration of that model. More information about that model will be given in Chapter 5. WL Delft Hydraulics (2007b) describes the first simulations of the several solution alternatives.

Parallel to this model development, Witteveen & Bos and Boskalis Ltd. also investigated and proposed solutions for the turbidity problems (Witteveen & Bos, 2004b). In this report the solution of a silt trap is highly recommended, because its expected efficiency to mitigate turbidity and preferential conditions to finance the project; sand which will be taken from the deep silt trap can be sold on the sand market, for example for extension projects near Almere. However, the exact working of a silt trap in the Markermeer is unknown (Witteveen & Bos, 2004b), so Boskalis and RIZA are interested in a study on the functioning of silt traps, to increase silt trap efficiency and optimize the design. This thesis is a part of that study.

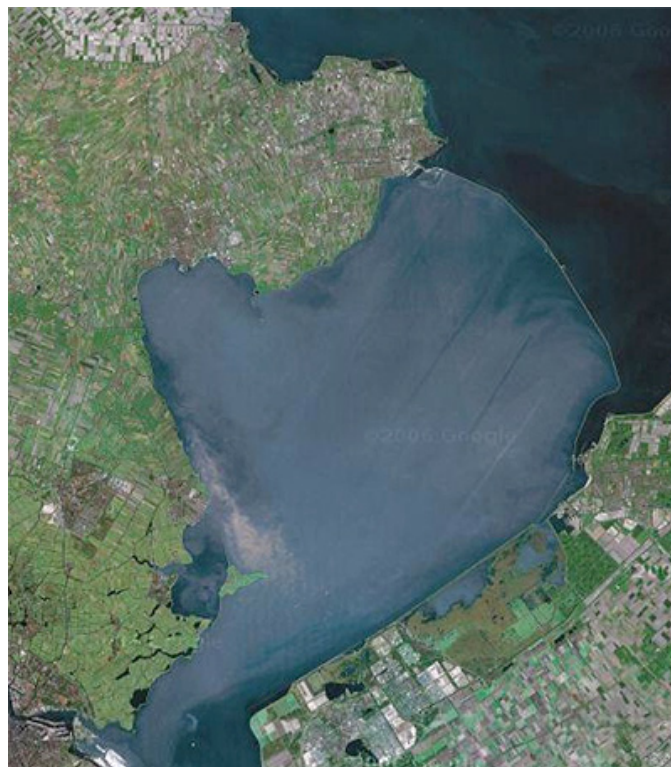


Figure 1.2: Satellite image of the Markermeer, which illustrates the turbidity problem. The bright appearance of the Markermeer reveals increase suspended sediment concentration, which is associated with higher turbidity. (maps.google.com)

1.2 Hypothesis

In Section 1.1 it is already mentioned that the exact working of a silt trap is not known. No detailed study to the effect of a silt trap in the Markermeer has been carried out before.

Early modelling studies (e.g. Van Duin, 1992) were set up as a 2D model of the Markermeer. The common idea was that the flow and sediment behaviour in the lake was a 2D horizontal process. Due to the very shallow water, the sediment concentration in the lake was considered to be uniformly distributed over the water column. For this reason 2D models were sufficient for modelling sediment transport. The idea about the working of a silt

trap was that the sediment will settle out from the water column in the silt trap, because of the decreasing flow velocity (turbulence intensity) above the trap.

Although the exact knowledge of the working of a silt trap was not present, in the past some deep pits have been dredged in the Markermeer (like the IJburg pit or Proefputten A and B). While dredging these pits in the Markermeer, construction experience was obtained. One of those experiences was that it was hard to keep those pits on a certain depth when dredging was carried out and just after it. Sedimentation rates inside these pits were a lot higher than expected from only settling of sediment from the water column (*Personal comment*).

More recent 3D studies (WL Delft Hydraulics, 2007b) also observed a low sedimentation rate (order few cm's/year) in pits when only settling of sediment is taken into account.

Probably a second mechanism is important for the infill of a silt trap or deep pit. This mechanism can be density currents.

Density currents can occur if a high concentration layer near the bed is present (causing a significant increase of fluid - mixture density) and a density difference between two locations exists. A flow is generated from the location with high density to the location with low density, driven by this density difference. Because this flow is in the high concentration layer near the bed, the sediment flux can be large. Near a silt trap those density differences can occur. The high concentration layer flows from the shallow part to the slope of the trap. On the slope the layer will accelerate due to gravity. For this reason the sediment flux to the trap can be much larger than the flux generated by settling of sediment from the water column.

Both mechanisms (settling and density currents) are explained in Figure 1.3. Because presently there is no scientific evidence for the existence of density currents in the lake, first a study to the mud dynamics in the Markermeer is carried out. This study focuses on the mud dynamics near the bed. After that the study will shift to the detailed mechanisms near a silt trap.

Before starting the study the following hypothesis is stated:

Silt traps can be filled by two mechanisms, settling of the sediment from the water column and density currents near the lake bed.

After this study this hypothesis will be accepted or rejected.

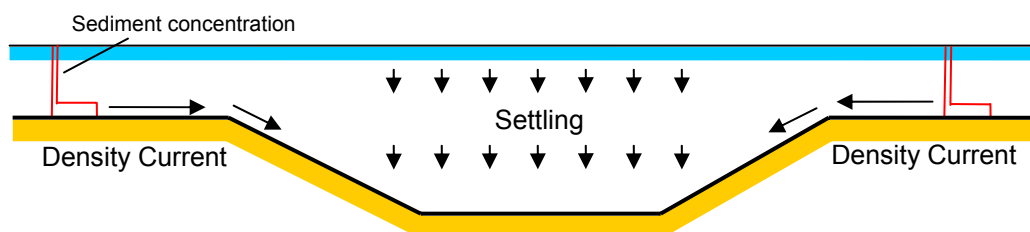


Figure 1.3: Two general mechanisms to fill a silt trap with sediment, settling and density currents. Density currents are generated by a high concentration layer near the lake bed and a density difference between two locations.

1.3 Objective of the study

This study focuses on the mud dynamics in the Markermeer and the effects of a silt trap as a solution for the turbidity problem. Aim of the study is to answer the following central question:

Is a silt trap an effective measure to improve the water quality in the Markermeer?

In this question, 'water quality' can be considered as an overall main property of ecological value of the lake. Several underlying factors determine the water quality of the lake, for example pollution, nutrients, light penetration (turbidity) and more. The problem of light penetration is a problem of turbidity, which is influenced by some factors, like algae, vegetation, sediment concentration. Figure 1.4 shows a schematic picture of this classification.

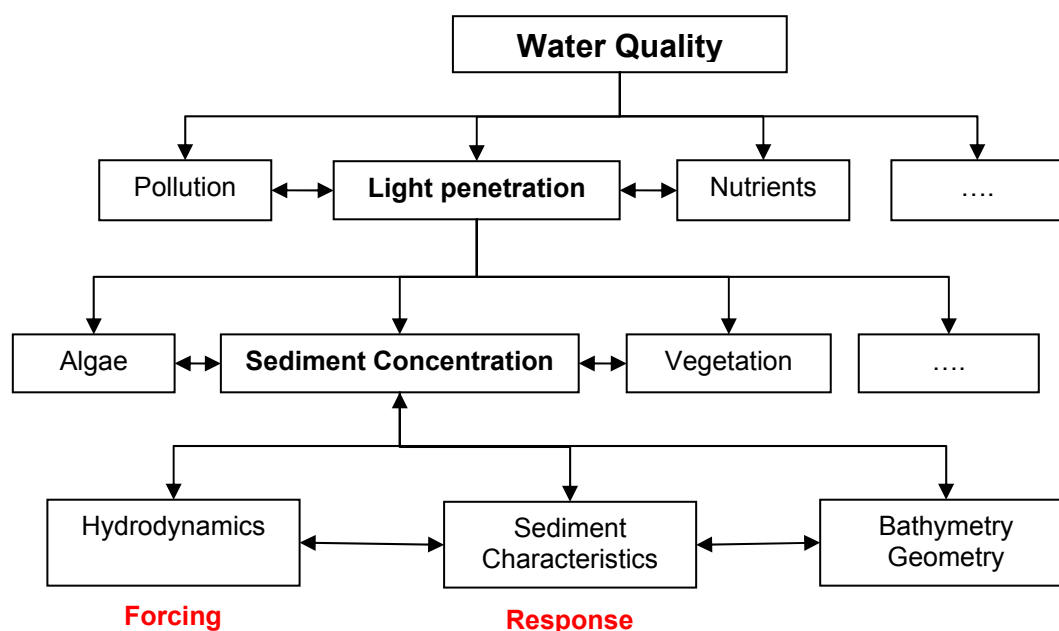


Figure 1.4: Schedule of the water quality problem. This schedule shows the relation between sediment concentration and water quality. In this study the focus will be on the sediment behaviour.

This study is restricted to the effects of a silt trap on sediment concentration in the water column. Biological processes like algal growth and vegetation development are left out of consideration. Because the sediment behaviour influences the water quality, this study will finally give advice about the effect of a silt trap on the water quality.

To assess the effects of a silt trap on the sediment concentration it is necessary to understand the both mechanisms which cause trapping of the sediment. Hypothetically two mechanisms are available:

1. Settling of sediment from the water column.
2. Flow of sediment into the silt trap as a density current, under the influence of density differences and gravity.

So far, the knowledge of the mud behaviour in the Markermeer is insufficient to determine if density currents can occur in the lake. Therefore the first main objective of this study is to determine if density currents can occur. This will be discussed in part I of this report. Two questions arise in that part:

- *What are the mud dynamics of the Markermeer?* (Chapter 3)
- *Can the mud in the Markermeer behave like a density current?* (Chapters 4 and 5)

In part II the detailed processes around a silt trap will be studied. The focus will be on dominant mechanism to fill a silt trap (settling or density currents) and its effect on the sediment concentration (second main objective). Also design parameters of a trap will be studied, to determine the optimal design of a trap in relation to reducing the sediment concentration. Two questions which arise in this part are:

- *What is the dominant process for the infill of a silt trap?* (Chapters 6 and 7)
- *What is an optimal design of a silt trap to reduce the sediment concentration?* (Chapter 7)

For this study the existing Delft3D mud model of the Markermeer (developed by Deltares, WL Delft Hydraulics, 2007a) is extended with a 3D online sediment transport computation to simulate the density currents near the bed. In this extended model the silt trap is implemented. The input of the model is based on field data, collected during a small scale measurement campaign, and previous studies.

1.4 Set up of the report

This section will describe the set up of this report and can be considered as a reading guide.

The report is divided into three main parts. The first part will focus on the mud dynamics in the Markermeer. The second part will describe the sediment behaviour near a silt trap and the final part will summarize the results; the main conclusions and recommendations will be discussed.

Part I consists of the Chapters 2 to 5 and will answer the first two sub questions stated in the previous section. Chapter 2 is an introduction to the Markermeer. Physical characteristics of the lake will be discussed, for example wind climate, geological composition of the lake bed or the water balance. Chapter 3 will give more detail of the hydrodynamic processes in the lake (Section 3.1) related to the sediment transport and the overall morphology (Section 3.3). Both chapters contain information from literature.

In Chapter 4 the field measurement campaign is discussed. A detailed set up of the campaign is outlined, proceeded with all results. All data from the measurement campaign is presented in appendix A.

The study continues with the Delft3D model. In Chapter 5 the set up (Section 5.2) and calibration (Section 5.3) of the large scale model of the Markermeer are discussed. Results of the calibration are shown in appendix B. Both Chapters 4 and 5 will give a definite answer to the question if density currents can exist in the Markermeer.

After this chapter the study switches to the small scale process near a silt trap. In Chapter 6 first the results of a literature study to the hydrodynamic processes near a trap are given (Section 6.1), followed by the sediment transport processes. Also an estimation of the magnitude of the density currents is given (Section 6.2).

Chapter 7 continues with the Delft3D model as set up in Chapter 5. However in this chapter the silt trap is implemented. First the adaptations to the large scale model of the Markermeer are given (Section 7.1 and 7.2). These adaptations were needed to implement the silt trap. In Section 7.3 the results of the model are discussed and compared to the theoretical expectations of Chapter 6. Chapters 6 and 7 give answer to the last two sub questions of this study. All results of the silt trap model are presented in appendix C.

Finally the main conclusions are drawn in Chapter 8 (Section 8.1), followed by a discussion about the shortcomings and utility of the silt trap model (Section 8.2). At last recommendations are given (Section 8.3) for future research on the mud dynamics in the Markermeer and the sediment behaviour near a silt trap.

All figures and tables are numbered according to the chapter numbers. For example: Chapter 2 starts with Figure 2.1, 2.2, etcetera. Chapter 3 continues with 3.1, 3.2..... The figures and tables in the appendix start with a A,B or C, according to which part of the appendices it belongs. For example appendix A starts with Figure A.1 and appendix B with Figure B.1. The same numbering is used for all equations.

Part I: Mud dynamics in the Markermeer

2 The Markermeer, a general description

This chapter is an introduction to the physical characteristics of the Markermeer. These physical characteristics are a background for all physical processes. Information is taken from reports and publications of previous studies.

2.1 History

The Markermeer is a large shallow lake in the centre of the Netherlands. Until 1932 it was part of the Zuiderzee, which was an inland sea connected to the North Sea. The Zuiderzee was a tidal bay, with water flowing in and out according to the tide. With the tide, sediment and salt water were transported in and out of the Zuiderzee. Due to this tidal flow a difference in bed sediment developed from north to south. In the southern part, where tidal flow velocities are low, fine sediment is accumulated. In the northern part the bed sediment is coarser. Due to larger flow velocities, only the coarse sediment can settle. Also a difference in salinity was observed; the southern part the Zuiderzee was less saline because of several fresh water sources.

In 1932 the construction of the Afsluitdijk was finished, according to the plans of ir. Cornelis Lely. The Zuiderzee became the IJsselmeer and was separated from the sea from that moment. Tidal influences disappeared and the lake became a fresh water lake.

In the years 1950 until 1968 large scale land reclamation projects were carried to, resulting in the Flevoland polder's and the Noordoostpolder in the southeast part of the IJsselmeer (Figure 1.1). Finally in 1975 the construction of the Houtribdijk between Enkhuizen and Lelystad was finished and the IJsselmeer was divided in two parts: IJsselmeer in the north and Markermeer in the south. The original plan was to drain the Markermeer as well into one big polder (the Markerwaard). However until now this is only a plan, so nowadays the Markermeer has mostly the same topographic character as in 1975 (Van Duin, 1992).

2.2 Topography

The Markermeer can be considered as a closed lake with a surface area of about 68000 hectare and a water volume of 2.5 billion m³. The west border is formed by the coast of the province of North Holland. The southeast border is the coast of Flevoland and in the northeast part the Houtribdijk is located, which separates the IJsselmeer and the Markermeer. Around the lake several towns are located. Ships can sail in and out of the lake through some locks, some of them with discharge sluices (Figure 2.1)

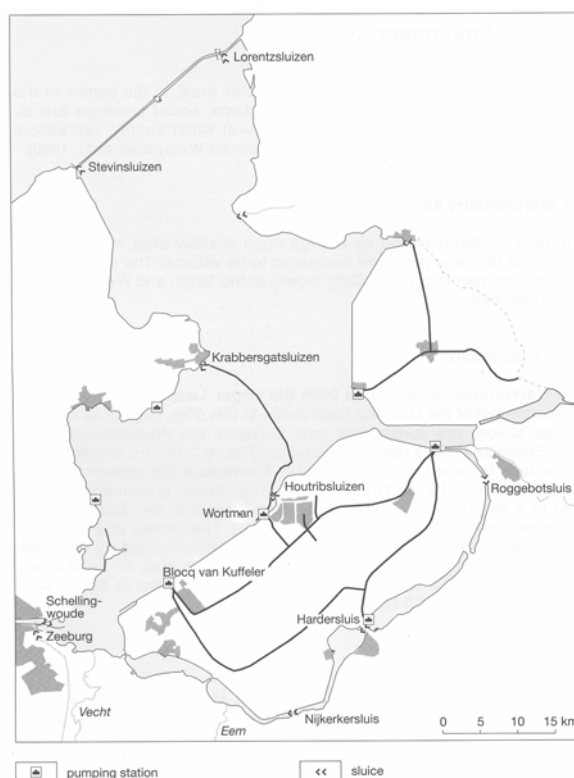


Figure 2.1: Topographic overview of the Markermeer. Locations of the locks are shown. (Van Duin, 1992)

2.3 Water depth and water balance

The Markermeer is a very shallow lake with a mean water depth of 3.6 m. The water level in the lake is kept at -0.20 m NAP (Nieuw Amsterdams Peil) in the summer (April till October) and -0.40 m NAP during winter. This difference exists because of the functions of the lake. In summer this function is mainly fresh water reserve and water supply. In winter this function is to facilitate drainage of the surrounding polders (Van Duin, 1992). It might be possible that the water levels in the lake will increase in the coming decades, because of global warming and sea level rise. The drainage of the Markermeer water to the sea is driven by water level differences with the IJsselmeer. So if the sea level will rise, the water level inside the lake will have to rise as well. This water level rise can have significant effects on, for example, the safety of the dikes. Other solutions (for example, pumping water to the IJsselmeer) for this problem might be more promising.

The differences in water depth in the lake are small. The lake bottom is gently sloping towards the west. The west part of the lake has a water depth of 2 m, the east part around 4 m. Overall, more than 89 % of the area has a water depth between 2 m and 5 m. Larger depths can be found in local sand pits and shipping channels. In the IJmeer a deep sand pit is located of 500 hectares and a depth of about 30 m. A shallow area is located near Enkhuizen, which is called the 'Enkhuizerzand'. The depth profile of the lake is shown in Figure 2.2.

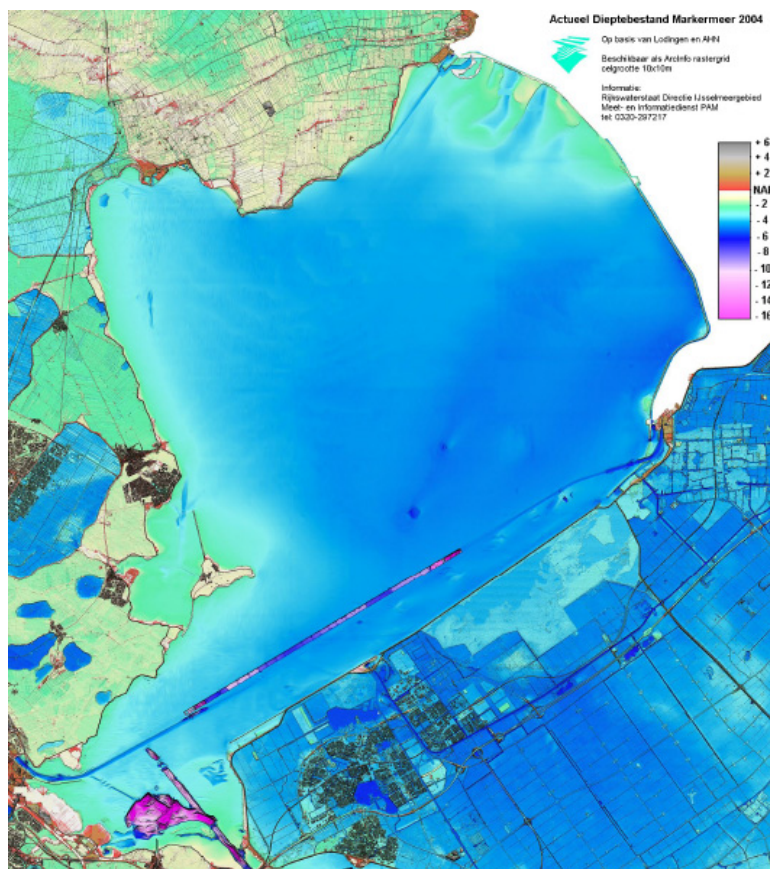


Figure 2.2: Depth profile in the Markermeer. The IJburg pit and the navigation channel are purple. The rest of the lake is very shallow. (Witteveen & Bos, 2004a)

The water balance of the Markermeer is shown in Figure 2.3. This is what the situation was in 1988. The balance is determined by precipitation and evaporation, in and outflow of water through locks, discharge sluices and rivers, infiltration and storage. Royal Haskoning (2006) estimates some values of the water fluxes (for the year 1988): discharge of water 1.1 billion m³ per year (excluding evaporation 500 million m³ per year), total supply 1.4 billion m³ per year (excluding precipitation 600 million m³ per year). The water balance can

be closed by assuming infiltration into and from the bed through groundwater transports. The average residence time of the water is about 6 to 18 months.

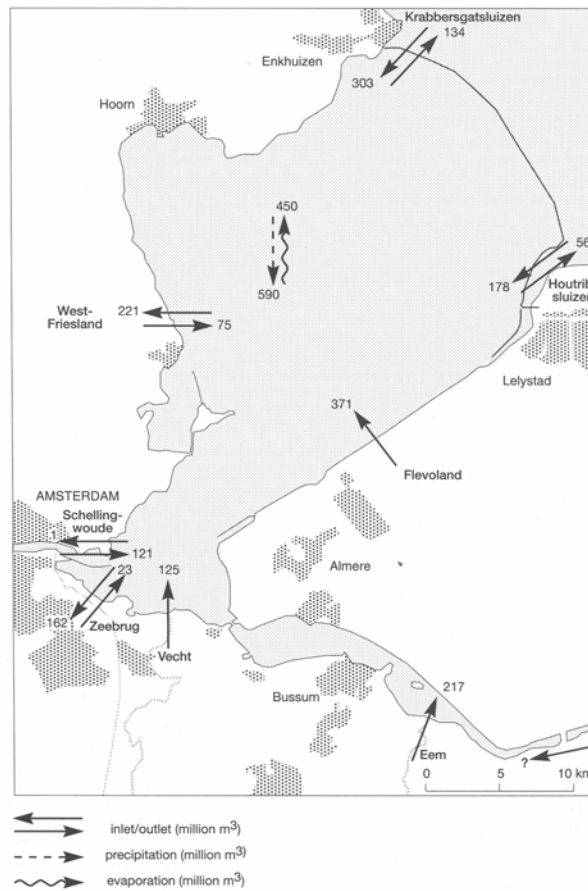


Figure 2.3: Water balance of the Markermeer in the year 1988. This water balance is closed by assuming infiltration into and from the bed. (Van Duin, 1992)

2.4 Geology and sediment characteristics

The upper part of the bed of the Markermeer is formed in the Holocene. A cross section of the different sediment layers from west (Volendam) to east (Lelystad) is shown in Figure 2.4.

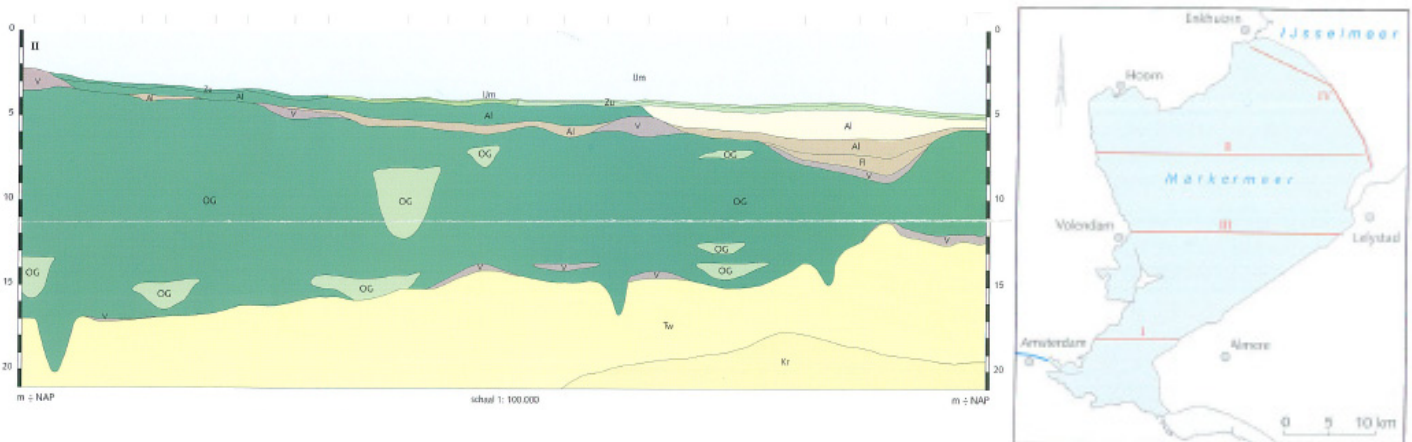


Figure 2.4: Geological profile of the Markermeer, cross section west to east, number II (figure right). (Rijkswaterstaat, 1995) In the west side of the lake the clay layer is much thicker (15 m) than in the east (5-10 m).

The colours in the picture represent different sediment types: dark yellow is sand (modest fine, with clay), yellow is fine sand (with clay), light green is light clay, green is clay and purple is peat.

The bed mainly consists of clay, with some fine and coarse sand layers in the western part. The clay layers in the west are about 15 m thick and in the east about 5 to 10 m. Near Enkhuizen the sand layer is thicker (approximately 5 m), which is called the 'Enkhuizen zand'. In the west part, also some peat layers are found. The present situation of the top layer of the bed is shown in Figure 2.5

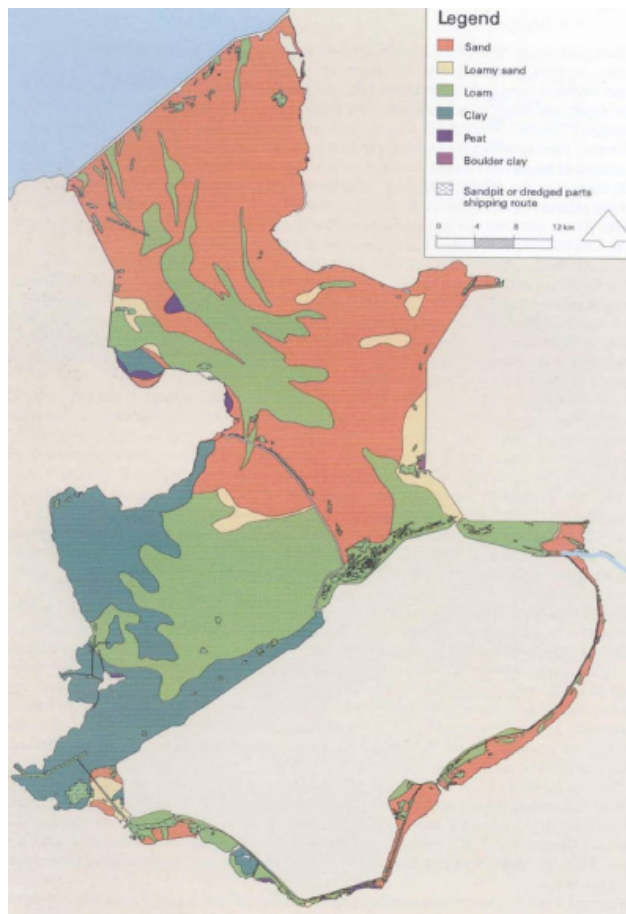


Figure 2.5: Sediment composition of the top layer of the bed. The top layer mainly consists of clay (dark green) and loam (green). (Royal Haskoning, 2006)

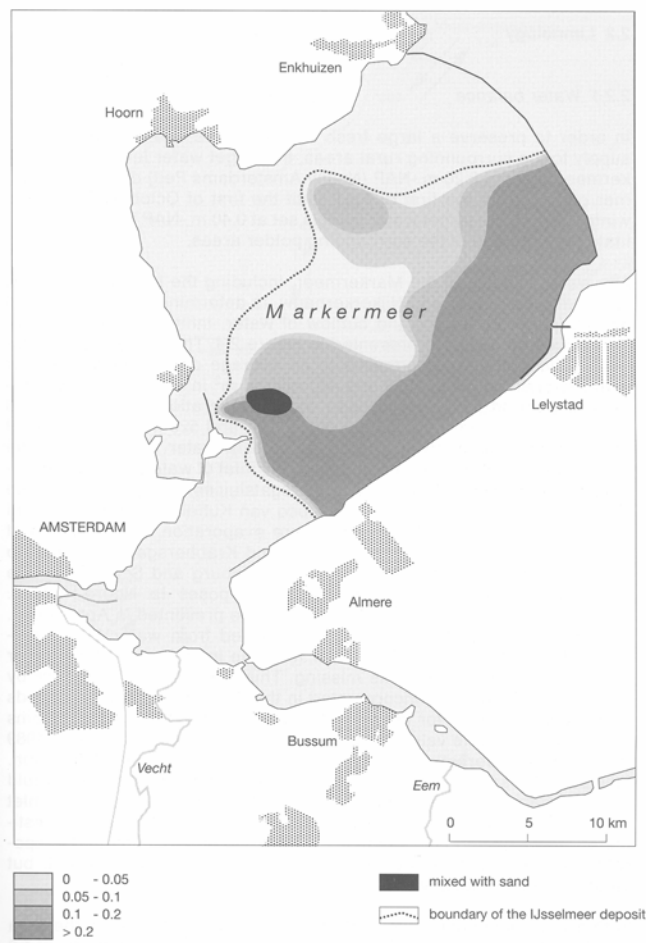


Figure 2.6: Location of the IJsselmeer deposits and its thickness. Situation of 1988. (Van Duin, 1992)

On top of the oldest sediment layers a layer of fine silt is found, covering 60 % of the area of the lake. This layer is called 'IJsselmeer deposit' and originates partly from eroded material of older deposits and partly of sediment from the river IJssel. The water and lutum content of this layer is high. In Figure 2.6 the extent and thickness of this layer is shown for the situation of 1988. Figure 2.7 shows the behaviour of this IJsselmeer deposit layer during some decades. It is clearly shown that the layer is transported to the deeper part of the lake, the east side.

Van Duin (1992) refers to a thin oxic mud layer which is found on top of all deposits. This layer contains freshly deposited sediment with a water content of 95% and is found over the entire surface of the lake (Van Duin, 1992). According to the measurements (Chapter 4) this layer can be considered as the fluffy layer.

The field measurements carried out for this study show that this fluffy layer is not found all over the lake. In Section 3.3.2 a complete sketch of the layer composition is given.

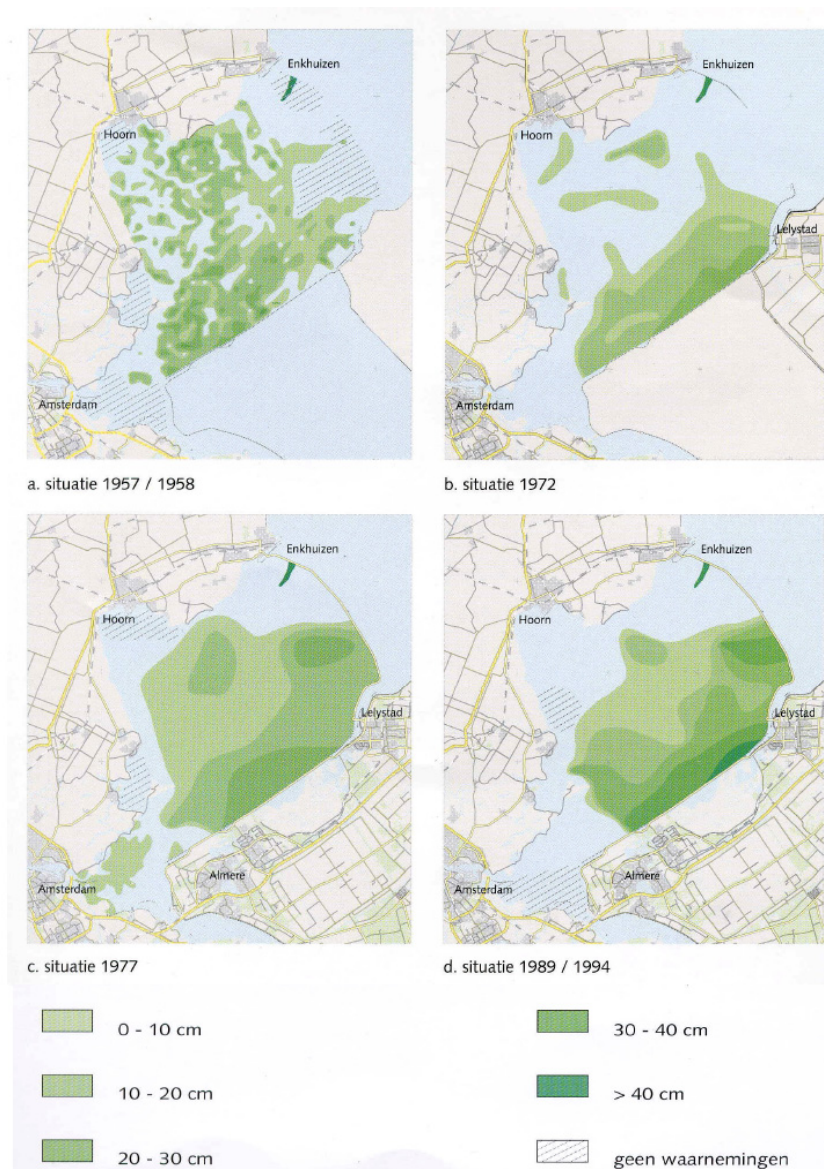


Figure 2.7: Behaviour of the IJsselmeer deposit layer, years 1958-1994. The layer is transported to the south east part and increases in thickness. (Rijkswaterstaat, 1995)

As mentioned in Chapter 1 the suspended sediment concentration in the Markermeer is much higher than for example in the IJsselmeer. The background concentration in the Markermeer is average 30 mg/l and maximum concentration about 250 mg/l. Comparing to the Ketelmeer (5 mg/l and 100 mg/l) or lake Balaton in Hungary (15 mg/l and 170 mg/l) this is much more. (Van Kessel, 1999).

2.5 Wind climate

The wind climate of the Markermeer area will be described according to the KNMI wind measurements at station Schiphol. There are some other wind stations near the Markermeer like, Wijdenes, Lelystad and Houtribdijk. Visser (2007) mentioned that the values of Schiphol are the most representative for the Markermeer area. Other stations can behave like a land station if the wind is from a specific direction. For this reason other stations can underestimate the wind speed.

An extensive wind data set is available on the website of the KNMI (www.knmi.nl). Every hour the wind speed and direction are recorded. Wind speeds are measured at a height of 10 m, the so called U_{10} (equation 3-1). The results of the measurements are shown in the figures below. It is shown in the graphs that the yearly dominant wind direction is southwest and also the stronger winds are from direction southwest.

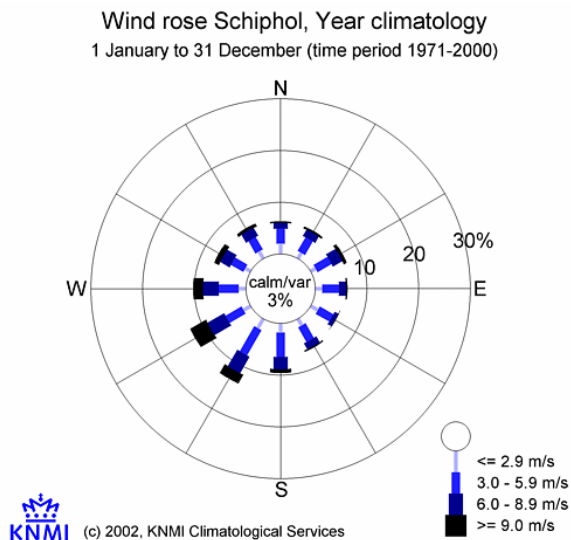


Figure 2.8: Wind rose Schiphol. (www.knmi.nl)

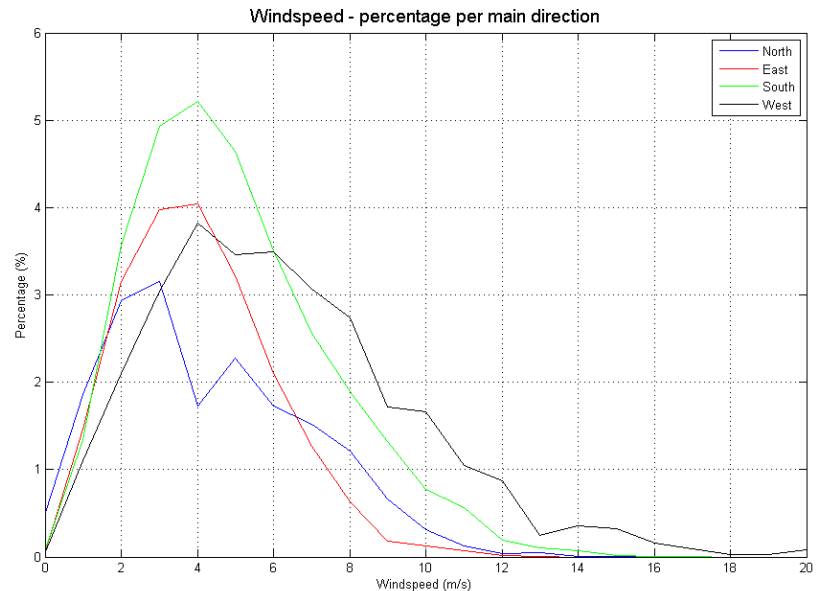


Figure 2.9: Wind speed and percentage of occurrence for different directions.

The data do reveal some seasonal spreading in the wind direction. In the spring, winds usually come from the north, in summer from the west, and in autumn and winter from the southwest. These variations appear in the model when using a real data set of wind measurements.

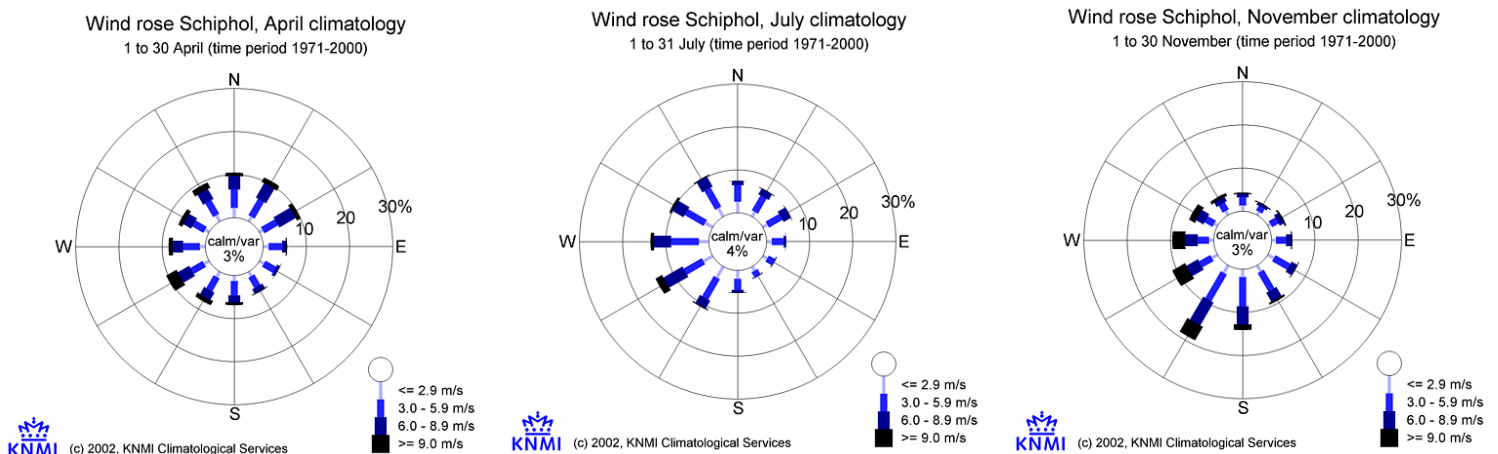


Figure 2.10: Seasonal variations of the wind speed and direction, location Schiphol
During spring winds are from the north/northwest. During summer from the west and in the winter from southwest. (www.knmi.nl)

Because wind is the only generator of currents and waves (the Markermeer is a closed body of water), proper modelling of the wind field is necessary to predict the currents and waves.

3 Large scale processes in the Markermeer

This chapter will give an introduction to the overall hydrodynamic processes in the Markermeer and the relation to the sediment behaviour and morphology. Section 3.2 will discuss the basic processes in cohesive sediments. These processes are important to understand the sediment behaviour in the lake. Most of the information is taken from literature.

3.1 Hydrodynamics

3.1.1 Wind driven currents and circulation

The large scale flow pattern in the Markermeer is mainly dominated by the wind induced flow. In Chapter 2 it was mentioned that the Markermeer can be considered as closed lake. Only a little amount of water is flowing in and out. Locally, current velocities can be affected by discharge through sluices or other in- and outlet system, but this is not important for large scale wind driven circulation. In Royal Haskoning (2006) a first order computation is given about the flow velocities in the lake generated by the wind. Although it is a rough computation, it estimates the order of magnitude of the flow. All equations and values in the computation in the following section are taken from Royal Haskoning (2006).

If wind is blowing over the lake, it will exert a shear stress on the water surface given by,

$$\tau_{wind} = c_1 \rho_{air} U_{10}^2 \quad (3-1)$$

c_1 is a coefficient and has a value of 0.0033, ρ_{air} is the density of air (1.0 kg/m^3) and U_{10} is the wind speed (m/s), 10 m above the water level.

Figure 3.1 shows a schematic picture of the reaction of the water body on the wind forcing: the wind causes a water level difference in the lake, called a wind set up.

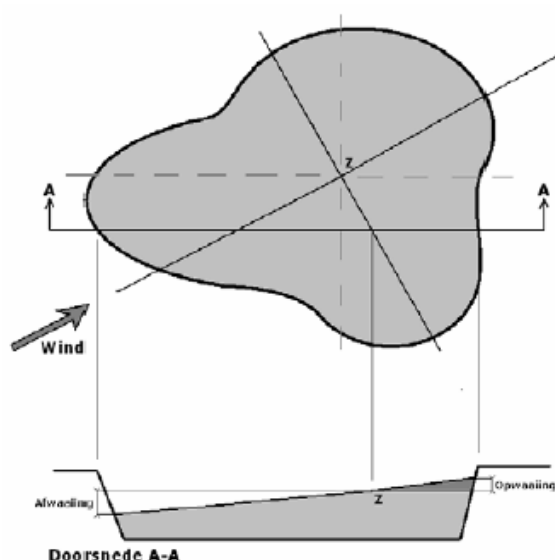


Figure 3.1: Schematic situation of wind setup in a lake. (Visser, 2007)
 The water is pushed from the wind side of the lake to the other side.

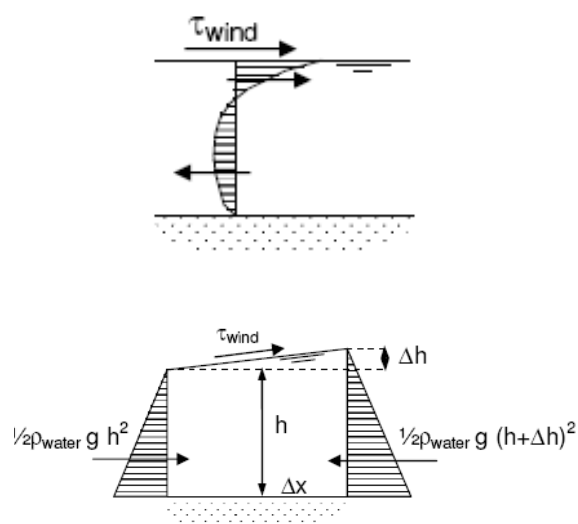


Figure 3.2: Water level and velocity profile due to wind forcing. (Royal Haskoning, 2006)
 In the upper part of the water column, flow is in the same direction of the wind; in the lower part against the wind direction.

The total water level difference can be computed using the force balance shown in Figure 3.2, which reads,

$$\tau_{wind} \Delta x = \frac{1}{2} \rho_w g (h + \Delta h)^2 - \frac{1}{2} \rho_w g h^2 \quad (3-2)$$

Δh^2 can be neglected, because it is much smaller than h . The water density is set to the value for fresh water, $\rho_w = 1000 \text{ kg/m}^3$. Equation 3-2 then becomes,

$$\Delta h = \frac{c_1 \rho_{air} U_{10}^2}{\rho_w g h} \Delta x = 4.10^{-6} \frac{U_{10}^2}{gh} \Delta x \quad (3-3)$$

Due to the wind setup and water level difference a pressure gradient is present over the lake. This gradient generates vertical and horizontal currents and circulation. The equilibrium velocity profile due to wind is shown in Figure 3.2. In the upper part of the water column the velocity is in the direction of the wind, in the lower part the velocity is against the wind direction. This profile is schematic, in reality also horizontal circulation will occur, which affects this velocity profile. The horizontal circulation is shown on the next page.

Royal Haskoning (2006) estimates the flow velocity in the lower part by assuming that in the lowest 30% of the water column the flow is comparable with flow without wind (a logarithmic profile). The flow velocity is then computed by,

$$U = C \sqrt{(0.3h)i} \quad (3-4)$$

with i is the water level gradient (-) and C is the Chezy coefficient ($50 \text{ m}^{1/2}/\text{s}$). The bottom shear stress induced by flow is given by,

$$\tau_b = \rho_w g (0.3h)i \quad (3-5)$$

Royal Haskoning (2006) calculated these velocities and shear stresses for several values of the wind speed in the Markermeer, using a fetch of 27 km and a water depth of 4 m. Results are shown in Table 3.1.

Wind (Bft)	4	5	6	7	8
Windspeed (m/s)	6	10	12	15	20
Occurrence (days/year)	280	148	59	17	3
Wind set-up (m)	0.10	0.28	0.40	0.62	1.10
Gradient (mm/km)	3.7	10.2	14.7	22.9	40.8
Flow velocity near bed (m/s)	0.10	0.17	0.21	0.26	0.35
Bed shear stress by flow (Pa)	0.04	0.12	0.17	0.27	0.48

Table 3.1: Wind setup and resulting flow velocity and bed shear stress for several wind speeds in the Markermeer. (Royal Haskoning, 2006)

As already mentioned this is a rough estimation. In the Markermeer a wind set up is generated, causing a return current. However this return current is not only near the bed, but also a horizontal circulation is generated. This results in a complex 3D flow pattern in the lake. This pattern is dependent on the wind speed and direction. For example, the flow pattern will look completely different for winds from the north than for winds from the west. A clear example of the 3D large scale circulation in the lake is shown in the Figures 3.3 and 3.4. These plots are results of the large scale Markermeer model (Chapter 5). At the time the plot is taken, the wind direction is from southwest with a speed of 11.5 m/s. The southwest direction is the dominant wind direction, so this flow pattern will occur most of the time.

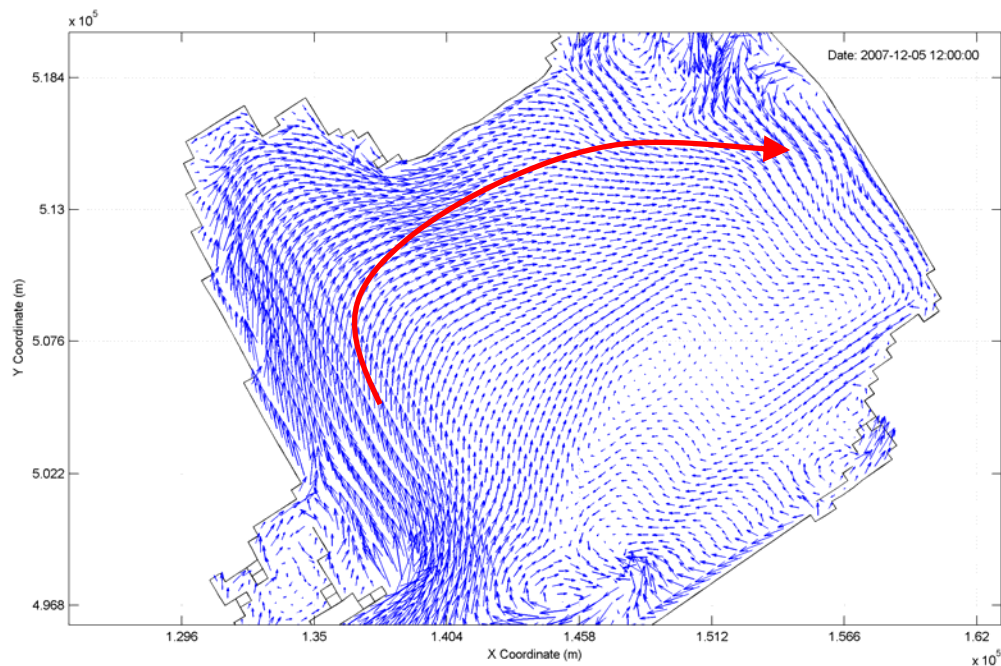


Figure 3.3: Horizontal velocity (m/s) in the upper layer in the vertical, wind SW, 11.5 m/s
 The flow is mainly from the southwest part (IJmeer) to the northeast and concentrates in the north part of the lake.

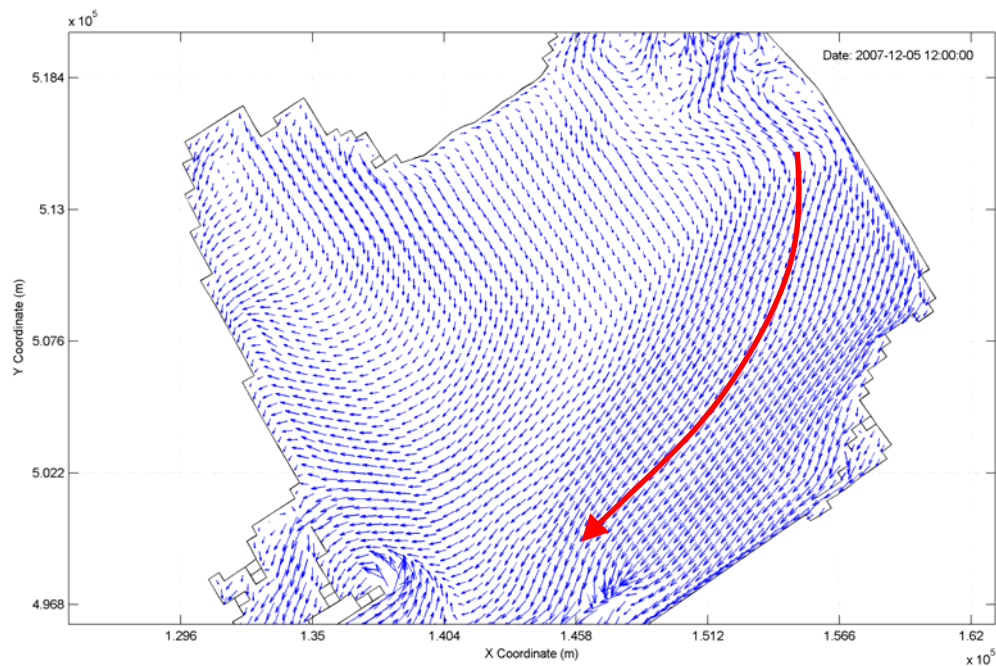


Figure 3.4: Horizontal velocity (m/s) in the lowest layer in the vertical, wind SW, 11.5 m/s
 The flow near the lake bed concentrates in the south part of the lake and is from the northeast to the southwest.

It is shown that in the upper layer the circulation is in the north part of the lake to the northeast and in the lowest layer in the south part of the lake to the southwest.

3.1.2 Wind generated waves

In the Markermeer waves are generated by the wind. Because of the closed water body, no waves from outside can enter the area, all waves are generated locally by the wind. Holthuijsen (2007) gives a description of wave growth in limited water depth, with a constant depth and wind speed.

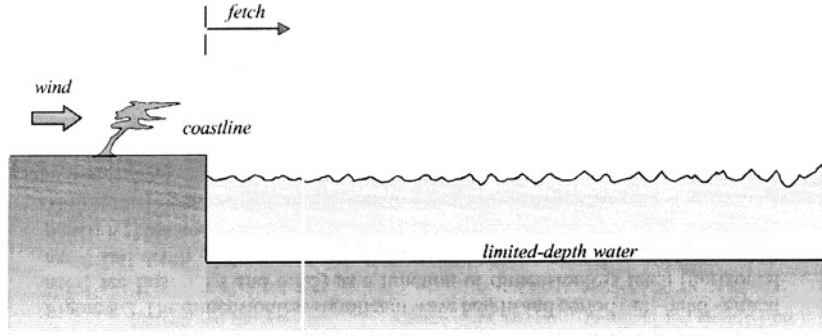


Figure 3.5: Schematic situation of wave growth in limited water depth and constant wind speed. (Holthuijsen, 2007)

The Markermeer is a shallow lake with limited depth (average 3.6 m) and without large depth differences, so the 'constant and limited depth' criterion is valid for the Markermeer. The wave height and wave period can be computed using several dimensionless parameters, which are,

- Depth: $\tilde{h} = \frac{gh}{U_{10}^2}$, with h is water depth (m). (3-6)

- Fetch: $\tilde{F} = \frac{gF}{U_{10}^2}$, with F is the fetch (m). (3-7)

- Wave height: $\tilde{H}_{m0} = \frac{gH_{m0}}{U_{10}^2}$, with H_{m0} is the zero moment wave height (m). (3-8)

- Wave period: $\tilde{T}_{peak} = \frac{gT_{peak}}{U_{10}^2}$, with T_{peak} is the peak wave period (sec). (3-9)

The wave height and period are computed by (3-10) and (3-11),

$$\tilde{H} = \tilde{H}_{m0} = \tilde{H}_{\infty} \tanh\left(k_3 \tilde{h}^{m3}\right) \tanh\left(\frac{k_1 \tilde{F}^{m1}}{\tanh\left(k_3 \tilde{h}\right)^{m3}}\right)$$

$$\tilde{T} = \tilde{T}_{peak} = \tilde{T}_{\infty} \tanh\left(k_4 \tilde{h}^{m4}\right) \tanh\left(\frac{k_2 \tilde{F}^{m2}}{\tanh\left(k_4 \tilde{h}\right)^{m4}}\right)$$

Values of the constants are according to Holthuijsen (2007),

$k_1 = 4.14 \cdot 10^{-4}$	$m_1 = 0.79$
$k_2 = 2.77 \cdot 10^{-7}$	$m_2 = 1.45$
$k_3 = 0.343$	$m_3 = 1.14$
$k_4 = 0.10$	$m_4 = 2.01$
$\tilde{H}_{\infty} = 0.24$	$\tilde{T}_{\infty} = 7.69$

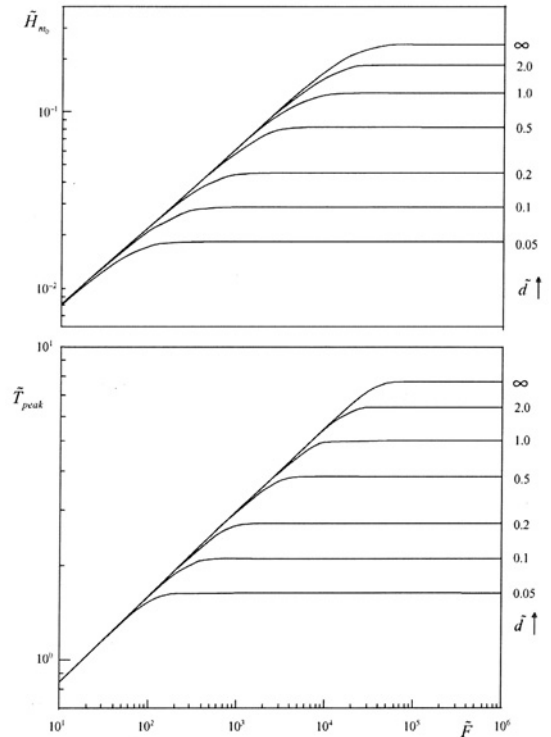


Figure 3.6: Wave growth curves. Dimensionless H_s and T_p as a function of fetch F . (Holthuijsen, 2007) Waves grow to a maximum if the fetch is large. This is shown in flattening of the curves.

General results of these formulas are shown in Figure 3.6. It is shown that the wave height and period grow with increasing fetch and depth. Royal Haskoning (2006) estimates the wave growth for several wind speeds (comparable with the computation for wind set up and velocity), using the same formulas (3-9 and 3-10), but different values for the constants. Also the wave length and orbital velocity near the bed are calculated. The wave length (L , (m)) is calculated using the Airy equation,

$$L = \frac{gT^2}{2\pi} \tanh\left(\frac{2\pi h}{L}\right) \quad (3-12)$$

The near bed orbital velocity (amplitude) follows from,

$$\hat{u}_b = \frac{\pi H_s}{T \sinh\left(\frac{2\pi h}{L}\right)} \quad (3-13)$$

The results of the computations are shown in Table 3.2. These values give an indication of the wave characteristics in the Markermeer. Although this is (again) a rough estimation, it shows the order of magnitude of the waves in the lake.

Wind (Bft)	4	5	6	7	8
Windspeed (m/s)	6	10	12	15	20
Occurrence (days/year)	280	148	59	17	3
Significant wave height (m)	0.40	0.64	0.73	0.86	1.03
Wave period (s)	2.5	3.1	3.4	3.7	4.2
Wave length (m)	9.3	14.4	16.4	18.9	22.3
Amplitude orbital velocity near the bed (m/s)	0.07	0.23	0.31	0.41	0.56

Table 3.2: Wave height, period and length for several wind speeds in the Markermeer.
(Royal Haskoning, 2006)

For both computations (flow and wave due to wind) carried out by Royal Haskoning (2006), time dependency is neglected. Waves and wind set up will have to grow in time during the first hours of a storm. In these computations it is assumed that the storm will last for a long time; the equilibrium situation will occur. The values shown in Tables 3.1 and 3.2 can be considered as the equilibrium values. In reality, waves and flow velocities will be lower in the first hours of a storm.

Two examples of computed wave heights with the Delft3D model are shown in Figure 3.7. Both situations are with same wind speed (12 m/s), but from different direction. The left figure is the situation of wind from the west northwest. The right figure shows the situation with wind from the south.

In both figures a dependency of the wave height on the fetch is shown. Largest wave heights are found at the locations where the fetch is longest. The order of magnitude of the wave height corresponds to the estimations shown in Table 3.2. The wind speed of 12 m/s corresponds by a wind of 6 Bft. The wave height is estimated at 0.73 m (Table 3.2). Comparing to the results of the Delft3D model, this value can be considered as an average value of the wave height. In the estimation a constant fetch of 27 km is used. In reality the fetch is not constant. For this reason higher and lower values of the wave height can exist.

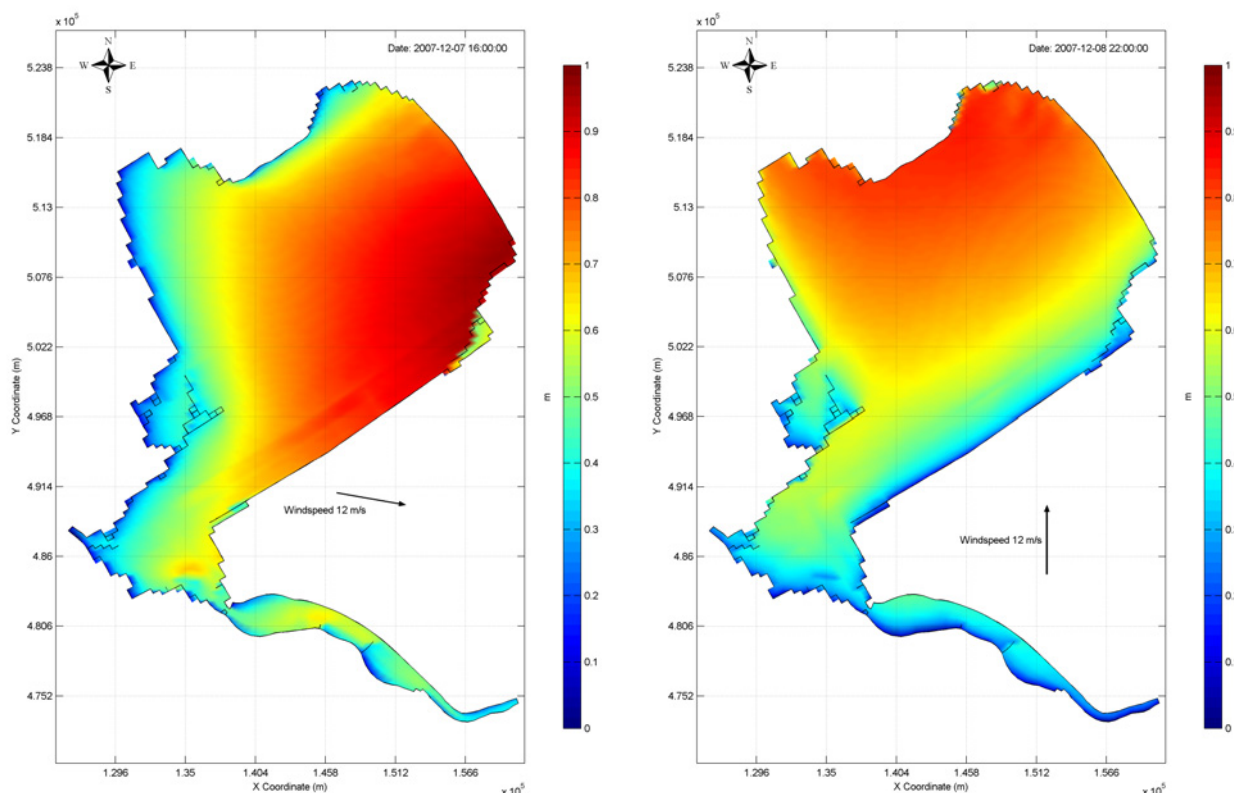


Figure 3.7: Computed significant wave heights (m) in the lake, during 2 wind directions: south (right) and west northwest (left). Larger wave heights are found if the fetch is larger.

3.2 Sediment transport processes in cohesive sediments

This section will discuss some general processes of cohesive sediments. These processes can be important for the Markermeer, because the sediment in the Markermeer consist of mostly cohesive sediment. Knowledge of these processes is useful for understanding the sediment behaviour in the lake. The next section starts with a first introduction to cohesive sediments.

3.2.1 Cohesive sediments

Cohesive sediments (fine sediments) have, in comparing to non cohesive sediments like sand, a complete different behaviour in the water column. Most important characteristic in comparing to sand is its cohesiveness (as the name already reveals). The sediment can stick together. This can cause many complicated processes which determine the transport and fate of this material under influence of flow, waves and winds. An overview of most of the processes is shown in Figure 3.8. This section will give a summary of the nature of cohesive sediments. Due to the existence of a large amount of cohesive sediment in the Markermeer, all processes shown in Figure 3.8 can occur, but not all processes are of major importance.

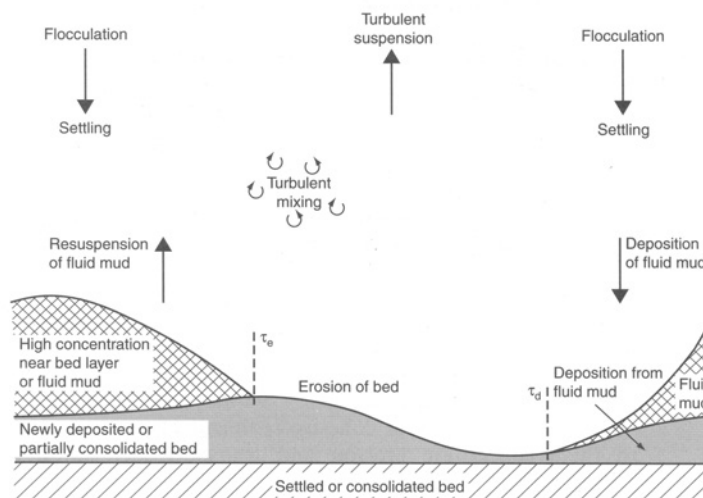


Figure 3.8 : Processes of cohesive sediments. (Whitehouse, 2000)

Cohesive sediment, or mud, can be defined as a fluid – sediment mixture consisting of clay, silt, sand, water, organic material and sometimes gas. These components in this mixture can vary in space and time and are dependent on meteorological – hydronamic conditions, biological activity, history, and many other variables. The behaviour of cohesive sediment is strongly dependent on these mixture components. Therefore modelling of cohesive sediment can be complicated. For each case (field) measurements are important for proper input values of the models.

The solid phase of the composition can be characterized by the particle size distribution. In Figure 3.9, classifications for several standards are shown.

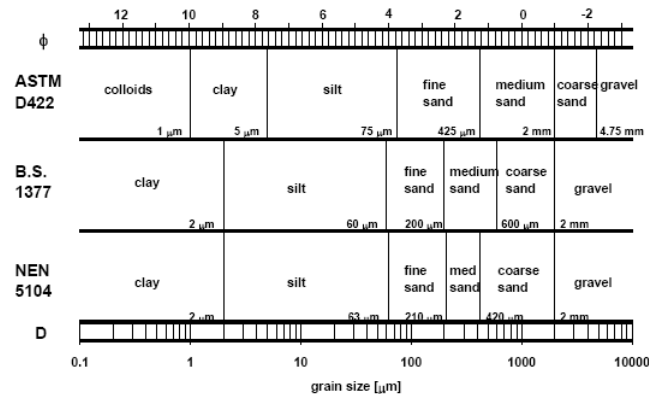


Figure 3.9: Classification of grain sizes for different standards. (Winterwerp, 2004)

A distinction is made between clay, silt, sand and gravel based on the grain size, not by their composition. All fractions can contain mineral and organic material. Another definition is: Fines (< 45 μm).

To classify the type of soil, often a sand-silt-clay triangle is used. In Figure 3.10 such a triangle is shown according to the Dutch standard, NEN 5104.

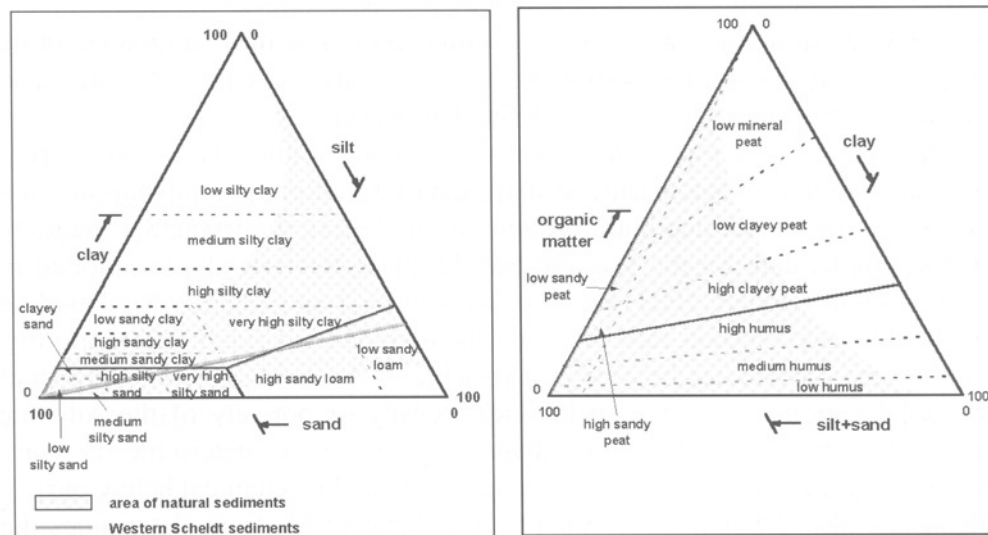


Figure 3.10: Triangular classification diagram according to NEN 5104

The organic component of cohesive sediments consists primarily of organic polymers and can originate from outside a sedimentation area, for example by erosion of peat layers on the west shore of the Markermeer (Haskoning, 2006) or be generated by biological processes. The organic matter can have large effects on the flocculation process (Section 3.2.3) and the stability and strength of the bed (Section 3.2.5). The amount of organic matter in the suspended sediment can be significantly large in the Markermeer (up to 50 %, according to appendix Table A.1). Because of the significant amount of organic material, this should be taken into account in the models of the Markermeer. However this is not

implemented in the model yet, because the characteristics of the organic material are not known. Further research should investigate these properties.

The mineral composition of cohesive sediment is often formed by silicates. Most common groups of silicates are quartz, feldspar and clay material. Clay materials are to a large extent responsible of the cohesive behaviour of mud, because of the flat shape of the particles (layered like structure) and an electric charge, which interacts with the water. The most important clay minerals are: kaolinite (two layer structure), montmorillonite (three layer structure), illite (three layer structure) and chlorite (four layer structure). Three types of clay minerals are shown in the microscopic photo (Figure 3.11).

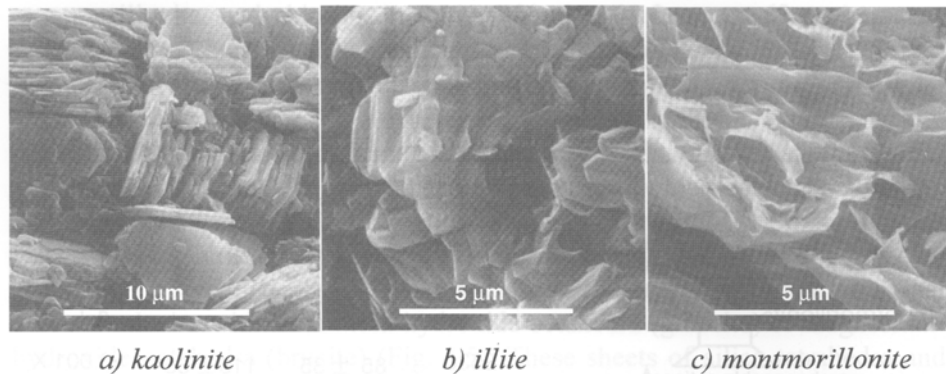


Figure 3.11: Three different types of clay minerals, microscopic picture. (Tovey, 1971)

Cohesive sediments are found all over the world in a large variety of modes. The appearance and behaviour of the sediment is not only determined by small scale processes, shown in Figure 3.8. Also local environmental circumstances (waves, flow, wind, bathymetry, etc.) can play an important role in the appearance of the mud sediment. The various occurrences of mud can generally be described according to a three layer system (Figure 3.12)

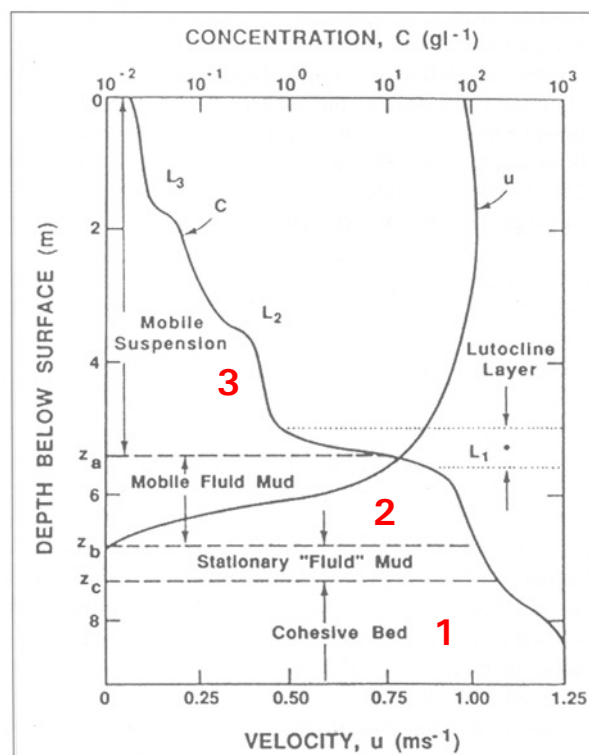


Figure 3.12 : Typical three layer system of mud sediment in the water column and the bed. Layer 1: consolidated bed, Layer 2: Fluid mud, Layer 3: suspended Sediment. (Ross and Metha, 1989)

The three layers are defined as follows:

1. Consolidated bed. Consolidated beds are always present in natural systems of cohesive sediments. The consolidated mud layer has a concentration larger than 300 kg/m³. In general consolidated mud layers have been accumulated for some time. In time the density and bed strength increases. Consolidation is discussed in Section 3.2.5.
2. Fluid mud suspension layer with concentrations in the range of 10 to 300 kg/m³. Fluid mud is found in many navigation channels and harbour basins. This layer can be subdivided into 2 layers:
 - Laminar (viscous) lower layer (100 to 300 kg/m³).
 - Turbulent upper layer (10 to 100 kg/m³)This layer contains freshly deposited material. The strength of this layer is lower than the consolidated bed.
3. Suspension layer with concentrations in the range 0 kg/m³ to 10 kg/m³.

A quite different distinction is made by Winterwerp (1999):

- High Concentrated Mud Suspension (HCMS) with concentrations of a few 100 to 1000 mg/l. The suspension behaves Newtonian with the main flow. HCMS have interaction with the turbulent flow field, which is an important property.
- Low Concentrated Mud Suspension (LCMS) with concentrations in order of 10 to a few 100 mg/l. This suspension does not affect the turbulent flow field.

In the Markermeer these two types of mud suspensions can also be recognized. In the water column the concentration is most of the time below 100 mg/l. Only during large storms it can become higher. So the water column behaves as a LCMS. Near the bed the concentrations can increase to even 1000 mg/l. This layer can behave as a HCMS. This is an important distinction between the water column and the near bed layer.

3.2.2 Settling

Settling of mud (flocs) is an important process in the behaviour of cohesive sediments. In many model studies the settling velocity is a parameter to characterize the sediment fraction. Also in this study the two sediment fractions of the model are characterized by their settling velocity (Chapter 5). However, predicting the settling velocity is difficult, because of processes like flocculation and hindered settling. These processes cause a changing settling velocity in time.

In suspensions with concentrations increasing up to about 1 g/l an increase of settling velocity is observed, as a result of flocculation. If the concentration becomes larger than about 10 g/l the settling velocity decreases due to hindered settling. Hindered settling is the effect that settling velocity of the flocs reduced due to an upward flow of fluid displaced by the flocs (Van Rijn, 2005). Winterwerp (1999) presents seven processes which influence the settling velocity of particles in suspension:

- Return flow and wake formation. If a particle falls through the water column, it creates a return flow, because of the displaced water. Particles close to that falling particle will be affected by that return flow.
- Dynamic or flow effect is the effect that particles near other particles have on the velocity gradients and pressure distribution.
- Particle – particle collisions can cause a hindered settling of individual particles, so settling velocity is decreased.
- Particle – particle interaction is the interaction of particles by mutual attraction and repulsion by electrical charges or others.
- Viscosity. Sediment particles in a fluid can change the viscosity of the fluid mixture (in case of high concentrations) and therefore also the settling velocity.
- Buoyancy. Particles in a saline environment will have a different settling velocity when the same particles are in a fresh water environment.

- Cloud formation. Particles in the wake of another particle will be dragged by this particle. This will enhance the wake of the group, catching more particles and a cloud of falling particles is formed.

There are some empirical formulas to predict the settling velocity of a mud particle/floc. The settling velocity of a single mud floc in still water (settling column) is (Winterwerp, 1999):

$$w_{s,r} = \frac{\alpha}{18\beta} \frac{(\rho_s - \rho_w)g}{\mu} D_p^{3-n_f} \frac{D^{n_f-1}}{1 + 0.15 \text{Re}_p^{0.687}} \quad (3-14)$$

With α and β coefficients depending on the shape of the particles, $\text{Re}_p = w_{s,r} D / \nu$ is the Reynolds particle number, D_p the particle floc size and n_f a coefficient. Hindered settling can be described according to the classical hindered settling formula of Richardson and Zaki (Winterwerp, 1999),

$$w_s = w_{s,r} (1 - k\phi)^n \quad (3-15)$$

with k is about 1 and n is a function of the particle Reynolds number, with values $2.5 < n < 5.5$. Although this formula is often used for cohesive sediments, it may be not correct according to Winterwerp (1999). Therefore in Winterwerp (1999) a more sophisticated formula is used, including the effect of return flow,

$$w_s = w_{s,r} \frac{(1 - \phi_*)^m (1 - \phi_p)}{1 + 2.5\phi} \quad (3-16)$$

The factor $(1 - \phi_*)$ accounts for the return flow and m is a coefficient.

If the suspended sediment concentration is further increased (more than 10 g/l) the fluid – mud mixture forms a space filling network and the settling velocity becomes zero. At this so called ‘gelling point’ the volumetric concentration ϕ becomes unity (1) by definition. The gelling concentration can be obtained from,

$$c_{gel} = \rho_s \left(\frac{D_p}{D} \right)^{3-n_f} \quad \text{and} \quad \phi = \sum \frac{c}{c_{gel}}, \quad \text{so } c = c_{gel} \text{ at the gelling point.} \quad (3-17)$$

The settling process is important for modelling of the silt trap, because settling is one of the major processes that fill a silt trap (Section 1.2). An important process which can affect the settling velocity is flocculation. This process will be discussed in the next section.

3.2.3 Flocculation

Flocculation is a characteristic property of cohesive sediments. It can significantly influence the sedimentation characteristics of the sediment; larger flocs normally have a larger settling velocity.

Winterwerp (2004) defines flocculation as: ‘... a reversible process and is the result of simultaneously occurring aggregation and floc break-up processes’. Aggregation is the result of mutual collisions of, and subsequent adherence between the particles. Break-up is caused by turbulent stresses and mutual collision. So flocculation requires particle collisions and this is governed by three mechanisms:

- Brownian motion of the particles. The number of collisions is linearly proportional to the sediment concentration.
- Differences in settling velocity because of different sizes of particles. Larger particles, which have a larger fall velocity, may ‘fall’ on the smaller ones.

- Turbulent mixing due to the presence of velocity gradients. One way this process will form flocs by collision, but if turbulent shear is high flocs will be broken up.

Winterwerp (1999 and 2004) however concluded that the first two mechanisms are probably small in estuarine and coastal environments, so turbulence is most important. Other factors that affect the flocculation process are:

- Particle size and concentration. Small particles and a large concentration intensify the process, because the distance between the particles is small. Therefore a higher chance of collisions is present.
- Salinity. This will be less important in the Markermeer, because it is a fresh water lake.
- Temperature. A higher temperature enhances the process, because of higher chance of collision.
- Organic material. The presence of organic material in the sediment intensifies the process, because of the binding properties of organic material. The sediment in the Markermeer mud contains a significant amount of organic material, measured in the field campaign (Chapter 4). Due to this organic binding, flocculation can be an important process in the Markermeer as well, although it is a fresh environment.

Figure 3.13 shows an example of a mud floc (taken from the Merwede). Macro flocs can have sizes in the range of 0,1 to 1 mm, miniflocs of order 0,01 to 0,1 mm and individual mud particles are smaller than 0,01 mm. Large flocs, about 1 mm, can have a density of 1 to 10 kg/m³ in excess of the fluid density, while individual particles have a excess density of 1600 kg/m³.

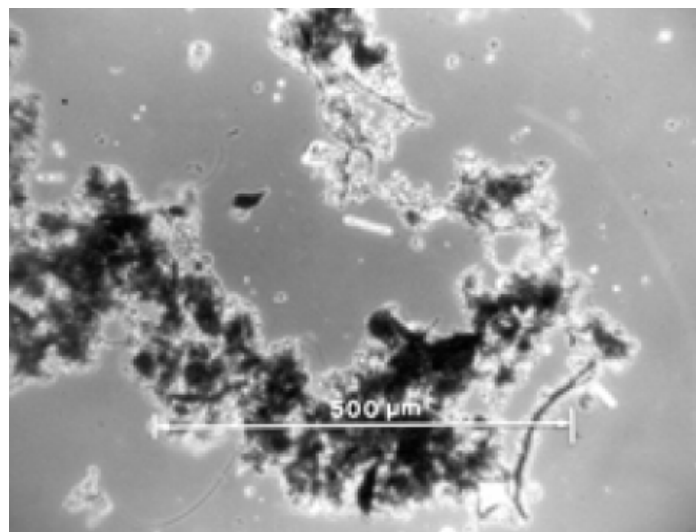


Figure 3.13: Mud floc taken from the Merwede. (Winterwerp, lecture presentation)
A larger mud floc consists of smaller flocs. Flocculation causes an aggregation and break up of flocs.

Present knowledge of the mud in the Markermeer can not give a definite conclusion about the existence of flocculation in the lake. For this reason it is not known if flocculation can occur in the Markermeer and what the influence is on the sediment transport processes.

3.2.4 Deposition and sedimentation

The result of the settling process is deposition and sedimentation of the material on the lake bed. Winterwerp (2004) gives a clear definition of both (different) processes:

- Deposition is defined as the gross flux of cohesive sediment flocs on the lake bed.
- Sedimentation is defined as the net increase in bed level, so the sedimentation rate is the deposition rate minus erosion rate.

Deposition occurs if the bed shear stress is lower than a critical value for deposition, τ_d . Two critical bed shear stresses for deposition can be distinguished, a lower minimum value, $\tau_{d,full}$ and an upper maximum value, $\tau_{d,part}$. The deposition process can be divided into three parts (Van Rijn, 2005):

- **Full deposition.** All particles and flocs are deposited. The bed shear stress τ_b is smaller than the bed shear stress for full deposition, $\tau_b < \tau_{d,full}$. The deposition rate then becomes, $D = c_b w_{s,b}$, with $w_{s,b}$ the settling velocity near the bed and c_b the concentration near the bed.
- **Partial deposition.** Strong, large mud flocs will be deposited, while the small and relative weak flocs will be broken up and stay in suspension. The bed shear stress in this range is $\tau_{d,full} < \tau_b < \tau_{d,part}$.
- **No deposition.** No sediment flocs will be deposited if the bed shear stress is larger than the maximum bed shear stress for deposition, $\tau_b > \tau_{d,part}$. There are no flocs in the water column with a shear strength larger than $\tau_{d,part}$. The deposition rate is zero, $D = 0$.

Typical (experimental) values for $\tau_{d,full}$ are between 0.05 and 0.15 N/m² and for $\tau_{d,part}$ between 1.5 to 2 N/m². For low concentrations (smaller than 0.3 kg/m³) the flocculation effect is less important and all particles will be fully deposited if $\tau_b < \tau_{d,full}$. In this case the classical Partheniades – Krone formula for deposition can be applied,

$$\frac{dh\bar{c}}{dt} = -D = -w_s c_b \left(1 - \frac{\tau_b}{\tau_{d,full}} \right) \quad (3-18)$$

3.2.5 Consolidation and bed strength

Van Rijn (2005) defines the consolidation process as follows: a process of floc compaction under the influence of gravity forces with a simultaneous expulsion of pore water and a gain in strength of the bed material. So, consolidation is a process that only can occur near or in the bed. Three consolidation stages can be distinguished:

- Initial stage (days). Processes of hindered settling and consolidation occur at the same time. Freshly deposited flocs are grouped in an open structure with large pore volumes. The bed surface level sinks linear with time t .
- Secondary stage (weeks). The pore volume is further reduced. Pore water can escape through small drains. The bed surface level sinks with \sqrt{t} or $\log(t)$.
- Final stage (years). Flocs are broken down, pore volume is further reduced.

In Table 3.3 (Van Rijn, 2005) several consolidation stages are shown, each with its corresponding densities (these densities are an indication).

Consolidation of mud layers is affected by:

- Initial thickness of the mud layer.
- Initial concentration of the mud layer.
- Permeability of the mud layer, which is a function of sediment composition, size, organic content, salinity and temperature.

Consolidation will increase the density of the bed material, but also causes an increase of the strength of the bed. This means that a more consolidated bed is less easily eroded and less sediment can be brought in the water column when a storm period takes off again.

Consolidation Stage	Rheological behaviour	Wet sediment density (kg/m ³)	Dry sediment density (kg/m ³)
Freshly consolidated (1 day)	Dilute fluid mud	1000 - 1050	0 - 100
Weakly consolidated (1 week)	Fluid mud (Bingham)	1050 - 1150	100 - 250
Medium consolidated (1 month)	Dense fluid mud (Bingham)	1150 - 1250	250 - 400
Highly consolidated (1 year)	Fluid - solid	1250 - 1350	400 - 550
Stiff mud (10 years)	Solid	1350 - 1400	550 - 650
Hard mud (100 years)	Solid	> 1400	> 650

Table 3.3: Density ranges of consolidated mud for several stages. (Van Rijn, 2005)

The strength of the mud bed can be expressed in the critical bed shear stress for erosion, $\tau_{c,e}$. This parameter depends on bed material characteristics, such as mineral composition, organic content, salinity, bed structure, etc. Experimental results show that $\tau_{c,e}$ is strongly dependent on the deposition and consolidation history. Due to consolidation, the density of the bed increases in time (Table 3.3). The critical erosion shear stress is related to the sediment concentration (dry density). Typical values for $\tau_{c,e}$ are given by Van Rijn (2005) for example for the Ketelmeer (a border lake of the IJsselmeer, close to the Markermeer), depending on the sediment concentration (dry bed density). Values are shown in Table 3.4.

	$c = 100 \text{ kg/m}^3$	$c = 150 \text{ kg/m}^3$	$c = 200 \text{ kg/m}^3$	$c = 300 \text{ kg/m}^3$
Ketelmeer $\tau_e \text{ (N/m}^2\text{)}$	0.10 - 0.20	0.20 - 0.25	0.25 - 0.35	0.50 - 0.70

Table 3.4: Critical shear stress for erosion in the Ketelmeer. (Van Rijn, 2005)

3.3 Morphological processes

3.3.1 Literature

In literature there is information available from early studies on the large scale (Markermeer scale) morphology and mud behaviour in the lake, but it is based on some assumptions and uncertainties. In general the behaviour can be split up in a long term part (erosion and sedimentation) and short term part (exchange of mud between water column and bed) according to Royal Haskoning (2006). The whole process is summarized in Figure 3.14 and is described in Royal Haskoning (2006). Next paragraphs are taken from that report.

Long term

The long term morphological behaviour is mainly characterized by net erosion on the west side of the lake and net sedimentation on the east side. The sediment transport process is mainly driven by a combination of wind, waves and currents. The west side of the lake is very shallow. Waves can exert a large shear stress on the bed.

Because of consolidation of the mud layers, the bed has a certain strength. Erosion only occurs if the wind speed is 5 Beaufort or higher. The erosion flux is small, about 7 kg/m² per year (total net erosion and sedimentation about 1.2 Mton per year), and so the effect on the total sediment concentration in the water column will be limited. The erosion speed on the west side will decrease during the coming decades, because of two effects. First is the consolidation of the sediment layers. Due to consolidation the mud layers will increase in strength; the critical erosion shear stress will increase. The other effect is caused by the erosion itself. Due to erosion the water depth will increase and consequently the wave impact on the bed will decrease. However the net erosion is only estimated at 1 cm/year, so this process will last for decades.

This erosion flux is not based on measurement data, but is estimated with rough values of the wave height and flow velocities, for example data from Table 3.1 and 3.2. For this reason, also the erosion fluxes are rough estimates. Detailed research should be carried out to determine the exact erosion locations and erosion fluxes.

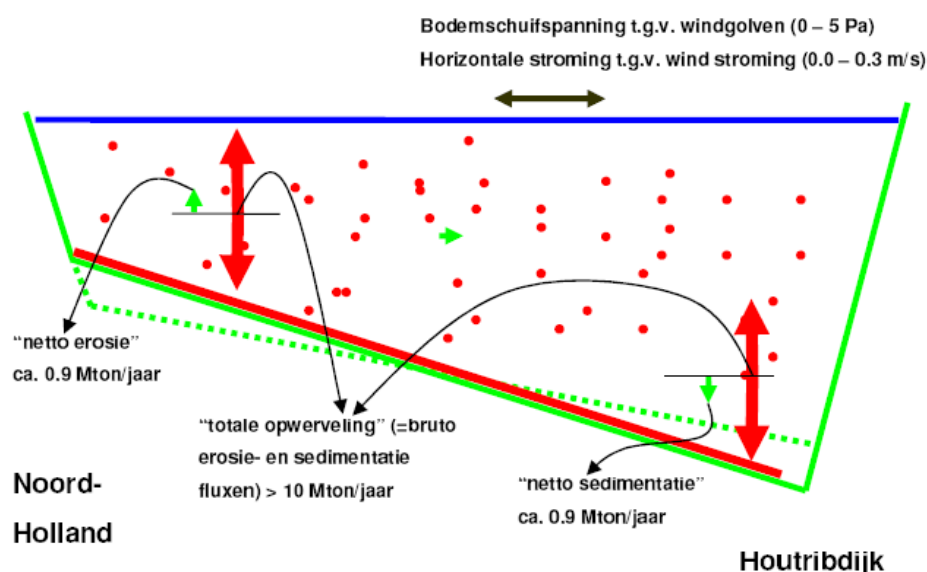


Figure 3.14: Large scale morphological behaviour of mud, conceptual model. (Royal Haskoning, 2006)
 The west side of the lake is an erosion area (net flux 0.9 Mton/year). The east side is a sedimentation area (net flux also 0.9 Mton/year).

Short term

The short term morphological processes in the lake are dominated by the behaviour of the fluffy layer (Section 2.4). This layer is rapidly eroded during the beginning of the storm periods, resulting in a sediment concentration of about 100 mg/l in the water column and will settle after storms. The concentration will in that case drop till 10 – 50 mg/l.

The layer is present almost in the entire area of the lake and resuspension will already occur at low wind speeds, at Beaufort 3. The sediment concentration is dominated by the erosion and sedimentation of this fluffy layer. The gross erosion/sedimentation flux is estimated at 70 kg/m² per year. Because of this rapid resuspension the sediment concentration in the water column is high during large periods of time. For this reason the fluffy layer is one of the main causes of the turbidity problem in the lake.

Unfortunately there are some important uncertainties about this fluffy layer. Especially the amount of the organic mud component in the fluffy layer is not known. This organic component can have influence on for example the erosion, deposition, settling and consolidation of the fluffy layer.

Also the thickness of this fluffy layer across the lake is not known. Measurements are carried out to obtain information about this layer. Results of these measurements are given in Chapter 4.

Mud balance

A total overview of the main mud transports in the lake is obtained from a mud balance. The mud balance of the Markermeer can be written as:

$$\text{Import} - \text{Export} + \text{Sources (erosion)} - \text{Sinks (accumulation/sedimentation)} = 0$$

Biological effects are neglected in this balance. This mud balance is coupled with the water balance. Water is flowing in and out of the lake. The water contains suspended mud sediment. For this reason these discharges of water change the mud balance. The four parts can be estimated (Royal Haskoning, 2006):

- *Import*: total import of water is 1.4 billion m³ per year (Section 2.3) with an average concentration of 20 mg/l. This results in 30 kton per year supply of sediment.
- *Export*: total export 1.1 billion m³ per year with an average concentration of 30 mg/l. This also results in 30 kton per year. The import - export part is in balance.
- *Sources*: Royal Haskoning (2006) estimates the total production (erosion) of sediment about 900 kton per year. This is in the same order as the estimated erosion of 1.2 Million m³ per year by Witteveen & Bos (2004a). Comparing to the import and export part of the balance, it can be concluded that the erosion source is dominant.
- *Accumulation*: Accumulation is in this case the same as sedimentation and is estimated by

$$A = w_s c, \text{ with } w_s = \text{fall velocity (m/s)}, C = \text{concentration (g/l)} \quad (3-19)$$

According to Van Duin (1992) this flux is estimated at 126 kg/m²/year ($w_s = 0.1$ mm/s and $c = 40$ g/l), which results in a mud layer of 0.5 m/year.

Overall it is assumed that the net sediment balance is zero.

3.3.2 Conceptual model of bed composition of the Markermeer

To understand the mud behaviour in the Markermeer it is necessary to know the sediment composition of the bed. In Chapter 2 and the previous sections attention is paid to the bed composition. However a clear picture is not given. For that reason this section will give a kind of summary about the bed composition. The total schematic picture is shown in Figure 3.15.

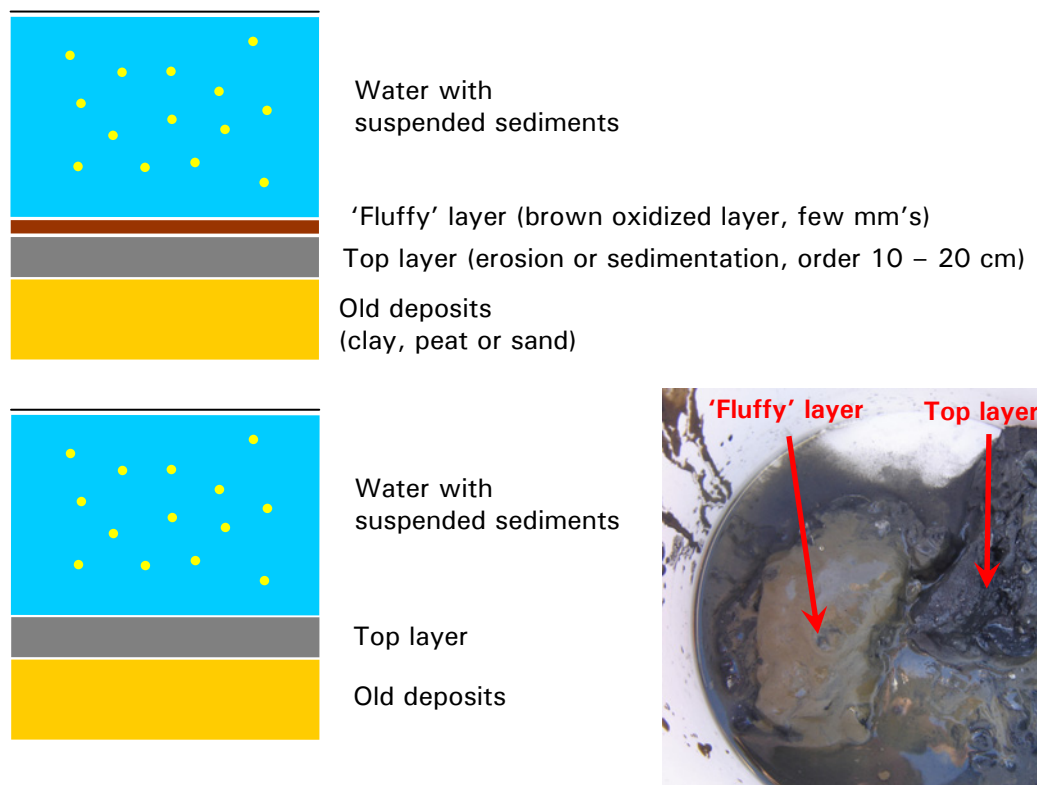


Figure 3.15: Conceptual lay out of the bed in the Markermeer
 The bed consists of a layer (grey) on top of old deposits (yellow). At some locations a fluffy layer (brown) is present. This layer is a few mm's thick. In the picture right the fluffy layer (brown layer) and top layer (grey) are also shown.

Concerning the fluffy layer, in general there are two possible situations in bed composition. Situation one is with a small brown 'fluffy' layer on top of the bed and situation two is without this fluffy layer. Both situations are shown in Figure 3.15.

This fluffy layer is a very mobile layer. It can be resuspended into the water column during already moderate conditions (Wind Bft 3 or higher). If this fluffy layer is suspended it is transported according to the wind driven circulation. This fine material will only settle if turbulence intensity is decreased a lot. Because of this dynamic behaviour, the locations of where this layer is present can vary in space and time. At a certain moment in time a fluffy layer can be present at a specific location, but some time later the situation can be completely different.

The oldest deposits are found in the deepest part of the bed. The composition of these old layers is shown in Figure 2.4.

On top of these old deposits a layer of some softer material is deposited. In the eastern part of the lake this layer contains the IJsselmeer deposit (Figures 2.6 and 2.7). During storm periods this layer can (partly) erode. This erosion will increase the amount of suspended sediment. Consequently this will give higher sediment concentrations in the water column (especially near the bed).

This soft mud layer consists of coarser material than the 'fluffy' layer. The water content and organic content are lower, for this reason this layer is not brown (oxidized), but grey, (Figure 3.15). The strength of this layer is higher, because this layer is (partly) consolidated. This layer is only eroded during storm periods.

4 Field Measurements

This chapter describes the field measurement campaign at the Markermeer, which is carried out in autumn of 2007. The campaign is set up in cooperation with WL Delft Hydraulics and IHE Delft (institute for water education). Both organizations are working at the Markermeer project.

Delft Hydraulics developed a Delft3D model of the Markermeer for the analysis of several solutions for the turbidity problem (Section 1.1 and WL Delft Hydraulics 2007a). To improve this model, good quality data is needed. At two locations in the lake, measurement poles were installed to collect this data. These are the measurement poles FL 41 (near Marken) and FL 42 (middle of the lake). At these locations several parameters are measured with a frequency of every 10 minutes: wave heights, current velocities, turbidity, chlorophyll and phosphorus. Also some bed samples are taken at both locations for physical analysis. To carry out proper calibration of the model, data of two locations in the lake is insufficient. For this reason a measurement campaign was set up to collect spatial distributed data.

In this campaign students from IHE cooperated with Delft Hydraulics. Their focus was on collecting data of ecological parameters of the water column and the bed. This data will be used in the development of the ecological model of the Markermeer.

For this MSc study specific measurements were needed to assess if the sediment in the Markermeer can behave as a density current (second main question in this study, Section 1.3). These special measurements are added to the campaign.

The two objectives of the measurement campaign were:

1. To collect spatially distributed data about the bed and water column characteristics of the Markermeer. This data is used as input and calibration data for the WL model of the Markermeer and the ecological model of IHE students. Parameters which are measured at each location are: grain size distribution, turbidity, chlorophyll, phosphorus, nutrients, pH, conductivity, temperature and organic content (both from water column as bed samples).
2. To collect data to assess if the sediment in the Markermeer can behave like a density current near the bed. For this objective special measurements are carried out, which will be described in this chapter. All these measurements will focus on the sediment concentration close to the bed and the occurrence of a soft mud layer in the bed. Density currents can occur if a high sediment concentration layer or soft mud layer is present near the bed, causing an increase in mixture density. If there is a density difference between locations, a density current is generated. The occurrence of a high concentration layer can be an indication for the existence of density currents. For this reason the measurements focus on the concentration near the bed. These measurements are special, because similar measurements were not carried out before. The results will give new insight in the sediment behaviour close to the Markermeer bed. A detailed description of each measurement type is given in the different sections.

4.1 Spatially distributed sediment and water column data

To collect spatially distributed sediment and water column data (objective 1) in total 71 measurement locations are visited during 5 days in the end of November 2007. The locations were spread all over the lake and are plotted (each measurement day separately) in Figure 4.1.

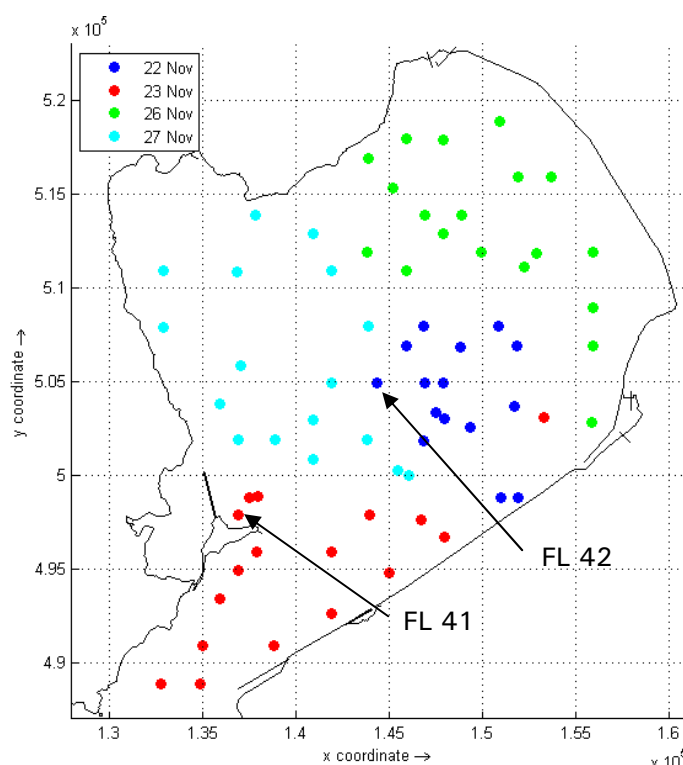


Figure 4.1: Measurement locations of the field campaign, separated for each measurement day. The locations of the measurement poles (FL 41 and FL42) are shown in the figure.

On every location at least one disturbed bed sample is taken with a Van Veen Grab (Figure 4.2). Also a Conductivity/Temperature/Depth (CTD), Turbidity (with an Optical Back Scatter, OBS) and chlorophyll measurement of the water column is carried out (Figure 4.3). The bed samples are taken with a Van Veen Grab, because by using this device the samples can be taken quickly to get a good total overview of the bed characteristics of the lake. The samples are analyzed at IHE.



Figure 4.2: Van Veen Grab.
Used for taking bed samples.



Figure 4.3: CTD, OBS and Chlorophyll sensors.
Used for water column measurements.

For this study the results of the OBS measurements are used. These measurements give information about the sediment concentration profile. More information about the OBS measurements is given in Section 4.1.2.

4.1.1 Fluffy layer

During the execution of the campaign the bed samples, taken with the Van Veen Grab, gave a quick indication of the sediment type of the upper layer of the bed. Especially the presence of the fluffy layer on every measurement location is determined quickly. The fluffy layer is defined as the brown mud layer, shown in Figure 4.4. This layer is very thin and the water content is high. This layer is mentioned in Section 3.3.2.

In earlier studies this layer was also noticed. For example in Chapter 2 it is mentioned that Van Duin (1992) found a thin layer of oxic mud over the entire surface of the lake. This layer can also be considered as the fluffy layer.

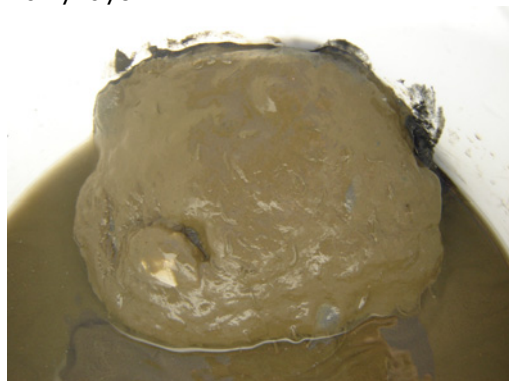


Figure 4.4: Brown fluffy layer (few mm's thick) on top of the grey mud layer.

The water content in this layer is higher than in the more grey mud layers beneath and the strength is less.

During the field campaign the fluffy layer was found at 52 measurement locations out of 71 in total (Figure 4.5).

In contradiction to the results of Van Duin (1992) this layer is not present all over the lake. Especially on the west shore (erosion area, Royal Haskoning, 2006) no fluffy layer exists. Also near the 'Enkhuizen Zand' in the north, this thin layer is not found during the campaign. However these results should be interpreted carefully. This fluffy layer is very mobile and after a period with stronger winds, the situation can be completely different.

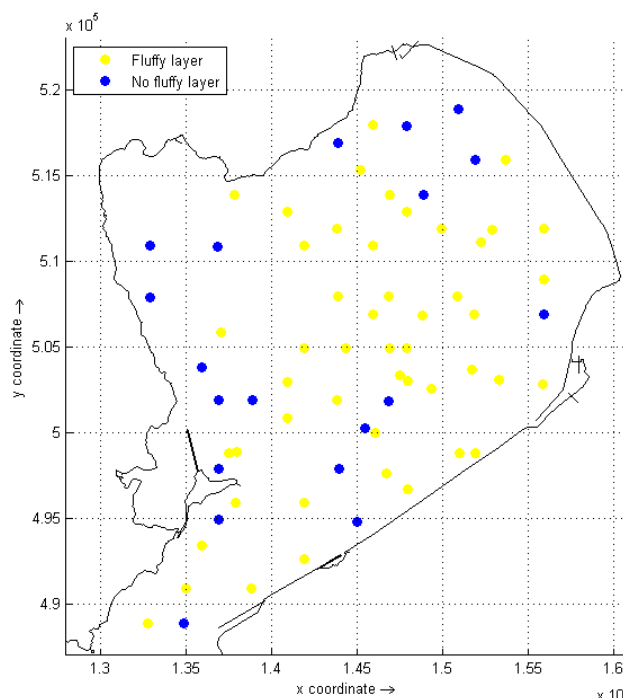


Figure 4.5: Locations where the fluffy layer is found (yellow) and where not (blue).

4.1.2 Turbidity

On every measurement location a vertical profile of the turbidity is recorded with an Optical Back Scatter (OBS). When the measurement ship was located steady on the measurement location, the OBS was put in the water, was slowly lowered to the lake bed and slowly pulled back. An OBS sends light into the water column. This light is scattered due to the presence of sediment particles and will reflect back to the OBS. The backscatter is recorded by the device. Because the scatter is a function of particle size, particle structure and sediment concentration, this backscatter can be translated into sediment concentration (if one assumes that the particle size and structure do not change). To do this translation calibration measurements are needed.

In the week before the measurement campaign the optical backscatter is calibrated to Normal Turbidity Units (NTU), so the output of the signal of the device is NTU. In theory there is a linear relationship between NTU and sediment concentration in the water.

This relation is however specific for each area. Considering the Markermeer as one area, one calibration relation is determined for the whole lake. Several calibration samples spread over the lake are taken. In total 9 samples are collected (with a range between 20 and 120 NTU) and analyzed. The results are given in appendix A-1. For this Markermeer area the linear relation between NTU and sediment concentration is,

$$[\text{mg/l}] = 0.9212 \times [\text{NTU}] \quad (4-1)$$

According to this relation every depth profile of turbidity is translated to sediment concentration profiles.

During the recording of the turbidity profile over the vertical, the OBS measured with a frequency of one measurement per 3 seconds. This results in a vertical resolution of one measurement per 10-20 cm, depending on the vertical speed of the sensor. This speed varied, because it was pulled in and out by man. Over the vertical about 20 turbidity points are recorded. Final sediment concentration profiles as shown in Figure A.2 and A.3 in appendix A are obtained.

The profiles in the appendix are split up in uniform and non uniform profiles. In the figures also the bed level is indicated by the black/brown line. These data is taken from the echo sounding measurements. Two typical profiles (one uniform, one non uniform) are also shown in Figure 4.6.

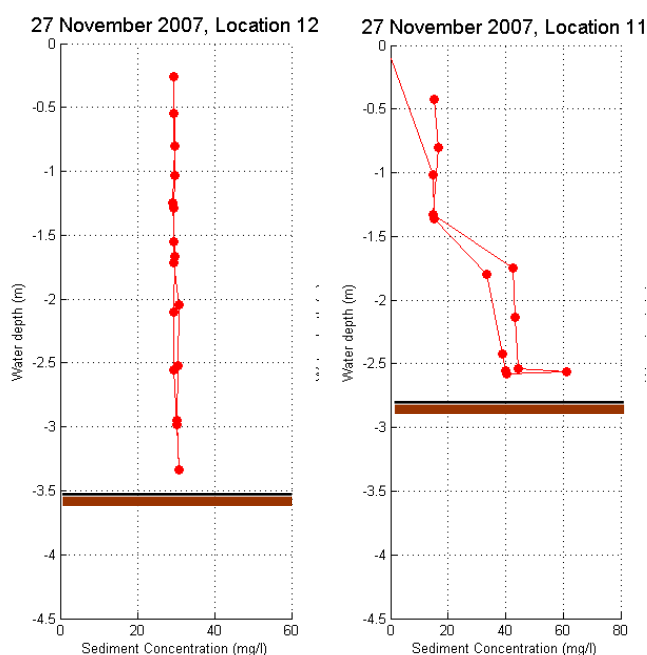


Figure 4.6: Sediment concentration profiles measured by the OBS sensor, uniform and non uniform.

Van Duin (1992) stated that the sediment concentration is uniformly distributed over the vertical and therefore a 2D model can be applied. The first four profiles in the appendix show that well mixed conditions occur, but the last four profiles do not support Van Duin's findings; they reveal a non uniform profile with higher concentrations near the bed. This is an indication that 3D modelling should be applied for detailed processes. These profiles are found especially during or after rough weather conditions. These profiles also support the idea that the sediment can behave like a density current (objective 2 of the campaign), because of the higher sediment concentration near the bed.

Some other interesting things can be found in the calibration sample data (Table A.1). Royal Haskoning (2006) stated that it was not clear what the amount of organic cohesive sediment is in the Markermeer and what influence

this organic component has on the sediment behaviour. Early mud models of the Markermeer are based on inorganic material, for example the WL model (WL Delft Hydraulics, 2007a). The calibration data (Table A.1) shows that the amount of organic material can be significant in the water column, up to 60 % in mass. For proper modelling of the sediment behaviour in the lake, the organic material should be included in the model. For this study it is however neglected, because of the uncertainty of the characteristics and the complication it will give for the modelling of the silt trap.

4.2 Echo sounding

4.2.1 Description and objective

Echosounding techniques are commonly used techniques in nautical surveys for determining the water depth or bed profile. The basic concept of an echosounder is to send a sound wave to the lake bed. This wave will be reflected on the bed and the returning wave is recorded by the echo sounder.

The time between transmitting the wave and recording the reflected wave is measured. The water depth is determined by dividing this time by the propagation speed of sound in the water. This propagation speed is dependent on the temperature, salinity and water depth.

The sound waves, produced by the echo sounder, can have different frequencies and each type of frequency will reflect on a different density gradient on the bed. The high frequency

wave reflects on the transition between water and low density layer (top layer, soft mud), a small density gradient. The low frequency reflects on the transition between the low density layer (soft mud) and high density layer (consolidated bed), a large density gradient. Low frequency echo sounders will therefore record a larger water depth than high frequency echo sounders. The low frequency wave penetrates through the soft mud layer (top layer). This property is used in this measurement campaign. The top layer measured by the echo sounder can be considered as the top layer defined in Section 3.3.2.

The objective in this type of measurement is to determine if soft mud layers exist in the bed of the Markermeer and to measure their thickness. If a soft mud layer near the bed exists, this can be an indication that the sediment can behave like a density current. For this measurement type a dual frequency echo sounder (33 kHz and 210 kHz) is used simultaneously. By subtracting the two depth values of both echo sounders the thickness of the soft mud layer is determined. On every measurement location (Figure 4.1) this measurement is carried out. Finally a spatial pattern of the thickness of the soft layer is obtained.

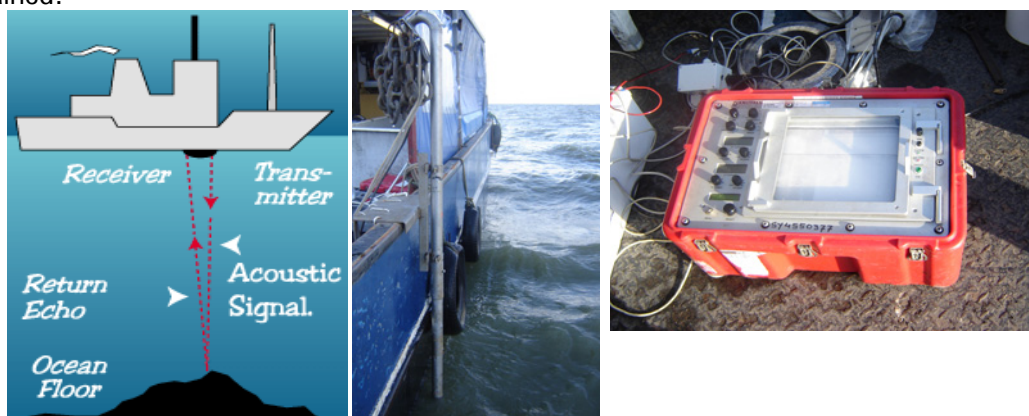


Figure 4.7: Principle of the working of an echo sounder (left) and the transducer in practice (right).

On every location the echo sounder recorded for about 10 to 20 seconds, resulting in 200 water depths records per location. Figure 4.8 shows a record of water depths at one location. The red line shows the water depth of the high frequency echo sounder, the blue line the low frequency. On the x axis the measurement number is plotted, in total about 200 per location.

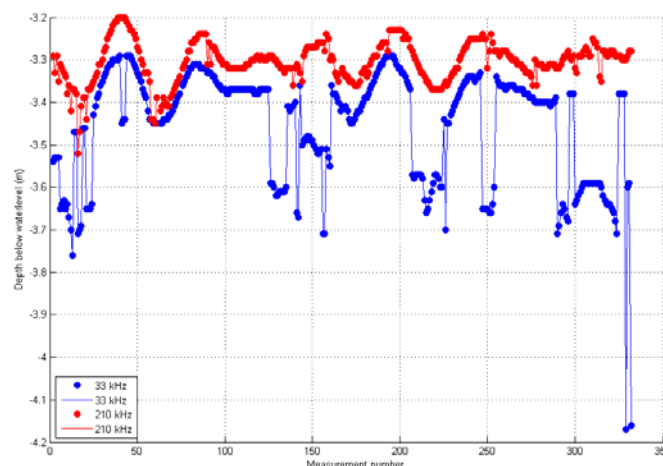
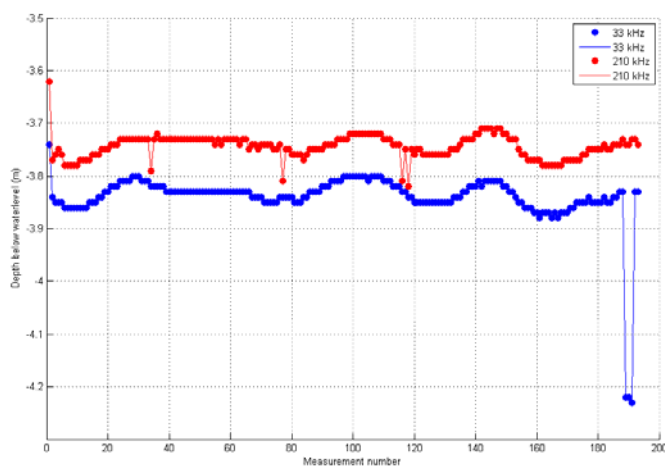


Figure 4.8: Echo sounder data, location 12 on 26th of November. **Figure 4.9:** Location 14 on 23th of November. Red line is HF, blue line LF echo sounder. Difference between both lines is the thickness of the mud layer.

Unfortunately there is small and large scatter in the data. Figure 4.8 shows small waves in the data. These waves are a result of the movement of the ship. Despite of these scatter a difference between both echo sounder types is measured. This difference is the thickness of the soft mud layer, about 10 cm in Figure 4.8.

Figure 4.9 shows large fluctuations and outlier data points (for example the last 2 points in Figure 4.9 are outliers). These outliers are removed from the datasets if the difference with the 'average' data points is more than about 30 - 40 cm.

After this removal of outlier data points the mean water depth of both echo sounder types is calculated. Subtracting these two water depths, the mean thickness of the soft mud layer is obtained. Also the standard deviation (σ) of this thickness is computed by,

$$\sigma = \sqrt{\frac{1}{n-1} \sum_{i=1}^n (d_i - \bar{d})^2} \quad , \text{with mean thickness value } \bar{d} = \frac{1}{n} \sum_{i=1}^n d_i \quad (4-2)$$

d is the thickness of the soft layer (m) as a result of both echo sounder measurements, n is the number of measurements at one location. All results are given in appendix A-2, Table A.2.

4.2.2 Results

On every location the mean water depth of both echo sounders is calculated, as well as the mean thickness of the soft layer and the standard deviation (Table A.2). The average mean thickness of the soft mud layer of all points is about 10 cm. In Figure A.4 the thickness of the mud layer in each location is plotted in the Markermeer map. Interpolation between the points is carried out with a cubic spline interpolation. This results in an indicative picture of the thickness of the soft mud layer across the lake. This figure should be interpreted carefully, because some regions cover insufficient data points, which yields poor interpolation results. Overall can be concluded that the thickness of the layer is larger in the south of the lake (close to Flevoland), about 15 cm and less in the middle (about 5 cm).

This overall picture shows a good agreement with the location of the IJsselmeer deposit layer (Figures 2.6 and 2.7). This layer is also present at the southeast part of the lake and is located at the top of the bed. Apparently this layer consists of soft mud and is recorded by the echo sounder. However a real evidence of a correspondence between these measurements and the location of the IJsselmeer deposits is absent.

In Figure 4.10 a histogram of the data is shown. On the x axis the thickness of the soft mud layer is plotted. The number of measurements in each thickness bin is plotted on the y axis. The modus of the thickness is about 8 to 10 cm. Even layers with a thickness of 30 cm are measured.

An important conclusion is that the soft mud layer exists all over the lake (even if it has no uniform thickness). According to this conclusion a density current near the bed of the lake can occur. Nevertheless, the density of the soft mud layer is not known and can not be determined with this data. Future measurements should be carried out to determine this density.

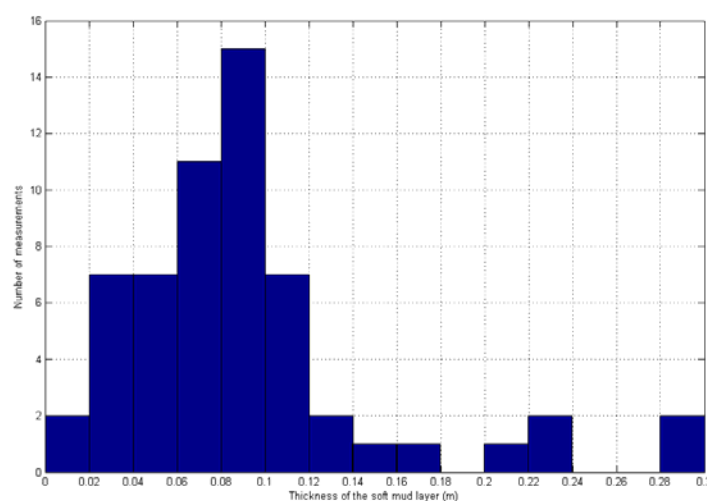


Figure 4.10: Histogram of the thickness of the soft mud layer. The modus of the measurements is 8 – 10 cm. The maximum thickness which is measured is about 30 cm.

4.3 Cesium measurements

4.3.1 Description and objective

To assess the behaviour of sediment around a silt trap, it will be helpful to know the sedimentation rate inside and outside historical pits. In the Markermeer two pilot pits are dredged in the early 1980's (Proefput A and Proefput B, locations shown in Figure 4.14).

If the sedimentation rate inside a deep pit is a lot higher than the net sedimentation rate in the neighbouring shallower parts of the lake, other processes than only settling from the water column occur in a deep pit. The difference in sedimentation rate can be explained by the density current effect.

The objective of this part of the measurements is to determine the sedimentation rate on different locations in the lake, especially in the two historical deep pits. These pits are almost filled up completely over the last 20 years. A higher sedimentation rate inside these pits than outside, can be an indication of the existence of density currents.

Sedimentation rates can be determined by Cesium measurements of cores of bed material. This technique is used in this study, in cooperation with Medusa Explorations BV in Groningen. The principle of Cesium distribution and the age of sediment is explained in the part below (text taken from Medusa):

The isotope ^{137}Cs is a radioactive element which is brought into the environment during nuclear tests in the years '50/'60 and during the Chernobyl accident in 1986. Due to the binding capacity of the clay parts in the mud, cesium is bound to mud particles and can not be brought in the water due to the strong binding force. Mud sediments can be produced by different sources: erosion of old peat layers, algae growth and resuspension of mud. Sediments that are produced after 1986 from erosion of peat layers or algae growth do not contain cesium. Also sediments produced before 1945 (start of nuclear tests) do not contain cesium. Sediments from 1945 to 1986 do.

In an ideal situation with constant sedimentation and no distortion of the bed a sediment core will contain two peaks in cesium content, shown in Figure 4.11.

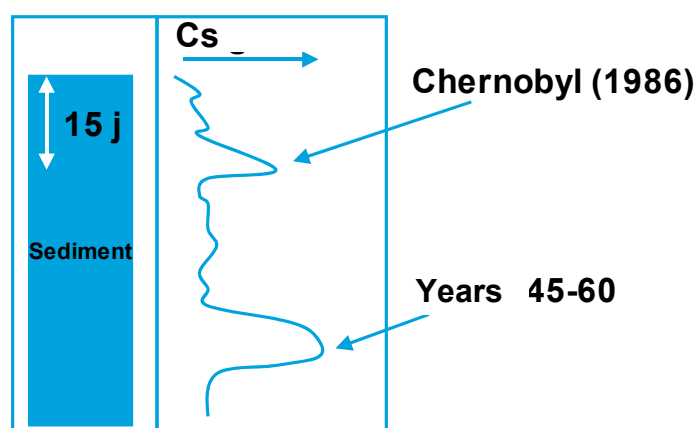


Figure 4.11: Schematic distribution of Cesium in a core.
The sedimentation rate is determined by the depth of the 86 layer divided by about 20 years.



Figure 4.12: Beeker sampler and core in practice.

During the measurement campaign at the Markermeer sediment cores are taken with a Beeker sampler (Figure 4.12). These cores are split up into vertical parts and for each part the cesium content is measured. A peak in cesium content indicates the Chernobyl layer. The sedimentation rate is calculated by dividing the depth of the Chernobyl layer in the core by time expired after 1986.

The beeker sampler can take cores with a maximum length of 1 m with a diameter of 7 cm. The minimum amount of sediment for a cesium measurement is 300 ml material. For this reason the cores are split up into part of about 20 – 25 cm length.

The vertical resolution of the cesium profile is consequently also 20 – 25 cm. This means that a detailed profile, such as shown in Figure 4.11, is not obtained. The cesium profile will be more discontinuous and the Chernobyl layer will be represented by one layer of 25 cm thick. A typical cesium profile is shown in Figure 4.13.

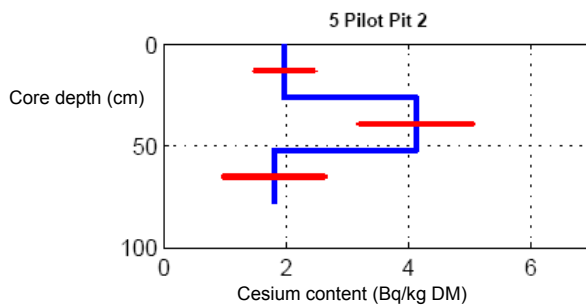


Figure 4.13: Typical cesium profile.
86' layer is located between 25 – 50 cm.

At ten locations in the lake, cores are taken for cesium analysis (Figure 4.14). Two cores are taken inside the historical tests pits (number 2 and 7), one near the measurement pole FL42 (number 1) and others on both sides of the lake. The measurements in the lab are carried out by a 'Nal detector' at Medusa Explorations. The wet samples are put in a Marinellibeaker. The total activity of the nuclides is determined by a full spectrum deconvolution of the signal. The activity concentrations are computed by dividing by the mass of the sample and the dry material percentage. This percentage is measured by the loss in weight of the sample in 6 hours at a temperature of 130 °C. Besides the measurement of cesium, also kalium, uranium and thorium contents are determined. This is because of the strong binding of cesium to mineral parts (uranium and thorium are found in mineral sediments). The content of cesium is corrected by dividing by the concentration of both elements.

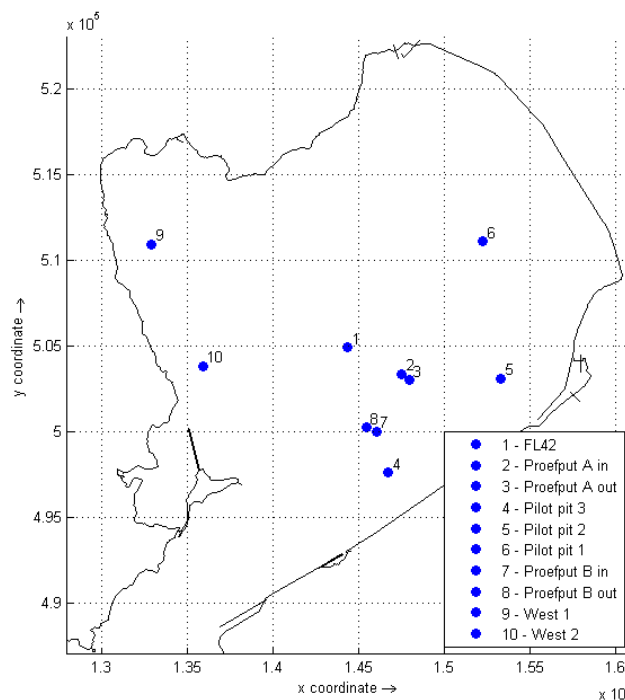


Figure 4.14: Locations where Beeker samples have been taken during the campaign. 2 and 7 illustrate the location of the former pilot pits. Number 1 is the measurement pole FL 42.

The results of the measurements are given in the Table A.3 and Figure A.6 in appendix A-3. In the table also the mud percentage is given. This percentage can be estimated using the amount of thorium. Sand has a Th value of 5 Bq/kg DM and Clay 45 Bq/kg DM. The mud percentage is calculated by,

$$mud\% = \frac{Th - 5}{45 - 5} \quad (4-3)$$

4.3.2 Results

In appendix A Figure A.6 the cesium profiles of each measurement location are shown. One important result can be obtained from the cesium profiles. The cores taken inside the former pits A and B contain much more cesium per kg dry material than all the others. Theoretically cesium can bind easier to fine material. For this reason the high cesium content in the cores inside the former pits indicates that fine sediment can accumulate in deep pits.

Field observations (bed samples taken by the Van Veen Grab) also reveal finer sediments and higher water contents in the top layer inside the former pits. Unfortunately no conclusion can be drawn about the sedimentation rate inside the pits, because no clear Chernobyl layer can be found in both cores. But the fact that fine sediment can accumulate inside the pit is an important conclusion. Which process causes this accumulation (settling or density current) can not be determined with this data.

In other places around the lake this Chernobyl layer is found. For example at 'Pilot Pit 2' (Figure 4.13) and 'West 1' a higher concentration is found at a depth of 25 – 50 cm in the bed. This is the 1986 layer, so all the sediment above is accumulated in the 22 years after it. This is an average net sedimentation rate of about 1.1 cm per year. Remarkable is that this Chernobyl layer is found at the top layer just outside the both pits ('Proefput A out' and 'Proefput B out'). Due to this it can be concluded that no net sedimentation will occur in the neighbouring of deep pits, probably because of sediment attraction of the pits. Sediment near the bed will flow in the pit and will not settle at the shallower parts close by. This mechanism can be caused by density currents near the bed. However this is only a hypothesis.

According to the data, no clear sedimentation or erosion area in the Markermeer can be pointed out. Early studies stated that the western shore of the lake is an erosion area and the eastern shore is a sedimentation area (Royal Haskoning and WL Delft Hydraulics, 2006). This hypothesis can not be rejected or confirmed by this data.

4.4 Argus Surface Monitor (ASM)

4.4.1 Description and objective

To assess if the sediment in the Markermeer can behave like a density current near the bed it is necessary to determine the sediment concentrations near the bed. Especially the behaviour during several weather conditions is interesting. The sediment concentration was already measured during the campaign, using an OBS device (Section 4.1.2). However this data are not sufficient enough for several reasons:

- Turbidity measurements (OBS) are carried out from a ship during the measurement campaign. Sediment concentrations during extreme conditions, like heavy storms, are not measured, because in such conditions it is not possible to sail out with the ship. Sediment concentrations during storms are important for understanding the behaviour of the mud. During these periods the sediment concentration and sediment transport can become high.
- The vertical resolution of the OBS measurements is too low. Especially the sediment concentration near the bed is important for the generation of density currents. The OBS sensor measured some sediment concentrations near the bed, but only one or two data points per location.
- The time resolution of the OBS measurements is too high. The sediment concentrations measured by the OBS are measured at one location at only one moment of time. Data about the dynamic behaviour of the concentration layer near the bed at one location will be useful.

For this reasons supplementary measurements are carried out after the campaign, using an Argus Surface Monitor (Figure 4.15). This device can measure sediment concentrations near the bed (up to 1 m above), with a vertical resolution of 1 cm and can be installed in the bed for measuring continuously for weeks. The principle is the same as an OBS, but with a high resolution.

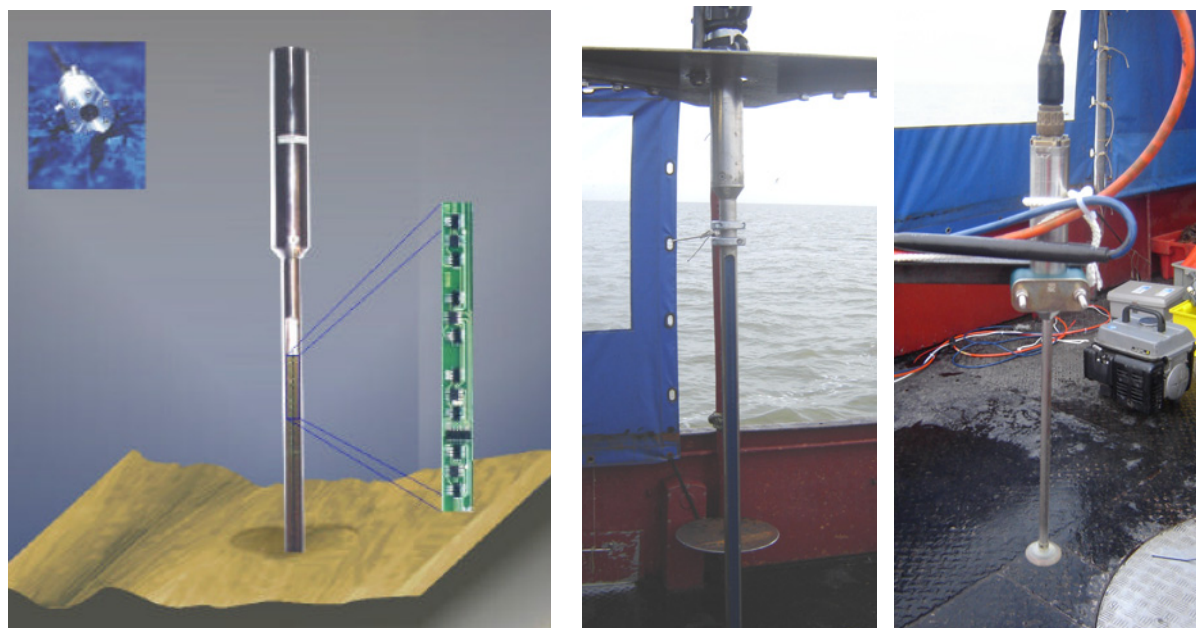


Figure 4.15: Argus Surface Monitor, schematic (left), in reality (mid) and EMC (right).

In the lowest 1 m of the device several OBS sensors are measuring turbidity with a vertical resolution of 1 cm and a time resolution of 10 min. The output value is reflectivity: the amount of infrared laser light which is reflected by the sediment in the water. This reflectivity value can be translated to sediment concentration using the same calibration principle as the OBS. Mud concentrations from 5 to 5000 mg/l can be measured with an accuracy of 10 %. In the upper part of the device (thicker part) temperature, water depth (pressure) and inclination are recorded simultaneously.

The ASM is placed at the Markermeer bed (using a steel frame for support) near measurement pole FL42 (10 m to the south west of it) for the period 4/12/2007 12:00 to 18/12/2007 10:30. At the steel frame, also an EMC (Electromagnetic Current Meter) is installed (about 25 cm above the bed) to measure flow velocities at that height above the bed. Wave heights are recorded at the pole FL42. So the total hydraulic conditions are measured during the period.

The wind characteristics during the measurement period are recorded at location Berkhout. Every 10 minutes, wind speed and wind direction were recorded. The results are shown in Figures A.14 and A.15 in appendix A. These hydrodynamic conditions and wind data are important for interpretation of the ASM data.

The objective of this part of the measurements is clear: to give insight in the sediment concentration profile near the bed during several conditions, to assess if a density current can occur.

Calibration of the ASM is carried out after the measurement period in the laboratory. Original Markermeer sediment is used for the preparation of the calibration mixtures. The sediment is taken from the Markermeer from the brown fluffy layer and stored in the refrigerator. In total 9 calibration measurements are carried out inside a bucket. Reflectivity values are taken from the lowest 6 measurement sensors of the ASM, because these sensors are most reliable (not influenced by light from outside). During the measurement a water-sediment sample is taken (200 ml) and analyzed on grain size and sediment concentration. Results are shown in Table A.4 in appendix A-4. The last two samples are omitted, because these samples are outside the measurement range of the ASM and are not reliable for this reason. Although there is some large scatter in the data, a linear relation between reflectivity and sediment concentration can be found, according to the following equation,

$$[\text{mg/l}] = 1.8153 \times [\text{Reflectivity}] \quad (4-4)$$

This conversion formula is used by the analysis of the output of the ASM.

4.4.2 Results

In appendix A-4 Figures A.8 till A.13 results of the ASM measurements are shown for several moments of time. Each figure consists of two subplots. The first plot shows the sediment concentration (x axis) from 0 to 100 cm above the bed (y axis) for a specific moment in time. The second plot shows the zero order moment wave height (H_{m0} , y axis) during the measurement period. The thick black line indicates the time of which the concentration profile (of plot one) is measured. The wave height at that time can be determined in that plot. Also the current velocity (measured by the EMC) at that specific time is given (in mm/s). The vector is in the net current direction.

In the first subplot also a theoretical profile is fitted through the data, to determine if the measurements can be described according to a theoretical model.

The theoretical model of the sediment concentration profile (green line) is taken from Winterwerp (2004). The basis is an advection-diffusion equation for the vertical (1D), where horizontal gradients are neglected,

$$\frac{\partial c}{\partial t} - \frac{\partial}{\partial z}(w_s c) - \frac{\partial}{\partial z}\left(\Gamma_T \frac{\partial c}{\partial z}\right) = 0 \quad (4-5)$$

c is the sediment concentration (kg/m^3), w_s the fall velocity (m/s) and Γ_T the eddy diffusivity (m^2/s). This is a simplified model. Other assumptions are:

- The eddy diffusivity is parabolic over the vertical.
- Vertical velocity profile is logarithmic.
- No sediment fluid interaction.
- No complex 3D flow structures.

In the Markermeer situation these assumptions are not completely applicable. For example the velocity profile is not a logarithmic profile; wind effect deforms this profile. However this fit gives an order of magnitude of the different values. The equilibrium solution of equation 4-5 is,

$$\frac{c}{c_a} = \left[\frac{a/h(1-z/h)}{z/h(1-a/h)} \right]^\beta, \text{ with } \beta = \frac{\sigma_T W_s}{\kappa U_*} \quad (4-6)$$

Where c_a is a reference concentration at level a (in this situation a is taken at 20 cm), h is the water depth (m). β is the Rouse number and is used in this situation as a calibration parameter, for each plot the β is fitted. According to the results, it can be concluded that this theoretical profile agrees with the data. An important conclusion about the β number is: the higher the β number, the higher the concentration near the bed (the profile is strongly non uniform). For $\beta \downarrow 0$ the concentration profile becomes a straight line.

In general, during the periods of growing and decreasing wind speeds a strongly non uniform sediment concentration profile can be generated (with β number of 0.28, Figure 4.17), with a thin layer of high concentrations near the bed (up to about 700-800 mg/l). This layer can cause density currents near the bed. This non uniform profile develops if the wave height becomes larger than about 0.5 m. This is shown in Figures A.8 and A.9. In Figure A.8 the wave height is about 0.5 m, but a uniform profile of about 80 mg/l is measured. In Figure A.9 the wave height is increased to 0.6 m and high concentration layer is measured. According to Table 3.2 wave heights of 0.5 m are already developed at wind 4 to 5 Bft, which are moderate conditions. Winds of 4 to 5 Bft. will often occur in the Markermeer area. For this reason it is expected that a high concentration layer near the bed will be generated often.

During calm weather the concentration profile is homogeneous over the vertical and density currents can not be generated. An example is shown in Figure A.13. The concentration is decreased to about 30-40 mg/l, the waves and current velocities are low (wave height is only 0.05 m, current velocity 10 mm/s).

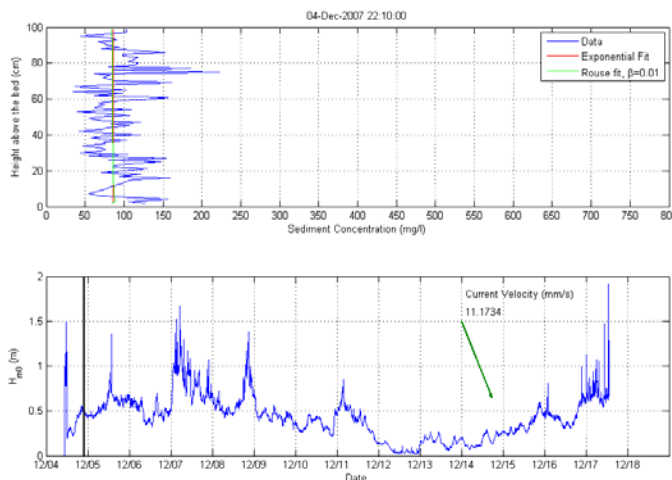


Figure 4.16: ASM result 4th of December 2007 22:10. The wave height is about 0.5 m. The concentration profile is uniform over the vertical.

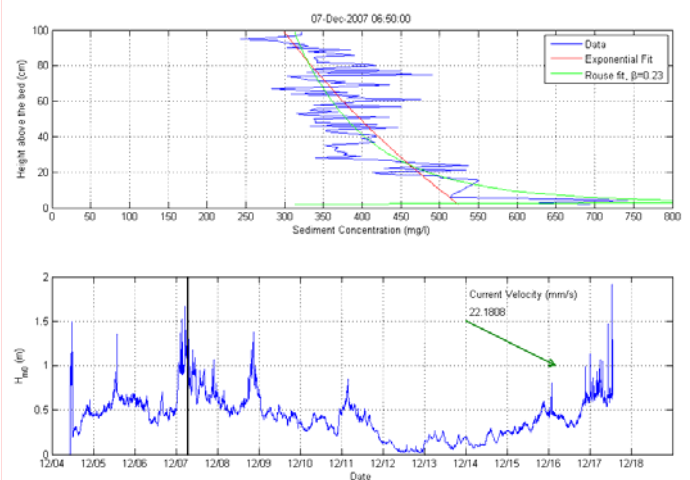


Figure 4.17: ASM result 7th of December 2007 6:50. Wave height is increased to more than 1 m. More sediment is suspended in the water column (concentration about 300 mg/l). The high concentration layer near the bed is increased to about 800 mg/l.

Storm periods are important for the generation of a high concentration layer near the bed. During increasing and decreasing wind forcing, a strong non uniform concentration profile can be build up. The total time of the measurements was about 14 days and during this period 4 storm periods are recorded, at the 3rd, 5th, 7th and 8th (each about 1 day long, Figure A.14). Measuring during this time of the year was useful. During spring and summer, conditions will be less heavy and the possibility of measuring a high sediment concentration layer is less.

4.5 Overall observations

According to all measurements the presence of a layer with higher sediment concentration near the bed exists in the Markermeer. This layer can exist if wind forcing is increased, larger than 4 or 5 Bft. Also a soft mud layer in the bed is recorded by the echo sounder. Important observations are as follows:

The *turbidity measurements* with an OBS give higher concentrations near the bed on several locations. These higher concentrations can be a factor 2 higher in the water column.

Echo sounding measurements indicate that a soft mud layer near the bed exists, with an average thickness of about 10 cm. Such a soft mud layer can behave as a density current. The density of this mud layer is not known, but the presence of the layer is important information.

The results of the *cesium measurements* of this campaign can not give a clear definite answer to the question how a deep pit is filled (by settling or density currents). The mud cores taken inside the pits were not deep enough; no layer with high cesium content (Chernobyl layer) was detected. Nevertheless there are other results which are interesting. Just outside the pits the Chernobyl layer is at the top of the bed. This means that no net sedimentation has occurred in these areas, which can probably be explained by the sediment attraction of the pits. Probably a high sediment concentration layer near the bed flows into the pit and consequently can not accumulate close to the pit. Another important conclusion

is that fine sediment can accumulate in pits. This is indicated by a high cesium content in the sediment cores taken inside former pits.

Measurements with the *Argus Surface Monitor* are in principle the same as the OBS sensor, but with a higher vertical resolution near the bed and a higher time resolution. The sediment concentrations near the bed measured by the ASM are a lot higher (up to about 700-800 mg/l) during times of increasing or decreasing wind speeds in a storm situation. A strong non uniform concentration profile can occur if wave heights are about 0.5 m or higher. The high concentration layer near the bed can cause density currents. During times with low wind speeds, this profile becomes uniform with low values (30-40 mg/l) and no density currents will come into existence.

4.6 Conclusion

The main question of this chapter was:

Can the sediment in the Markermeer behave like a density current near the bed?

To answer this question some specific measurements are carried out, which are described in detail in the text above. According to all measurements it can be concluded that the sediment in the Markermeer can behave like a density current, because a higher sediment concentration layer near the bed is measured.

For this reason the density effect is included in the Markermeer model. Density effects can have a significant influence on the sediment behaviour near the silt trap.

5 Large scale Delft3D model

This chapter considers the large scale Markermeer model of this study. This large scale model is set up to give insight in the mud dynamics of the lake, especially near the bed. On top of that, the large scale model should also give an answer to the question: Can the mud in the Markermeer behave like a density current? This is one of the main questions of this study. The field measurements (Chapter 4) clearly show that this can occur, but the model should confirm these results.

The model is calibrated to the field measurement data (wave height and sediment concentration) and will be used as a reference model for the model of the silt trap. This means that after calibration of the large scale model, the silt trap is implemented and the effects of the trap are determined by using that model. More about the implementation of the silt trap in the model can be found in Chapter 7.

In general, this large scale Markermeer model is based on the Delft3D model of the Markermeer, developed by Deltares (WL Delft Hydraulics at that moment: this model is further referred as WL model). A detailed description of that model is given by WL Delft Hydraulics (2007a) and the model will be shortly discussed in Section 5.1. For this study some adaptations were implemented to the WL model, therefore this chapter starts with a short description of that model. The other sections of this chapter will give information about the set up, calibration and results of the model used in this study.

5.1 Markermeer model WL Delft Hydraulics

As already mentioned in Section 1.1, Deltares is involved in the total Markermeer project. Its main task is to set up a mud model of the Markermeer, based on Delft3D, which can be used as a model to analyze several policy measures in the Markermeer for the turbidity problem. The final goal of the model development is to develop a model that can predict currents, erosion, sedimentation, mud concentration and light extension in relation to the weather conditions.

At the start of this MSc study the WL model was still in an early development phase. The most up to date version (December 2007) is described in WL Delft Hydraulics (2007a). The Markermeer model used in this MSc study is based on this version; for this reason a short introduction to the WL model is given in this section.

The objectives of the WL model, version December 2007, were:

- Optimisation of the computation time.
- Calibration and validation of the model based on existing measurement data.
- Sensitivity analysis on the calibration parameters.
- Simulations with test scenario runs for the turbidity measures.

The model is set up as a coupled FLOW – WAVE (SWAN) model for the hydrodynamic part. The sediment part is modelled with Del-WAQ. Del-WAQ is used because by using this module, ecological processes can be included, for example light extension or algae growth (Del-WAQ is developed for ecological modelling). In a later stadium of the model development these ecological components will be implemented.

There is no online coupling between the hydrodynamic part and the sediment part. The sediment part is simulated as a post process of the hydrodynamic part. This is an important difference between the WL model and the large scale Markermeer model used in this study. However in the WL model erosion and sedimentation processes are included in the Del-WAQ part. These processes are not present in the model of this study. Erosion and sedimentation parameters (such as the critical shear stresses) in the WL model are not based on measured data, but are a result of the calibration process of the model. The WL model is calibrated on

a limited dataset, based on available field data. The calibration is carried out on the following parameters,

- Water levels of 7 days in the year 2002, including 1 storm period. These calibration results show good results. Water levels are predicted by the model within an accuracy of 10 % in a storm period and within a few percent during moderate conditions. Due to this calibration result it is concluded that water levels are well predicted by the model.
- Total suspended sediment concentration over the year 2006 at one location in the lake. In the year 2006 only 11 measurements are carried out. These measurements show good agreement with the model results. However only 11 points in time are compared at one location. For the model in this study this is not enough to conclude that the sediment concentration is well predicted.
- Overall spatial pattern of sediment concentration in the top layer is compared to remote sensing pictures. The overall pattern seems quite good, but remote sensing picture can only be used when the sky is clear. Therefore the model is not calibrated by rough weather conditions. Also no calibration has been carried out for a complete sediment concentration profile, only the upper layer of the water column.
- The data from the measurement poles (FL 41 and FL 42) is not used yet, because this data was not available at the moment of calibration. This data will be used in a later calibration.
- No wave height and no current velocity calibration have been carried out yet. It is assumed that these hydrodynamic processes are correctly computed by the model. According to the results of this MSc study this is not true for wave heights (Section 5.3.1).

In the WL model the sediment is schematized in two fractions: one fine fraction and one coarse fraction. Sediment parameters such as settling velocity, critical shear stress and erosion rate are results of calibration.

In the WL model the total year 2006 is simulated for analyzing the effect (a decrease in sediment concentration) of several solution measures for the turbidity problem.

Conclusions from those simulations are:

- The sediment concentration in the water column is variable in space and time. Therefore calibration should also be based on spatially distributed data. For this reason the measurement campaign is carried out.
- Waves and currents both influence the sediment concentration in the water column, both processes are important to include in the model.
- The model is usable to study the effects of several measures, although the model is not completely calibrated.

Also some recommendations are given for further studies:

- The flocculation process can be important for the sediment behaviour in the water column. This process should be included in the model.
- The model does not include sediment fluid interaction in the form of density effects. So density currents are not included.

This last recommendation is important for this MSc study, because according to the field measurements, this process can occur in the lake and should therefore be included in the model. This process can also be important for the infill of the silt trap.

The Delft3D model, developed for this study, is set up to include this density effect. Some adaptations on the WL model are made to establish this.

The Del-WAQ module is not able to simulate density currents. Therefore the sediment behaviour is modelled with the sediment part in FLOW. Density currents near the bed are

generated if a high sediment concentration layer near the bed can be build up. The model should describe the sediment concentration in the same order as the field measurements. For this reason this model is again calibrated on the sediment concentration, but now on the concentration near the bed, measured by the ASM. Also calibration for wave heights is carried out.

The final objective of the model of this study is to give insight in the effects of a silt trap on the sediment behaviour. Comparing to the WL model, this model is set up for a *detailed study to one of the measures* (the silt trap), while the WL model is used for a *large scale study to the effect of several alternative measures together*, on a higher spatial scale (total scale of the lake).

In the next sections the set up and calibration of the large scale Markermeer model will be described in more detail.

5.2 General lay out of the model

5.2.1 Software

The software which is used to carry out the simulations is the Delft3D software, developed by Deltares. According to the manual (WL Delft Hydraulics, 2006a) Delft3D is suited for a multi disciplinary approach and 3D computations for coastal, river and estuarine areas. It can carry out computations of flows, sediment transport, waves, water quality, morphological developments and ecology. The software is composed in several modules. In this study the modules FLOW (version 3.54.23.00) and WAVE (version 3.00.05.786) are used.

Delft3D FLOW is a multi dimensional 2D or 3D hydrodynamic (and transport) simulation program which calculates non steady flow and transport phenomena according to tidal or meteorological forcing. Delft3D WAVE simulates the propagation of random, short crested wind generated waves and is based on the SWAN model, developed by Delft University of Technology.

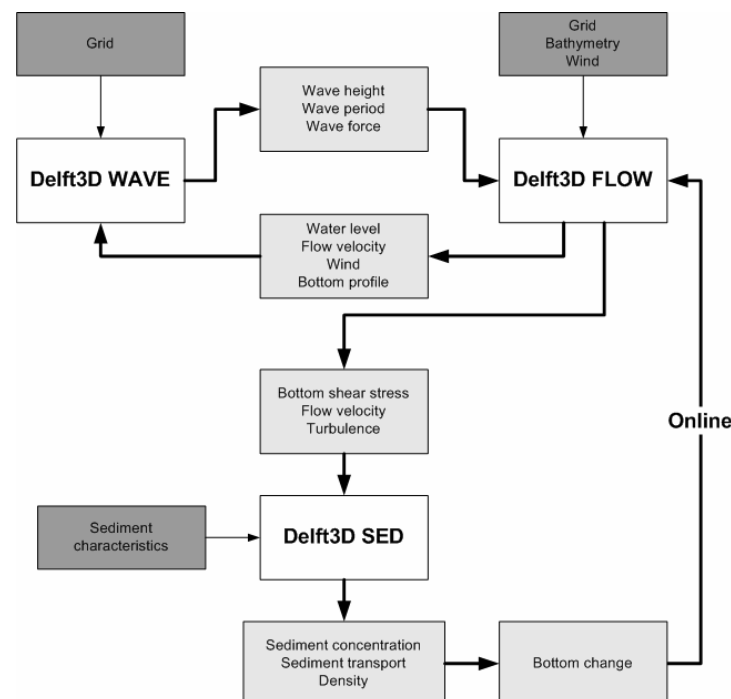


Figure 5.1: Schematic set up of the Delft3D modelling software
 The model consists of three main parts: FLOW, WAVE and SED.
 An online coupling between the three main parts is established.

In this study an online coupling between FLOW and WAVE is established, because of the interaction and influence between flow phenomena and waves. Also an online coupling between the sediment part (SED) and FLOW is established, because of simulating density currents (which is typical a sediment flow interaction). Online coupling means that one process influences the other (for example flow velocity influences waves), but also the other way around (waves influence the flow velocities). This two way coupling is taken into account for flow and waves, but also for the effect of sediment on the flow (via density effects and sediment concentration). A schematic picture of the software is shown in Figure 5.1.

5.2.2 Domain, grid and bathymetry

The first step in setting up a numerical model is to schematize the natural system (area) to a certain domain. With this domain the borders of the model are determined. Also the total Markermeer area is schematized in one domain.

The Markermeer is part of a larger body of water, containing the Markermeer and several small border lakes (IJmeer, Gooimeer and Eemmeer). Since the Markermeer is in open connection with these lakes, the modelling domain should include these lakes to make sure that the water balance is correctly simulated. For example during time of wind from southwest, water is pushed against the Houtribdijk. The water level on the northeast part of the lake becomes higher and on the southwest a water level decrease will establish. Water will flow from the border lakes to the Markermeer. If wind is blowing from the northeast the situation is the other way around, the water level in the border lakes (and on the southwest part) will increase. Because of this dynamic interaction of the border lakes with the main part of the Markermeer, the border lakes should be implemented in the model. Also in the WL model these border lakes are included in the domain.

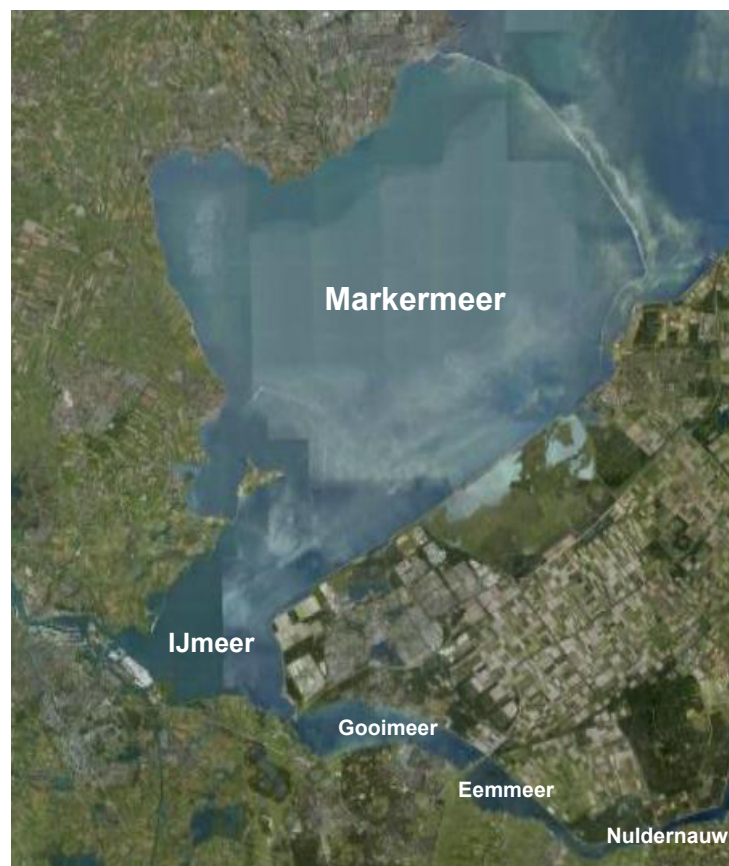


Figure 5.2: Overview of the modelling domain.
The domain consists of the Markermeer and the border lakes: IJmeer, Gooimeer, Eemmeer and Nuldernauw.

All borders of the domain are closed borders. No water is flowing in or out of the domain. In reality there is some discharge through the lake system, for example inflowing of water flow the river Vecht or the North Sea Channel. Also the discharge sluices in the Houtribdijk will exchange water with the IJsselmeer. This in and out flowing water contains sediment and therefore changes the amount of sediment in the lake. However these fluxes are negligible to the total amount of sediment in the lake. Especially if only 11 days are simulated. In Section 3.3.1, the mud balance, it is mentioned that the total import of sediment by these fluxes is about 30000 kg/year. This is about 850 kg for 11 days. The total amount of sediment which is put in the model is about 600000 kg. The total import of sediment in these 11 days is than only 0.0014 % of the total amount in the lake and therefore it is neglectable. Consequently, no open boundaries are added.

Horizontal grid

The grid that is used in the model is shown in Figure 5.3. The grid is based on the coarse grid of the original WL model. A coarse grid is used to save computation time. The detailed simulations of the silt trap will be carried out on a local fine grid. For calibration of the large scale model this coarse grid is sufficient. The grid resolution is on average about 500 x 400 m. In total there are 142 grid cells in M direction and 80 in N direction (M and N are local grid coordinates of the Delft3D model).

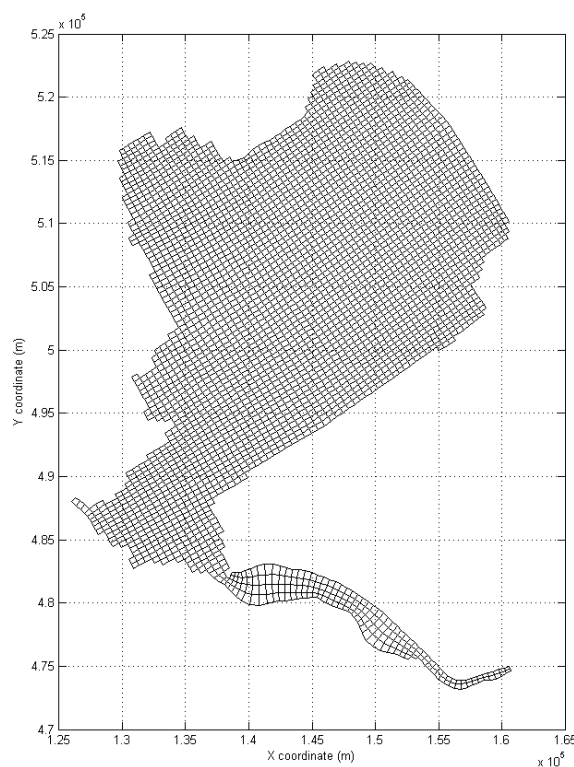


Figure 5.3: FLOW and WAVE grid of the model
The resolution is about 500 x 400 m
In total there are 3727 grid cells.

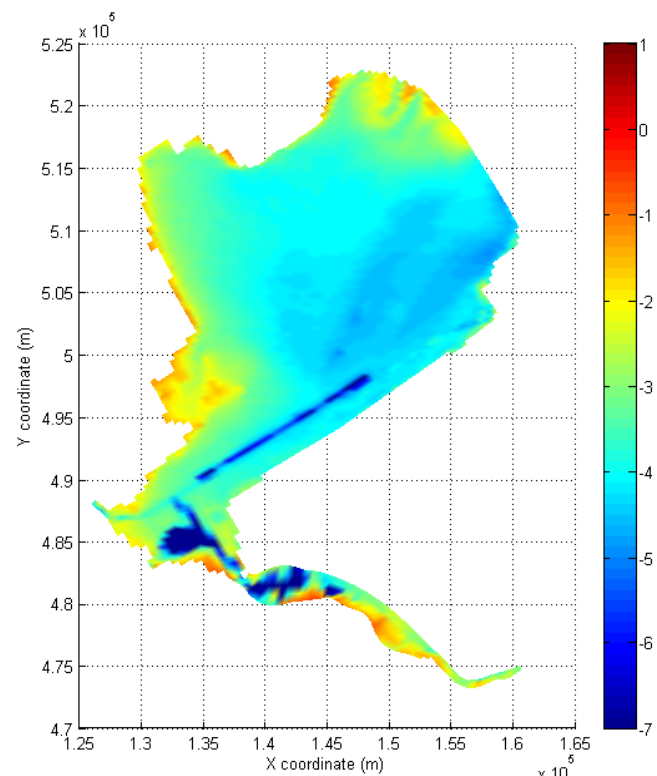


Figure 5.4: Bathymetry of the Lake as implemented in the model (situation 2006).

Vertical grid

This model is set up as a fully 3D model, with several computational layers in the vertical. This set up is based on the WL model of the Markermeer. The reason for 3D modelling is described in Figure 5.5. The velocity profile according to wind forcing is schematically given in the left picture (also Figure 3.2). In the Markermeer the profile can be a bit different, depending on the location in the lake. However a difference in flow direction between the upper part and lower part of the water column is characteristic.

If a depth average 2DH model is used, the velocity profile will be represented by only one velocity (picture middle). Using a fully 3D model, the vertical will be split up in several layers, with for each layer its characteristic velocity. It is clear that the 3D profile describes

the real profile best. Especially when sediment behaviour near the bed is important (which is the case in this study), the return current near the bed can have significant influence. 3D modelling should be applied.

This 3D modelling is a new concept in modelling of the Markermeer and is first described and modelled in the WL model. Earlier models, like Van Duin's model (1992), are 2DH models with depth average flow velocity and sediment concentrations. Due to these newer insights in 3D flow patterns, this 2DH modelling can not longer be applied in the Markermeer.

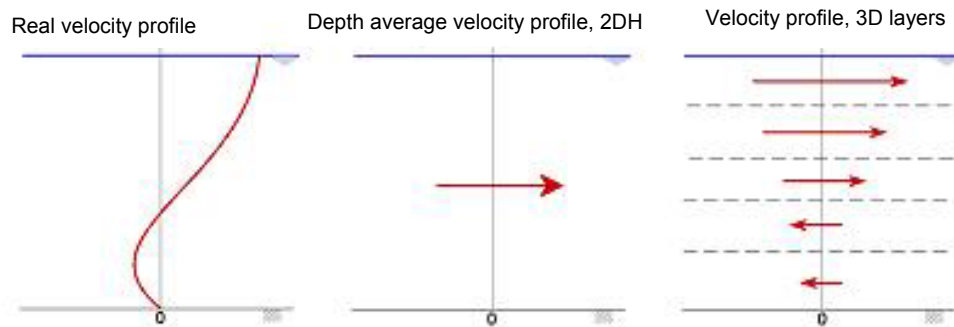


Figure 5.5: Differences between 2DH and 3D modelling in velocity profile. (WL Delft Hydraulics, 2007a) Left the real velocity profile due to wind. In 2DH modelling (middle) a depth average velocity is computed. The 3D velocity profile (right) matches better with reality.

In this study the vertical is split up in 20 layers, each with an equal proportionality of 5 % of the water depth. The original WL model has 7 layers, but in this model 20 layers are used. This is done for the simulation density currents. A higher resolution gives a better insight in that process.

There are two types of vertical layers that can be used in Delft3D, sigma-layers and z-layers. The difference between the two is explained in Figure 5.6. Sigma layers divide the water column in 20 layers on every location. If the water depth increases, also the grid height, Δz , increases. z layers have a fixed Δz and with increasing water depth, more layers are generated. In this model sigma layers are used, because of the modelling of the density currents. This can only be done by using of sigma layers. It is also not possible to make a coupling between FLOW and WAVE while using z-layers. This is another reason to use sigma layers.

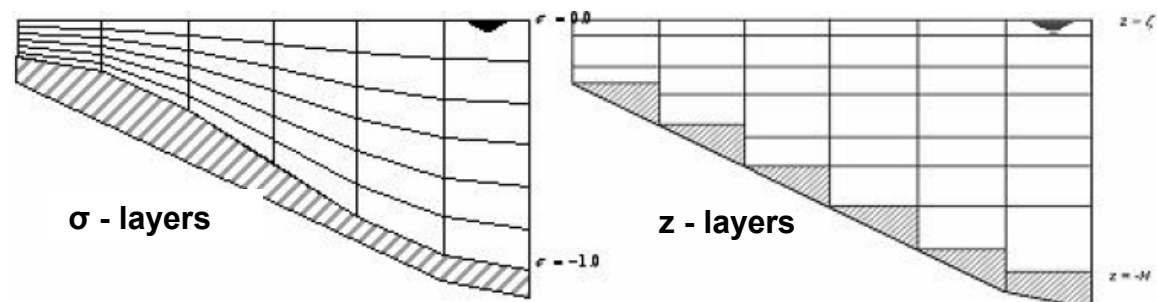


Figure 5.6: Schematic picture of sigma-layers (left) and z-layers (right). (WL Delft Hydraulics, 2006a). Z layers have a fixed grid height, sigma layers have a proportionality of the water depth.

Bathymetry

The bathymetry which is used in the model is shown in Figure 5.4. This is the situation of 2006 and is based on echo sounding measurements of Rijkswaterstaat. The resolution of the depth samples was larger than the grid resolution, so grid cell averaging is applied to translate the depth samples to the grid cells. Depth points are imposed at the corners of the grid cells. This bathymetry schematization is based on the WL model.

5.2.3 Sediment characteristics and morphology

Sediment is modelled by the means of 2 fractions of sediment, both representing of mud (cohesive sediment). The reason for using two fractions in the model is because of the different behaviour of both fractions. The first fraction represents the finest material, which is mostly permanent in suspension, already during moderate conditions. This fine fraction can be considered as material from the fluffy layer (Section 3.3.2).

The second fraction is brought in the water column only during storm situations. This behaviour is typical for the Markermeer and is also observed during the field measurements. Therefore one fraction has a small settling velocity and the other with a larger. This concept is also used in the WL model, although with some different values for the parameters. The characteristics of both fractions are shown in Table 5.1.

Name	Type	Reference Density Hindered Setting (kg/m ³)	Specific Density (kg/m ³)	Dry Density Bed (kg/m ³)	Settling velocity w_s (mm/s)	$\tau_{c, sed}$ (N/m ²)	$\tau_{c, e}$ (N/m ²)	Initial C water column (kg/m ³)	Initial C $K = 20$ (kg/m ³)
Mud1	Cohesive	100	2650	500	0.025	$1 \cdot 10^{-15}$	100	0.0125	1.25
Mud2	Cohesive	100	2650	500	0.800	$1 \cdot 10^{-15}$	100	0.025	2.5

Table 5.1: Characteristics of the two sediment fractions, implemented in the model.

The settling velocities are based on values used by Van Duin (1992) and in the WL model (WL Delft Hydraulics, 2007a). But finally they are results of the calibration process. Also the initial sediment concentrations of both fractions are an outcome of the calibration. More information about the calibration will be given in Section 5.3.

Table 5.1 shows that the critical shear stress for erosion $\tau_{c, e}$ is set to a very high value. The critical shear stress for sedimentation $\tau_{c, sed}$ (which is in this case the same as the critical shear stress for deposition, τ_d) is set to a very low value. Consequently no sedimentation and erosion can occur.

In reality erosion and sedimentation will occur, but the reason for not taken this into account in the model is for the sake of simplicity. Erosion and sedimentation parameters, such as the critical shear strengths, are hard to calibrate. These parameters are spatially different, depending on detailed soil characteristics, for example the consolidation rate of the bed. Proper modelling of these processes requires good field data about the strength of the bed, but this data is not present yet for the Markermeer. Therefore it is decided to put this out of the model.

A consequence of this modelling approach is that the sediment concentration in the lowest layer can be significantly overestimated. If the sediment settles from the water column, during calm conditions, it will be stored in the lowest layer and no interaction with the bed can occur. This means that during calm conditions sediment concentration in the lowest layer will increase to about 5 g/l (if all the sediment is settled in the lowest layer). According to the Argus Surface Monitor measurements only about 30 mg/l is measured near the bed (Figure A.13). This is a large difference between the model and the measurements. However it is no problem if this lowest layer is considered as a part of the bed. Above this lowest layer the sediment concentration can indeed drop to values of about 30 mg/l.

If conditions become heavier again, resuspension occurs and results will fit better to the data (more about this effect in Sections 5.3 and 5.4). This schematization effect should be kept in mind for the interpretation of the model results.

An important morphological process included in this model is the effect of sediment concentration on fluid density. Due to sediment concentration differences, density differences can occur and therefore density currents (Section 6.2). The field data show that

this effect can occur (Section 4.6). For this reason it is included in the model. This density effect is not implemented in the original WL model of the Markermeer. This is one of the most important developments with respect to the WL model.

5.2.4 Boundary and initial conditions

Initial conditions are based on the initial conditions of the WL model of the Markermeer. The initial water level over the lake is set to – 0.26 m, with respect to reference level (N.A.P.). The initial current velocities in all layers over the lake are set to 0 m/s, for both u and v direction.

The initial conditions for sediment concentrations of both fractions are shown in Table 5.1 and Figure 5.7. An initial concentration profile is imposed for the water column and the lowest layer. In layer 1 till 19 a low sediment concentration is set, in layer 20 a high concentration. This higher layer ‘represents’ a transition layer between the water column and the consolidated bed. This layer can be considered as the high concentration layer measured in the field campaign with the ASM (Section 4.4) The values for both fractions differ and are a result of the calibration process.

Boundary conditions at the edge of the computational domain are not imposed, because all boundaries are closed boundaries. At the water surface and at the bed there are boundary conditions. At the water surface a wind condition is set. This wind condition is also the forcing of the model (Section 5.2.5). At the bed a boundary condition is imposed due to bottom friction. Bottom friction will give a bed shear stress, which is computed in the model according to the manual (WL Delft Hydraulics, 2006a),

$$\vec{\tau}_{b,3D} = \frac{g\rho_w \vec{u}_b |\vec{u}_b|}{C_{3D}}, \text{ with magnitude of the bottom shear stress, } |\vec{u}_b| = \rho_w \vec{u} \cdot \vec{u} \quad (5-1)$$

C_{3D} is the Chezy value ($m^{1/2}/s$) and is set at the default value in this model, $C_{3D} = 65 m^{1/2}/s$. ρ_w is the water density ($1000 kg/m^3$) and u_b the bottom velocity (m/s).

The boundary condition becomes,

$$\frac{\nu_v}{h} \frac{\partial u}{\partial \sigma} \bigg|_{\sigma=-1} = \frac{1}{\rho_w} \vec{\tau}_b \quad \text{in u direction} \quad (5-2)$$

$$\frac{\nu_v}{h} \frac{\partial v}{\partial \sigma} \bigg|_{\sigma=-1} = \frac{1}{\rho_w} \vec{\tau}_b \quad \text{in v direction} \quad (5-3)$$

h is the water depth (m), u and v the components of the current velocity (m/s) and ν_v is the vertical eddy viscosity (m^2).

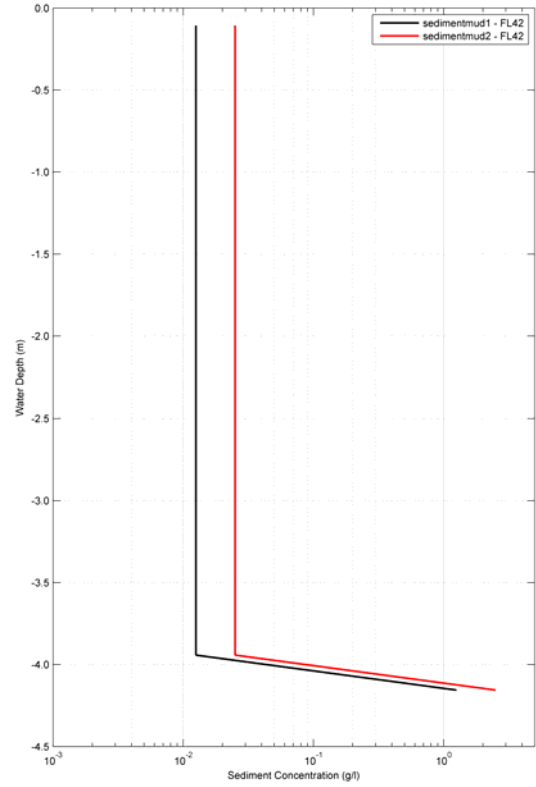


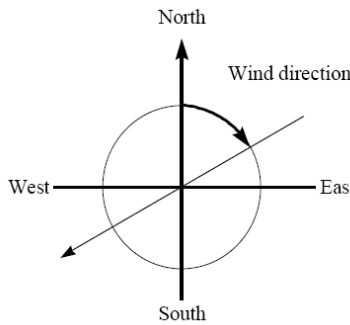
Figure 5.7: Initial sediment concentration profile. Near the bed a high concentration layer is imposed.

5.2.5 Forcing

In Section 5.2.2 it is already mentioned that no open boundaries are implemented in the model. This means that the forcing of the system is only due to the wind. Wind causes wave growth and water level set up. Due to pressure gradients over the lake, a large scale wind driven circulation pattern occurs (Section 3.1.1). The wind is the driving factor in the whole system.

Therefore a proper description of the wind must be implemented in the model. In this model, real wind measurements are used for this forcing. The measurements are taken from location Berkhout. Every 10 min a wind speed and wind direction (in degrees, 0 degrees is North, Figure 5.8) is obtained from that data set (Figure 5.9). Visser (2007) mentioned that wind data of location Berkhout might be not accurate (Section 2.5). However, wind data from location Schiphol for the year 2007 were not available at the moment of modelling.

Wind exerts a shear stress on the water surface. This shear stress can be regarded as a boundary condition for the water surface boundary. In Delft3D this shear stress is computed by a very common used equation,



$$\left| \vec{\tau}_{wind} \right| = \rho_a C_d U_{10}^2 \quad (5-4)$$

ρ_a is the air density (1.0 kg/m^3), U_{10} the wind speed at a height of 10 meters above the water level (m/s) and C_d is a drag coefficient. The drag coefficient is linear dependent on the wind speed. In this model the default values are used, resulting in a linear formula for C_d value as a function of the wind speed U_{10} ,

Figure 5.8: Nautical definition wind direction. (WL, 2006)

$$C_d = 0.000066 U_{10} + 0.00063 \quad (5-5)$$

The free surface boundary in the model becomes (WL Delft Hydraulics, 2006a),

$$\left. \frac{\nu_v}{h} \frac{\partial u}{\partial \sigma} \right|_{\sigma=0} = \frac{1}{\rho_w} \left| \vec{\tau}_{wind} \right| \cos(\theta) \quad \text{in } u \text{ direction} \quad (5-6)$$

$$\left. \frac{\nu_v}{h} \frac{\partial v}{\partial \sigma} \right|_{\sigma=0} = \frac{1}{\rho_w} \left| \vec{\tau}_{wind} \right| \sin(\theta) \quad \text{in } v \text{ direction} \quad (5-7)$$

θ is the angle between the wind stress vector and the local direction of the grid lines.

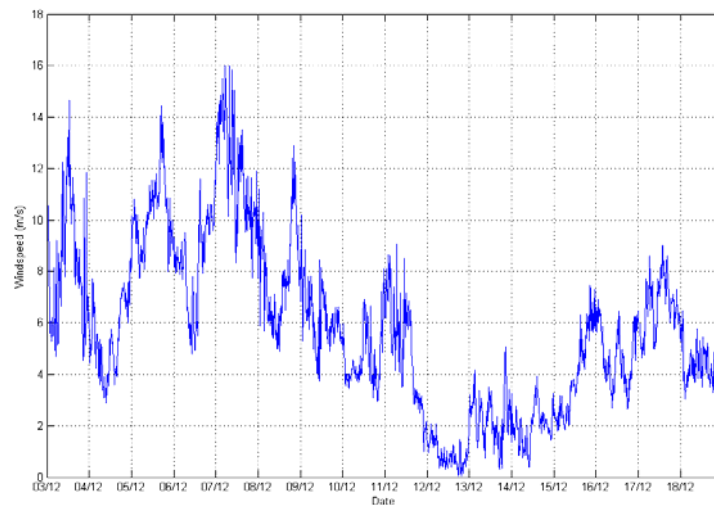


Figure 5.9: Wind speed during modelling period, measured in Berkhout.

In the first half of the period four storms are recognized, each with a peak wind speed of about 14 m/s. The duration of each storm is about one day.

5.2.6 Time

The time frame of the model is set as the same period as the Argus Surface Monitor measurements. In this period good quality data is available to carry out a proper calibration. Also the wind forcing in that period is interesting, because of the several storms which occur (Figure 5.9). Because of the limited computation time, not the whole period is used. The reference time for the computation is set at:

3 December 2007 0:00

The computation period is 11 days in total, so:

3 December 2007 0:00 – 14 December 2007 0:00

The time step in the model is set to two minutes, so $\Delta t = 2$ min. For numerical stability this is acceptable. To determine the stability of the model the courant number (CFL) is computed. The courant number is given by,

$$CFL = U \frac{\Delta t}{\Delta x} \quad (5-8)$$

Taking $U = 0.4$ m/s and $\Delta x = 400$, CFL becomes 0.12, which is smaller than 1. This is sufficient for numerical stability.

The output of the model is stored every 60 minutes. The online coupling between the FLOW and WAVE part of the model is every 120 min. So every 2 hours a new wave computation is carried out. This coupling is set to 2 hours instead of 1 hour (which is default) to save computation time. The SWAN computation is namely the dominating factor for the total computation time. The accuracy of the computation will hardly change and is even better than the WL model, because in this model a 3 hour coupling is used.

Other, more detailed, model settings are given in appendix B-1.

5.2.7 Cohesive sediment processes

In Section 3.2 some general processes in cohesive sediments are described. Although this Markermeer model is set up for cohesive sediment, not all processes are implemented in the model. This section points out which process is implemented and which is not.

The *settling process* is important for modelling of the silt trap, because settling is one of the major mechanisms that fills a silt trap (Section 1.2). In the Delft3D model settling is taken into account by defining a characteristic settling velocity for each fraction (Table 5.1).

The *hindered settling effect* is determined according to the formula of Richardson and Zaki (equation 3.15), by using the n coefficient with a value 5 and imposing a gelling concentration (in the large scale model 100 g/l). This means that the sediment concentration can not be larger than 100 g/l, the settling velocity is than 0 mm/s

Flocculation can be an important process for the sediment behaviour in the Markermeer. Nevertheless, flocculation is not taken into account in this Markermeer model. It is not implemented in the model, because the dynamic floc aggregation and break down processes are not implemented in this version of the Delft3D software. If it was, it was even hard to model the process, because it is dependent on many parameters and processes.

Unfortunately no research has been carried out on the flocculation behaviour of the sediment in the Markermeer. It is therefore hard to give a good estimation of the process.

Indirectly, flocculation is accounted for in the model by using two fractions: one with a small settling velocity and one with a large. The mud fraction with a large settling velocity can be considered as a fraction with a representative large mud floc. This floc is a result of flocculation, but it can not break up or aggregate in the model. In reality this breaking up and aggregation of flocs are dynamic processes and can influence the settling of sediment in the lake and also in the silt trap. In the end, these processes will influence the effectiveness

of the silt trap. Further developed models of the Markermeer should include this flocculation process for a better description of the sediment behaviour near a silt trap.

The *consolidation process* and the *increase in bed strength* can be important processes in the Markermeer and the silt trap.

However the consolidation process is also not implemented in the model. Consolidation can not be accounted for in the version of Delft3D used for this study. Consolidation is a complicated process and is only implemented in some trial versions of Delft3D.

As a consequence, the sediment in the model will behave different than in reality. If the sediment is transported in the pit, it will stay in the lowest computational layer and will not consolidate or increase in strength. The sediment can easily be brought in the water column again due to turbulent mixing. Not only inside the silt trap, but also in other parts of the lake this modelling effect will be present.

However the model only simulates 11 days in total. The time scale for significant consolidation process is longer. For this reason, the consolidation in those 11 days of simulation is negligible. This model schematization will not influence the results to a large extent.

5.3 Calibration

As mentioned in the introduction to this chapter, the objective of this large scale model is to assess the mud dynamics in the Markermeer and to give an answer to the question if density currents can occur near the bed. For this reason, it is not necessary that the model predicts the sediment concentration exactly right on every moment of time. Because of the rough schematization (only 2 fractions, coarse gird, no erosion/sedimentation) this is probably not possible. But to give proper insight in the sediment behaviour the order of magnitude of the sediment concentrations should agree with the measurements.

The WL model already showed that the large scale sediment concentration patterns in the upper layer of the water column can be described by the model. For simulation density currents the sediment concentration profile over the vertical should be right. Calibration of this model will for this reason focus on the sediment concentration profile, especially near the bed. Model results are compared to measurements of the ASM, because the ASM measured sediment concentration profiles in time. Unfortunately only on one location these profiles are measured, near pole FL42. Consequently only on this location calibration can be carried out. One recommendation of the WL model was to use a spatially distributed calibration. For the ASM data this is not possible; this should be done in future model developments.

For the hydrodynamics, the WL model showed that water levels computed in the model match quite good with measurements, so no further calibration is needed. Wave heights are not calibrated in that model. However waves can be very important for the sediment concentration profile, for example for stirring up of the sediment. For this reason this model is also calibrated to wave heights, measured at the pole FL42. This section gives a description of the calibration process to the two parameters, wave heights and near bed sediment concentration. The final results are presented in appendix B.

5.3.1 Wave height

For the calibration of the wave height, wave data from the measurement pole FL 42 is used. This is the same data set as shown in the results of the measurement campaign (for example Figures A.8 till A.13).

Significant wave heights computed by the model at the same location as pole FL 42 are compared to the measurements. The results of the calibration process are shown in the appendix, Figures B.1 and B.2 and Figure 5.10. At the end (red line) the wave heights computed by the model fits the measured wave heights quite well. Figure B.2 (red dots) shows the scatter round the line $y = x$. This scatters is not very large. The correlation coefficient (R) can be computed by,

$$R(X,Y) = \frac{\text{Cov}(X,Y)}{\sqrt{\text{Cov}(X,X)\text{Cov}(Y,Y)}} \text{ , with } \text{Cov}(X,Y) = E[(X - \mu_x)(Y - \mu_y)] \quad (5-9)$$

Here X and Y are vectors (one the model data, other the measurement data), E the mathematical expectation value and μ the mean value. The correlation coefficient between the measured and modelled significant wave height at pole FL 42 is 0.85, which is quite good.

To get this good match between the measurements and the model, some adaptations to the model had to be made. If the wave heights are computed with default values of SWAN, the waves will be underestimated. This is a known problem of SWAN: under prediction of waves in shallow lakes with only wind forcing (Westhuysen et al, 2006). Therefore some different settings are implemented. These measures are taken:

- A new formulation for the whitecapping process. Problems according to the whitecapping computation are already recognized by Westhuysen et al (2006). In this publication a new formulation is given. This new whitecapping formulation is implemented in the model. The major difference in this new formulation is that the whitecapping formulation is nonlinear and that this expression is combined with a new wind input term, which is more accurate for young waves.
- The bottom friction for waves is not taken into account (only for waves, fiction for the FLOW part is still in the model). This means that energy dissipation of waves due to bottom friction is zero. Waves therefore can grow larger, wave heights become larger. Physically it is not right to switch of the friction; waves will 'feel' the bottom and loose some energy. However for the model results it is better to neglect the friction.
- More iterations (to a maximum of 30) and stricter iteration criteria. The wave computation will be more accurate when using more and more stricter iterations. A disadvantage of this measure is the increasing computation time.
- The coupling between FLOW and WAVE is set to 2 hours instead of 3 hours (used in the WL model). Using more up to date wind data and current velocities this will result in better model computations for the actual wave heights. Also this measure will increase the computation time.

The effect of these measures is shown in Figures B.1/5.10 and B.2. The green line in 5.10 is the computed wave height before these measures, the red line after these measures are implemented. The blue line indicated the measured wave heights at the pole. The red line agrees better with the blue line than the green line. The maximum order of the wave height is about 40 % higher when using the new settings. This can also be shown in Figure B.2. The red dots show that using the new settings wave heights are higher. The green dots show that the modelled wave height can not be higher than 0.8 m, however the measured wave height is up to 1.4 m.

However, the correlation coefficient computed in the old and new situation (correlation with the measurements) does not change. In both situations $R = 0.85$.

The reason that this correlation coefficient is not increased in the new settings is the somewhat overprediction of the wave height at the 5th of December (Figure B.1). The model predicts higher wave heights (about 1 m maximum) than the measurements (about 0.7 m). The model results might be correct, because the storm at the 5th of December is almost the same in magnitude and direction as the storm at the 7th of December. Wind speeds are 14 to 15 m/s for both storms and the direction is 240 to 270 degrees. One expects somehow the same wave climate at the 5th of December as during the 7th. But the measurements show significant lower waves than the model. Maybe the measurements are not correct during the 5th of December and consequently cause some differences.

If one compares the results of this calibration process of this model with the WL model, an improvement is established. No wave data were available for calibration for the WL model

and therefore default values were used. The calibration process shows that the results of the WL model are wrong and that waves are underestimated by using the old model settings. Further model developments should start with the settings from the model of this study.

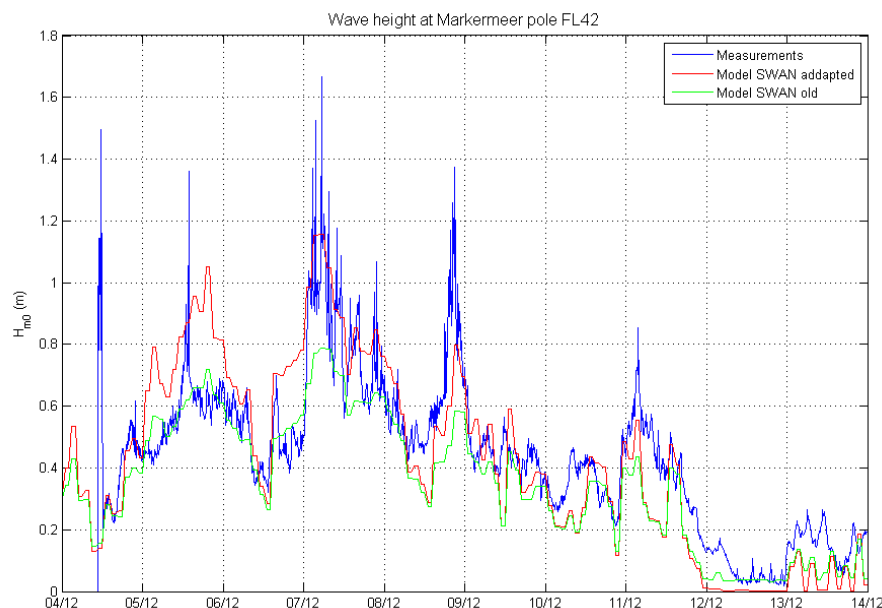


Figure 5.10: Time series of significant wave height, measurements (blue) and model old (green) and model adapted (red). The results of the adapted model show good similarity with the measurements.

5.3.2 Sediment concentration

For calibration according to sediment concentration, data from the Argus Surface Monitor is used. A complete description of the measurement set up and results is given in Chapter 4. In this section those results are compared to the results of the calibration process of the model.

The calibration parameters of the model are: fall velocities and initial sediment concentrations of both fractions. In each simulation these values are changed and the computed sediment concentration profiles at the location of pole FL42 are compared to the results of the ASM. Finally, the order of magnitude of the concentration should be the same in the model as in reality, for several weather conditions. The starting values for the settling velocities are 0.025 mm/s for the fine fraction and 0.412 mm/s for the coarse fraction. Both values are based on results of the study of Van Duin (1992). At the end of the calibration, the settling velocity of the coarse fraction increased up to 0.8 mm/s to give better results in the lowest part of the water column.

The initial sediment concentration is actually the total amount of sediment that will be in the lake system. Erosion and sedimentation is neglected, therefore no sediment can be brought in or taken from the model domain. Calibration of these values is important for the final results. At the end, the initial concentrations shown in Table 5.1 in Section 5.2.3 give quite good results.

Figures B.3 and B.4 show sediment concentration profiles on specific times. The blue line indicates the measured sediment concentration. The red line is the model result of the final calibration setting (this is run 14 in Table 5.2)

In all plots the order of magnitude between model and measurements matches. In some plots, like B.3 (middle plot) and B.4 (last plot) the effect of neglecting sedimentation and erosion is shown. At these times the weather is calm and the sediment will stay in the lowest layer, which can be regarded as bottom. Consequently the sediment concentration in this layer is overestimated by the model. In the other plots it is shown that the model predicts the sediment concentration quite well, even the higher sediment concentration near the bed and higher up in the water column.

To compare the modelled sediment concentration to the measured concentration, a time series of the concentration is useful. However to make a time series of the sediment concentration close to the bed it is not right to include the lowest layer. In this lowest layer the concentration is overestimated in times of calm weather, due to the model effect.

For this reason the upper 10 cm of the ASM measurements are averaged and compared to the model results at the same water depth (around – 3.3 m). This time series is shown in Figure B.5 and 5.11. In this plot also the results of some other calibration runs are shown. The settings of the calibration runs are given in Table 5.2.

Fraction	Mud 1			Mud 2			Waves
	w_s (mm/s)	Initial C (kg/m ³) k = 1-19	Initial C (kg/m ³) k = 20	w_s (mm/s)	Initial C (kg/m ³) k = 1-19	Initial C (kg/m ³) k = 20	Settings old/new
Run 1	0.025	0.025	2.5	1	0.025	2.5	Old
Run 4	0.025	0.025	2.5	0.8	0.025	2.5	Old
Run 6	0.025	0.025	2.5	0.8	0.025	2.5	Old
Run 12	0.025	0.025	2.5	0.8	0.025	2.5	New
Run 14	0.025	0.0125	1.25	0.8	0.025	2.5	New

Table 5.2: Settings of some calibration runs for the Markermeer model.

Seven different parameters are changed during the calibration process (Table 5.2). The parameters are settling velocity, initial sediment concentration water column, initial sediment concentration lowest layer for both fractions and the wave settings. Wave settings ‘old’ means default wave settings, before adaptations are carried out. ‘New’ settings means after adaptation.

Figure 5.11 shows that runs 1, 4, 6 and 12 over predict the sediment concentration according to the measurements. Especially at the 5th of December and in the last part of the simulation this can be a factor 2. The difference between these runs in sediment concentration is not very much, although run 12 gives some higher sediment concentrations. This can be explained by the fact that waves are higher in run 12, because of the new wave formulation. Apparently the settling velocity has little influence on the concentration. There is some difference between run 1 and run 4 (the settling velocity of mud 2 is decreased), but the effect is not strong.

Conversely, the initial sediment concentration has a large influence on the sediment concentration in the water column. The effect of this initial concentration is shown by comparing run 14 to the other runs. In run 14 the total amount of the mud 1 fraction is halved. As a consequence the sediment concentration in the water column decreases and run 14 fits the measurements best.

The overall concentration pattern of run 14 shows good agreement with the measurements, but some differences are shown at 7th and 12th of December.

At the 7th, the model predicts significant lower concentrations than measured. This is also because of the model effect of neglecting erosion (there is a lack of sediment in the model). On the 7th of December a large storm occurred, which gave a large load on the bed and therefore large erosion in reality. This is not included in the model; the total amount of sediment can not increase and the concentration will be less. Figure B.6 (appendix) also shows this effect. The maximum sediment concentration in the model is about 200 mg/l. At that moment all the sediment will be in the water column and the concentration can not increase. This is only a problem during extreme conditions, because at that time erosion will be strongest. During the other (less strong) storms in the period this effect is much less.

The other main difference between run 14 and the measurements is on the 12th of December. In this period the wind forcing is that low, that even the fine fraction can settle out of the water column. As a consequence the concentration will be extremely low.

However the model overestimates the concentration. This is due to the fact that the settling velocity of the fine fraction (mud 1) is a bit too low and the concentration decreases too slowly. At the end, on the 13th of December the match is better. Because this period is not

very interesting for turbidity and this period is not simulated in the silt trap model, it is chosen not to change the settling velocity of the fine fraction.

Also the wave computation in SWAN during these 2 days is not very accurate. The iteration processes of SWAN gives worse results when wind speed is low. This defect is already mentioned in WL Delft Hydraulics (2007a): At low wind speed, SWAN needs more iterations to get a good result.

During low wind speeds, the wave height is also lower and consequently the bed shear stress is less. Resuspension due to waves in this period is less or even not existing. Correct computation of the wave heights is less important in this period.

Finally it can be concluded that the model predicts the sediment concentration in the right order. Together with the good hydrodynamic results it is concluded that the model is calibrated well enough to model the effects of the silt trap on the sediment behaviour.

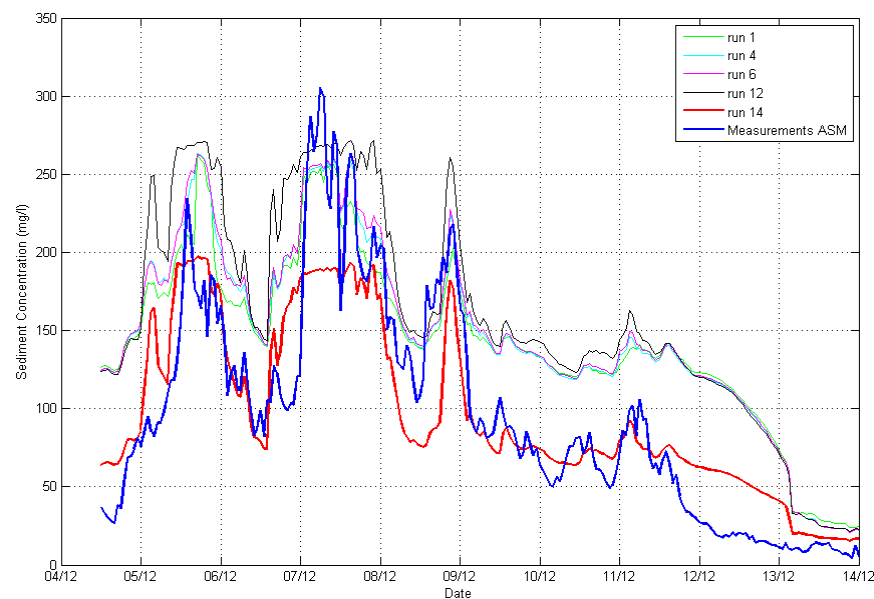


Figure 5.11: Time series of sediment concentration averaged over upper 10 cm of ASM (about 1 m above the bed), measurements (blue) and several model simulations. Run 14 shows good similarity with the measured sediment concentration.

5.4 Results

One of the important results from the model is about the behaviour of the two fractions. Knowledge of the different behaviour of those fractions is useful to understand the results of the silt trap model in the coming chapters. For this reason some plots of the sediment concentration of both fractions are shown in appendix B, Figures B.7 and B.8.

Each fraction has its characteristic behaviour, which depends on the wind forcing:

- The fine fraction (mud 1) is uniformly distributed over the vertical during already moderate condition. This is shown in the first three plots (1,2 and 3) in Figures B.7 and B.8 (black line is the fine fraction). Conditions differ a lot between these times, but the sediment concentration is mostly uniform over the vertical. If the wind forcing is further decreased (to a few m/s) the fine fraction can also settle. This is shown in the last plot (4) in Figure B.8 and 5.13. In the upper part of the water column the sediment concentration for the fine fraction decreases drastically. Because this fine fraction is already suspended in the water column at low conditions, it is responsible for a high turbidity in the Markermeer. To decrease the

sediment concentration by means of a silt trap, this fine fraction should be caught in the trap in some way.

- The sediment concentration profile of the coarse fraction (mud 2) is much more variable in time than the fine fraction. The behaviour is directly linked with the wind forcing. During moderate conditions most of the sediment is in the lowest layer. If the wind forcing increases, resuspension occurs and the sediment concentration increases due to the suspension of mud 2 until an equilibrium-type profile is reached. This is the case in the second plot (2) in Figure B.7 and 5.12. If the forcing is decreased, the profile collapses immediately and the sediment will stay in the lowest layer again. Due to this coarse fraction layers with high sediment concentration and sharp luctoclines can occur near the bed. This can cause density currents. Just like the field measurements also the model results give reasons to believe that density currents can occur in the lake.

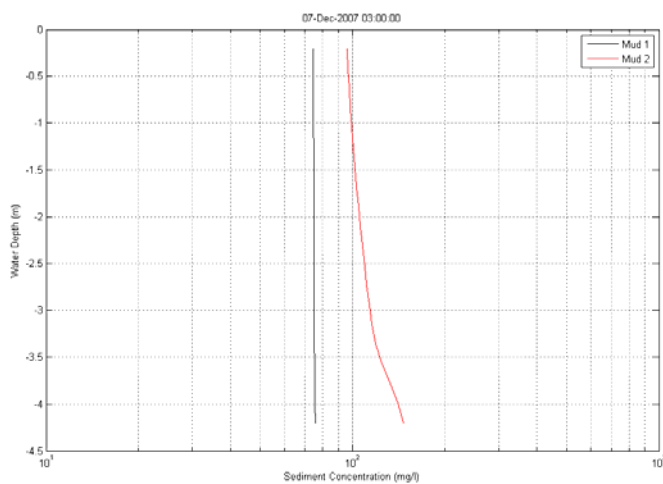


Figure 5.12: Sediment concentration of both fractions. 7 Dec. 3h00, fine (black) and coarse (red). Both fractions are completely mixed in the water column.

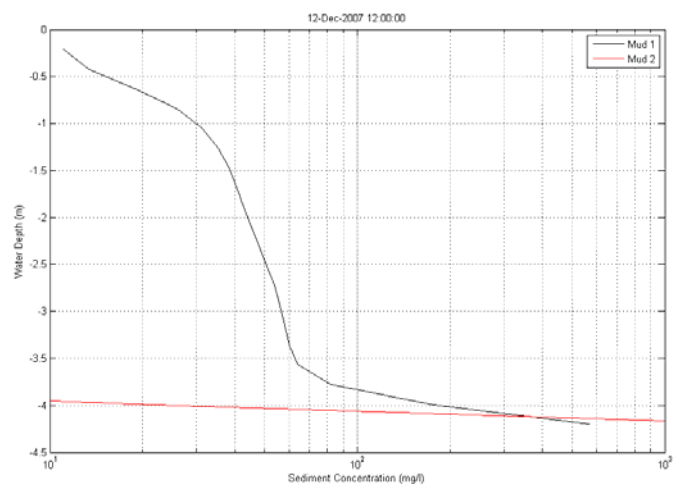


Figure 5.13: Sediment concentration of both fractions. 12 Dec. 12h00. The coarse fraction is already settled. The fine fraction starts to settle out.

Another important result of the model is the influence of waves on the sediment concentration. Waves can have influence on the sediment concentration in the wave column due to several processes:

- Waves cause bed shear stress on the lake bed. If the shear stress exerts a certain critical value, the bed can erode. Due to erosion the amount of sediment in the water column is increased. Because erosion and sedimentation is not taken into account in this the model of this study, this process does not play a part.
- Waves cause wave driven flow. This wave driven flow increases the turbulent intensity in the water column and as a result an increase in mixing of the sediment. Wave driven flow is implemented in the Delft3D model, so this process has influence on the sediment concentration.
- Waves itself also increases the turbulent intensity and therefore influence the mixing process. Also this process is implemented in the model.

To assess the influence of waves on the sediment concentration, one model run is carried out without wave computation (so no SWAN computation). The other input parameters are unchanged. The results of that run are shown in Figure B.9 and are compared to the results of run 14 and the ASM measurements. It can be concluded that waves have a significant influence on the sediment concentration. Especially during storm periods the concentration computed by the run without waves is less than run 14, with waves. For example at the 7th of December the concentration computed in run 14 is about 200 mg/l. By neglecting waves this drops to about 150 mg/l, which is a decrease of 25 %. A consequence of this lower

turbulent intensity due to the absence of waves is that the sediment will stay in the lowest layer; the mixing is less. This consequence is shown in Figure B.10. This figure shows the sediment concentration profile on 8th of December 0:00. The red line (run 14 including waves) fits the measured data of the ASM (blue line) very well. The black line (run 14, without waves) shows that the sediment stays in the lowest layer. The difference between the red and black line is only due to this wave effect.

The conclusion that waves are important for sediment concentration modelling in the Markermeer was somehow expected, because this is also one of the conclusions of the study of Deltares (WL Delft Hydraulics, 2007a and Section 5.1). The results of this the model are a confirmation of the findings in that report.

5.5 Conclusion

The purpose of the development of this new large scale Markermeer model is to further develop the WL model of the Markermeer. Density currents must be implemented in the model to assess the influence of a silt trap on the sediment behaviour. The model should also give insight in the mud dynamics in the lake.

To reach these two purposes the model should describe the sediment concentration in the same order as the measurements of the Argus Surface Monitor. For the model, the same time period is simulated as the measurement period of the ASM; real wind characteristics of that period are used as a forcing of the model. Calibration has been carried out to the sediment concentration profile near the bed and the wave height. With respect to the existing WL model this is new, because that model was not yet calibrated to such detailed data sets.

Finally it can be concluded that the model describes the hydrodynamic and sediment behaviour to the right order of magnitude. The model is good enough to assess the effects of the silt trap.

The behaviour of both fractions in the model does match with the results of the field measurements and previous studies.

Also according to the results of this Delft3D model, it can be concluded that density currents can exist in the Markermeer. Density currents might have an influence on the sediment behaviour near a silt trap.

The silt trap model should therefore include this density effect. A detailed description of this model will be given in Chapter 7.

Part II: Silt traps as a mitigation measure for turbidity

6 Processes in and around a silt trap

In this part of the study the focus will shift from the large scale Markermeer to the small scale processes around a silt trap. This chapter describes the theory about the hydrodynamic and sediment behaviour near a silt trap. Section 6.1 considers the effect of the silt trap on the local current pattern and waves. Section 6.2 will discuss sediment transport processes near the trap.

This chapter is important for understanding of the behaviour of fine sediments near a silt trap. That subject will be extensively discussed in Chapter 7 according to the results of the Delft3D model of the silt trap.

6.1 Hydrodynamics

6.1.1 Flow

Over the last decade research is carried out on the effects of dredged channels on the flow pattern and sediment transport. The results of two studies are useful for this section,

- Jenssen et al (1999a) describes the results of a numerical model of the 3D flow pattern and sediment transport near a dredged channel. Also a comparison between a 2DH and 3D model is made.
- Van Rijn (2005) gives a description of the hydrodynamic and sediment transport processes in navigation channels. It is also mentioned that this situation is comparable with deep sand mining pits.

The silt trap in the Markermeer, which is investigated in this study, is in fact also a deep 'sand mining' pit. Van Rijn (2005) describes the processes around pits in the coastal region. The pits are relatively shallow as compared to the water depth in the surrounding area. Due to the focus on the coastal region the sediment transport is mainly driven by tidal currents. In the Markermeer currents and waves are driven by wind (Section 3.1), so the situation is quite different. Another difference is that the studies of Van Rijn (2005) and Jensen et al (1999a) are set up for navigation channels instead of deep silt traps, which is subject of this study. Nevertheless, results of both studies are useful for understanding the basic processes and are for this reason presented in this section. Although, some results can not be applied directly to the situation of the silt trap in the Markermeer.

Effect on flows

In general, the dimensions of the silt trap are small with respect to the total scale of the Markermeer. Consequently there will be no significant influence of the silt trap on the large scale flow pattern in the lake. Only effects in the direct vicinity of the silt trap are expected. However, these effects can be important for the sediment transport near the silt trap. Understanding of the hydrodynamic processes is therefore important. The influence of the trap on the local current pattern is determined by:

- Trap dimensions (length, width, depth and slope angle).
- Magnitude of the current velocity.
- Bathymetry of the local area (shoals near the silt trap).
- Angle between the main axis of the trap and direction of approaching current, the inlet angle (α_0 , Figure 6.1).

With respect to the last variable, Van Rijn (2005) and Jensen et al (1999a) distinguishes three basic cases:

- Flow parallel to the main axis of the trap ($\alpha_0 = 0^\circ$).
- Flow perpendicular to the main axis of the trap ($\alpha_0 = 90^\circ$).
- Flow oblique to the main axis of the trap ($0^\circ < \alpha_0 < 90^\circ$).

In the Delft3D silt trap model the orientation of the silt trap with respect to the wind direction (and therefore also the current direction near the surface) is investigated. Only the first two cases are simulated, parallel and perpendicular flow.

The study carried out with the Delft3D model also investigates the influences of the slope angle and depth of the trap, which are other important pit parameters.

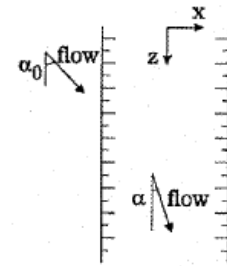


Figure 6.1: Definition of flow angles. (Jensen, 1999a)

Parallel ($\alpha_0 = 0^\circ$)

The situation of a flow parallel to the silt trap is illustrated in Figure 6.2. Inside the trap area the depth average flow velocity will exceed the depth average flow velocity outside the trap. This can be explained as follows (Jensen et al, 1999a):

The longitudinal pressure gradient ($\partial p / \partial z$) is constant across the trap. The driving force of the flow is equal to the water depth times the pressure gradient. A larger water depth causes a larger driving force and consequently a larger flow velocity.

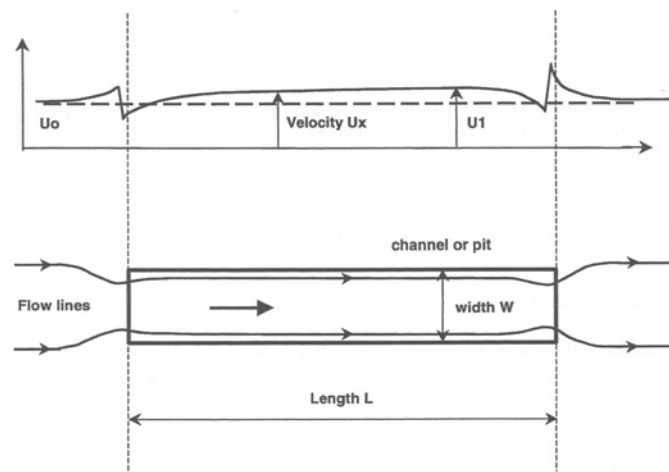


Figure 6.2: Flow parallel to the silt trap. (Van Rijn, 2005) Just upstream and downstream of the trap flow contraction occurs (left and right side) Inside the trap the depth average flow velocity is higher than outside.

Just upstream of the trap, flow contraction will occur. This distortion of the flow results in areas of increase and decrease of the velocity at the edge of the trap. This will also occur at the downstream end of the trap. The depth average flow velocity in that contraction zone, just upstream of the trap, can be estimated by assuming a logarithmic velocity profile (Van Rijn, 2005),

$$u_{con} = \left(\frac{2h_0}{(h_1 + h_0)} \right) u_0 \quad (6-1)$$

With the index '0' stands for outside the trap and '1' for inside the trap. h is the water depth (m) and u the depth averaged flow velocity (m/s).

The flow velocity inside the trap can be calculated by the Chezy equation (by assuming the water surface slope constant),

$$u_1 = u_0 \left(\frac{C_1}{C_0} \right) \sqrt{\frac{h_1}{h_0}} \quad (6-2)$$

The depth average flow velocity inside the trap is larger than the average velocity outside. Equation 6-2 shows that the flow velocities inside the trap increase proportionally with the square root of the expansion in depth.

This increase in velocity does not occur when the length of the trap is small comparing to the width, $L < 2W$.

Perpendicular ($\alpha_0 = 90^\circ$)

The situation of flow perpendicular to the trap is shown in Figure 6.3. In this situation the depth average flow velocity will decrease inside the silt trap.

This can be explained by depth average continuity. The discharge just outside the trap is equal to the discharge inside the silt trap (over a certain width). Due to the increase in cross section inside the trap (depth increases), the depth average flow velocity will decrease.

In case of steep slopes, 1:5 and steeper, flow separation can occur near the upstream end, causing eddies and energy dissipation. Flow velocities near the water surface are hardly influenced by the pit, because of inertial effects.

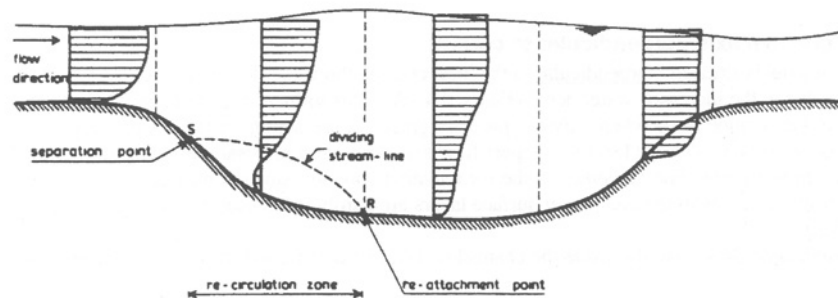


Figure 6.3: Flow profiles near the silt trap (perpendicular case). The depth average flow velocity decreases inside the trap. (Van Rijn, 2005).

In the silt trap model the difference in water depth is much larger (4.5 m outside to 16.5/21.5 m inside the trap). Probably the velocity profile will look different than in Figure 6.3. In the model slopes of 1:15 and 1:20 are implemented, so flow separation is not expected. In reality the slope will be steeper (1:4 to 1:10). In reality flow separation can occur.

The depth average flow velocity inside the trap is calculated by the continuity equation (Van Rijn, 2005) ,

$$u_1 = u_0 \left(\frac{h_0}{h_1} \right) \quad (6-3)$$

The velocity profile inside the trap is a linear combination of a logarithmic profile and a perturbation profile and is (Van Rijn, 2005),

$$u(z) = A_1 u_h \ln \left(\frac{z}{z_0} \right) + \left(1 - A_2 \ln \left(\frac{z}{z_0} \right) \right) u_h F \quad (6-4)$$

with u_h is the flow velocity near the surface (m/s), A_1 and A_2 coefficients and F the perturbation profile, described by,

$$F = 2((z - z_0)(h - z_0))^t - ((z - z_0)(h - z_0))^{2t}, \text{ with } t \text{ a coefficient.} \quad (6-5)$$

Oblique ($0^\circ < \alpha_0 < 90^\circ$)

In most of the time the current will have an oblique inlet angle with the trap axis. Also in the model the flow will definitely not be exactly parallel or perpendicular. In the situation of flow with an oblique inlet angle, the effects of parallel and perpendicular flow occur simultaneously. This results in refraction of the streamlines shown in Figure 6.4.

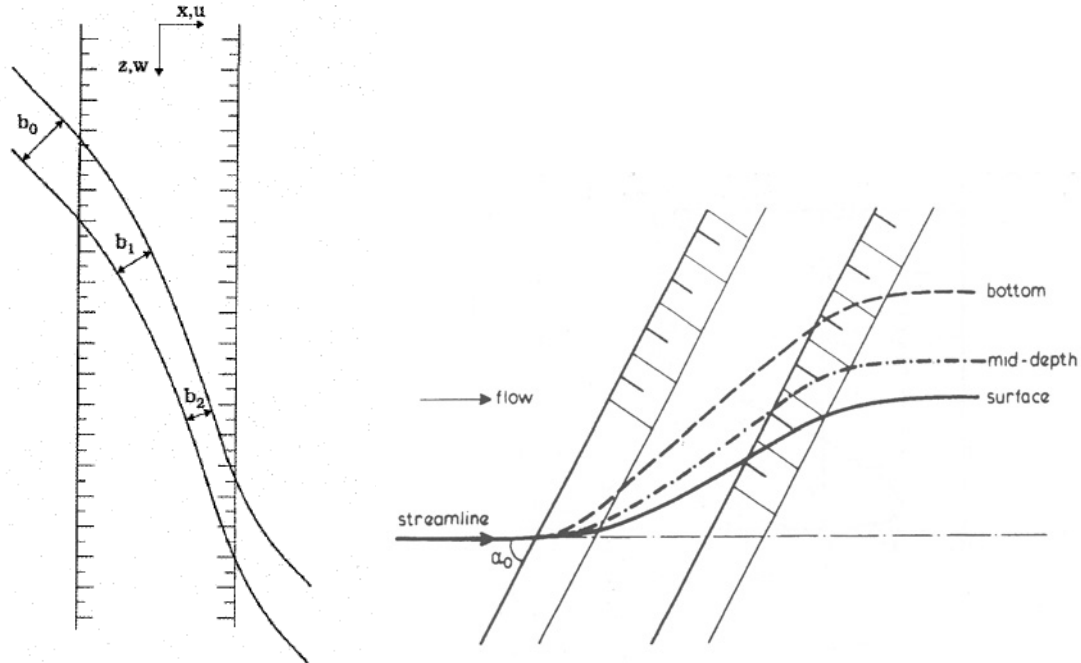


Figure 6.4 : Refraction of the streamlines in case of a flow with oblique inlet angle. Left: contraction of the stream lines. (Jensen, 1999a) Right: the refraction is stronger near the bottom of the trap. (Van Rijn, 2005)

The refraction of the depth average flow velocity is caused partly by the decrease of the flow component perpendicular and partly by the increase in the flow component parallel. The following relation is obtained (Jensen et al, 1999a) for the refraction,

$$\frac{u_1}{u_0} = \frac{b_0}{b_1} \frac{h_0}{h_1} \quad (6-6)$$

b is the width of the stream lines (Figure 6.4)

The refraction near the bottom of the trap is stronger than at the water surface, because the velocities are small near the bottom. To calculate the equilibrium velocity vector a combination of equations 6-2 and 6-3 is made,

- The velocity component normal to the axis is inversely proportional to the water depth $h_0 v_{0,normal} = h_1 v_{1,normal}$
- The velocity component parallel to the axis follows Chezy's law, $v = C\sqrt{hi}$

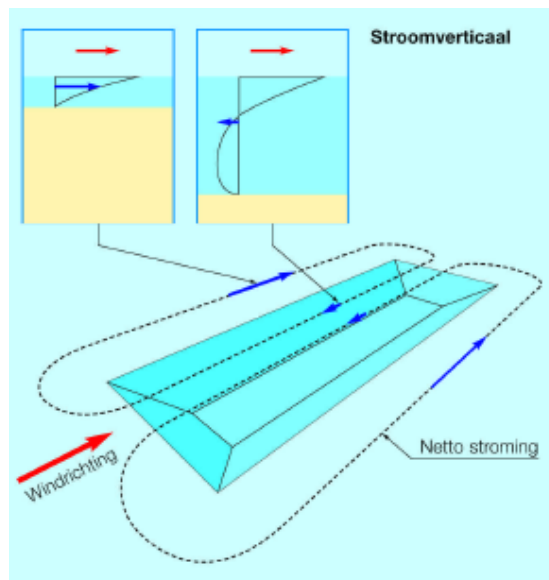
This results in the following equations (Van Rijn, 2005),

$$v_1 = v_0 \sqrt{\left(\frac{h_0}{h_1}\right)^2 \sin^2 \alpha_0 + \left(\frac{C_1}{C_0}\right)^2 \left(\frac{h_1}{h_0}\right) \cos^2 \alpha_0} \quad \text{Velocity magnitude} \quad (6-7)$$

$$\cot(\alpha_1) = \left(\frac{C_1}{C_0} \right) \left(\frac{h_1}{h_0} \right)^{1.5} \cot(\alpha_0) \quad \text{Velocity direction} \quad (6-8)$$

Wind driven flow

As mentioned in the introduction to this section, the flow pattern in the Markermeer is dominated by wind driven flow. The effect of a silt trap on the local flow pattern is somewhat different than described by Van Rijn and Jensen et al. A schematic picture of the flows around a silt trap with wind driven flow is shown in Figure 6.5.



Just outside of the trap (left of the trap) the net flow velocity (blue arrow) is in the same direction of the wind. Inside the trap a strong current near the bottom of the trap (in the lower part of the water column) is generated and has an opposite direction of the wind. In the upper part of the water column the flow is indeed in the direction of the wind. However, the net current is opposite to the wind direction. This means that the trap attracts the flow, just as in the situation of a parallel trap. Flow attraction can therefore be important for an increase in accumulation in the silt trap.

Figure 6.5: Flow pattern near a silt trap with wind driven flow. (Witteveen & Bos, 2004b)

The trap causes an attraction of the flow: the net flow is to the trap.

2DH and 3D modelling

Jensen et al (1999a) compared the results of a 3D flow model near a dredged channel with the results of a 2DH model. The conclusions are very clear:

'To predict the detailed flow behaviour and the direction and magnitude of the bed shear stress in particular, a 3D flow description is necessary.'

The current refraction, described in Figure 6.4 is a complex 3D process. The near bed flow is refracted more than the near surface flow. This difference causes a complex secondary flow pattern. This pattern will not be obtained if a 2DH model is used.

A well-modelled magnitude and direction of the flow velocity and bed shear stress are crucial for an accurate prediction of the sediment transport. To assess the efficiency of the silt trap a 3D model is necessary. This is again evidence that only a 3D model can be used to determine the transport and fate of the sediment in the lake and especially near a silt trap.

6.1.2 Waves

In analogy to currents, waves can approach the pit parallel, perpendicular or oblique to the axis of the trap. During most of the time there will be an angle between the wave direction and the main axis of the trap. In Figure 6.6 the possible effects of a channel on the wave direction are shown. This situation is near the coast, but is also valid for the Markermeer situation.

Waves with a very small approach angle will be reflected on the slope of the trap, causing reduced wave heights in the pit. If the angle is larger and clear oblique approach occurs ('crossing waves' in Figure 6.6), shoaling and refraction effects occur simultaneously and cause a disturbed wave pattern inside the pit.

In general waves propagating over the deep silt trap, will have a lower wave height inside the trap, because of the larger water depth. Wave celerity will increase inside the trap,

yielding curved wave crests. The wave energy will be reduced on the side slopes by refraction (Van Rijn, 2005).

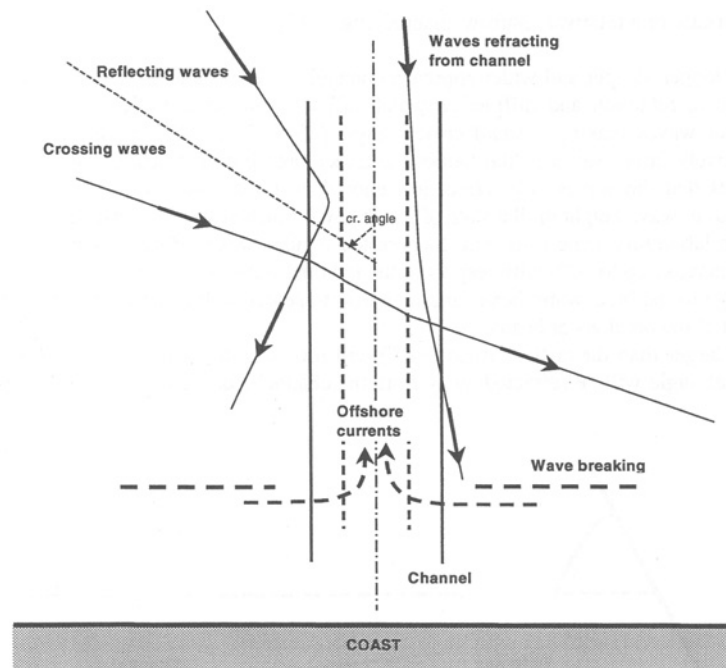


Figure 6.6: Wave direction near a channel or silt trap. (Van Rijn, 2005)
 Several processes can occur: reflecting if the incident angle is small.
 Refraction will occur if the waves cross the trap.

6.2 Sediment transport processes

This section will describe the two mechanisms that will cause an infill of the silt trap: settling of sediment from the water column and density currents (Section 1.2). Jensen et al. (1999b) give an extensive analysis of the sediment transport near dredged channels. This section only focuses on the two mechanisms.

6.2.1 Suspended sediment transport – settling

The settling of sediment from the water column (sediment in suspension) to the deeper parts of the silt trap is the result of a redistribution of sediment over the vertical. This redistribution is caused by a change in flow velocity and turbulence intensity above the trap. The distribution of sediment in suspension can be determined by using the advection – diffusion equation of the sediment concentration, c . This equation is (Jensen et al, 1999),

$$u \frac{\partial c}{\partial x} + v \frac{\partial c}{\partial y} + w \frac{\partial c}{\partial z} = w_s \frac{\partial c}{\partial z} + \frac{\partial}{\partial x} \left(\nu_T \frac{\partial c}{\partial x} \right) + \frac{\partial}{\partial y} \left(\nu_T \frac{\partial c}{\partial y} \right) + \frac{\partial}{\partial z} \left(\nu_T \frac{\partial c}{\partial z} \right) \quad (6-9)$$

u, v and w are the flow velocities in three main directions (m/s). ν_T is the eddy viscosity (m^2/s), which is used as a turbulent mixing coefficient.

The left part of the equation is the advection part. The three right parts describe the turbulent mixing in three directions. The advection and mixing is balanced by settling of the sediment (first right part). The settling velocity (w_s) is influenced by many processes, which are discussed in Section 3.2.

6.2.2 Density currents

The sediment concentration has influence on the density of the water in the Markermeer. If the sediment concentration in a volume of water increases, the density of that water volume increases, assuming that the volume does not change. If there is a density difference

between two locations (for example inside and outside a silt trap) a density current is generated. Density currents can have a large effect on the efficiency of a silt trap. This efficiency will be investigated in the silt trap model (Chapter 7). This section gives a rough estimation of the order of magnitude of the density currents.

The effect of sediment concentration on the density of the fluid is computed by the equation of state (Winterwerp, 2004),

$$\rho(S, T, c^{(i)}) = \rho_w(S, T) + \sum_i \left\{ \left(1 - \frac{\rho_w(S, T)}{\rho_s^{(i)}} \right) c^{(i)} \right\} \quad (6-10)$$

$\rho_w(S, T)$ is the density of water (kg/m^3) as a function of the temperature (T) and salinity (S). $\rho_s^{(i)}$ is the solid density of the mud (kg/m^3) fraction i and c the concentration of the fraction. With the equation of state, sediment concentration can be 'translated' into mixture density. The sediment induced density currents are accounted for by gradients in the momentum part of the Navier-Stokes equations ($\partial \rho / \partial x, \partial \rho / \partial y, \partial \rho / \partial z$). Density currents are only generated if there is a density gradient in horizontal or vertical direction.

A rough analysis of the density effect can be carried out using the well known Bernoulli equation, which is in the general form along a stream line (Kranenburg, 1998),

$$\frac{1}{2} \rho_0 u_0^2 + p_0 + \rho_0 g z = \frac{1}{2} \rho_1 u_1^2 + p_1 + \rho_1 g z \quad (6-11)$$

u is the flow velocity (m/s), ρ the density (kg/m^3), z the water depth (m), p the outside pressure and g the gravitation acceleration (9.81 m/s^2). The subscript 0 and 1 denote location/situation 0 (base) and new situation/location 1.

Figure 6.7 shows a schematic picture of the generation of a density current near a silt trap. In situation 0 a high concentration layer near the bed is present, with density ρ_2 and thickness z_2 . Just inside of the silt trap this layer is not present. This is the initial situation of the set up of the silt trap model (Section 7.1.3). If the initial flow is neglected in situation 0, the Bernoulli equation becomes,

$$\rho_1 g z_1 + \rho_2 g z_2 = \frac{1}{2} \rho_1 u_1^2 + \rho_1 g (z_1 + z_2) \quad (6-12)$$

The current generated by density effect just near the bed can be computed by,

$$u_1 = \sqrt{\frac{2(\rho_1 g z_1 + \rho_2 g z_2 - \rho_1 g (z_1 + z_2))}{\rho_1}} = \sqrt{\frac{2(\rho_2 g z_2 - \rho_1 g z_2)}{\rho_1}} = \sqrt{2 \Delta \rho g z_2}, \quad (6-13)$$

with, $\Delta \rho = \frac{\rho_2 - \rho_1}{\rho_1}$

The average velocity in the high concentration layer is then about half of it,

$$\overline{u_1} = \frac{1}{2} \sqrt{2 \Delta \rho g z_2} \quad (6-14)$$

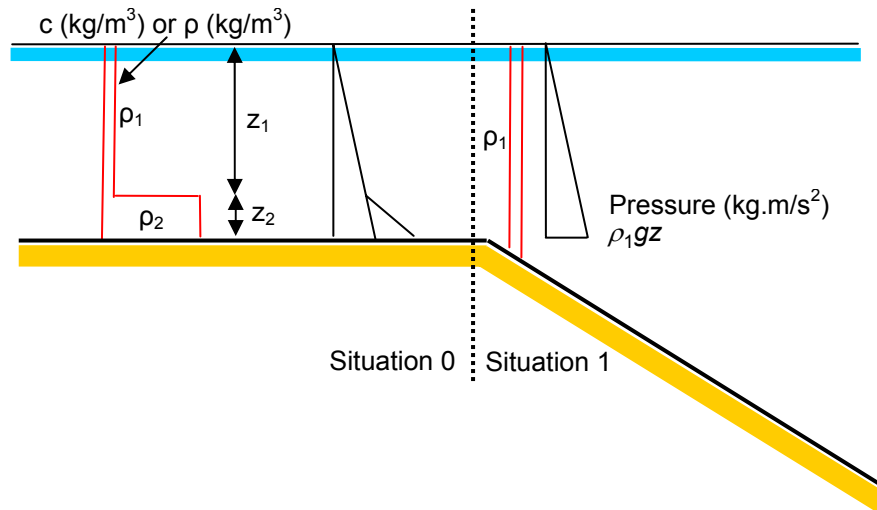


Figure 6.7: Schematic picture of a density current near a silt trap.

A density current is generated if density differences exist between 2 locations (0 and 1).

That difference between ρ_2 and ρ_1 is shown at layer z_2

In the Markermeer the thickness of the high concentration layer z_2 is about 10 to 20 cm. This is based on the echo sounder measurements (Section 4.2).

In this analysis with the Bernoulli equation, several assumptions are made. First of all it is assumed that no initial flow in situation 0 is present. In reality there will be a flow, also in the high concentration layer. Secondly the magnitude of the density difference is an initial difference. In situation 1 also a high concentration layer will originate, due to advection and diffusion of sediment from situation 0. The density difference will decrease, resulting in a decrease of the magnitude of the density current.

Third important assumption in this approach is that bed friction is not taken into account. In reality the flow in the high concentration layer will be influenced by friction with the consolidated bed. As a result the flow velocity will be lower. If this friction term is included in the formulation, the following formula will be obtained, taken from Kranenburg (1998),

$$\bar{u}_1 = \frac{1}{2} \sqrt{\Delta \rho g z_2} \quad \text{with } \bar{u}_1 \text{ is the average velocity of the high concentration layer.} \quad (6-15)$$

This formula calculates an average flow velocity in the high concentration layer which is about $\sqrt{2}$ times less than the formula derived from Bernoulli. Figure 6.8 shows the results of both formulas as a function of the sediment concentration. It can be concluded that the average flow velocities in the layer due to this density effect can become significantly high compared to the wind driven flow velocities (Table 3.1). Those velocities are in the order of about 0.10 to 0.20 m/s. The flow induced by density currents can become about 0.05 m/s, which is 25 to 50 %. Because this is relatively large, one can expect some influence of the density effect on the results of the model simulations about the silt trap. This influence is one of the research topics of this model study of the silt trap and will be described in Chapter 7.

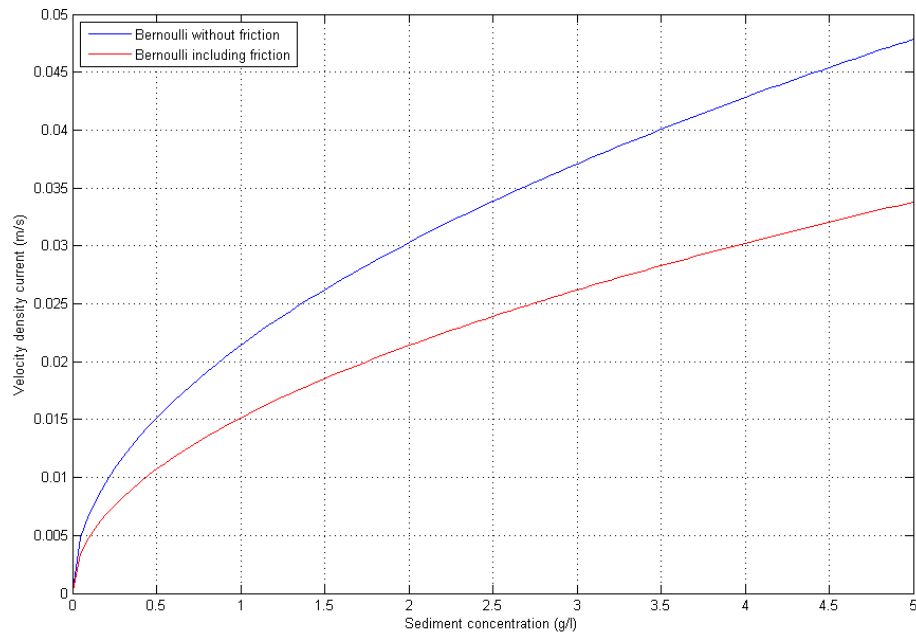


Figure 6.8: Velocity of the density current as a function of the sediment concentration. The velocity is proportional to the square root of the sediment concentration. The red line illustrates the results including friction with the bed. The blue line is the result without friction. The velocity including friction is $\sqrt{2}$ times less than without friction.

7 Delft3D model of the silt trap

This chapter describes the Delft3D model of the silt trap and can be considered as the main chapter of the report. The results of the model will give an answer to the main questions of this study:

- What is the dominant mechanism for the infill a silt trap?
- What is an optimal design of a silt trap to decrease the sediment concentration in the water column?

Finally the results of the model will give a definite answer to the question if a silt trap can be an effective measure to improve the water quality. These questions will be answered in the end of this chapter and in Chapter 8. First, a description of the general lay out of the silt trap model will be given in Section 7.1. Most of the characteristics of the large scale Markermeer model are also implemented in the silt trap model (the silt trap is set in the Markermeer model). For this reason only the differences between both models are discussed. Much attention is paid to the results of the different simulations. This is the main part of the study and will be described in Sections 7.2 and 7.3.

7.1 General lay out

7.1.1 Grid and bathymetry

First step in the set up of the silt trap model is the schematization of the silt trap itself. The length, width, depth and lay out of the silt trap are determined to schematize the trap in the model. For this study the lay out is based on early work about silt traps, which is discussed in 'Transparante Markermeren' (Witteveen & Bos, 2004b). In this report a typical silt trap of 80 hectare (2000 x 400 m, 50 m deep) is designed. This silt trap is shown in Figure 7.1.

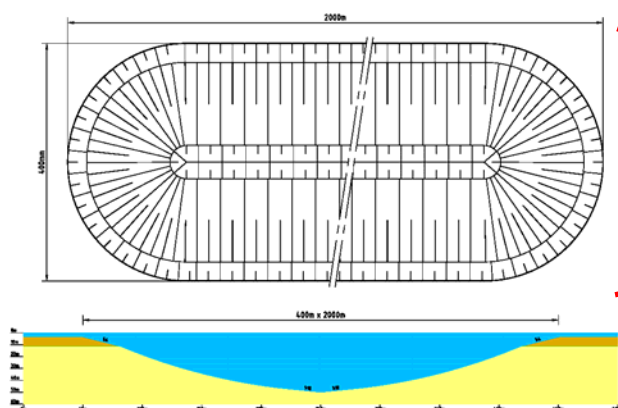


Figure 7.1: Design of the silt trap in the report 'Transparante Markermeren'. (Witteveen & Bos, 2004b)
The trap has an area of 80 hectare and a depth of 50 m.

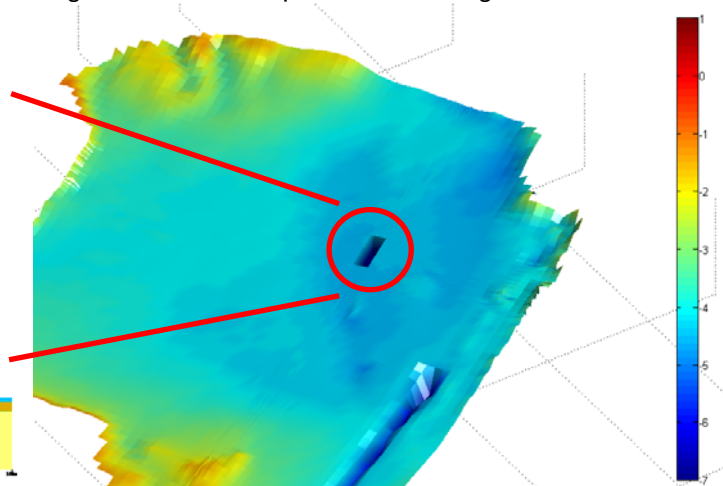


Figure 7.2: Location of the silt trap in the bathymetry of the Delft3D model.

The silt trap is small as compared to the overall size of the Markermeer. This has important consequences for the computation grid. In the silt trap area the grid should be finer than for the total model, to have sufficient resolution to simulate the physical processes near a silt trap. For this reason a finer grid is generated in the silt trap area. Outside the silt trap area the grid is the same as the grid of the large scale Markermeer model. The location of the silt trap in the bathymetry of the lake is shown in Figure 7.2. The trap in the model is a rectangular trap with a length of 2000 m, a width of 600 m and a depth of 16.5 m or 21.5

m below reference level (thus about 12 m or 17 m deeper than the surrounding area). The width is slightly larger than the width of the trap in Figure 7.1. This is for numerical accuracy. The depth is determined on wave penetration to the bottom of the trap.

Waves exert a shear stress on the bed of the trap. This bed shear stress decreases with increasing water depth. The depth of the trap must be large enough to restrain waves to have influence on the bed.

However the depth can not be too large, because of inaccurate model effects of strong vertical gradients in the grid. Depths of 16.5 m or 21.5 m are a compromise. In the simulations two depth values are used to assess the effect of a deeper and steeper trap on the sediment behaviour. The slopes of the trap are set to 1:20 and 1:15.

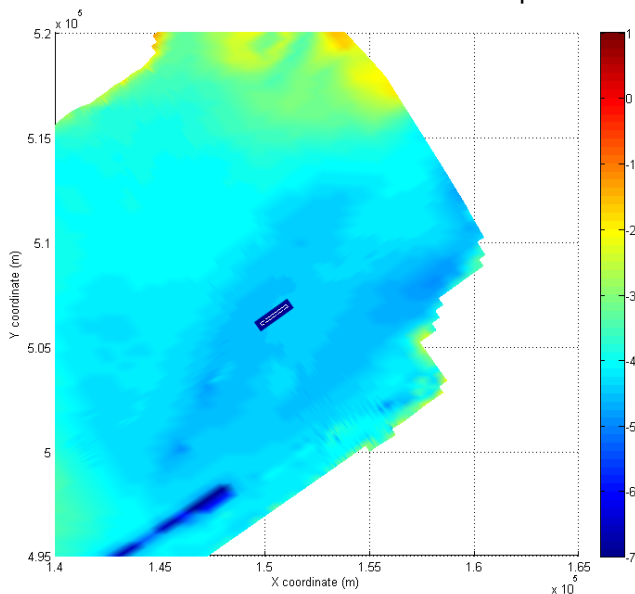


Figure 7.3: Location of the silt trap, parallel.

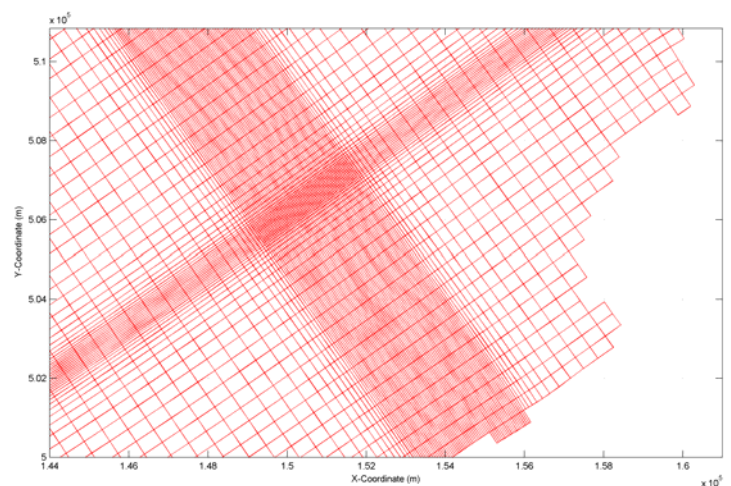


Figure 7.4: Grid of the silt trap model, parallel.
Refinement in the silt trap area.

The location of the silt trap in the Markermeer is shown in Figure 7.3, the grid in Figure 7.4. The location of the trap in the Markermeer is determined on the flow velocity and flow direction pattern which occur in the total Markermeer. If the wind is from the southwest (which is the dominant wind direction), water flows to the northeast in the upper layer of the water column and to the southwest near the bottom of the lake (Figure 3.4). For the trap configuration shown in Figure 7.3, the flow is parallel to the trap. If the trap is rotated over 90 degrees, the flow is perpendicular to the trap. Comparing both situations the effect of the orientation of the trap on the sediment behaviour can be studied.

The grid is not uniform in grid size. In the silt trap area the grid size is 50 x 50 m, because of the fine resolution needed for computational accuracy. The slope of 1:20 and 12 m difference will be divided over 5 grid cells, which is good for accuracy reasons. To save computation time the grid cells to the borders of the domain are larger. In these areas the grid has the same size as in the Markermeer model without trap. A gentle transition between the fine and coarse part of the grid is established.

In the vertical, the water column is divided into 20 layers, just like in the Markermeer model. However in that model the height of the layers has an equal proportionality of 5 % of the water depth. In the silt trap model the height of the layers is not equally distributed, the layers near the bed are finer. The reason for this is to have a higher resolution near the bed, to have more information about the behaviour of density currents near the silt trap. The layer distribution is shown in Table 7.1.

k	1	2	3	4	5	6	7	8	9	10	11	12	13	14	15	16	17	18	19	20
%	6.5	6.5	6.5	6	6	6	6	6	6	6	6	6	6	6	3	2	1.5	1	0.5	

Table 7.1: Height of the vertical layers (k = 1 top layer, k = 20 lowest layer) as a percentage of water depth.

The vertical grid near the silt trap is shown in Figure 7.5. This figure shows that the grid cell height becomes larger with increasing water depth (this is a characteristic of the sigma grid, Section 5.2.2). The grid cells are higher in the silt trap area.

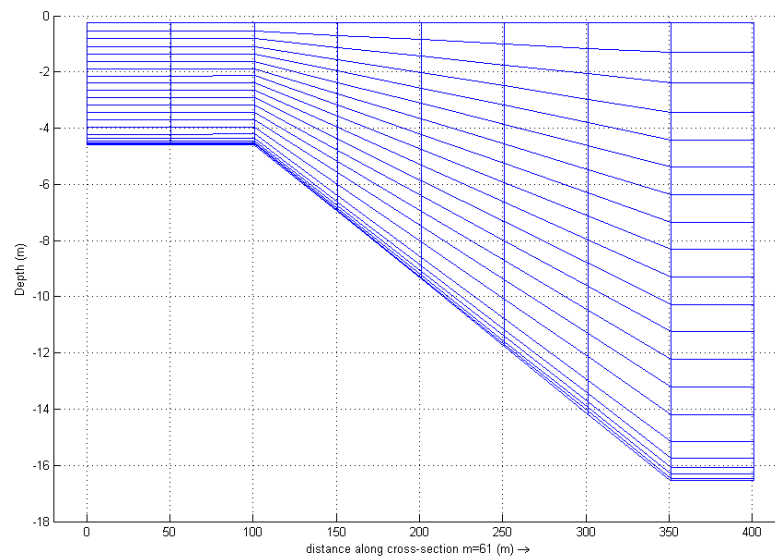


Figure 7.5: Part of the vertical grid near the silt trap. In the area with a large water depth, the grid height is also larger.

The bathymetry of the trap is already discussed in the previous part, but again shown in Figure 7.6 for completeness. The silt trap is implemented in the model as a rectangular shaped trap, with straight slopes. The bottom of the trap has an area of 15 hectare (1500 x 100 m)

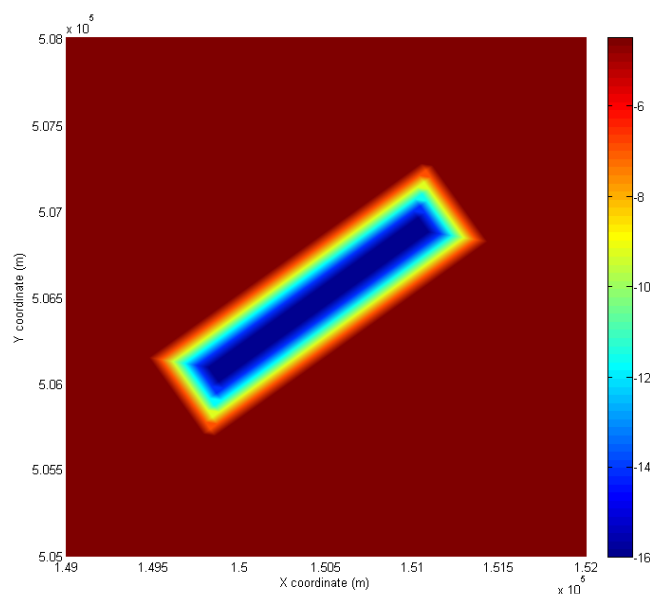


Figure 7.6: Bathymetry of the silt trap model. The silt trap has a depth of 16.5 or 21.5 m. The surrounding area about 4.5 m.

7.1.2 Initial conditions

The initial conditions (water level, velocity and sediment concentrations) are mostly the same as in the Markermeer model (Table 5.1). The calibration results showed that, by using these conditions, the sediment concentrations match the field measurements. The concentration profiles shown in Figure 5.7 are also imposed in this model. However in the area where the silt trap is located the initial high concentration layer near the bed is absent; in the silt trap model this layer has also the low initial concentration, just like the other layers in the vertical. This difference in initial concentration in the silt trap area is

implemented, because by using this model set up, the total sedimentation rate of the silt trap is obtained. This model set up can be considered as a schematic representation of the situation just after the dredging of the silt trap. The high concentration layer near the bed is also absent just after dredging the trap, it is removed by dredging. The simulation period of the model can be considered as the period of about 10 days just after the dredging.

In the reference case (situation without trap) the normal initial sediment concentration profile is used, because then there is no trap and the high concentration layer is not removed by dredging.

7.1.3 Sediment characteristics

The sediment characteristics in this silt trap model are the same as finally obtained in the calibration process of the large scale Markermeer model (Table 5.1). Using these settings the sediment behaviour is modelled quite well. The only modification to these settings is the gelling concentration (reference density for hindered settling). In the large scale model this parameter is set to 100 kg/m^3 , which is a high value. However in that model this parameter had no influence, because of the large grid height near the bed (0.20 m, 5 % of the water depth). If all the coarse sediment (mud 2) settles in the lowest layer, the concentration in that layer is approximately 3 g/l. In the silt trap model, the lowest layer is only 0.02 m (only 0.5 % of the water depth). If in this model all the sediment will settle, then the concentration will become 30 g/l. This high sediment concentration does not correspond to the measured sediment concentration. For this reason the gelling concentration is set to about 3 g/l, to avoid unrealistic high concentration layers near the bed. For sensitivity analysis the gelling concentration is also increased in two runs, to 10 g/l.

7.1.4 Observation points and cross sections

For the analysis of the model results observation points and cross sections are defined. The location and names of the observations points and cross section are different for the parallel and perpendicular case.

In appendix C Figures C.1 and C.2 the locations of the observation points are shown. 3 points are inside the trap (one in the middle, two on both edges). Other points are just outside the trap, on the edge. At these points all hydrodynamic and sediment parameters are stored with a time interval of 10 minutes, starting at the 3th of December.

In appendix C Figures C.3 and C.4 the cross sections are shown. The cross sections are defined at the edge of the trap and enclose the trap (four cross sections, one for each side of the trap). Sediment transport through these sections is calculated for each mud fraction separately, with a time interval of also 10 minutes.

The total accumulation of sediment in the silt trap can be calculated with the transports through these cross sections. This analysis will be explained in Section 7.3.2.

7.1.5 Other input parameters

Time frame

Because the number of grid cells is increased by refining the grid for the silt trap area, also the computation time is increased. To keep the total computation time equal, the simulation period is shortened with 2 days to,

3-12-2007 0:00 – 12-12-2007 0:00

Comparing to the large scale model, the last two days are omitted. In Section 5.3.2 it is already mentioned that during these two days the wave computations are not reliable. For this reason these days are left out of the simulation period. The time step is kept the same, $\Delta t = 2 \text{ min}$.

The Courant number in the silt trap area changes, because the grid is finer in that area. Taking $\Delta x = 50 \text{ m}$, instead of 400 m (coarse grid) and $U = 0.40 \text{ m/s}$, the Courant number is 0.96. This is still less than 1 and therefore acceptable.

7.2 Alternative scenarios

7.2.1 General

The objective of the silt trap model is to answer the questions stated in Chapter 1 and in the introduction to this chapter. Several simulations are carried out to assess the influence of density currents, silt trap orientation and silt trap dimensions on the effectiveness of the trap.

In total 14 simulations and 1 reference simulation are carried out. This reference simulation is the situation that no silt trap is implemented in the model, but other model settings are the same as in the simulations with the silt trap. This reference simulation will be the basis of the other simulations; all simulations will be compared to that simulation. The results of this reference simulation will be discussed in the next section.

In Table 7.2 a schedule of all simulations is shown.

Name of simulation	Effect sediment concentration on fluid density	Silt trap orientation to the wind	Silt trap slope	Silt trap depth (m)	C_{gel} (kg/m ³)	Critical shear stress sedimentation
Parallel 1	Yes	Parallel	1:20	16.5	3	$\tau_{c, sed}$ low
Parallel 2	No	Parallel	1:20	16.5	3	$\tau_{c, sed}$ low
Parallel 3	Yes	Parallel	1:15	21.5	3	$\tau_{c, sed}$ low
Parallel 4	No	Parallel	1:15	21.5	3	$\tau_{c, sed}$ low
Parallel 5	Yes	Parallel	1:15	21.5	10	$\tau_{c, sed}$ low
Parallel 6	No	Parallel	1:15	21.5	10	$\tau_{c, sed}$ low
Parallel 7	Yes	Parallel	1:15	21.5	3	$\tau_{c, sed}$ high in trap
Parallel 8	No	Parallel	1:15	21.5	3	$\tau_{c, sed}$ high in trap
Perpendicular 1	Yes	Perpendicular	1:20	16.5	3	$\tau_{c, sed}$ low
Perpendicular 2	No	Perpendicular	1:20	16.5	3	$\tau_{c, sed}$ low
Perpendicular 3	Yes	Perpendicular	1:15	21.5	3	$\tau_{c, sed}$ low
Perpendicular 4	No	Perpendicular	1:15	21.5	3	$\tau_{c, sed}$ low
Perpendicular 5	Yes	Perpendicular	1:15	21.5	3	$\tau_{c, sed}$ high in trap
Perpendicular 6	No	Perpendicular	1:15	21.5	3	$\tau_{c, sed}$ high in trap
Reference	Yes	No silt trap	-	-	3	

Table 7.2: Schedule of the different alternative simulations of the silt trap model and the different settings.

The parameters that are varied in the simulations are:

- Effect of sediment concentration on fluid density. This effect can be switched on and off in the Delft3D model. The effect of the sediment concentration on the fluid density is described by the equation of state (equation 6-10). If this effect is not taken into account the fluid density is the same as the water density (1000 kg/m³) and no density currents are generated in the model.
- Orientation of the silt trap to the wind. This also means: orientation of the silt trap to the near bed flow, because the direction of the near bed flow is opposite of the wind direction at the location of the trap. Two alternative situations are investigated: parallel and perpendicular to the wind direction. The lay out of the model in both cases will be given in Section 7.2.3.
- Silt trap dimensions, which are slope and depth of the trap. These parameters are varied to give recommendations about the optimal design of the silt trap.
- The gelling concentration. This parameter is only varied for sensitivity analysis, not to give advice about the silt trap.

- Critical shear stress for sedimentation. In the large scale Markermeer model the critical shear stress for sedimentation ($\tau_{c, \text{sed}}$) is set to a very low value $1 \cdot 10^{-15} \text{ N/m}^2$. Consequently no sedimentation occurs, all sediment is kept in the water column. In the first simulations this setting is also applied. So inside the trap the sediment also kept in the water column. This is not true in reality. Especially inside the trap sedimentation occurs and the sediment is removed from the water column. To assess the maximum sedimentation rate, in 4 simulations the $\tau_{c, \text{sed}}$ is set to a very high value at the bottom of the trap, 100 N/m^2 . In that case full sedimentation occurs.

In the next sections more detailed information will be given about the several alternative simulations.

7.2.2 Reference case – Validation

The reference simulation is carried out to get a reference case, to which all other simulations can be compared. This reference case is the present situation in the Markermeer, without silt trap being dredged in the lake. The bathymetry of the large scale model is also used in the reference simulation.

In this simulation three important adaptations to the large scale model (Chapter 5) are carried out. These adaptations can probably influence the sediment behaviour,

1. The horizontal grid is refined locally in the silt trap area.
2. The vertical grid is refined near the bed for the completed model domain.
3. The gelling concentration is set to a lower value.

These adaptations should not change the sediment behaviour to a large extent. In Chapter 5 it was mentioned that the large scale model is well calibrated for simulations of the silt trap; the model including these adaptations should not change this result. To check the effects of these adaptations, the sediment behaviour in the reference case is compared to the behaviour in the large scale model. Sediment concentrations at the location of the measurement pole (FL 42) are compared in the same way as described in Chapter 5. This comparison can be considered as validation of the modified model to the calibrated model.

The results are shown in Figure C.5. The green line is the reference simulation, the red line run 14 (last calibration run) and the blue line are the ASM measurements. The green line shows the same pattern as the red line, but predicts a slightly higher sediment concentration in time, except at the 7th of December. At that day the concentration is lower than in run 14.

It can be explained that the sediment concentration is a bit higher in the reference case. This is due to the lower gelling concentration. Because of this lower gelling concentration (3 g/l in the reference case) the settling velocity is reduced more than in run 14 (gelling concentration 100 g/l).

According to equation 3-15, ϕ is higher if C_{gel} is lower (sediment concentration is the same). Because ϕ is higher the reduction of the settling velocity is higher (according to Richardson and Zaki equation). If the settling velocity is lower, the sediment is easier resuspended into the water column and the concentration becomes higher.

However, the increase in concentration is not large and during some times the green line describes even better the measurements (for example the 8th of December). For this reason it is concluded that the adaptations to the model do not have a large influence to the sediment behaviour. The model can be used to assess the effects of the silt trap.

7.2.3 Silt trap orientation and dimensions

One of the main objectives of this study is to give an advice about the optimal design of the silt trap. 'What design of the trap gives the highest reduction in sediment concentration?' Several basic design parameters of the trap are varied: orientation, slope of the trap and depth of the trap. The effectiveness of the trap is also highly dependent on the location of the trap in the Markermeer. In this study it is decided to fix this location. This study focuses

on the different physical processes near a trap on a local scale; future studies should look at the most efficient location in the lake.

Two orientations of the trap are investigated: parallel and perpendicular. Both alternative situations are shown in Figure 7.7. This study will assess the effect of the orientation of the silt trap for both typical flow patterns. This assessment can be used by determining the orientation of the trap when the exact location is chosen. Because this study focuses on the basic processes it is irrelevant where the silt trap is located in this model.

The slope and depth of the silt trap are coupled in these simulations. If the trap is deeper, the slope will be steeper. This is done to get the same grid resolution in the silt trap. In the simulations a slope of 1:15 and 1:20 is used. These slopes are gentler than the slope will be in reality. The silt trap will be dredged with slopes varying from 1:4 to 1:10. However for numerical aspects it was not possible to implement such steep slopes in this model. To get a reliable computation the grid must be even finer and consequently computation time will be longer.

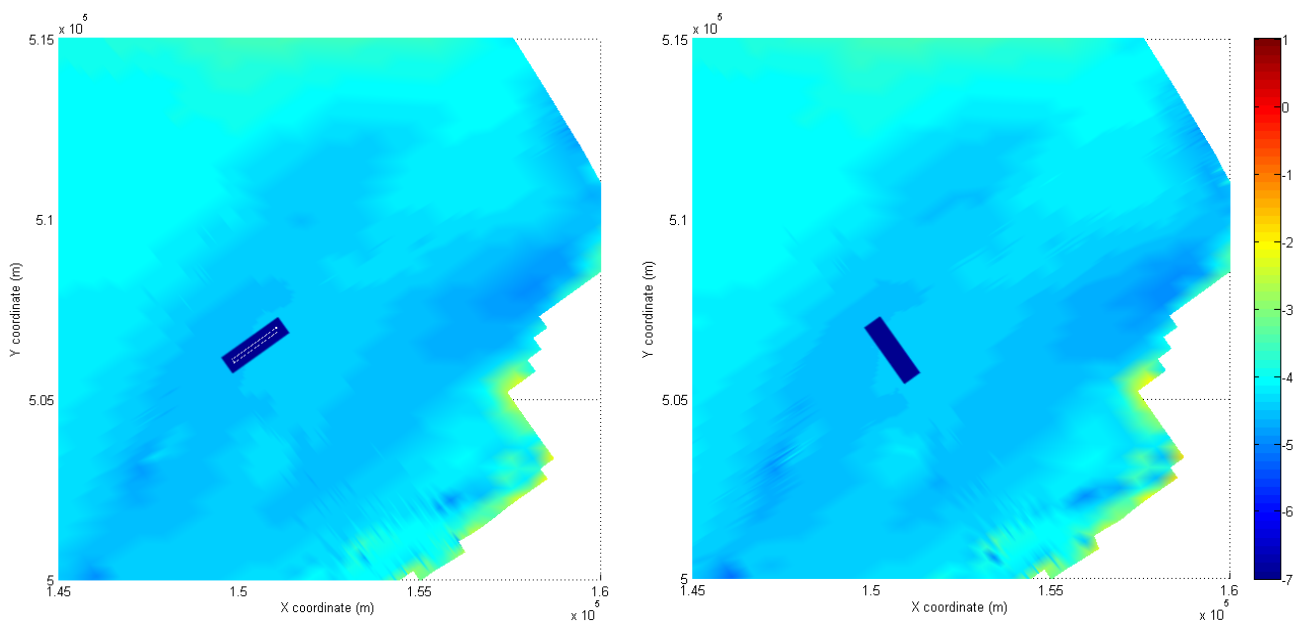


Figure 7.7: Two alternative orientations of the silt trap, parallel (left) and perpendicular (right).

7.3 Results

7.3.1 Comparison to the hydrodynamic theory

Unfortunately no data is available about the hydrodynamic processes and sediment behaviour near a deep pit in the Markermeer. Consequently no validation of the Delft3D model of the silt trap can be carried out. It is hard to determine if the model predicts all processes near a silt trap correctly. However in Chapter 6 basic theory is described about the flow patterns and sediment behaviour near and in a silt trap. Also an estimate is made about the influence of sediment concentration on the density currents. In this section the results of the model are compared to the theory, to determine the reliability of the model.

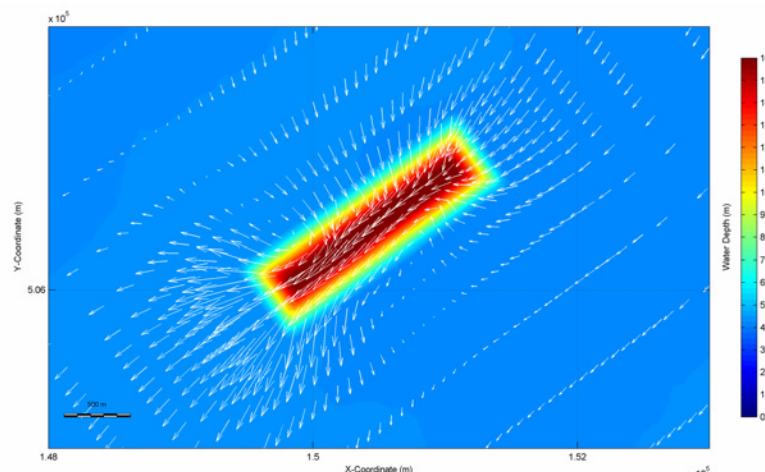


Figure 7.8: Depth average flow velocity situation trap parallel, 7-12 12h00.

Flow

Van Rijn (2005) and Jensen et al. (1999) describe the theory about the flow patterns near a dredged channel. This theory can also be applied for sand mining pits. A distinction is made in parallel and perpendicular flow with respect to the main axis of the trap. For parallel flow, flow contraction occurs in the area of the silt trap and the depth average velocity increases (Figure 6.1). According to the model results in Figure 7.8 and C.6 in appendix C the same flow contraction and flow divergence pattern can be recognized. Just upstream of the silt trap, the flow accelerates and contraction occurs. In this situation the silt trap 'attracts' the flow. Just downstream of the silt trap the flow velocity decreases and the flow diverges.

In Figure C.7 the perpendicular situation is shown. However the flow direction is not exactly perpendicular of the silt trap, but slightly oblique. Therefore this situation is compared to Figure 6.4 (theoretical oblique flow). In this figure a refraction pattern is shown, with the effect of refraction increasing close to the bed. This refraction pattern is also reproduced by the model. Flow approaches the silt trap in northeast direction. Inside the trap the flow is refracted to the north direction and just downstream of the trap the flow is again northeast.

Although the theory given in Chapter 6 was developed for a different situation than in the Markermeer case (navigation channel near the coast), it appears that the flow patterns reproduced by the model correspond quite well to this theory.

Waves

Van Rijn (2005) stated that, in general, waves will have a lower wave height above the silt trap, when they propagate over the trap. Figure C.8 shows the wave height in time for three points near the silt trap during simulation parallel 1. Also the reference case is added to the plot; the situation without silt trap.

The figure shows that the wave height slightly increases in the area of the silt trap. Especially the high waves (wave heights up to 1 – 1.5 m) increase even more in the situation with the silt trap. The increase in wave height is about 5 to 10 cm, which is about 5 to 10 %. This slight increase in wave height can be explained from wave focussing in the trap, due to refraction on the slopes of the trap. Waves will be refracted to the centre of the trap, resulting in an increase in wave energy and interaction. The wave height increases. This process is illustrated in Figure 7.9.

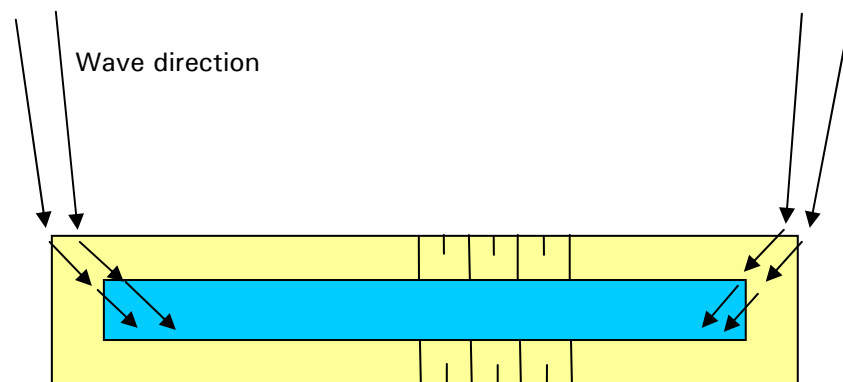


Figure 7.9: Schematic situation of refraction pattern of waves near a trap (not to scale). This refraction pattern causes an increase in wave energy and wave height above the silt trap.

This increase of wave height causes higher turbulence intensity in the water column above the silt trap. For this reason the sediment can settle less easily in the trap. However the increase in wave height is not extremely high, so no large influence on the settling process is expected.

7.3.2 Effect density currents

Comparison to the theory

In Section 6.2.2 a rough estimate of the effect of sediment concentration on the density current is made. This estimate is based on the basic theory of Bernoulli and is carried out for the initial situation of the model. Initial situation means no sediment is available the inside the silt trap and just outside a high concentration layer is imposed near the bed. In this situation a flow in the order of several centimetres per second can be generated by the density current (about 2 to 3 cm/s).

In the model the density effect can be determined by comparing the simulations parallel 1 and 3 (including the effect) to parallel 2 and 4 (not including the effect). Just in the initial situation (at the time of 3th of December 0:10) and on the edge of the silt trap (observation points 55,90 and 68,90) the horizontal flow velocity and sediment concentration profiles are shown in Figures C.9, C.10 and 7.10.

In the plots of the horizontal velocity a difference in horizontal velocity is shown near the bed between parallel 1 and 3 (red and purple line) and parallel 2 and 4 (green and black line). This difference is due to density currents in the direction of the silt trap. The magnitude of the density current is about 2 to 3 cm/s, just as estimated in theory. The sediment concentration near the bed is about 1.2 g/l (for all simulations). According to Figure 6.13 the flow velocity in the density current can be determined for this concentration. This is also 2 to 2.5 cm/s.

Figure C.11 shows that these density currents can also be generated if the initial effect is already disappeared. This plot is taken at the 10th of December 6:00, towards the end of the simulation period. The magnitude of the density current is even higher (about 5 cm/s) than in the initial situation.

The model describes the effect of density currents according to the theory very well.

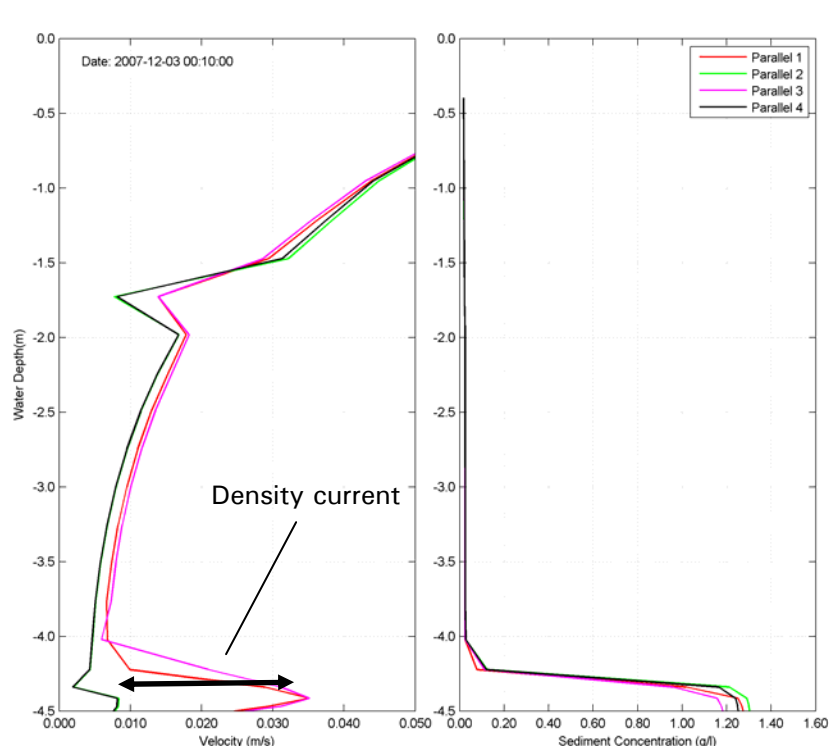


Figure 7.10: Velocity (left) and sediment concentration (right) profile on the 3th of December 0h10, location (55,90). Near the bed a density current is generated with velocity of 2 cm/s. This is the difference between the red/purple and the green/black line in the left figure at a water depth of -4.4 m. The discontinuity at a depth of -1.7 m is an initial effect of building up of the velocity profile.

Generation of density currents

Further analysis on the effect of density currents is shown in Figures C.12 and C.13. In both figures the first plot shows the difference in horizontal velocity between two simulations with and without the density effect, averaged over the lowest 4 grid cells in the vertical (about 20 cm near the bed). Actually this is the mean magnitude of the density current. The second plot shows the sediment concentration, averaged over the lowest 4 grid cells.

In the first plot in Figure C.12 it is shown that during most of the time no significant density current is generated (velocities less than 2 cm/s). There is a correspondence between the increase of sediment concentration and the magnitude of the density current. If the sediment concentration near the bed is increased rapidly to about 1 g/l a density current is generated of 2 cm/s or even more (e.g. at the 4th of December). At the 10th of December this is even 4 cm/s. This increase in sediment concentration corresponds to the forcing to the wind. If the wind speed drops, the sediment concentration profile in the water column collapses. This increase of sediment concentration near the bed is about 1 day after a storm period and can only occur if the wind speed is reduced for more than one day. In the period of the 5th to the 9th of December, the wind increases and decreases rapidly, three storm periods are recorded just after each other. No high concentration layer can be built up. Finally at the 10th of December the wind speed decreases for a longer time and the sediment concentration increases in the lowest layer.

It can be concluded that a density current can be generated if mild wind conditions occur for at least one day after a storm. During that day the coarse sediment can settle out of the water column, building up a high concentration layer near the bed. If the high concentration layer is increased to 1 g/l or more, a significant density current is generated.

Accumulation in the silt trap

To assess the effect of the density current on the accumulation of sediment in the silt trap, data from the cross sections are used. The total amount of sediment which is caught in the trap is a measure for the effectiveness of the trap. In the end if the silt trap functions properly it should catch the sediment.

The total amount of sediment accumulated in the trap is calculated from the cumulative total sediment transports through the cross sections (in m³). In Figure 7.11 the direction of positive transport is shown for each cross section in the parallel situation. The total amount of accumulated sediment is calculated by adding and subtracting the transports, according to the equation (7-1),

$$\text{Accumulation in silt trap}_{\text{par}} = \text{Transport}_{\text{north}} + \text{Transport}_{\text{west}} - \text{Transport}_{\text{south}} - \text{Transport}_{\text{east}}$$

This equation holds for the parallel situation. In the perpendicular case the formula is (7-2),

$$\text{Accumulation in silt trap}_{\text{perp}} = \text{Transport}_{\text{NW}} + \text{Transport}_{\text{SW}} - \text{Transport}_{\text{SE}} - \text{Transport}_{\text{NE}}$$

The total amount of accumulated sediment in the trap changes in time. Figure C.14 till C.17 show the results of these calculations. Figures C.14 and C.15 show the results of the simulations with a low critical shear stress for sedimentation inside the trap. Figures C.16 and C.17 show the results of the simulations also with full sedimentation in the deepest part of the trap.

According to Figures C.14 and C.16 it can be concluded that for the *fine fraction* the effect of density current on the infill of the trap is nil. For both orientations and for all simulations the lines are almost identical. However the fine fraction can accumulate in the trap. This is shown in Figure C.16. The lines representing the simulations with full sedimentation show a constant increase, which means that the fine fraction accumulates in the trap. At the end of the simulation period in total about 100 m³ is accumulated. This accumulation is not caused by density currents, because the lines for simulations with and without the density effect are almost identical. Advection and settling cause the accumulation of fine material in the trap. It is hypothesized that this accumulation occurs after a storm period. The fine sediment

in the water column above the trap can settle out in the trap if turbulence intensity decreases. The surface area of the trap determines the total accumulation in the trap.

For the *coarse fraction*, density effects can indeed play a part in the filling of the silt trap. Figures C.17 and 7.12 show a difference in the total amount of accumulated sediment in the trap for simulations with and without density effect. Simulations parallel 7 (red line) and perpendicular 5 (purple line) include this effect; parallel 8 (black) and perpendicular 6 (green) not.

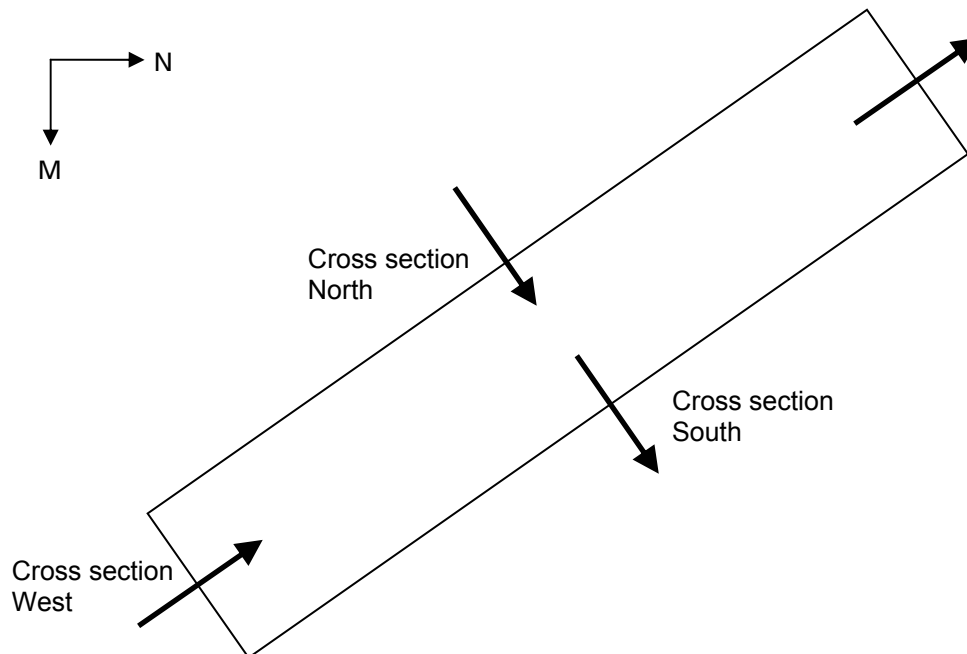


Figure 7.11: Direction of positive transport through the cross sections.

The amount of sediment accumulated in the trap by density current in the parallel case is $7590 - 6246 = 1344 \text{ m}^3$ at the end of the simulation period. This is about 18 % of the total amount in the trap. For the perpendicular case it is even more, $7866 - 6229 = 1637 \text{ m}^3$, about 21 %.

An important conclusion is that the increase of accumulated sediment for the perpendicular case is completely determined by the density effect. In the simulations without density effect (simulation parallel 8 and perpendicular 6) no difference is observed for the parallel and perpendicular case. In the simulations including this density effect (simulation parallel 7 and perpendicular 5) there is a difference. Consequently this difference is completely due to the increase in density current.

It can be explained that in the perpendicular case the density current is more important. In the perpendicular case there is no increase of flow velocity observed near the trap, in the parallel case it is. The parallel silt trap attracts the flow: flow is accelerated near the trap and also inside the trap the flow velocity increases (Figure 7.8 and Section 6.1). Figures C.28 and C.29 show this increase inside the trap.

Figure C.28 shows the horizontal velocity in the lowest layer ($k=20$) in time, for all simulations. The blue line is again the reference case. According to these results also a large increase in velocity is observed for flow inside the parallel silt trap. At the 7th of December the flow velocity increases from 0.05 m/s (reference, blue line) to 0.2 m/s (parallel simulations), about four times higher. But also between two storm periods the flow velocity is much larger. This increase in flow velocity causes a higher turbulence intensity in the water column and an increase in bed shear stress. Figure C.29 shows the bed shear stress in time. The same pattern of increase is shown as for the velocity in C.28.

Due to this increase in velocity, also the turbulence intensity increases. This results in a higher mixing of sediment in the water column for the parallel case. Because of this higher mixing the high concentration layer near the bed is generated less easily. Density currents are generated by the high concentration layer. Consequently for the parallel case the generation of density currents will be less, so the influence of density currents is less than in the perpendicular case.

Transport through each cross section

In Figures C.18 to C.21 the transport through each separate cross section is shown. Figures C.18 and C.19 show the parallel orientation of the trap, C.20 and C.21 the perpendicular case. Simulations parallel 4 (black line) and 8 (green line) are the simulations without density effect. Simulations parallel 3 (pink) and 7 (red) include this effect. For all directions the total transport through the cross section is larger if the density effect is not included. This effect is larger by the transports out off the trap (Figure C.18): the difference between the red and green line out off the trap (cross section west, straight line) is larger than between the dashed red and green line (this transport is to the trap, cross section east)

This can be explained from the fact that the direction of the density current is always towards the trap (positive, direction of the slope). If the net transport is out of the trap (negative), this net out transport is decreases by the density current (always positive). If the density current is not taken into account the total net transport out of the trap is higher. Because of this decrease in net out transport due to density current on the slope, accumulation in the trap will be higher.

7.3.3 Orientation and depth of the silt trap

Orientation

The effect of the orientation on the effectiveness of the silt trap can be determined by two parameters,

- Total amount of sediment accumulated in the silt trap.
- Average sediment concentration in the water column above the silt trap.

The total amount of accumulated sediment in the silt trap is already discussed in the previous section (7.3.2) The conclusion of this analysis was that the silt trap with a perpendicular orientation to the dominant flow direction will catch more sediment. This is because the flow velocity (turbulence intensity) is not increased (as is in parallel case). Mixing is less and the density current is a more important mechanism in the perpendicular case.

The average sediment concentration above the silt trap is shown in Figure C.22 and C.23. This average concentration is calculated at the point in the centre of the silt trap ((61,90) for the parallel case and (80,72) for the perpendicular case). The sediment concentration is averaged over the first 3 m of the water column, for each sediment fraction separately.

Results for the *fine fraction* (mud 1) are shown in Figure C.22. It can be concluded that no significant decrease in sediment concentration is expected for the fine fraction. All lines are close to the reference simulation (blue line). Only a decrease of a few percent is expected. The turbidity problem in the Markermeer is caused by the fine material. For this reason the silt trap might be an ineffective measure. However, Figure C.16 showed that the fine fraction is caught in the trap; fine material is removed from the water column. The effect of this removal can not be observed in a decrease of sediment concentration for this short period. Only 10 days are simulated. The amount of fine material removed from the water column in these 10 days is too small, comparing to the total amount of fine fraction. For a longer period (years to decades) this removal might cause some reduction in total amount of the fine sediment in the lake and for this reason reduce the concentration. This is also proved by the following estimate:

The total volume of water in the lake is about $2.5 \times 10^6 \text{ m}^3$ (Section 2.2) The maximum sediment concentration of the fine fraction is about 80 mg/l. So in total about $1.95 \times 10^8 \text{ kg}$ fine material is present in the lake. The specific density is assumed 2650 kg/m^3 , this gives $7.4 \times 10^4 \text{ m}^3$ of fine material in the lake. The total accumulation of fine material during the 10 days of simulation is about 100 m^3 , this is about 0.13 % of the total amount. In this period 4 storms are present. Assuming 25 storms per year, about 1 % of the total amount of fine sediment can accumulate in the trap per year. In 20 years about 20 % of the fine sediment can be removed from the water column with this silt trap, if the production is neglected.

Although this is a rough estimation, based on many assumptions, it can be concluded that the silt trap will reduce the amount of fine material in the lake.

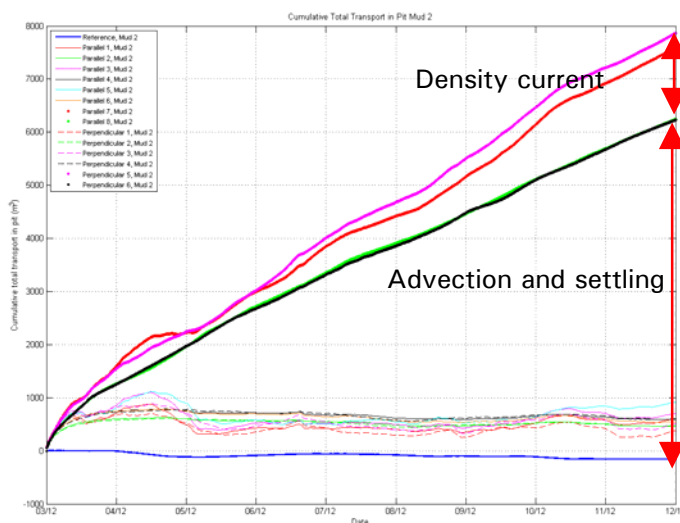


Figure 7.12: Cumulative Total Transport in trap Mud 2. Thick green/black: no density effect, thick red/purple: including density effect. The perpendicular trap has a larger accumulation than parallel trap.

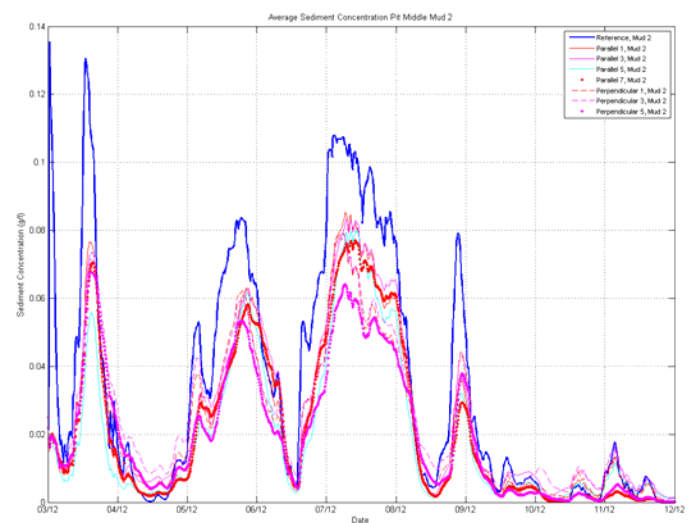


Figure 7.13: Average sediment concentration Mud 2, upper 3 m of water column. The blue line is the simulation without trap. Simulation perpendicular 5 (pointed purple line) gives highest reduction in sediment concentration

Results for the *coarse fraction* (mud 2) are shown in Figures 7.13 and C.23. The sediment concentration for the coarse fraction is dominated by the wind forcing. During times of strong winds the concentration of mud 2 is much higher than in calm periods. For example during the 7th of December a storm is present and the concentration increases to about 80 mg/l (reference simulation, blue line). At the end of the simulation, a calm period occurs and the concentration of mud 2 is almost zero in the water column. During the storm periods the silt trap can reduce the sediment concentration of this coarse fraction. The reduction can be high, up to 50 % during some storms (for example around the 9th of December).

Comparing to all simulations, the simulation perpendicular 5 (bold purple line) causes the highest reduction in sediment concentration. This is also the simulation in which the most sediment is accumulated in the silt trap. It can be concluded that the silt trap with a perpendicular orientation causes the highest reduction in sediment concentration during storm periods. For example during storm period at the 5th of December this is 82 mg/l to 52 mg/l, which is 37 %. At the 7th of December the reduction is from 107 mg/l to 64 mg/l, 40 % and at the end of the 8th of December it is even more: 79 mg/l to 38 mg/l, 52 %. These results are from simulation perpendicular 5. Other simulations show also a lower reduction during these storm periods. During periods with calm weather all simulations which include the density effect, show the same results.

In Figures C.24 to C.27 two cross sections of the silt trap during two storm periods are shown (5th and 7th of December). The figures show the sediment concentration above and close to the silt trap, over the whole water column. By using these figures the area of influence of the silt trap can be determined. The area of influence is the area in which is

sediment concentration is decreased, because of the silt trap. Figure 7.13 shows the longitudinal cross section of the trap on the 5th of December. At the upstream part (Northwest) the sediment concentration in the water column is higher (about 90 mg/l for the coarse fraction) than at the downstream end (about 60 mg/l). The coarse fraction is settled from the water column inside the trap. In the water column above the trap the sediment concentration is decreased. This decreases extends to about 1500 m downstream, outside the trap. The perpendicular cross section of the trap at the same moment in time is shown in Figure C.24. The influence area in perpendicular direction is only restricted to the area of the silt trap and a few 100 m next to it.

Overall it can be concluded that a silt trap will decrease the sediment concentration in the upper part (first few meters) of the water column above the trap. The influence area extends to about a few 100 meters close to the trap.

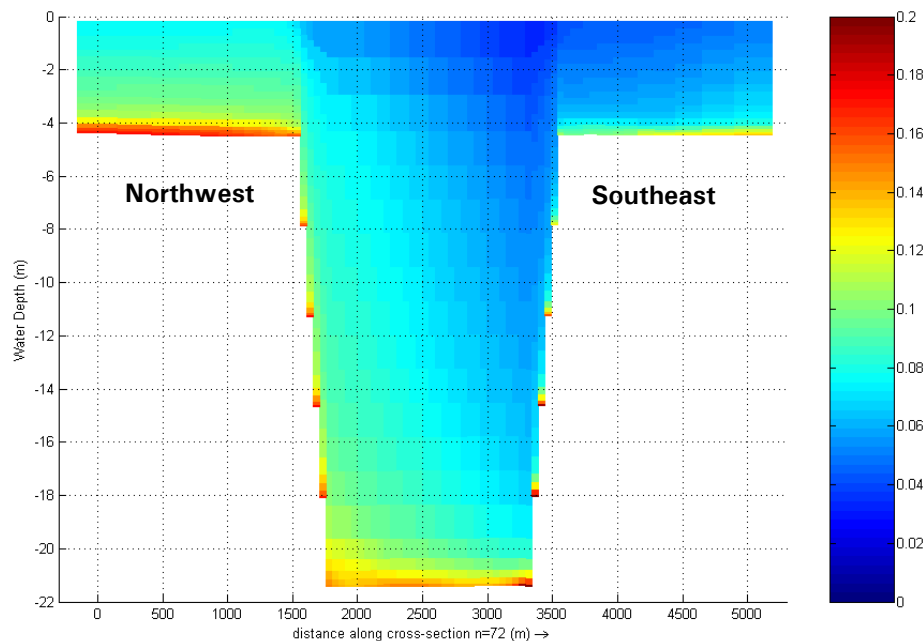


Figure 7.14: Sediment concentration Mud 2 (kg/m³), simulation Perpendicular 5, 5th of December 18h00. Cross section along line N = 72, longitudinal section. Decrease in sediment concentration is only just in the upper part of the water column, above the silt trap and about 1.5 km to the Southeast.

Again, comparing the total transport through each separate cross section an important difference is observed (Figures C.18 to C.21). For the perpendicular case the transport is mostly through the longer cross sections (Southwest and Northeast). The transport through the Northwest and Southeast cross sections (Figure C.20) is a order of 10 smaller than through the longer cross sections (Figure C.21).

In the parallel case there is no difference in sediment transport between the long and short sections. West and East (shorter sections, Figure C.18) show a same transport as North and South (longer sections, Figure C.19).

This can be explained by the fact that in the parallel case the flow through the short cross sections is accelerated, because of the 'flow attraction' of the silt trap. This effect is explained in Section 7.3.1. The total transport in time (S_{tot} , (m³/s)) through the total area of the section (A) is defined by,

$$S_{tot} = \rho_s \int_{A_{cross\ section}} u(z)c(z)dz \quad (7-3)$$

If the velocity u (m/s) is increased and the concentration (c) is the same the transport is increased. In the perpendicular case this increase in flow velocity does not occur in the shorter sections.

Depth and slope of the trap

Other design parameters of the silt trap are its depth and slope. Two alternatives are simulated: a trap with a depth of 16.5 m and a slope of 1:20 and a trap of 21.5 m deep and slopes 1:15. Results of both alternatives can be obtained by comparing the simulations parallel 1 and parallel 3 or perpendicular 1 and perpendicular 3. The effect on the accumulation in the silt trap is shown in Figures C.14 and C.15. The effect on the sediment concentration in Figures C.22 and C.23.

Overall it can be concluded that the depth and slope of the silt trap does not have a large influence on the accumulation and concentration. The trap with a larger depth (parallel 3, purple line) catches more coarse sediment (mud 2, C.15). Probably less sediment can be mixed up in the water column in the deeper parts of the trap, because of the low turbulence intensity. Consequently less sediment is transported out off the trap. However the difference between parallel 1 and 3 in accumulation is very little, only about a few 100 m³. This difference is calculated for the simulations with a very low critical shear stress for sedimentation inside the trap. A simulation with full sedimentation is not carried out for the two alternatives. So, the difference might be larger in reality.

Results of the sediment concentration (Figure C.23) show no difference between the two depths of the trap. Both alternatives show almost exact the same results, for the parallel case (normal line), as well for the perpendicular case (dashed line).

For this reasons it can be concluded that the depth and slope do not have a large influence on the behaviour of the sediment near the trap.

7.3.4 Overall observation and conclusions

Overall it can be concluded that a silt trap in general will catch sediment and will reduce the sediment concentration above the trap, for both orientations: parallel and perpendicular. Even the fine mud fraction will accumulate in the silt trap, although the sedimentation rate is low (about 1 % of the total amount of fine material in the lake per year). In the short period after the dredging of the silt trap, no decrease (only a few percent) in sediment concentration for the fine fraction is expected.

The conclusion that the silt trap catches sediment for both orientations is important. This means that for every wind direction and flow pattern sediment will accumulate in the trap.

An optimum efficiency will be reached when the trap is orientated perpendicular to the mean flow direction. In this case more sediment will accumulate. For the parallel trap, the flow is attracted to the trap, flow velocity increases, which results in a higher turbulence intensity and mixing of sediment in the water column. Density currents are generated less easily. The perpendicular case does not show an increase in flow velocity. So the importance of density currents in the perpendicular case is higher. Also a higher reduction in sediment concentration is expected.

About 20 % of the total amount of coarse sediment (Mud 2) accumulated in the trap is due to density currents. 80 % is due to advection and settling.

These results are all based on the model results of this study. All models are just a schematization of reality. Also this silt trap model has its shortcomings; some important processes in cohesive sediments are not implemented in the model. For example, erosion and sedimentation, consolidation and flocculation (Section 3.2) are not accounted for. These processes can influence the behaviour of sediment near the silt trap. In Chapter the results of the model will be discussed. Also recommendations are given for further model studies on the silt trap.

Part III: In summary

8 Conclusions, discussion and recommendations

This final chapter gives the conclusions of this study. In Chapter 1 the central question and the sub questions are stated. In Section 8.1 these questions will be answered.

In Section 8.2 the conclusions will be discussed in relation to the model set up. In the final Section 8.3 recommendations are given for further model research and field study on the mud dynamics in the Markermeer and especially on the sediment behaviour near a silt trap.

8.1 Conclusions

In this section each sub question stated in Chapter 1 is brought up and answered using the knowledge obtained from this study.

What are the mud dynamics of the Markermeer?

The mud dynamics in the Markermeer are governed by the behaviour of two sediment fractions: a fine and a coarse fraction. In reality a whole range in sediment fractions exists between fine and coarse. However, this rough schematization results in an easy understanding of the basic sediment transport processes in the lake.

The fine fraction has a very low settling velocity. The sediment concentration of the fine fraction is uniformly distributed (80 mg/l) over the water column during most of the time. During already moderate weather conditions (Bft. 3 wind speed) this fraction is mixed up in the water column. This fraction can only settle out if the wind speed is reduced to a few meters per second (1 to 2 m/s, which is Bft. 1 to 2 wind speed). If the fine material settles, it forms a thin layer at the surface of the bed, which is considered as the fluffy layer. This fluffy layer is already mentioned in previous studies (Van Duin, 1992) and is also found in the measurement campaign, which is carried out for this study. The fluffy layer consists of oxic mud, with a high water content. During the measurement campaign the fluffy layer is found at 52 locations across the lake, out of 71 measured locations in total. This layer is very mobile. If wind forcing increases, the layer is rapidly resuspended in the water column and transported according to the mean flow. It can only settle out if the wind forcing decreases drastically. This fine mud fraction is the main cause of the turbidity problem.

The coarse fraction has a high settling velocity and is suspended in the water column if wind speed Bft. 5 or higher occurs. The sediment concentration of this coarse fraction depends on the wind forcing. In storm periods the concentration is high, up to 100 - 150 mg/l. During times of mild weather conditions the mud is completely settled out and forms a high concentration layer at the bed surface.

In the Delft3D Markermeer model this two fraction schematization is also applied. By using this schematization the model results show good agreement with near bed sediment concentration measurements by the Argus Surface Monitor. Also the typical behaviour of both fractions is observed in the model results.

Waves have a large influence on the total sediment concentration in the water column. Waves cause an increase in sediment concentration due to erosion of bed material and an increase in turbulence intensity. Turbulence causes mixing of the sediment in the water column. If waves are not taken into account in the model, sediment concentrations drop with about 25 %.

Can the mud in the Markermeer behave like a density current?

Density currents can be an important mechanism for the infill of silt traps. It is indicated that density currents cause a rapid siltation of former pits that were dredged in the Markermeer. However the occurrence of density currents in the Markermeer has never been investigated and verified.

Usually a density current is generated if two conditions are fulfilled:

- A high sediment concentration layer near the bed is present. This high concentration causes a significant higher fluid density than the water density.
- There exists a density difference between two locations. Especially near a silt trap this difference can exist.

The presence of a high sediment concentration layer has never been investigated before. No detailed data were available about the sediment concentration near the bed. For this reason special measurements are carried out during the field measurement campaign.

According to all measurements, the presence of a layer with high sediment concentration near the bed can be confirmed. The turbidity measurements obtained by an Optical Back Scatter (OBS) showed higher concentrations near the bed on several locations. These concentrations can be a factor 2 higher than in the water column.

Echo sounding measurements indicate that a soft mud layer near the bed exists, with an average thickness of about 10 cm. The density of this mud layer is not known, but the presence of the layer is an important indication of the existence of density currents.

Measurements obtained by the Argus Surface Monitor (ASM) show very high concentrations near the bed during times of increasing and decreasing wind speeds in a storm period. Sediment concentrations in the lowest 20 cm of the water column can increase to about 700 – 800 mg/l. This results in a strong non uniform concentration profile over the vertical. This profile develops if wave heights are 0.5 m or higher.

Also the Delft3D Markermeer model predicts a high sediment concentration layer near the bed. The model is calibrated to the measurement data (wave height and sediment concentration). It can be concluded that the model results agree well with the measured sediment concentrations by the ASM. The high concentration layer consists almost completely of material of the coarse fraction (mud 2). Only during very mild conditions the fine fraction is also able to end up in the high concentration layer near the bed.

Overall conclusion: the first condition for the generation of density currents is fulfilled. High sediment concentration layers can exist in the Markermeer.

Density differences can exist near deep pits in the Markermeer. A theoretical analysis is carried out on the generation of density currents near a silt trap. This analysis reveals that the average flow velocities inside the high concentration layer due to density currents can become significantly high. The flow velocity due to density currents can be in order of 2 to 5 cm/s. Comparing to the wind driven flow velocities (0.10 to 0.20 m/s) this is an increase of about 25 to 50 %.

Also in the Delft3D Markermeer model this order of magnitude of flow velocities due to density currents is found. Further analysis reveals that density currents become significantly high (velocity in the layer is more than 2 cm/s) when the sediment concentration near the bed increases to 1 g/l. This increase in concentration is observed if mild wind conditions occur for at least one day after a storm. During that day the coarse sediment (mud 2) can settle out of the water column and build up a high concentration layer near the bed. If there is a period with several storms succeeding each other, the sediment is not able to settle out completely and no density currents are generated. Field measurements with the ASM showed sediment concentrations up to 800 mg/l, which is in the same order as the 1 g/l to get a significant density current.

So, both conditions fulfilled, it is indeed likely that density currents occur in the Markermeer.

What is the dominant mechanism for the infill of a silt trap?

In Chapter 1 a hypothesis is stated that the infill of a silt trap is caused by two mechanisms:

1. Settling of sediment from the water column.
2. Flow of sediment as a density current near the bed.

The previous question concluded that the last mechanism can occur in the Markermeer. The order of magnitude of the flow in the density current near the silt trap is about 2 to 5 cm/s. This density current causes an additional accumulation of sediment in the silt trap. In the model several simulations are carried out to assess the amount of sediment which accumulates in the trap through both mechanisms.

According to the model results it can be concluded that the fine fraction can accumulate in the silt trap. However the sedimentation rate is low, only a few percent of the sedimentation rate of the coarse fraction. The fact that the fine fraction can accumulate is important, because due to this process fine material is removed from the water column. This can result in a lower sediment concentration. A rough ballpoint calculation indicates that about 1 % of the total amount of fine material in the lake will accumulate in the trap per year.

The accumulation of fine sediment in deep pits is also concluded from the results of the cesium measurements during the field campaign. The cesium content in the sediment cores taken inside former deep pits, was significantly higher than in cores outside the pits. Theoretically, cesium can bind easier to fine material. For this reason the high cesium content in the cores inside the former pits indicates that fine sediment can accumulate in deep pits. This observation agrees with the results of the model. The accumulation rate can not be obtained from the cesium measurements.

The fine fraction is being transported into the trap by advection and settling. Density currents do not play a part for this fraction. The model shows the same results for the fine fraction in simulations with and without the density effect. For the fine fraction the settling mechanism is dominant.

For the coarse fraction both mechanisms occur. The total accumulation of this coarse fraction in the silt trap is much larger than for the fine fraction. Of the total amount (volume) of sediment accumulated in the silt trap about 20 % is produced by the density current mechanism. The remaining part, 80 %, is caused by advection and settling for the present configuration and conditions.

Overall, the hypothesis stated in Chapter 1 can be confirmed. The silt trap in the Markermeer is being filled by the two mechanisms: settling of sediment from the water column and by flow of sediment due to density currents.

What is an optimal design of a silt trap to reduce the sediment concentration?

The overall objective of the silt trap in the Markermeer is to reduce the sediment concentration in the water column. This reduction of concentration will improve the water quality in the lake, hence facilitates ecological enrichment. In general a reduction in sediment concentration is established by two processes, each with a different time scale:

- Reducing of the sediment concentration in an area near or above the silt trap. This is a direct effect of the silt trap and will play a part from the moment the trap has been dredged.
- Accumulation of sediment inside the trap reduces the total amount of sediment available for resuspension in the water column. If the removal of the sediment from the water column is larger than the production of sediment, the lake will become less turbid. This process will have a longer time scale.

Both processes are observed in the model. According to the model results, it can be concluded that a silt trap in general will catch sediment and will reduce the sediment concentration above the trap. For both orientations of the trap, parallel and perpendicular to

the main flow direction, this is observed. This means that for all wind directions and flow patterns sediment will accumulate in the trap.

However with some small changes in the design of the silt trap, the efficiency of the trap can be increased. An optimal efficiency is reached when the trap is orientated perpendicular to the mean flow direction

The higher efficiency of the perpendicular silt trap can be explained by considering the flow pattern near a silt trap. A silt trap with a parallel orientation will 'attract' the flow. Flow is accelerated just upstream of the trap. At the silt trap area the depth average flow velocity increases. Just downstream of the trap the flow velocity decreases again. This increase of flow velocity causes an increase of turbulence intensity in the area near the silt trap. Due to this increase in turbulence, the mixing of the sediment in the water column is larger. A high concentration layer near the bed (cause of the density current) can not be build up. In the case of a silt trap with perpendicular orientation, this increase in flow velocity does not occur. As a consequence the density current can be build up more easily and has a larger influence on the accumulation of sediment in the silt trap.

Due to the higher mixing of sediment in the water column for the parallel case, also the sediment concentration in the water column is higher. For this reason the reduction in sediment concentration is larger for the perpendicular case. This reduction can increase to about 50 % for the perpendicular case and is observed in the upper part of the water column above the trap and a few 100 meters next to trap.

For an efficient working of a silt trap, the trap should be orientated perpendicular to the main flow direction

The depth and slope do not have a large influence on the behaviour of the sediment near the trap. The model results show no large differences between the simulations with different depths and slopes of the trap.

With these answers to all sub questions the central question of this study can be answered. This question was:

Is a silt trap an effective measure to improve the water quality in the Markermeer?

Assuming a direct link between water quality and sediment concentration, it can be concluded that a silt trap is an effective measure to improve the water quality in the lake.

All different simulations show an accumulation of sediment inside the trap and a reduction of sediment concentration for the coarse fraction in the water column.

However the model results show no significant decrease in sediment concentration above the silt trap for the fine fraction. Especially this fine fraction is the cause of the turbidity problem. The fine mud is suspended in the water column during most of the time, causing a high turbidity. Decreasing this concentration is important for solving the turbidity problem. Because no reduction of sediment concentration for the fine fraction is observed in the model, a silt trap might be an ineffective measure. Nevertheless, an accumulation of fine sediment is observed in the silt trap. On a longer timescale the amount of fine sediment in the lake water column can be decreased (about 1 % of the total amount of fine sediment in the lake per year). For this reason the overall conclusion is:

Silt traps can be used as a mitigation measure for turbidity

Besides, the effect of a silt trap can be increased if it is used in combination with other measures to mitigate the turbidity, such as small dams that compartmentalize the lake. On a local scale in the lake the turbidity can be decreased by the use of both measures. It is hard to improve the water quality of the total lake by means of only one silt trap with a size of the silt trap adopted in this study. For example, it will take 20 years to decrease the total amount of fine material in the water column with 20 % (if no production is assumed). But to

improve the water quality of a small part of the lake it is a very effective measure. Silt traps should always be used in combination with different measures.

8.2 Discussion

The conclusions drawn in the previous section are all based on results of the model, which is set up especially for this study. In general, all models are just a schematization of reality. Also this model has its shortcomings; for example, some important processes in cohesive sediments are not implemented in the model. Erosion and deposition, consolidation and flocculation are not accounted for. These processes can influence the behaviour of sediment near the silt trap and will affect its efficiency. This section discusses model shortcomings and how these affect the results.

8.2.1 Erosion and deposition

The erosion and deposition process are not implemented in the model for the sake of simplicity. To include these processes in the model, at least a reliable estimate of the critical shear stresses for erosion and deposition ($\tau_{e,c}$ and $\tau_{d,c}$) is needed. The values for these model parameters should be based on field data about the bed strength. These data are not available and for this reason it is decided to exclude these processes. However both processes can have a large influence on the model results and the efficiency of the silt trap.

The main effect of erosion of the lake bed is production of 'new' mud sediment. If erosion occurs and sedimentation does not, the total amount of sediment in the lake water column will increase. To determine the long term efficiency of a silt trap, the total erosion flux should be determined. If the total erosion flux is larger than the total sedimentation rate inside the silt trap(s), a silt trap is not a good measure to solve the turbidity problem in the long run. In this situation the total amount of sediment in the lake increases, causing a higher turbidity if it is mixed up in the water column. Unfortunately, no detailed data are available about the exact location of the erosion areas in the lake, the erosion flux or the bed strength. Royal Haskoning (2006) gives an estimate of the flux, but this is not based on data. Also the results of the cesium measurements of the field campaign do not give a decisive answer about the erosion areas in the Markermeer (Section 4.3).

For the results of the silt trap model, the exclusion of the erosion and deposition processes can have a significant effect. In the model, the total amount of sediment does not change. Erosion does not occur, so no production of sediment took place. Deposition is absent, so no real removal of sediment occurs. All the sediment stays in the model domain. Only in four simulations deposition in the silt trap is implemented. The difference between those simulations and the simulations excluding deposition is large, but this is affected by the high critical shear stress (all the sediment will accumulate in the bed and is removed from the water column).

Implementing both processes should be the next step in the model research on the sediment behaviour near a silt trap. If erosion and deposition are implemented, the detailed processes near a trap will be simulated in a more realistic situation.

8.2.2 Flocculation

In Section 8.1 it is mentioned that the sediment concentration above the trap for the fine fraction does not decrease. Apparently, the turbulence intensity above the trap is high enough to keep the fine mud in suspension. The coarse fraction is able to settle out. In reality a whole range of sediment fractions exists from fine to coarse mud fraction, not only two. A typical process that can occur in cohesive sediments is flocculation (Section 3.2.3). If flocculation occurs, fine mud flocs can form coarser mud flocs, or the other way around. The flocculation process can influence the settling behaviour of the sediment and consequently affect the efficiency of a silt trap.

If the fine mud fraction can flocculate near the silt trap, it can form larger flocs and might be able to settle out of the water column. The sediment concentration will be more decreased

and more sediment is accumulated in the trap. Consequently, the efficiency of the trap will increase a lot.

However, the flocs can also break up if the turbulence intensity is very high. Consequently the material will be finer and is longer mixed up in the water column. In that case the efficiency of the trap will decrease.

Flocculation is presently taken into account in an aggregated manner (via settling velocities and different fractions). Dynamics of flocculation (aggregation and floc break up, Section 3.2.3) is not included.

On the other hand, it is not even known if dynamic flocculation can occur in the Markermeer. No specific measurements are carried out to the flocculation behaviour of the Markermeer mud. Before implementing the flocculation process in the model, this should be investigated.

8.2.3 Consolidation

The consolidation process is explained in Section 3.2.5. This process is not implemented in the model, because it is not implemented in the version of Delft3D, which is used in this study. Consolidation will increase the strength of the bed. For this reason, consolidation affects the erosion and sedimentation processes. For the model of the silt trap it can have influence on the results at two locations.

- Inside the silt trap consolidation has an effect on the accumulation of sediment in the bottom of the trap. Because of the sheltered area in the deep parts of the trap, the sediment layer in the trap can consolidate easier than outside. This means that the bed inside the trap will have a larger strength than outside.
- Outside the trap, in the shallow part, the bed can increase its strength due to the consolidation process. Especially during calm periods this increase in bed strength might be important. After periods of mild weather conditions the bed is less easily eroded. As a consequence less sediment is brought into the water column and the turbidity will be lower.

For this reason implementing consolidation in the model will probably increase the efficiency of the silt trap. However consolidation will not have a large influence on the model, as set up in this study. Only 10 days are simulated, including four storm periods. The sediment will not be able to consolidate in such a short period of time, under these conditions. So, the results of this model will not be influenced by the consolidation process. To assess the long term efficiency of a silt trap, consolidation should definitely be included in the models.

8.2.4 Effect silt trap on a longer time scale

As already mentioned in Section 5.1, the silt trap model in this study is set up for a detailed study to the processes around a silt trap. A high time- and spatial resolution is needed to study these detailed processes. This results in a high computation time; only a limited period can be simulated. In this study a period of 10 days is simulated with a computation time of 2 days. This period of 10 days is a period in the storm season (four storms are simulated), because a storm period is an important to study the sediment behaviour.

As a consequence of this modelling approach, the present model can not be used to determine the efficiency of the silt trap on a large time scale. Simulating one year will result in a computation time of 66 days. This is not usable. Models which must be able to give predictions on a longer time scale must be set up differently. The boundary conditions of those models should be reconsidered. For example a different wave and wind schematization must be used, to assess longer time scales.

These models should also include the consolidation and erosion/deposition process, because these processes can become important on large time scales. Total accumulation in the silt trap should be compared to the total production of sediment in the lake. The silt trap will, in the end, be efficient if the total accumulation is larger than the production. This comparison

can not be made with this model. A model set up for a longer time scale is also able to give predictions in the total life time of the silt trap. In the model of this study, the silt trap is a pit with a depth of about 20 m. The accumulation of sediment in the modelling period of 10 days causes a sedimentation of only 10 – 15 cm (depends on the settings of the bed density).

In reality it can take about 20 years to fill a deep Markermeer pit completely. The behaviour of the sediment near a silt trap can change if the trap becomes significantly shallow. If the trap is very shallow, waves can penetrate to the bed, causing an increase in turbulence intensity and bed shear stress. The settling of the sediment in the trap is reduced due to this higher turbulence. The shallower trap will have no different influence on the density current mechanism than a deep silt trap. As a consequence the density current mechanism will become more important for the total accumulation in the trap.

These effects of the silt trap on a longer time scale can not be simulated by the silt trap model developed for this study. This is an important limitation of the model. For this reason it is hard to give a prediction of the efficiency of the silt trap on a longer time scale.

8.2.5 Ecology

The final important limitation of this study has to do with the ecology. The main objective of the silt trap is to improve the water quality. Water quality governs the ecological potential. Many parameters determine the water quality (Figure 1.4). In this study it is assumed that the water quality is only determined by the sediment concentration. To a large extent this assumption will hold, but in reality the situation will be more complex. Clear example of this complexity is the dynamic feedback mechanisms within the ecological system.

Algae growth is one of those feedback mechanisms and can have an important influence on the turbidity in the water column. Turbidity is not only determined by sediment concentration. The amount of algae in the water will also determine the turbidity and algae growth is coupled to sediment concentration.

For instance: if the sediment concentration decreases due to the silt trap, the first reaction is a decrease in turbidity. Because of this lower turbidity, the (sun) light can penetrate deeper into the water. This higher light intensity can stimulate the algae growth. If the algae growth is really high, the turbidity will increase again.

So, a decrease in sediment concentration can in the end result in still a higher turbidity, but due to a different cause. Because no real ecological model exists for the Markermeer, it is hard to give a prediction about these processes. To give a real good prediction of the effect of silt traps on the water quality, ecological processes should be included in the model.

The model developed in this study, together with the Deltares mud model of the Markermeer, can be considered as a important step in a total cycle to develop a complete hydrodynamic, sediment transport and ecological model of the Markermeer. In Section 8.3 some recommendations will be discussed for the next modelling and research steps in this cycle.

Ecological research on the Markermeer and the IJsselmeer is embedded in the 'Building with Nature' program (*Personal comment*, website www.ecoshape.nl). 'Building with Nature' is a recently set up research program focusing on a sustainable building in delta areas, so called ecodynamic building. In this program, many companies and institutes will cooperate: Boskalis, Van Oord, Deltares, Royal Haskoning, Universities and other institutes.

The Markermeer and IJsselmeer case will for instance focus on the realization of some pilot projects to improve the ecological value of the lake (for example a swamp). Also a complex study to the realization of an ecological regime shift in the lake will be carried out. Such a regime shift will establish a completely different ecological composition of the lake and an improvement of the water quality.

8.2.6 Numerical model effects

Accumulation due to density current

The total accumulation of sediment in the silt trap due to density currents is about 20 %, settling causes about 80 %. It seems that the density effect is of minor importance, although it will exist.

However the accumulation due to density currents in reality will be probably higher. In the model two important model effects can cause a decrease in density current effect in the model.

The first model effect is about the unrealistic sedimentation mechanism of the density current in the bed. In reality the density current will flow directly into the soft bed, in the model the mechanism is different.

In the silt trap model, sedimentation of sediment to the bed can only occur in the deepest part of the silt trap. In those grid cells the critical shear stress is set to 100 N/m^2 , so full sedimentation occurs. Only sediment from the lowest computational cell will accumulate in the bed. All layers above ($k = 1-19$) show a balance between settling and turbulence mixing. (Figure 8.1)

Sedimentation of the density currents in the model is as follows:

The density current first has to flow horizontally inside the lowest layer and will then accumulate in the bed. Because the thickness of the density current layer is not only one computation layer, some sediment from the density current can end up in the layers above the lowest layer. Consequently this sediment can be mixed up again and transported out of the trap.

In reality the density current will flow directly into the soft bed, not via the lowest part of the water column. Consequently less sediment will be mixed up from the density current and the accumulation rate via density current will be higher.

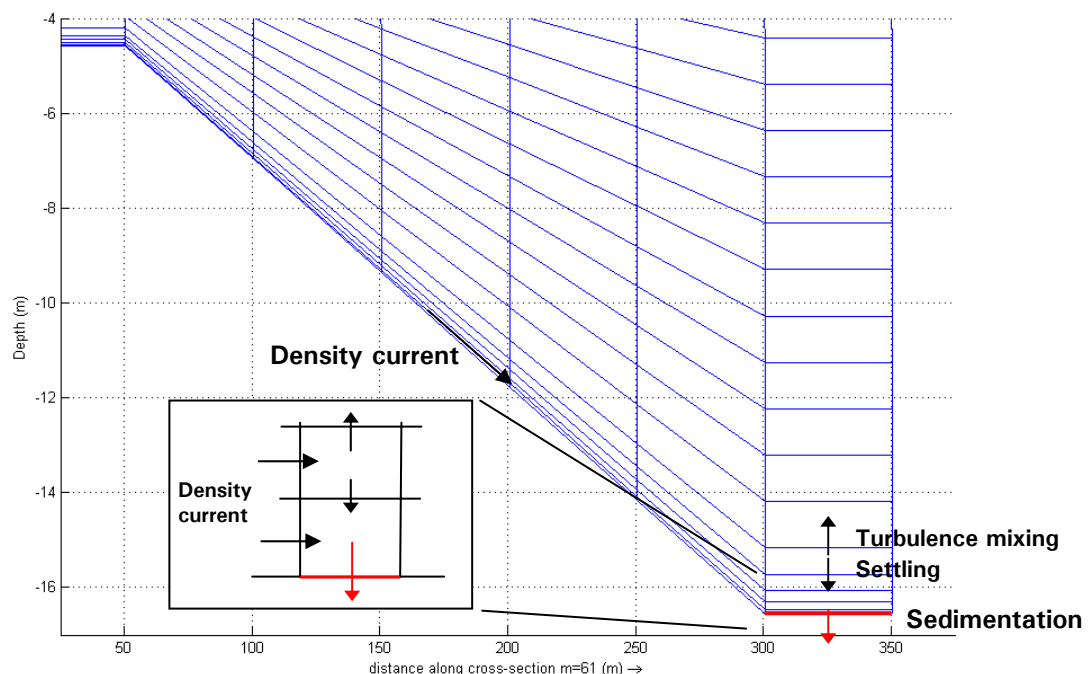


Figure 8.1: Explanation of the model effects. Sedimentation only occurs at the lowest layer. All layers above a balance between settling and turbulence mixing occurs.

Second model effect is that the sigma layer schematization has an influence on the results. The grid cell height inside the silt trap is larger than outside (Figure 8.1), because the water depth is larger. The effect on the density current is as follows: in the high concentration layer near the bed, the same amount of sediment is present in the lowest computation layer

inside and outside the trap. Because of the increased grid cell height inside the trap, the concentration is lower than outside. The same amount of sediment is distributed over a larger grid cell. Due to the decrease in concentration (due to this grid effect), the sediment can be mixing up more easily in the water column inside the trap (the layer is less stable). In reality this layer will keep its high concentration and will be more stable. Resuspension rates are smaller and accumulation rates will be higher. However, the same effect also holds for the settling process. If the sediment is advected into the trap, the sediment concentration decreases by an increasing cell size (if the same amount of sediment is advected). For this reason it can not be concluded that the density current effect will definitely be higher.

This sigma layer effect is also mentioned in WL Delft Hydraulics (2007a). In that study a local increase in sediment concentration just in the upper layer above the deep pits, is observed. This is explained as a model artifact. The grid cell height increases above the trap. The sediment will have to settle for a longer period to go out of the upper layer. For this reason the model predicted sediment concentration in the upper layer above deep pits will be higher for a longer time than in reality.

8.2.7 Utility of the model results

Although the silt trap model has its shortcomings (described in the sections above) the results of this study can be used in the design process of a silt trap in the Markermeer. This study reveals new insights in the mud dynamics in the Markermeer and sediment behaviour near a silt trap.

First, the occurrence of density currents in the Markermeer is proved, both from field measurements as from model results. Density currents can play an important role in the sediment behaviour near a silt trap. In the design of the silt trap this mechanism should be taken into account.

The second important result of the study is that the efficiency of the silt trap can be increased by the orientation of the trap. The efficiency of the silt trap can be increased if the silt trap is orientated perpendicular to the main flow at that location. In the design process this outcome can be used according to the following 5 steps:

1. An exact location and lay out of the silt trap should be determined. The choice for a location can be based on many different aspects, not related to only the physical processes of the trap. For example governmental laws, environmental issues or economical reasons can play a role. Also the lay out of the trap can be based on other aspects, like the interaction with other engineering measures to mitigate the turbidity.
2. When the location is determined, the flow pattern at that location should be defined. This can be obtained from a hydrodynamic model of the Markermeer. With knowledge of this flow pattern, the main flow should be determined.
3. The silt trap must be orientated perpendicular to the direction of the main flow. In this situation the trap has its highest efficiency.
4. The lay out of the silt trap depends on the existence of a main flow direction. If there exist a typical main flow the trap must be rectangular shaped, perpendicular orientated to the main flow. If the flow is from many different directions, the trap can be quadrangle to trap the most sediment from all directions.
5. The exact accumulation and reduction in sediment concentration can be determined by simulating the designed trap in a numerical model.

8.3 Recommendations

In this section some recommendations will be discussed considering the next steps in research on the mud dynamics in the Markermeer and model development and field study for the silt trap model. The focus will be on research on the sediment behaviour.

First, a detailed study to the existence of the *flocculation process* in the Markermeer should be carried out. Flocculation can be an important process in the behaviour of the fine mud fraction in the lake. Especially near a silt trap this flocculation can influence the efficiency of the trap.

Laboratory tests should investigate if the mud in the Markermeer is able to flocculate. If so, the flocculation characteristics must be determined to obtain input data for numerical models. The effect of the flocculation process on the mud behaviour near a silt trap can be studied by these numerical models.

The most recent commercial version of the Delft3D software is not able to include the flocculation process. For this reason a trial version must be used. Proper calibration of that model has to be carried out again to make sure the model is reliable.

Second, the *erosion processes* in the Markermeer should be investigated. In Section 8.2.1 the importance of the erosion process is already mentioned: if the total net production of mud (erosion of old mud layers) is higher than the net removal of mud sediment by means of the silt trap, the total amount of sediment in the lake is increased. In this case a silt trap is not an appropriate measure for turbidity. Detailed (field) study should be carried out to determine the exact erosion locations in the lake.

Results of this study should be:

- Location of the erosion areas.
- Estimation of the total erosion fluxes.
- Determination of the bed strength. For example the critical shear stress for erosion and the erosion constant (M) are important values.

Last two parameters can be determined in the laboratory using real bed material of the Markermeer. These parameters are important for implementation of the erosion process in the Delft3D Markermeer model.

The version of Delft3D used in this study is able to include this erosion effect. A first improvement in the model is to include the erosion effect. With knowledge of both parameters it can be easily established.

The last process in cohesive sediments that has to be investigated is *consolidation*. It is mentioned in Section 8.2.3 that consolidation can have a significant influence on the sediment behaviour near silt traps. Consolidation tests in the lab should be carried out to determine the consolidation characteristics of the Markermeer mud. Second step is to implement those results in the models. However this might be difficult, because also the consolidation process is only available in some trial versions of the Delft3D software.

Setting up the Markermeer model for this study reveals new insights in model development of the Markermeer. These insights result in some recommendations for future models of the Markermeer:

- Waves in the Markermeer should be modelled including the new wave model settings, used in this model. The calibration process showed that using these new settings a better agreement between model and wave measurements is obtained. Further research must be carried out to the effect of the wave bottom friction in the model. In this study this friction is switched off, but this is not a realistic schematization. It can also cause some problems with wave computations in the shallow part of the lake. Waves can become too high in those areas, because of the absence of friction. A better description of the wave friction parameter is needed.
- The sediment in the Markermeer is schematized in this model by the means of two fractions, one fine and one coarse fraction. The amount of sediment in the lake is based on calibration results. During times of heavy weather conditions the total available amount of sediment that can resuspend in the water column is too low, compared to the measurements. This problem can be solved by including erosion in the model or implementing an extra coarse fraction (coarse mud or even sand). This

coarse fraction can only resuspend during strong wind conditions resulting in a higher sediment concentration during a storm period. New calibrations should be carried out on the effect of the extra fraction.

- The model of this study is only calibrated at one location in the lake, the location of the measurement pole FL 42. WL Delft Hydraulics (2007a) already recommended that calibration should be carried out on different locations in the lake. For this study no detailed data were available at other locations. To improve the calibration of the model, new measurements (waves, flow velocity and sediment concentration) should be carried out on different locations. By using this data a better calibrated model can be obtained.
- In this model wind data from the measurement station Berkhout of the year 2007 are used. Visser (2007) mentioned that this measurement station might give inaccurate data; it can behave like a land station for specific wind directions and consequently underestimate the wind speed. Proper modelling of the wind speed and direction is necessary, because wind is the main forcing of the Markermeer system. Future models should use wind data from the measurement station Schiphol. Even better is to measure the wind speed and direction at measurement poles in the lake during a measurement campaign.

The application of state-of-the-art 3D mud models, in this study as well as the Deltares study has contributed importantly to our understanding of the Markermeer mud dynamics. Realization of a pilot silt trap in the Markermeer would be a prerequisite for future developments, including improved insight in silt traps efficiency, validation of basic model processes and the development of an integral ecological model for the Markermeer.

References

- BERLAMONT, J., OCKENDEN, M., TOORMAN, E., WINTERWERP J.C., (1993), The characterisation of cohesive sediment properties, *Journal of Coastal Engineering*, 21, 105-128.
- BLOM, G., DUIN, E.H.S. VAN, AALDERINK, H., et al. (1992), Modelling sediment transport in shallow lakes – interactions between sediment transport and sediment composition, *Hydrobiologia* 235/236, 153-166.
- DUIN, E.H.S. VAN (1992), PhD thesis: Sediment transport, light and algal growth in the Markermeer – a two dimensional water quality model for a shallow lake, Van Zee tot Land 59, Landbouwniversiteit Wageningen.
- DUIN, E.H.S. VAN, BLOM, G., LIJKLEMA, SCHOLTEN, M.J.M., (1992), Aspects of modelling sediment transport and light conditions in Lake Marken, *Hydrobiologia*, 235/236, 167-176.
- HOLTHUIJSEN, L.H. (2007), *Waves in oceanic and coastal waters*, Cambridge University Press
- JENSEN, J.H., MADSEN, E.O., FREDSE, J. (1999a) Oblique flow over dredged channels. I: Flow description, *Journal of Hydraulics Engineering*, Vol. 125, No. 11
- JENSEN, J.H., MADSEN, E.O., FREDSE, J. (1999b) Oblique flow over dredged channels. II: Sediment transport and Morphology, *Journal of Hydraulics Engineering*, Vol. 125, No. 11
- KESSEL, T. VAN (1997), PhD thesis: Generation and transport of subaqueous fluid mud layers, Delft University of Technology.
- KRANENBURG, C. (1998), *Dichtheidsstromen CT5302*, Lecture note Delft University of Technology
- MCANALLY, W.H., FRIEDRICHS, C., HAMILTON, D. et al. (2007a), Management of fluid mud in estuaries, bays and lakes – Part I: Present state of understanding on character and behaviour, *Journal of Hydraulic Engineering*, vol. 133, 1-9-22.
- MCANALLY, W.H., FRIEDRICHS, C., HAMILTON, D. et al. (2007b), Management of fluid mud in estuaries, bays and lakes – Part II: Measurement, modelling and management, *Journal of Hydraulic Engineering*, vol. 133, 1-23-38.
- MINISTERIE VAN V & W (2007), *Een ander IJsselmeergebied, een ander beleid*, Ministerie van Verkeer en waterstaat, projectgroep 'Een ander IJsselmeer', authors Bussink et al., Den Haag.
- NIEUWSTADT, F.T.M. (1998), *Turbulentie – theorie en toepassing van turbulente stromingen*, Epsilon Uitgaven, Utrecht
- RIJKSWATERSTAAT (1995), *Geologische en bodemkundige atlas van het Markermeer*, Rijkswaterstaat IJsselmeergebied, authors Lenselink and Menke, Lelystad.
- RIJN, L.C. VAN (2005), *Principles of sedimentation and erosion engineering in rivers, estuaries and coastal seas*, Aqua Publications
- RIZA (1991), *Een model voor resuspensie en sedimentatie van slib – Toepassing op het Markermeer*, RIZA notanummer 91.005, author Vlag, Lelystad.

- RIZA (2003), Afname van de driehoeksmossel in het Markermeer, Rijkswaterstaat RIZA rapport 2003.016, authors Noordhuis and Houwing, Lelystad
- ROSS, M.A. AND MATHA A.J. (1989), On the mechanics of luctoclines and fluid mud, Journal of Coastal Research, Special Issue 5: High Concentration Cohesive Sediment Transport, ed. A.J. Metha and E.J. Hayter, 51-61.
- ROYAL HASKONING AND WL DELFT HYDRAULICS (2006), Verdiepingsslag en maatregelen slibproblematiek Markermeer – Analyse kennisleemten en inventarisatie maatregelen, authors Van Ledden et al , Royal Haskoning and WL Delft Hydraulics.
- TOVEY, N.K. (1971), A selection of scanning electron micrographs of clays, University of Cambridge, Department of Engineering, Report CUED/C-SOILS/TR5a
- VISSEER, K.P. (2007), Golfbrekers in het Markermeer – Synergie voor veiligheid en ecologie, Hogeschool van Amsterdam and Rijkswaterstaat IJsselmeergebied.
- VLAK. D.P. (1992), A model for predicting waves and suspended silt concentration in a shallow lake, Hydrobiologia, 235/236, 119-131.
- WESTHUYSEN, A.J. VAN DER, ZIJLEMA, M., BATTJES, J.A. (2006) Nonlinear saturation-based whitecapping dissipation in SWAN for deep and shallow water, Journal of Coastal Engineering, vol. 54, 151-170
- WHITEHOUSE, R., SOULSBY, R., ROBERTS, W., MITCHENER, H. (2000), Dynamics of estuarine mud, HR Wallingford and Thomas Telford Limited, London.
- WINTERWERP, J.C. (1999), PhD thesis: On the dynamics of high-concentrated mud suspensions, Delft University of Technology
- WINTERWERP, J.C. AND KESTEREN, G.M. VAN (2004), Introduction to the physics of cohesive sediments in the marine environment, Developments in sedimentology 56, Elsevier, Amsterdam
- WINTERWERP, J.C. (2006), Stratification effects by fine suspended sediment at low, medium and very high concentrations, Journal of Geophysical Research, 111, C05012, doi:10.1029/2005JC003019.
- WITTEVEEN & BOS (2004a), Quick scan slibproblematiek Markermeer en Eem- en Gooimeer, Witteveen en Bos, project nummer Rw1390-1, author Van Leeuwen, Deventer
- WITTEVEEN & BOS (2004b), Transparante Markermeren – Als ecologische afronding van de Zuiderzeewerken, Witteveen en Bos and Boskalis b.v. Hydronic, authors Grimm, Groot and Loman.
- WL DELFT HYDRAULICS (1999), Handboek zoetwaterslib, WL Delft Hydraulics, authors Van Kessel and Vonk, WL Delft Hydraulics
- WL DELFT HYDRAULICS (2006a), Delft 3D – FLOW, user manual, WL Delft Hydraulics, Delft
- WL DELFT HYDRAULICS (2006b), Delft 3D – WAVE, user manual, WL Delft Hydraulics, Delft
- WL DELFT HYDRAULICS (2007a), Modelling slibhuishouding Markermeer, authors Hulsbergen and Kuijper, WL Delft Hydraulics
- WL DELFT HYDRAULICS (2007b), Scenarioberekeningen Markermeer, author Kuijper, WL Delft Hydraulics report, Q4408.50

Appendices

Appendix A: Field measurements

A-1: Turbidity measurements

Calibration of OBS sensor

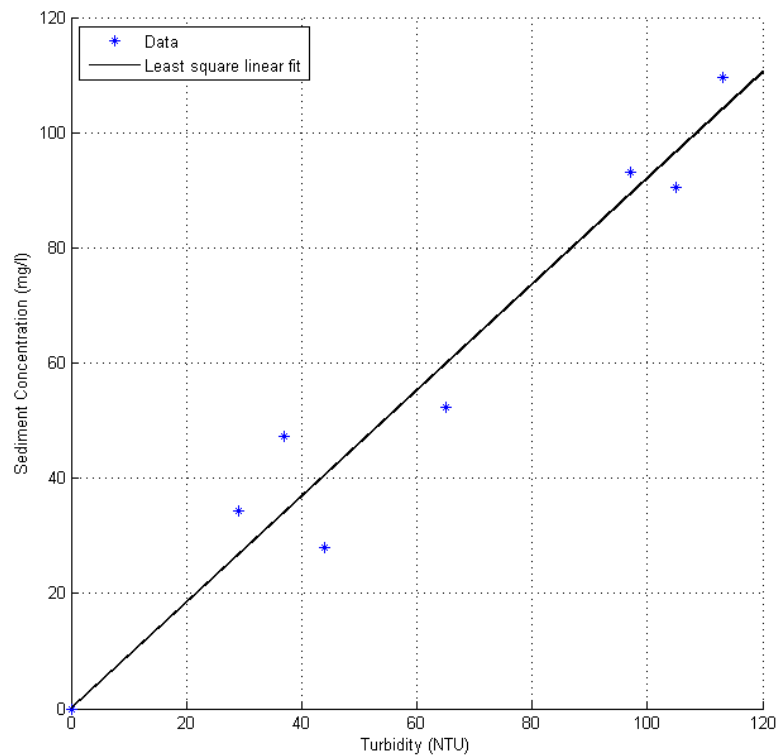


Figure A.1: Calibration Curve for OBS sensor.

Calibration Sample	Volume (ml)	Mass Sediment (g)	Mass Inorganic (g)	Mass organic (g)	Sediment Concentration (mg/l)	Turbidity (NTU)	D ₅₀ (µm)	D ₅₀ DeFloc (µm)	Comment
26/11 - 2	250	0.0196	0.0117	0.0079 (56%)	78.4	50	22	12	Outlier, omitted
26/11 - 4	250	0.0131	0.082	0.0049 (18%)	52.4	65	19	11	
26/11 - 5	250	0.0233	0.148	0.0085 (38%)	93.2	97	22	11	
26/11 - 9	500	0.0140	0.0071	0.0069 (58%)	28	44	19	12	
26/11 - 11	250	0.0226	0.0148	0.0078 (40%)	90.4	105	19	11	
26/11 - 13	250	0.0274	0.0186	0.0088 (38%)	109.6	113	20	10	
27/11 - 3	250	0.0118	0.0060	0.0058 (44%)	47.2	37	16	11	
27/11 - 5	250	0.0046	0.0022	0.0024 (28%)	18.4	60	17	10	Outlier, omitted
27/11 - 10	250	0.0086	0.0051	0.0035 (76%)	34.4	29	16	11	

Table A.1: Results of analysis of calibration samples of the OBS.

Calibration equation:

$$[\text{mg/l}] = 0.9212 \times [\text{NTU}]$$

Error: $R^2 = 0.9148$ Correlation Coefficient = 0.9574

Sediment concentration profiles

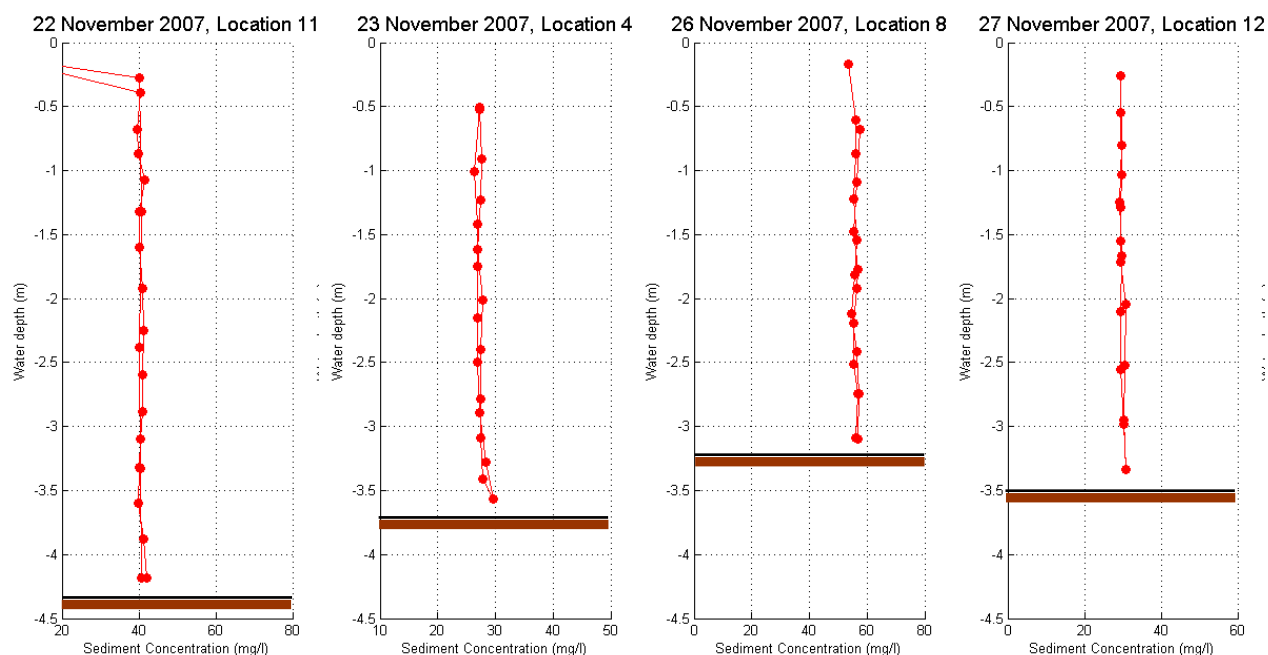


Figure A.2 : Sediment concentration profiles on several measurement days and locations. These profiles show a uniform distribution of sediment concentration over the water column.

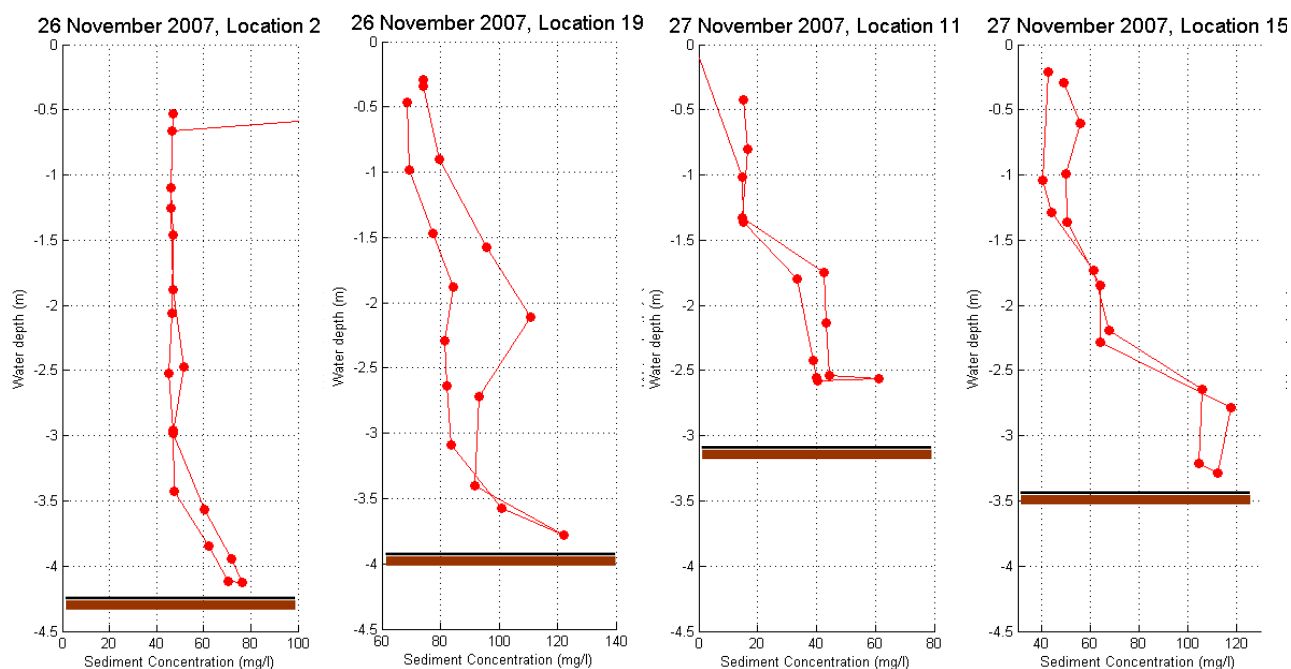


Figure A.3: Sediment concentration profiles on several measurement days and locations. These profiles show a non uniform distribution of sediment concentration over the water column. The sediment concentration near the bed is higher, at some location up to two times the concentration near the water column.

A-2: Echo soundings

Day	Location number	X (RD,m)	Y (RD,m)	Mean LF (m) 33 kHz	Mean HF (m) 210 kHz	Mean Thickness soft layer (m)	Median Thickness soft layer (m)	Std Thickness soft layer (m)
22/11/07	4	151901.3088	506879.7322	4.2114	4.1791	0.032278	0.03	0.018875
	5	150904.4646	507935.0578	4.2403	4.2083	0.031992	0.03	0.020626
	6	148873.937	506873.2823	4.3229	4.2744	0.048486	0.05	0.025149
	7	146881.0653	507951.4716	3.8238	3.8049	0.018900	0.02	0.019296
	8	145933.9396	506928.8342	3.8311	3.8241	0.006983	0.01	0.005782
	9	144396.9403	504909.736	4.0584	3.9692	0.089259	0.09	0.024678
	10	146944.6219	504909.9345	4.1555	4.0644	0.091101	0.09	0.047868
	11	147926.2805	504919.4918	4.4268	4.3493	0.077455	0.075	0.030816
	12 in pit	147552.9233	503360.7677	5.0005	4.8945	0.105977	0.11	0.064887
	12 out pit	147959.2807	503011.8388	4.4801	4.3830	0.097143	0.1	0.062599
	13	146879.8831	501841.7536	4.4565	4.3903	0.066207	0.07	0.024294
	14	149384.6232	502563.776	4.4649	4.2339	0.230992	0.21	0.100037
	15	151723.0342	503686.3564	4.4060	4.3826	0.023333	0.02	0.015143
	16	150994.6938	498819.9336	4.0457	3.9534	0.092362	0.09	0.031526
	17	151945.1083	498818.902	No data	No data	No data	No data	No data
23/11/07	1	146769.0126	497612.2235	4.1203	4.0620	0.058245	0.06	0.018285
	2	144994.4281	494815.6653	3.9753	3.8476	0.127662	0.11	0.073743
	3	141934.7848	492630.9559	3.7857	3.7554	0.030290	0.03	0.017147
	4	138859.7757	490891.4932	3.6985	3.6536	0.044880	0.04	0.017462
	5	134922.365	488887.3076	3.1678	3.0762	0.091556	0.11	0.045954
	6	132805.3241	488847.9596	3.6109	3.1163	0.494675	0.57	0.238375
	7	135002.3109	490886.2861	3.2186	3.1554	0.063230	0.06	0.030344
	8	135966.8242	493438.3793	No data	No data	No data	No data	No data
	9	136899.5086	494905.8647	No data	No data	No data	No data	No data
	10	137942.8186	495917.4605	2.9631	2.8800	0.083113	0.07	0.058430
	11	136931.6681	497890.8267	No data	No data	No data	No data	No data
	12	137517.4204	498802.9632	No data	No data	No data	No data	No data
	13	137973.6362	498871.944	No data	No data	No data	No data	No data
	14	141931.6286	495925.0788	3.3718	3.3018	0.070046	0.07	0.029048
	15	143975.3411	497916.3421	3.6524	3.5458	0.106647	0.11	0.028698
	16	147959.6116	496722.8241	3.1730	2.9423	0.230687	0.22	0.111619
	17	153331.7088	503117.839	4.1375	3.9313	0.206206	0.21	0.060374
26/11/07	1	155933.7263	506887.4432	4.2620	4.1651	0.096905	0.1	0.018731
	2	155971.2636	508923.5703	4.3403	4.1694	0.170875	0.16	0.061372
	3	155959.1186	511898.0909	3.8489	3.8105	0.038404	0.04	0.015087
	4	153684.3104	515917.817	No data	No data	No data	No data	No data
	5	151912.861	515915.8542	3.1393	3.0466	0.092683	0.09	0.036608
	6	150961.4017	518871.0001	3.1647	3.0550	0.109737	0.1	0.071754
	7	147923.7917	517897.9139	3.0626	3.0366	0.026000	0.02	0.020203
	8	145959.0104	517934.4953	3.2537	3.1572	0.096448	0.09	0.042452
	9	143886.6984	516904.1732	3.4221	3.3185	0.103598	0.11	0.025704
	10	145201.5426	515365.3328	3.6624	3.5695	0.092989	0.1	0.029500
	11	143853.9116	511882.2098	3.7185	3.6440	0.074512	0.07	0.039913
	12	145946.1061	510948.8989	3.8339	3.7446	0.089316	0.09	0.013765
	13	146908.6764	513911.0856	3.7448	3.6583	0.086551	0.09	0.016962
	14	147937.1882	512928.6018	3.7216	3.6593	0.062298	0.06	0.022867
	15	148888.318	513889.4093	3.6588	3.5806	0.078162	0.07	0.030805
	16	149958.8776	511896.3476	3.8327	3.7359	0.096816	0.1	0.026118
	17	152293.8867	511095.8196	4.2040	4.1554	0.048619	0.05	0.021164
	18	152939.3101	511844.7074	4.1530	4.0421	0.110867	0.11	0.030016
	19	155911.5047	502841.1326	4.0637	3.7590	0.304708	0.33	0.095227
27/11/07	1	146054.6905	500011.7087	4.8933	4.6014	0.291981	0.32	0.096232
	2	145469.3522	500242.5451	No data	No data	No data	No data	No data
	3	143827.7414	501902.4687	3.9797	3.9404	0.039286	0.04	0.017778
	4	141956.9038	504931.7501	4.0423	3.9565	0.085856	0.08	0.035745
	5	143888.1839	507941.4078	3.8808	3.8328	0.047937	0.05	0.018220
	6	141926.6787	510951.5114	3.7341	3.6779	0.056116	0.05	0.023516
	7	140952.3635	512907.7925	3.7877	3.7148	0.072905	0.06	0.034092
	8	137856.3911	513870.8727	3.8590	3.7026	0.156450	0.15	0.032063
	9	136894.8133	510878.4658	3.4367	3.3390	0.097651	0.1	0.022154
	10	132933.5664	510944.0255	3.0924	3.0287	0.063731	0.06	0.015226
	11	132903.0392	507893.4454	3.1588	3.0926	0.066207	0.055	0.051998
	12	137039.0759	505873.0307	3.5478	3.4349	0.112917	0.11	0.038814
	13	135916.7799	503831.5158	No data	No data	No data	No data	No data

	14	136918.6067	501915.205	3.1535	3.0441	0.109404	0.11	0.022680
	15	138889.5216	501916.9558	3.5032	3.4254	0.077750	0.08	0.018628
	16	140942.4807	502941.3317	3.9532	3.8318	0.121362	0.11	0.053654
	17	140938.6794	500857.6914	3.8934	3.8457	0.047736	0.05	0.016635

Table A.2: Results of echo sounding measurements.

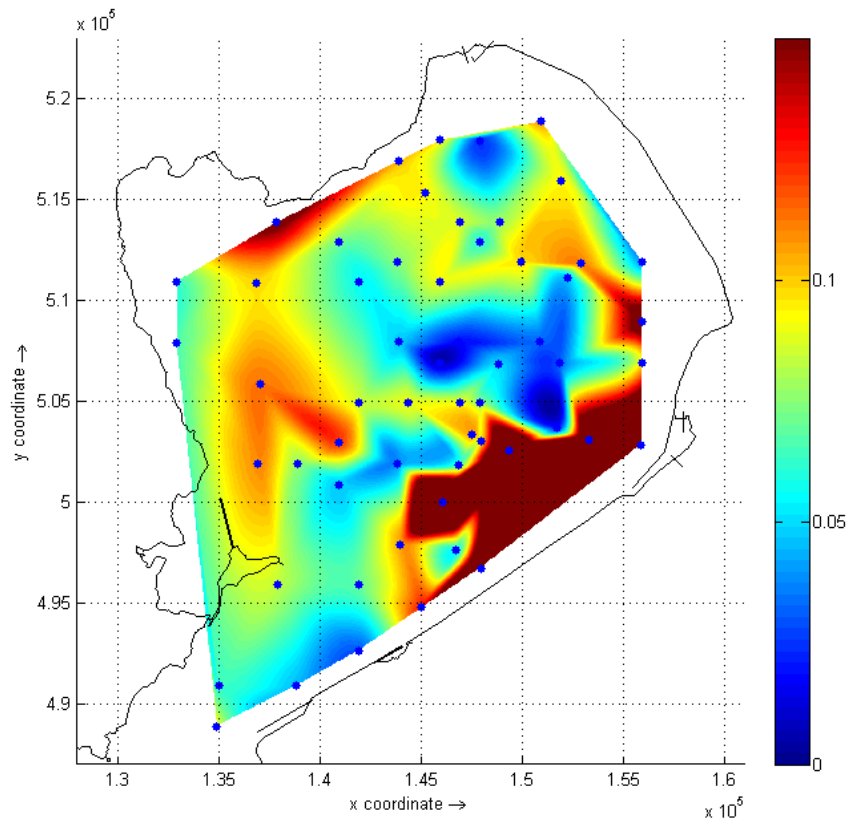


Figure A.4: Overview of thickness (m) of soft mud layer. The blue dots are the measurement locations. In the southeast part of the lake the soft mud layer is thicker than in the other areas of the lake (up to 15 – 30 cm).

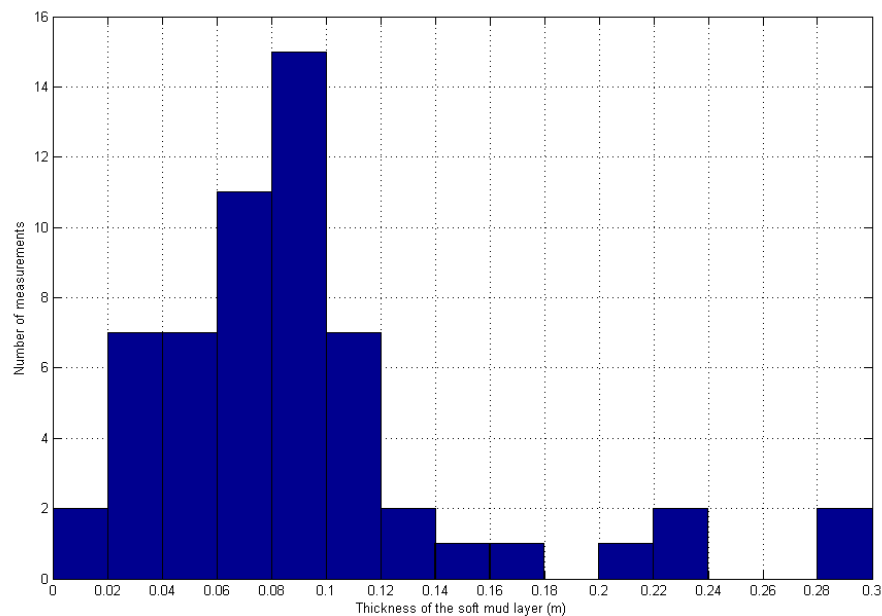


Figure A.5: Histogram of the thickness of the soft mud layer. The modus of the measurements is 8 – 10 cm. The maximum thickness which is measured is about 30 cm.

A-3: Cesium measurements

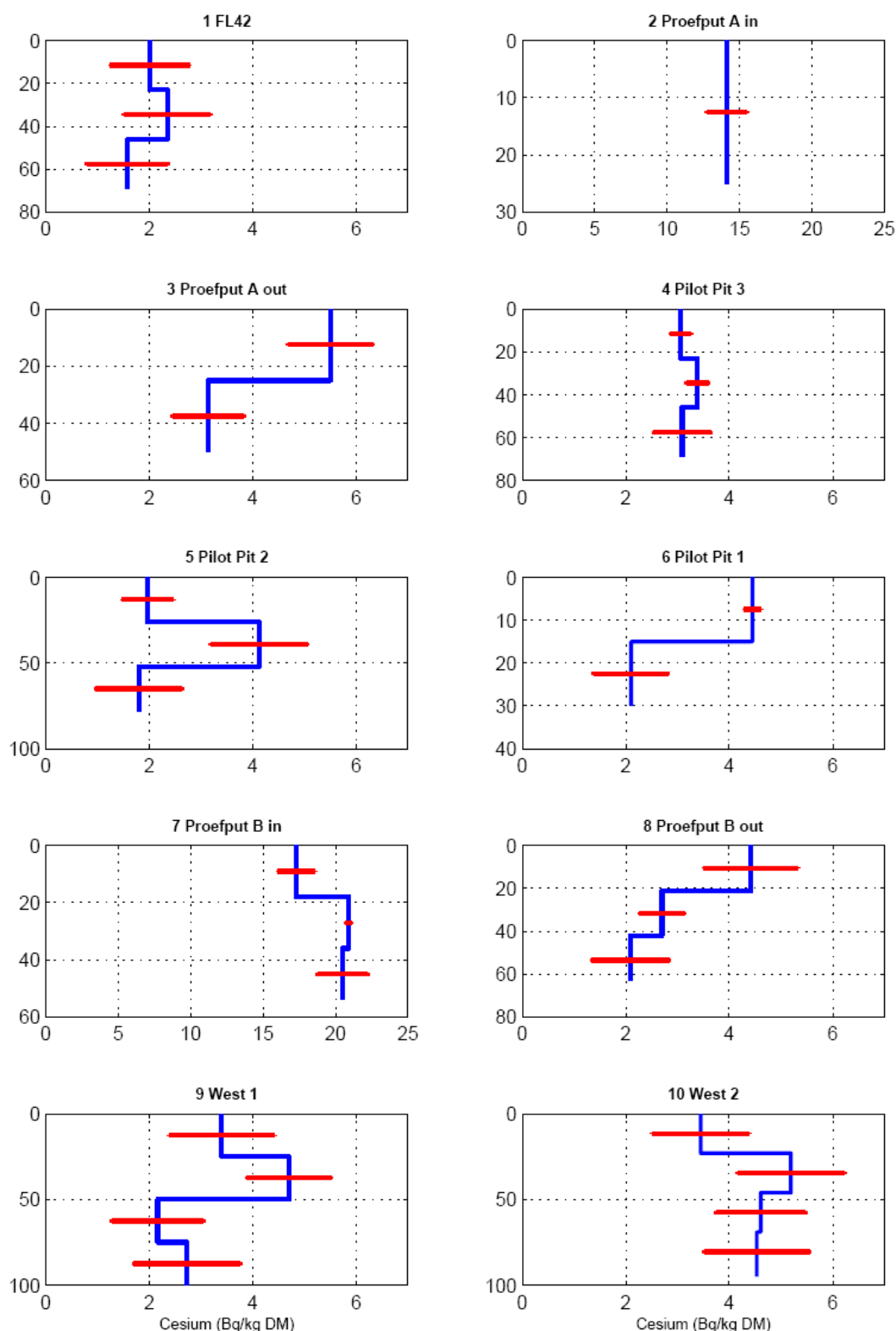


Figure A.6: Cesium profiles of measurement locations (blue) and uncertainty (red). At the locations 'Proefput A' and 'Proefput B' a much higher cesium content is measured. Just outside these pilot pits, the Chernobyl layer is near the surface.

Location	X (RD,m)	Y (RD,m)	Water depth (m)	Depth sample (cm)	Dry Material (%)	d Dry Material	Mud content (%)	40-K (Bq/kg DM)	dK	238-U (Bq/kg DM)	dU	232-Th (Bq/kg DM)	dTh	137-Cs (Bq/kg DM)	dCs	Cs /(U+Th)
1 - FL42	144396.9403	504909.736	4.05	0 - 23	63.9	0.297	56.75	453.6	14.9	25.2	1.13	27.7	1.02	2.01	0.764	0.038
				23 - 46	58	0.298	60	529.4	16.6	27	1.22	29	1.11	2.35	0.831	0.042
2 - Proefput A in	147552.9233	503360.7677	4.95	46 - 69	53.3	0.253	67.75	536.2	16.3	23.7	1.18	32.1	1.09	1.58	0.775	0.028
3 - Proefput A out	147959.2807	503011.8388	4.40	0 - 25	66.4	0.289	42.75	432.4	14.1	24.2	1.06	22.1	0.954	5.5	0.811	0.119
				25 - 50	72.4	0.314	55.75	435.2	12.6	23.7	0.956	27.3	0.87	3.14	0.684	0.062
4 - Pilot pit 3	146769.0126	497612.2235	4.10	0 - 23	50.6	0.279	61	516.7	3.68	25.6	0.272	29.4	0.248	3.06	0.189	0.056
				23 - 46	45.8	0.248	70.25	553	4.02	26	0.295	33.1	0.271	3.38	0.207	0.057
				46 - 69	45.3	0.249	65	503.8	10.6	27.5	0.795	31	0.728	3.09	0.548	0.053
5 - Pilot pit 2	153331.7088	503117.839	4.05	0 - 26	71.7	0.328	40.25	401.5	9.52	19.5	0.697	21.1	0.631	1.97	0.489	0.049
				26 - 52	55.6	0.274	57.75	516.7	17.9	25.3	1.3	28.1	1.16	4.12	0.934	0.077
				52 - 78	52.3	0.263	57	566.3	17.2	24.5	1.23	27.8	1.11	1.8	0.83	0.034
6 - Pilot pit 1	152293.8867	511095.8196	4.20	0 - 15	68.6	0.507	40.75	412	2.81	21.1	0.207	21.3	0.187	4.45	0.157	0.105
				15 - 30	65.4	0.789	48.25	452.1	13.9	23.1	1.03	24.3	0.937	2.1	0.712	0.044
7 - Proefput B in	146054.6905	500011.7087	4.75	0 - 18	29.5	0.235	71.5	565.5	18.3	27.3	1.36	33.6	1.24	17.3	1.27	0.284
				18 - 36	29	0.235	78.75	643.9	2.62	24.5	0.187	36.5	0.172	20.9	0.187	0.343
				36 - 54	29.6	0.275	70.75	704.1	25.1	20.6	1.69	33.3	1.56	20.5	1.7	0.380
8 - Proefput B out	145469.3522	500242.5451	-	0 - 21	49.4	0.294	67	544	17.1	25.3	1.26	31.8	1.16	4.42	0.909	0.077
				21 - 42	42.9	0.242	76	602.1	8.62	35	0.65	35.4	0.586	2.7	0.428	0.038
				42 - 63	50.1	0.252	58.5	469.8	15.1	28.3	1.14	28.4	1.03	2.09	0.741	0.037
9 - West 1	132933.5664	510944.0255	3.05	0 - 25	47.5	0.26	75	582.8	19.9	29.6	1.47	35	1.33	3.4	1.02	0.053
				25 - 50	44.7	0.23	71	652	15.4	31.5	1.13	33.4	1.01	4.7	0.811	0.072
				50 - 75	42.1	0.221	73.5	601.6	17.9	28.7	1.3	34.4	1.17	2.16	0.875	0.034
				75 - 100	43.6	0.229	70.25	607.9	19.8	30.1	1.45	33.1	1.33	2.73	1.02	0.043
10 - West 2	135916.7799	503831.5158	-	0 - 23	43.1	0.252	82.5	658.6	18.7	29.8	1.37	38	1.27	3.45	0.937	0.051
				23 - 46	45.7	0.254	76.25	662.3	19.8	29	1.42	35.5	1.31	5.19	1.03	0.080
				46 - 69	51.3	0.269	65	589.1	16	23.6	1.13	31	1.04	4.61	0.85	0.084
				69 - 95	53.2	0.283	52.5	544.2	18.7	28.5	1.37	26	1.22	4.53	1.01	0.083

Table A.3: Results of the cesium measurements.

A-4: Argus Surface Monitor

Calibration of the sensors

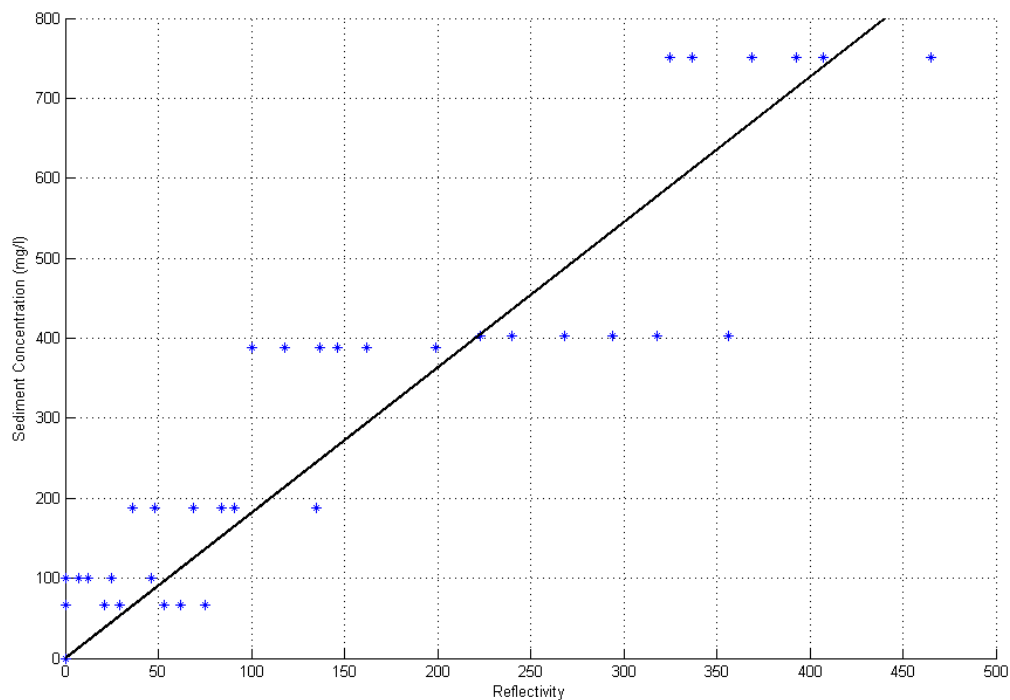


Figure A.7: Calibration Curve for Argus Surface Monitor.

Calibration Sample	Volume (ml)	Mass Sediment (g)	Sediment Concentration (mg/l)	Ref 91	Ref 92	Ref 93	Ref 94	Ref 95	Ref 96	D ₅₀ (μm)	D ₅₀ DeFloc (μm)	Comment
1	200	0	0	0	0	0	0	0	0	-	-	
2	200	0.0133	66.5	21	0	53	62	29	75	54	30	
3	200	0.0200	100	7	0	25	46	12	25	48	33	
4	200	0.0377	188.5	48	36	91	135	69	84	40	34	
5	200	0.0776	388	118	100	146	199	137	162	40	35	
6	200	0.0805	402.5	240	223	294	365	268	318	47	39	
7	200	0.1502	751	337	325	407	465	369	393	44	42	
8	200	0.5065	2532.5	616	622	722	792	666	676	42	42	Outlier, omitted
9	200	2.0673	10336.5	2045	2039	2352	2552	2002	2062	49	45	Outlier, omitted

Table A.4: Results of analysis of calibration samples for the ASM.

Calibration equation:

$$[\text{mg/l}] = 1.8153 \times [\text{Reflectivity}]$$

Error: $R^2 = 0.8497$ Correlation Coefficient = 0.9852

Concentration profiles

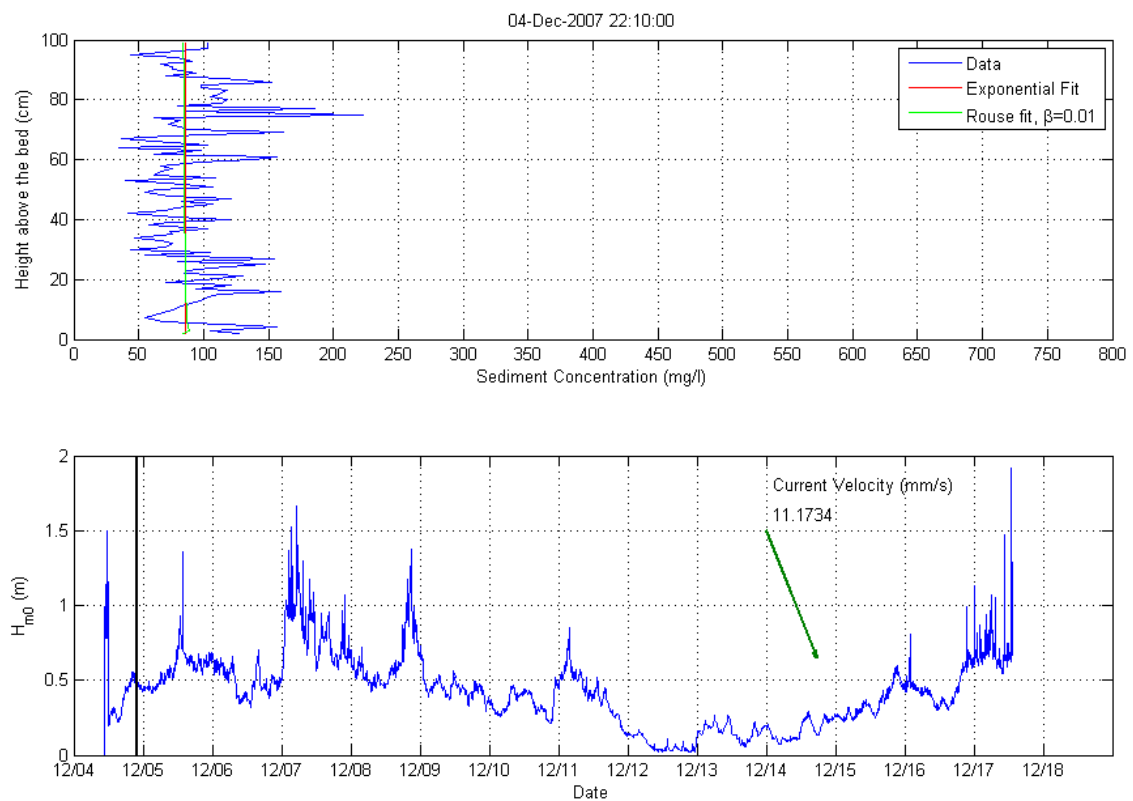


Figure A.8: ASM result 4 December 2007 22:10. The wave height is about 0.5 m. The concentration profile is uniform over the vertical.

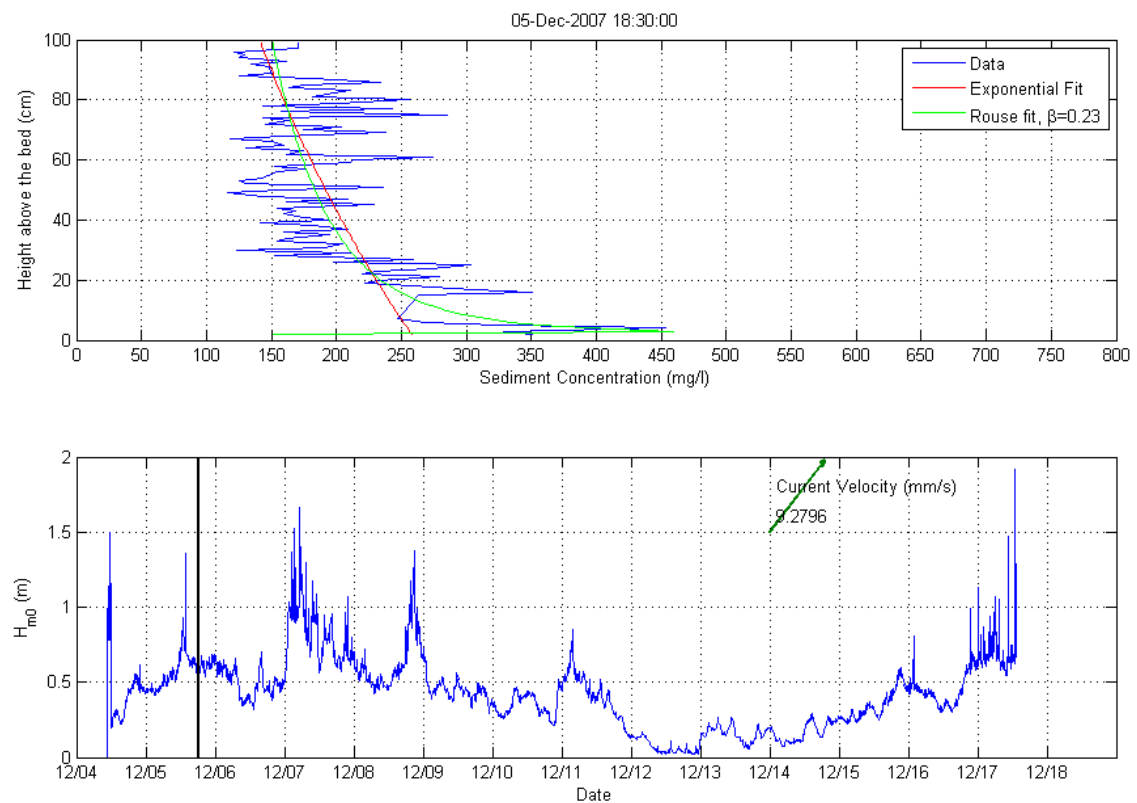


Figure A.9: ASM result 5 December 2007 18:30. Wave height is increased to about 0.6 m. The concentration profile shows a high concentration layer near the bed, up to 450 mg/l

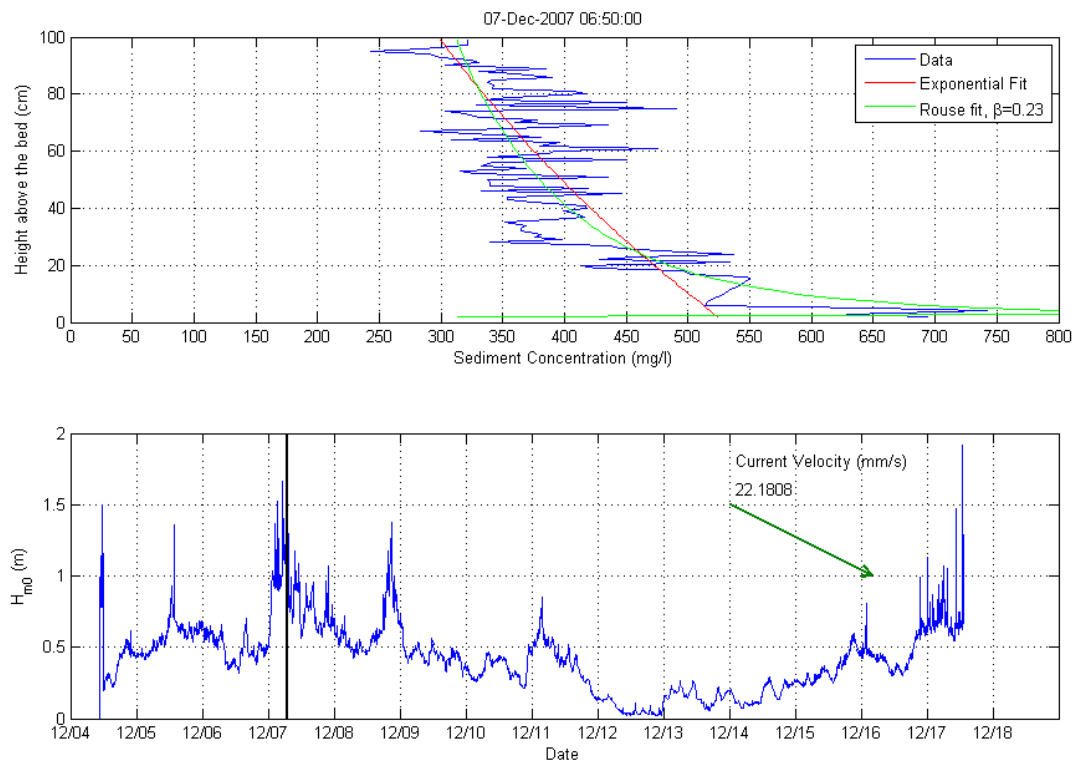


Figure A.10: ASM result 7 December 2007 6:50. Wave height is further increased to about 1 m and more. More sediment is suspended in the water column (concentration about 300 mg/l). The high concentration layer near the bed is increased to about 800 mg/l.

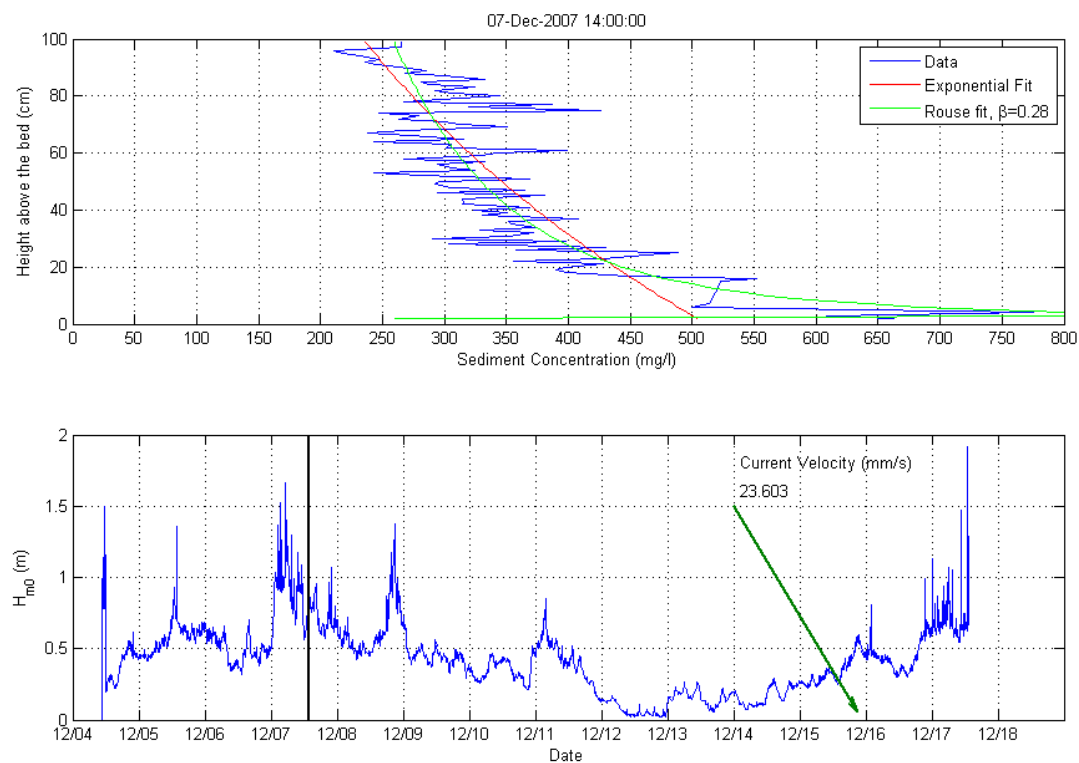


Figure A.11: ASM result 7 December 2007 14:00. The storm period is over. The wave height is reduced to 0.7 m. Sediment concentration in the water column is decreased to 250 mg/l. The high concentration layer near the bed is still present.

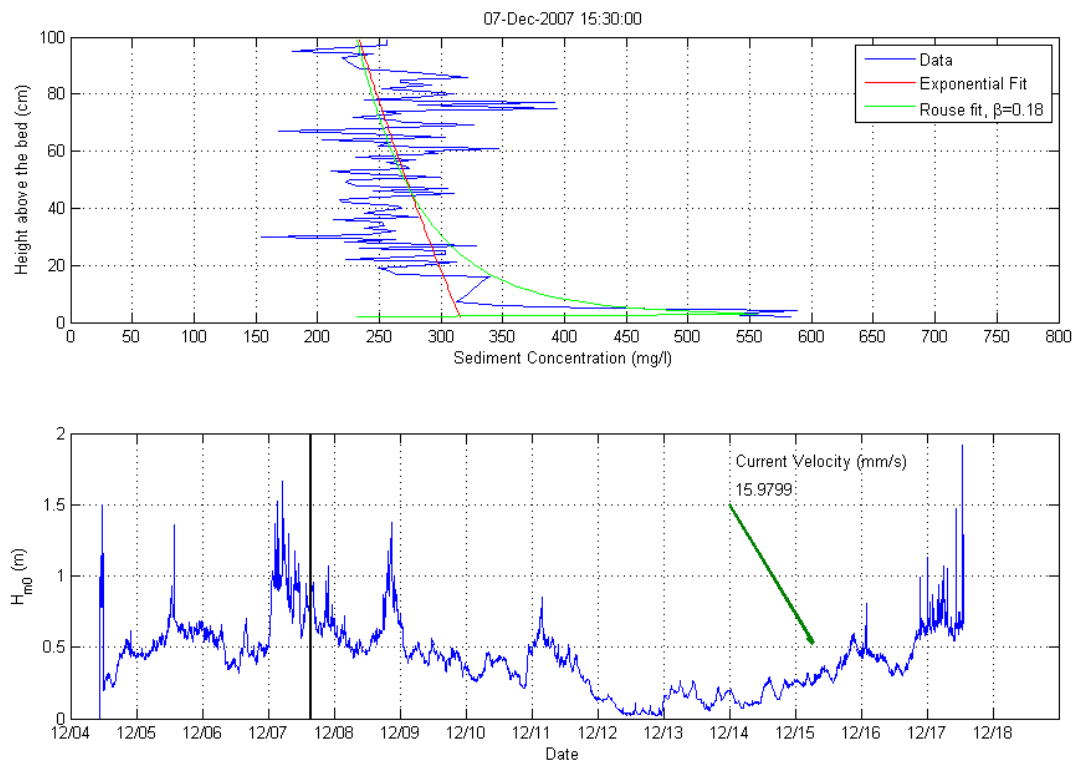


Figure A.12: ASM result 7 December 2007 15:30. Wave height is further reduced. The sediment concentration in the water column is still 250 mg/l. The high concentration layer is thinner and the concentration is decreased to 500 mg/l.

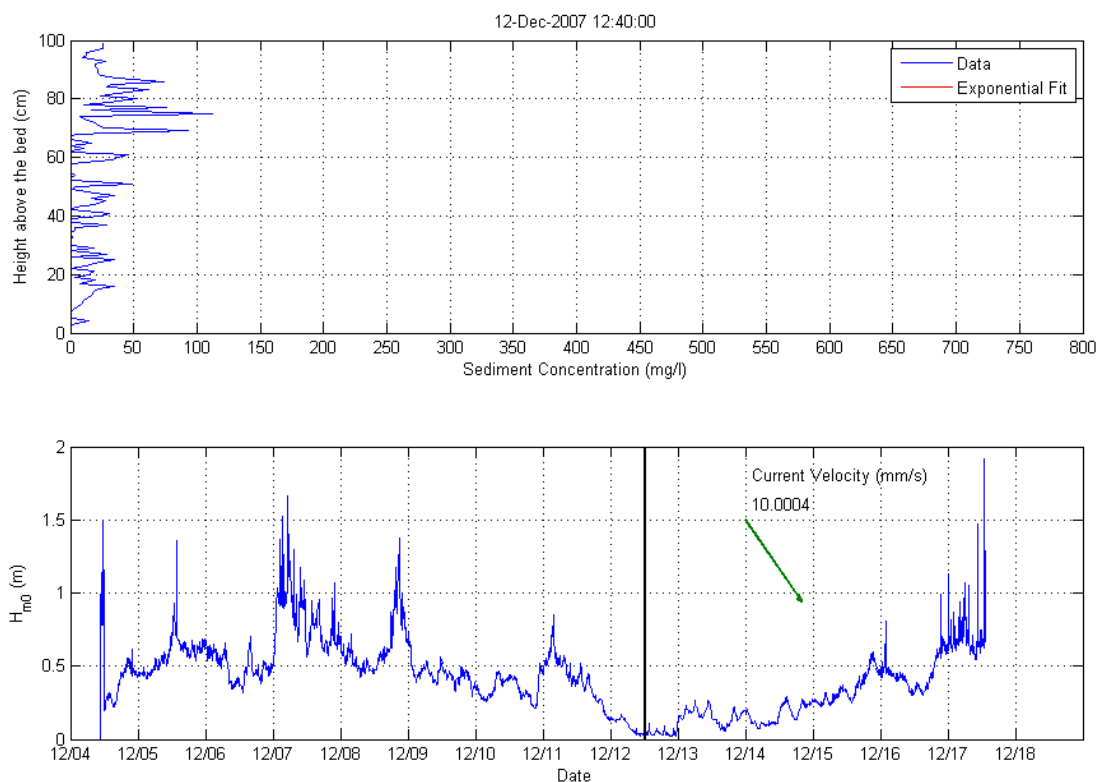


Figure A.13: ASM result 12 December 2007 12:40. Very calm period. Almost no waves. The sediment concentration in the water column is minimal, only 20 – 30 mg/l

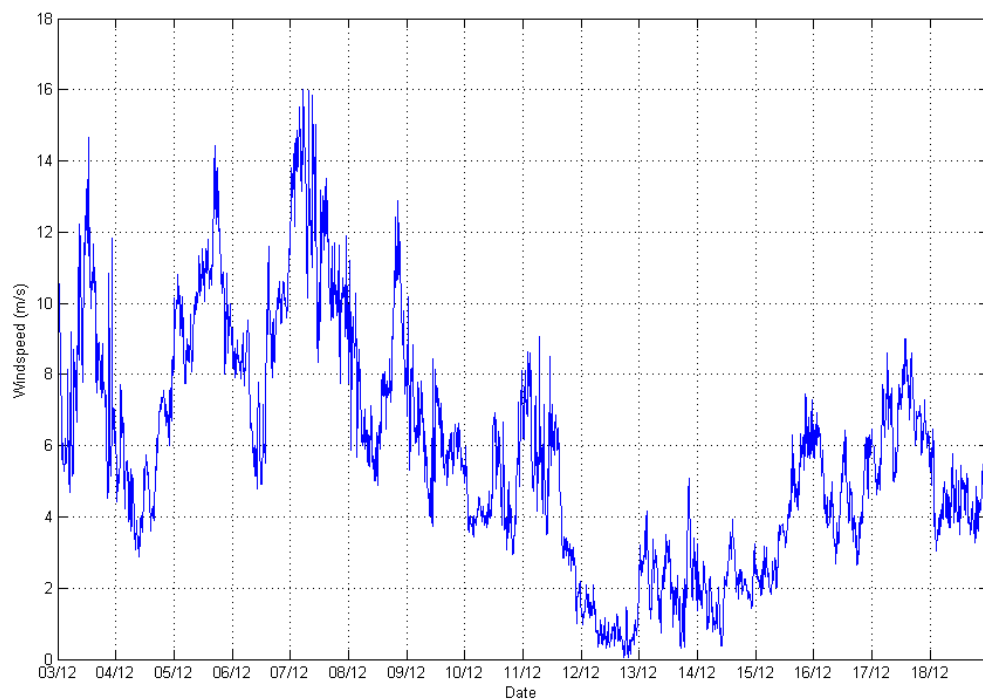


Figure A.14: Wind speed (m/s) during measurement period. In the period of 5 December to 9 December three storm periods occurred. After this period the conditions became calm.

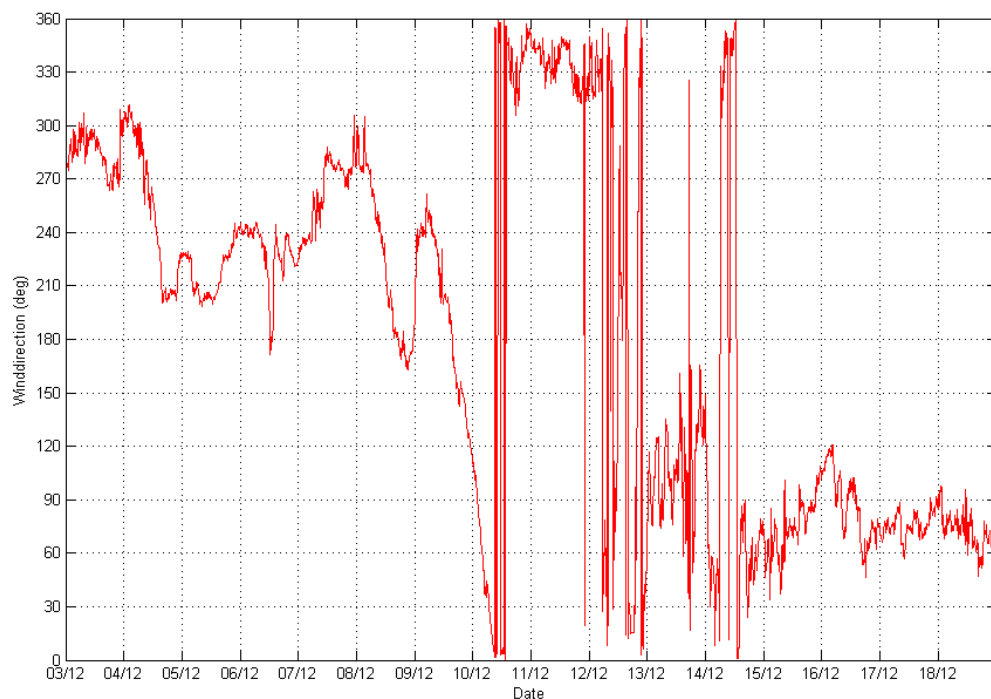


Figure A.15: Wind direction (deg) during measurement period. During the storm periods the wind is from 210 to 240 degrees, which is from the southwest direction.

Appendix B: Large scale Delft3D model

B-1: Other model settings

In this part of the appendix the other model settings of the large scale Markermeer model are described.

Viscosity

The viscosity and diffusivity values in the model are set to default values:

Horizontal eddy viscosity	= 1 m ² /s
Eddy diffusivity	= 10 m ² /s

The turbulence model used in this 3D model is the well known $\kappa - \epsilon$ model. This is in combination with density current modelling and 20 layers in the vertical the best choice. More information about the $\kappa - \epsilon$ turbulence model and its implementation in the Delft3D model is given in de Delft3D manual (WL Delft Hydraulics, 2006a).

WAVE: Physical processes and parameters

In SWAN several physical processes of waves can be taken into account. In this model it is not needed to implement all the processes in the computation. Some of the processes should be excluded or changed, because of the wrong behaviour of the model when using default values.

Depth induced breaking is included in the model, according to the Battjes & Jansen model with default values, $\alpha = 1.0$ and $\gamma = 0.73$. Nevertheless waves will not break in the model, because of the limited wave growth. For example, the maximum γ (which is defined as H_s/h), at the location of the measurements, pole FL 42 is 0.3 – 0.4. (Figure B.2)

Bottom friction is not included in the model. In default this is, but due to under prediction of the wave height this is switched off (explanation is given in Section 5.3).

Diffraction is not included in the model. This is default setting and this process is not important in this situation.

Wind growth is the process that waves will grow due to the wind. This is the main driving force of the Markermeer model, so this process is important.

Quadruplets wave interaction is also an important process in wind generated waves, so also this is included.

Refraction and frequency shift are included in the model, this is default.

Whitecapping is energy dissipation when waves become too steep. This is also an important process in wind generated waves, so it is included. However, whitecapping is not implemented according to the default values, but with a new formulation (according to Westhuysen et al 2006), because of under prediction of wave height in shallow lakes (explanation is also given in Section 5.3).

Wave set up is not included, because this is an important process in surf zone hydrodynamics, but not in this Markermeer model. The wave setup is not relevant for the large scale mud dynamics in the lake.

Numerical parameters

Numerical parameters for the SWAN model concern mostly the accuracy criteria for the iteration process. Comparing to the original WL model of the Markermeer the iteration criteria are stricter. This is because of the under prediction of the wave height. More and more accurate iterations will improve the results. Therefore the maximum number of iterations in each SWAN computation is set to 30 (default value is 15). The percentage of the accurate wet grid point should be 99 % (default 98 %) before stopping the iteration process. All relative changes are set to 0.01 m (default 0.02 m).

The spectral values for computing the energy balance in SWAN are set to default values. The number of directions is 36. The lowest frequency is 0.05 Hz and the highest 1 Hz. The number of frequency bins is 24.

B-2: Calibration results

Wave heights

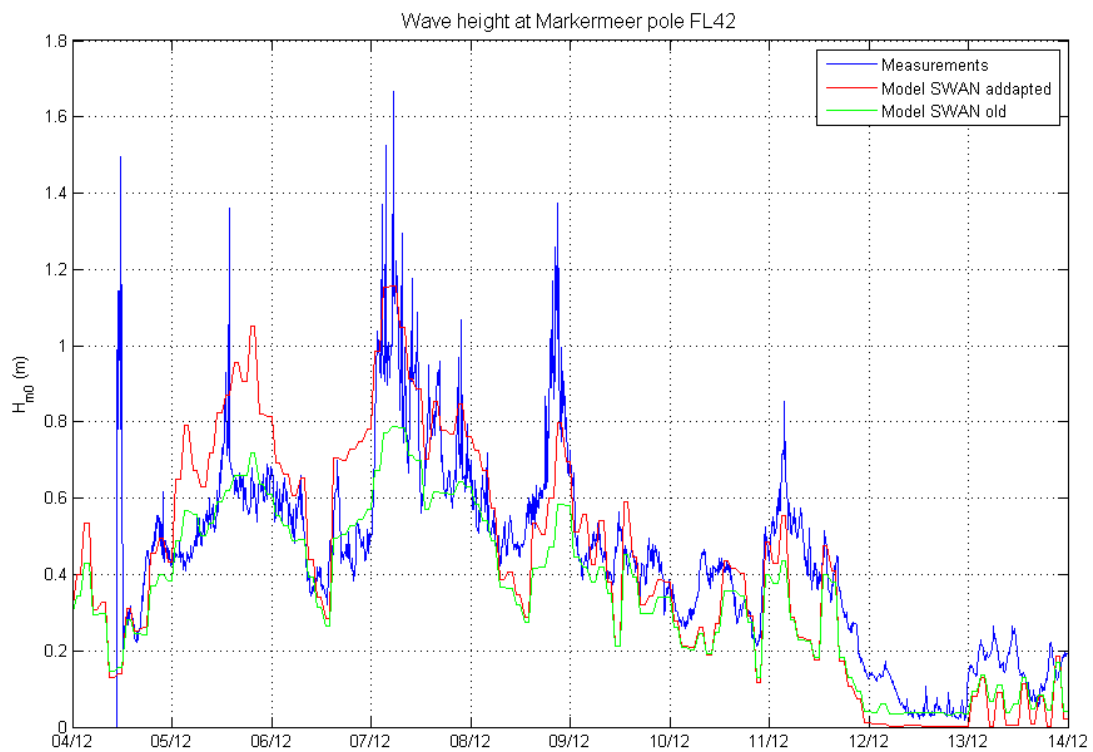


Figure B.1: Time series of significant wave height, measurements (blue) and model old (green) and model adapted (red). The results of the adapted model show good similarity with the measurements.

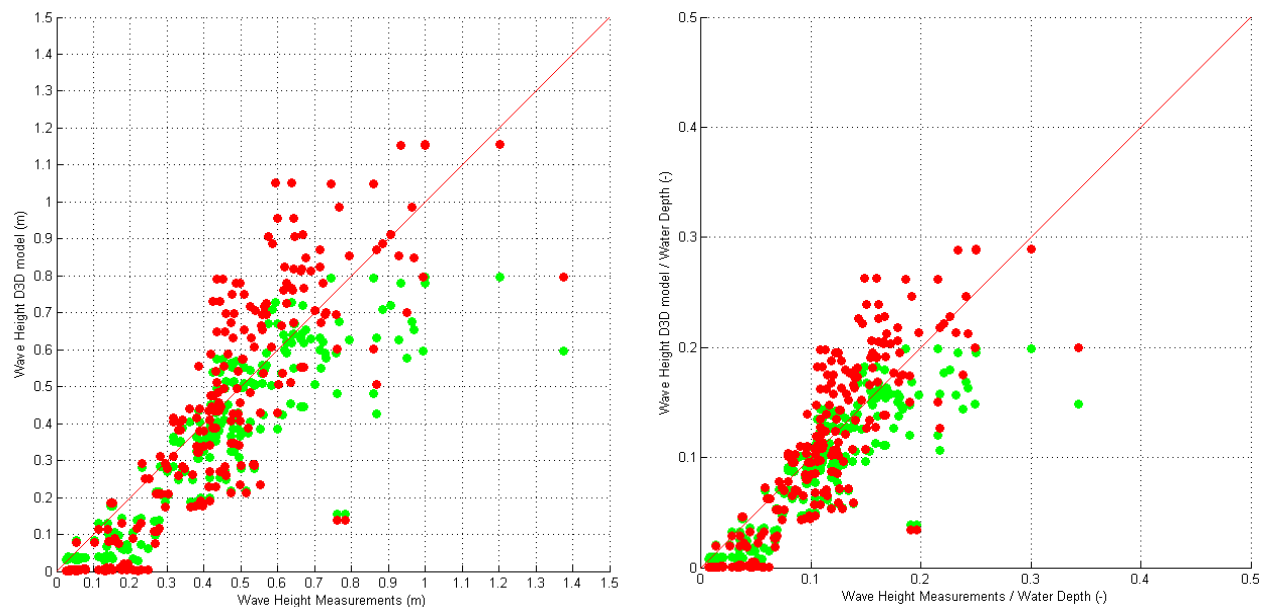


Figure B.2: Significant wave height, measurements (x axis) and model (y axis) compared and scaled to water depth (right).

Sediment Concentration

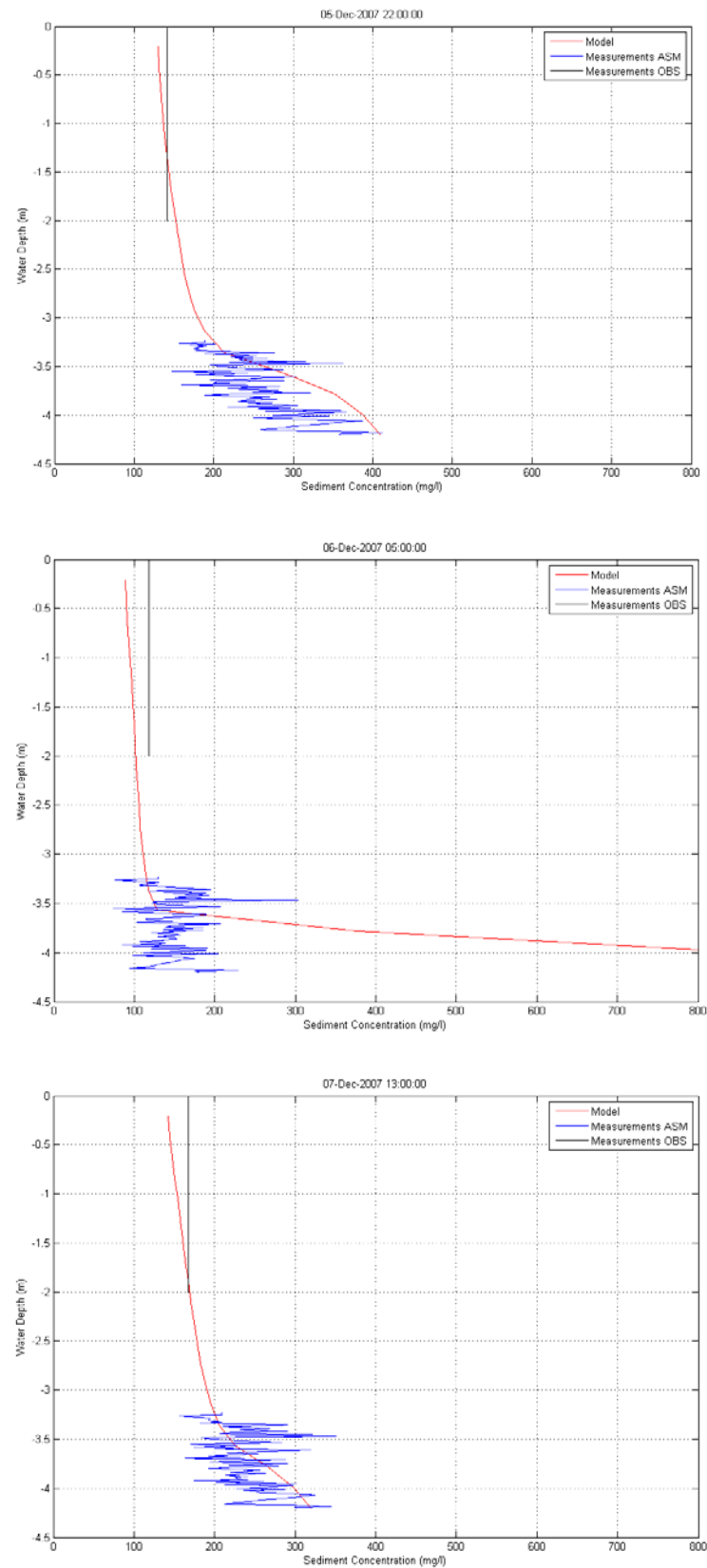


Figure B.3: Sediment concentration profiles, measured (blue) and model results (red) on several times. The model results give the same order of sediment concentration. Also the high concentration near the bed is well simulated.

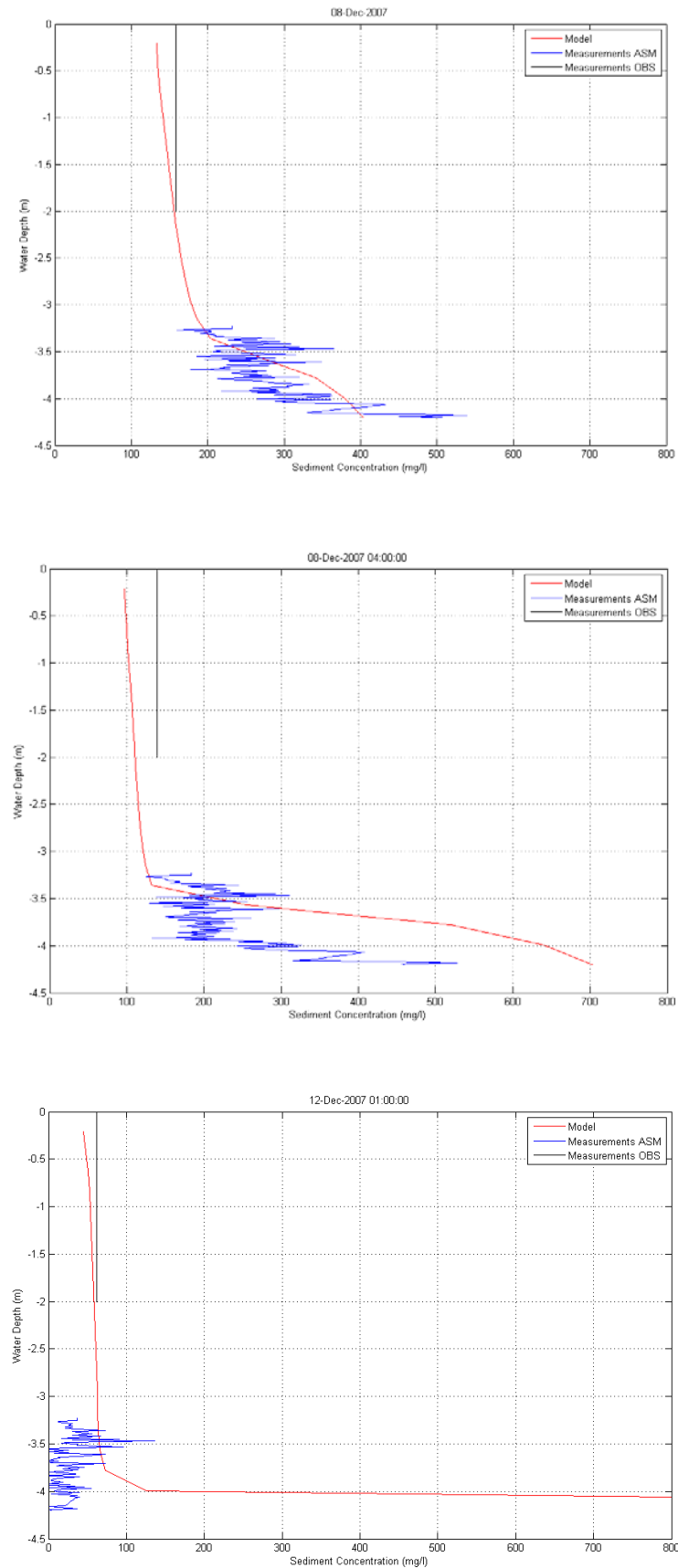


Figure B.4: Sediment concentration profiles, measured and model results on several times. In the last plot the modelling effect of neglecting sedimentation and erosion is shown. The model predicts a high concentration layer, almost all the sediment is 'stored' in the lowest layer.

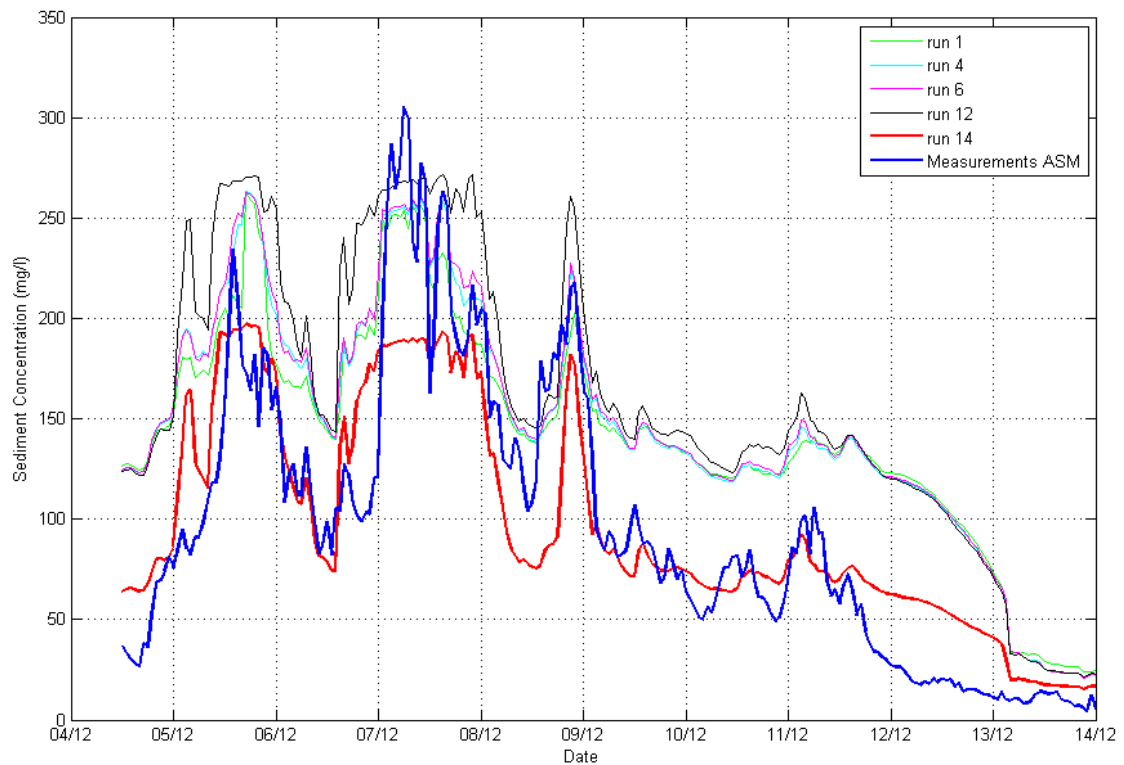


Figure B.5: Time series of sediment concentration averaged over upper 10 cm of ASM (about 1 m above the bed), measurements (blue) and several model simulations. Run 14 shows good similarity with the measured sediment concentration.

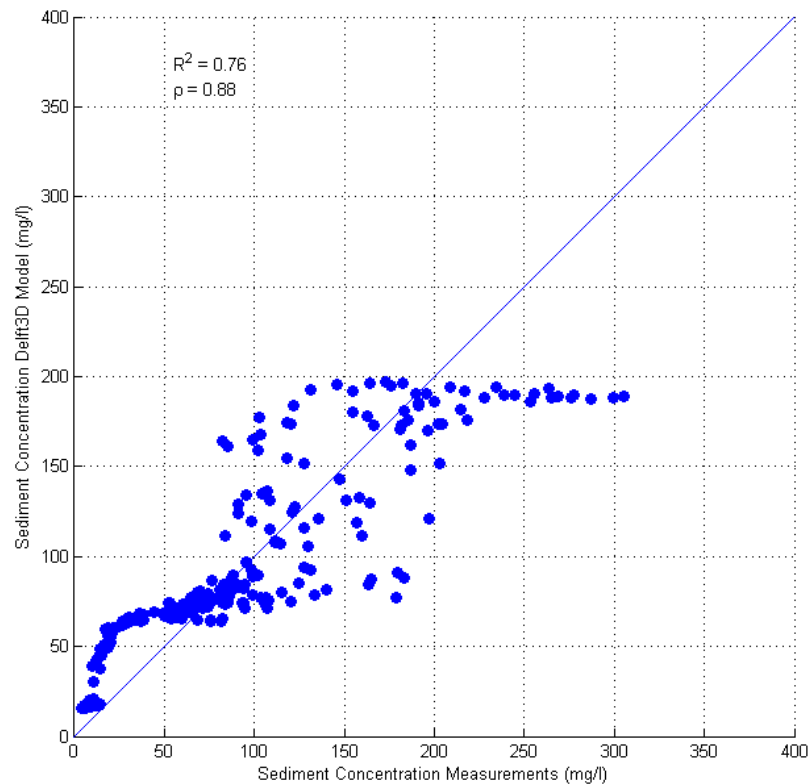


Figure B.6: Comparison of measured (x axis) and modelled sediment concentration (y axis) at the location of the ASM. Modelling results are of run 14. The sediment concentration in the model has its limit on 200 mg/l.

B-2: Results

Behaviour of both fractions

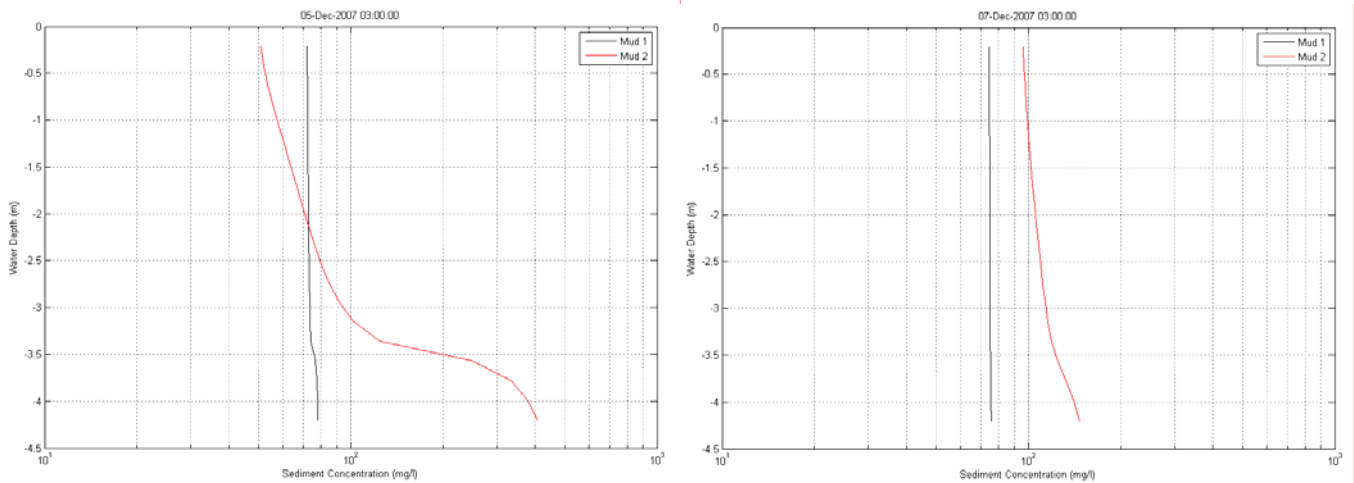


Figure B.7: Sediment concentration profiles of both fraction on several times, left (1) and right (2).

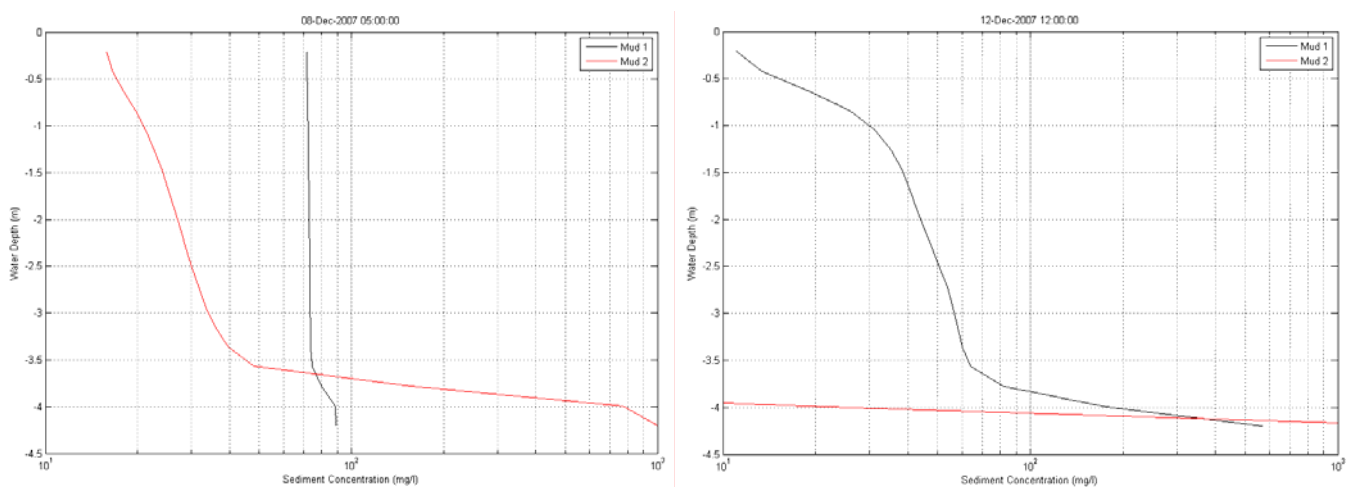


Figure B.8: Sediment concentration profiles of both fraction on several times, left (3) and right (4).

The fine fraction is completely mixed over the vertical during most of the time. The fine fraction can settle if wind forcing is decreased to very low intensity. The mixing of the coarse fraction is according to the storms periods.

Effect of waves on sediment concentration

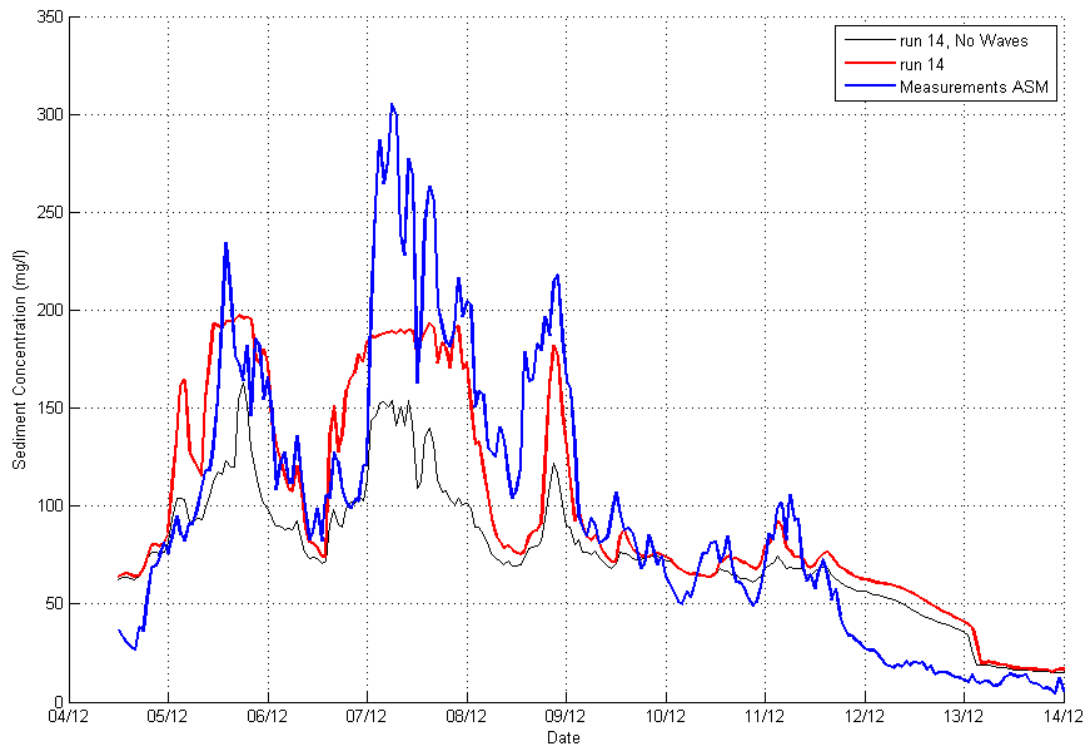


Figure B.9: Time series of sediment concentration upper 10 cm of ASM, measurements (blue) and model. One model run normal (run 14, red), one run without wave computation (black). The effect of waves on the sediment concentration is largest during storm periods. In the simulation without waves, the sediment concentration is about 25 % lower.

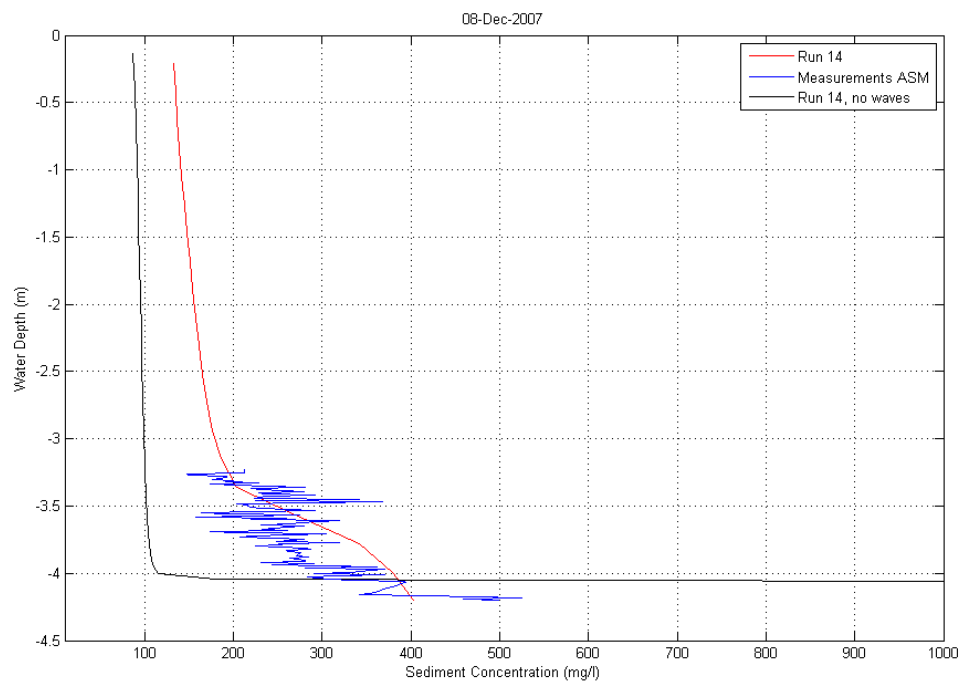


Figure B.10: Sediment concentration profile 8 December 2007. One model run normal (run 14, red), one run without wave computation (black). The simulation including waves corresponds better to the measurements. Without waves the turbulence intensity near the bed is less and the sediment is kept in the lowest layer.

Appendix C: Delft3D model of the silt trap

C-1: Observation points and cross sections

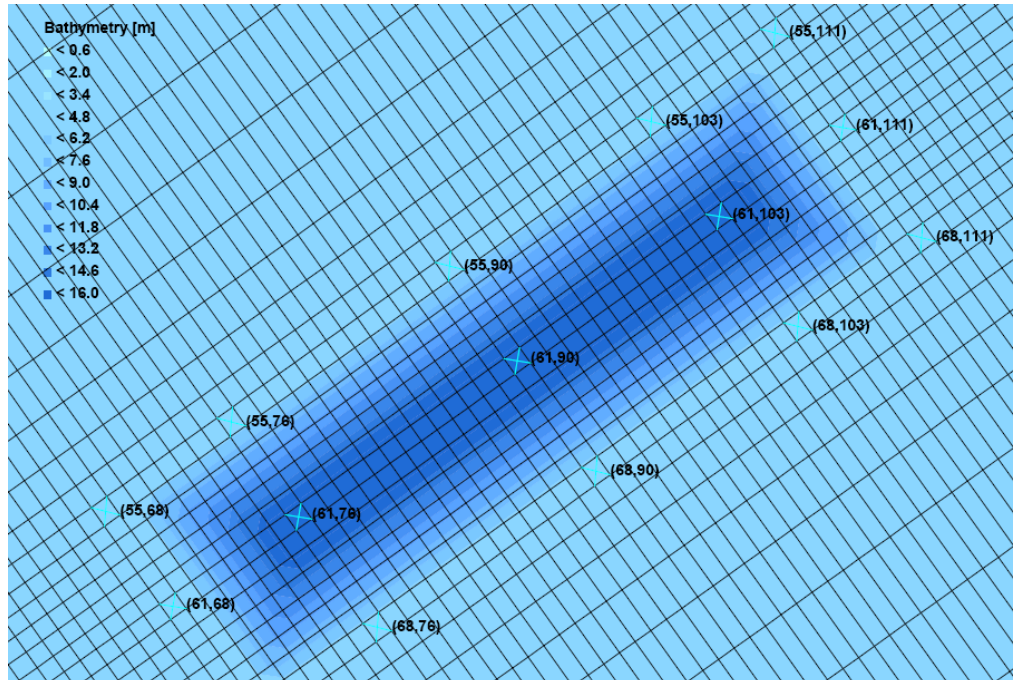


Figure C.1: Parallel observation points.

Three observation points are located inside the silt trap. 12 observation points just on the edge of the trap.

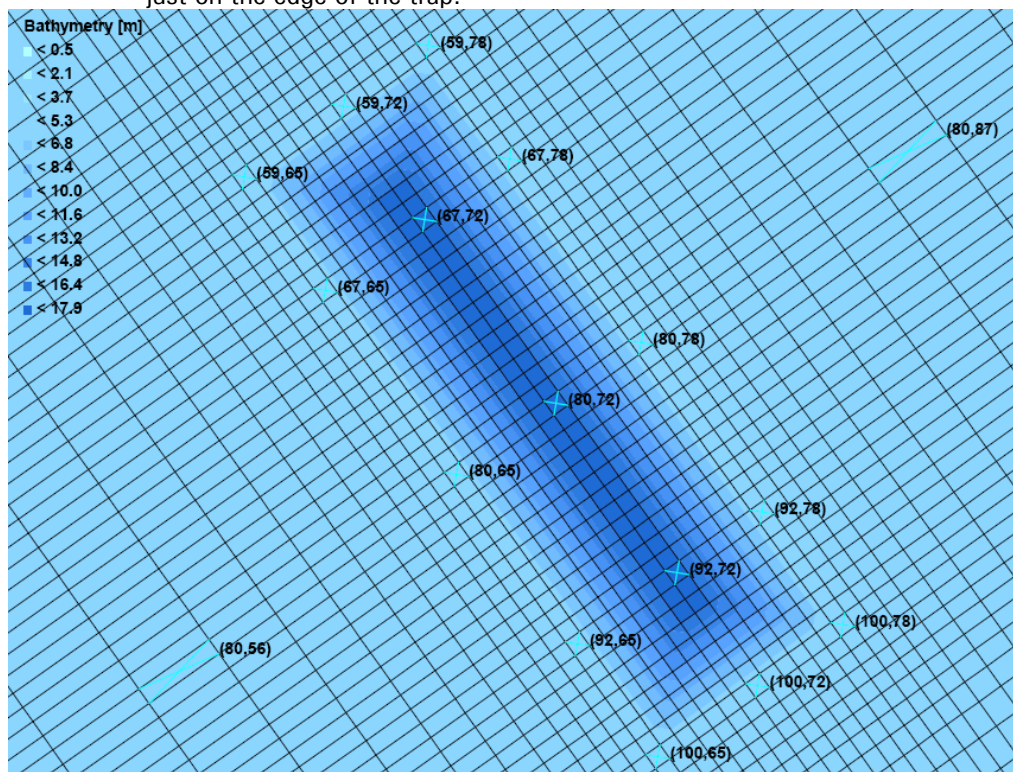


Figure C.2: Perpendicular observation points.

Three observation points are located inside the silt trap. 12 observation points just on the edge of the trap.

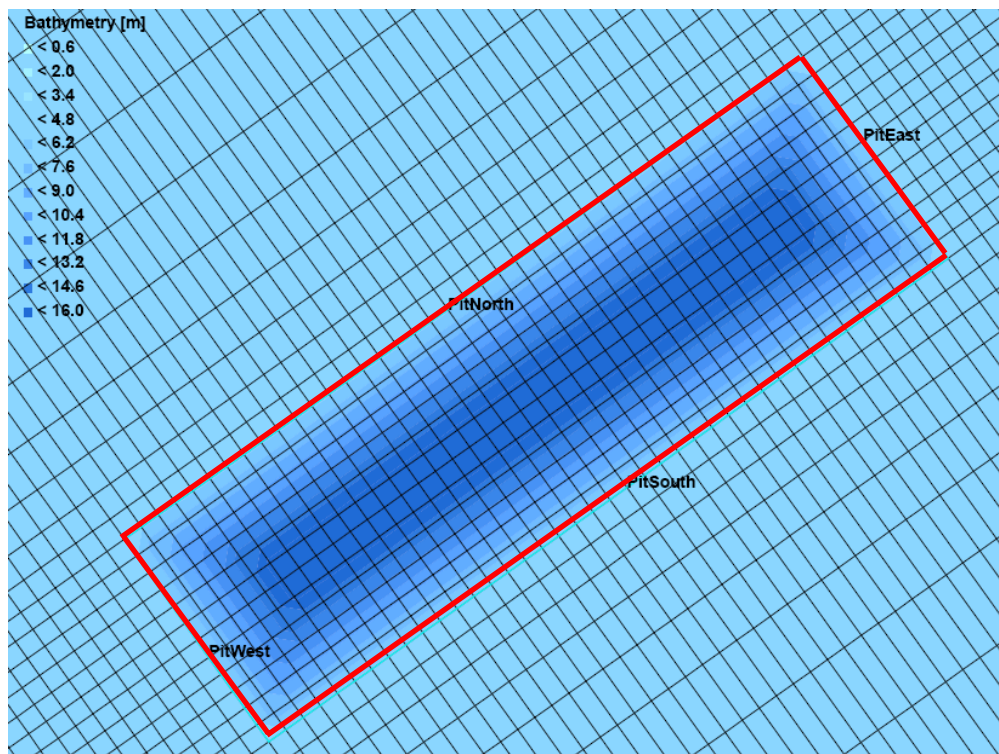


Figure C.3: Parallel cross sections. Four cross sections are defined: North, South, East and West.

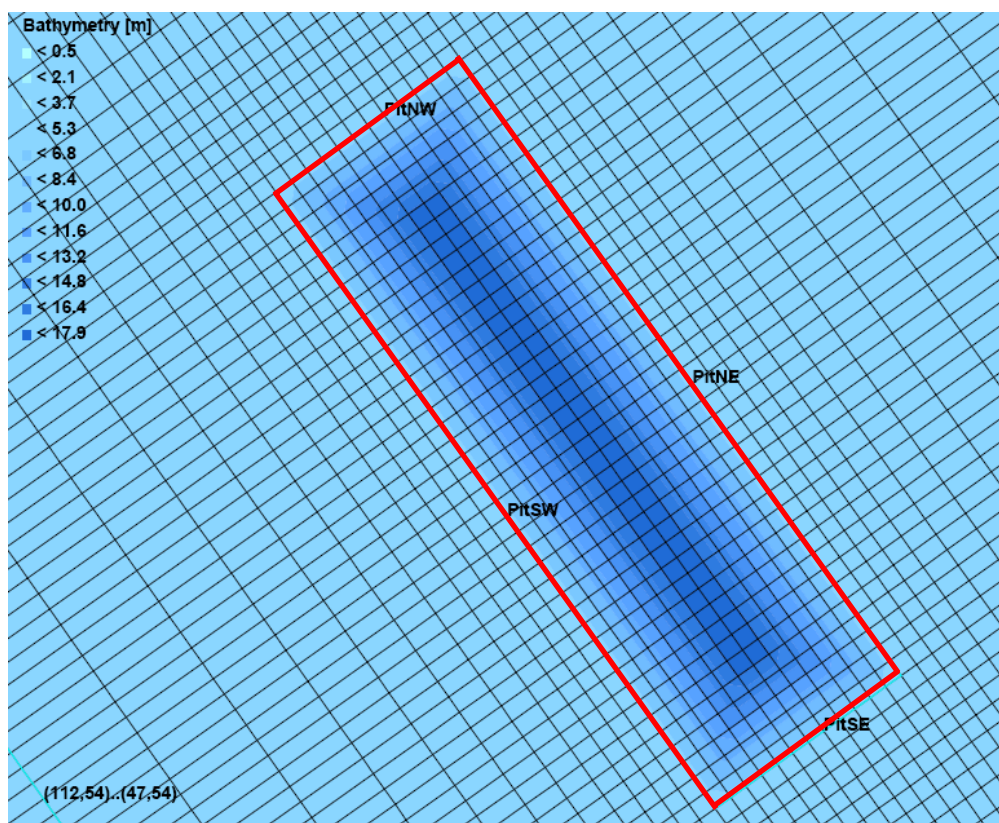


Figure C.4: Perpendicular cross sections. Four cross sections are defined: Northwest, Southwest, Northeast, Southeast.

C-2: Validation

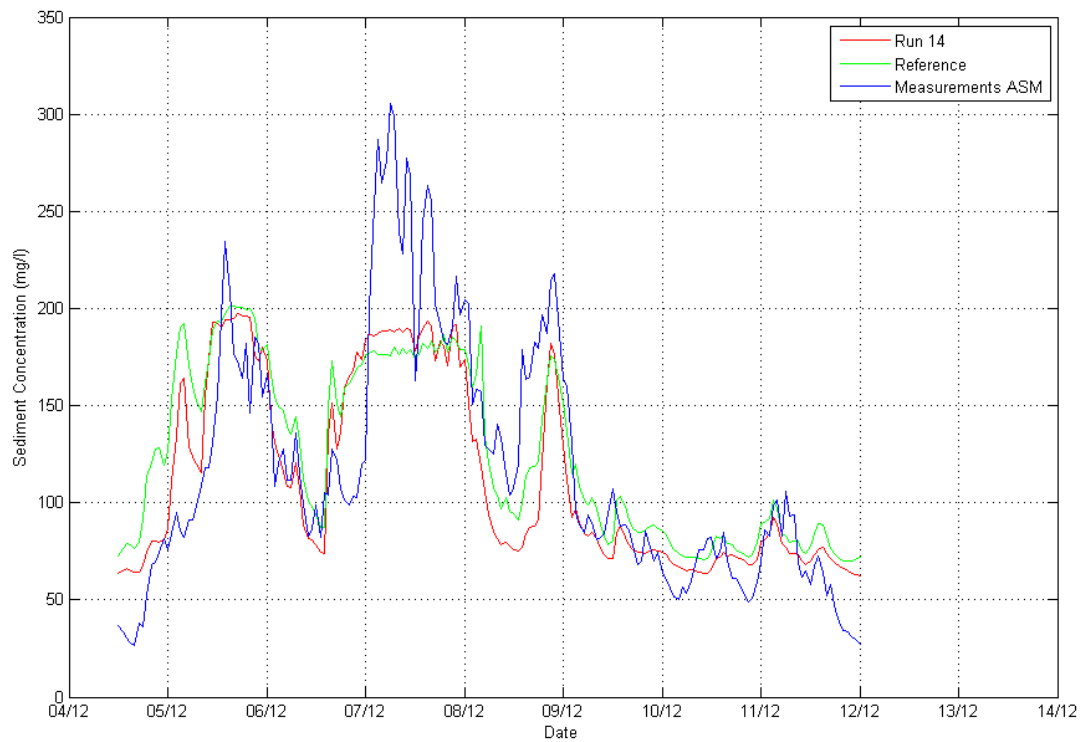


Figure C.5: Sediment concentration at location FL 42. Run 14 (red line), reference model (green line) and ASM data (blue line). The green line agrees well with the red line. Conclusion: the adoptions to the model do not have a large influence on the sediment concentration; the model can be used to assess the effects of the silt trap.

C-3: Comparison to theory

Flow

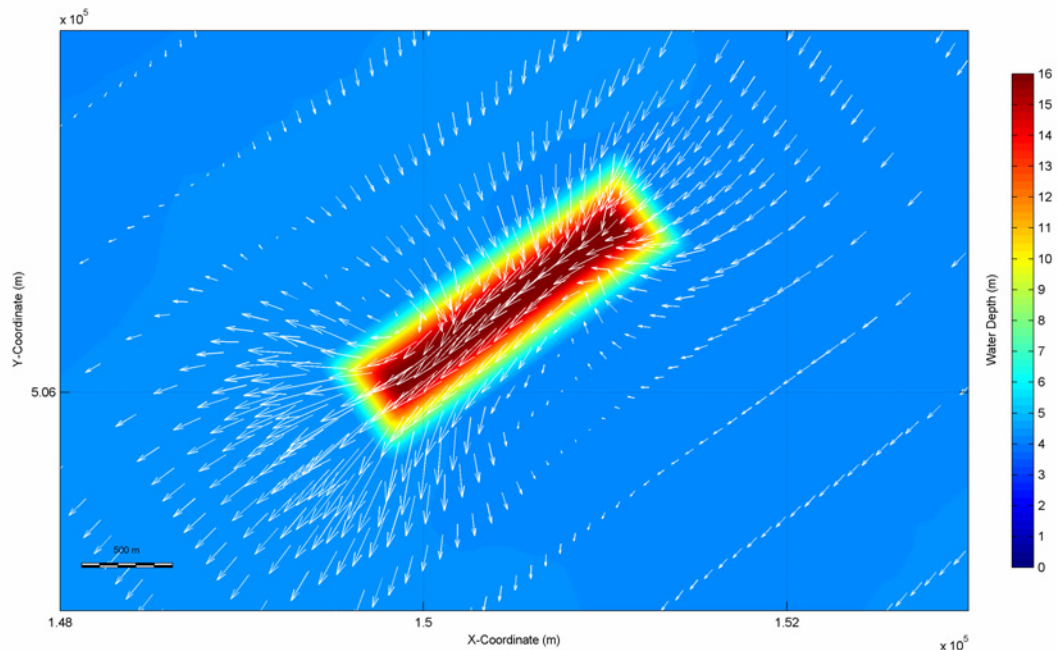


Figure C.6 : Depth average flow velocity situation trap parallel (simulation parallel 1). Time: 7th of December 12h00. Just upstream of the trap the flow accelerates and contracts. Just downstream the flow diverges and decelerates. This flow behaviour corresponds to the theory.

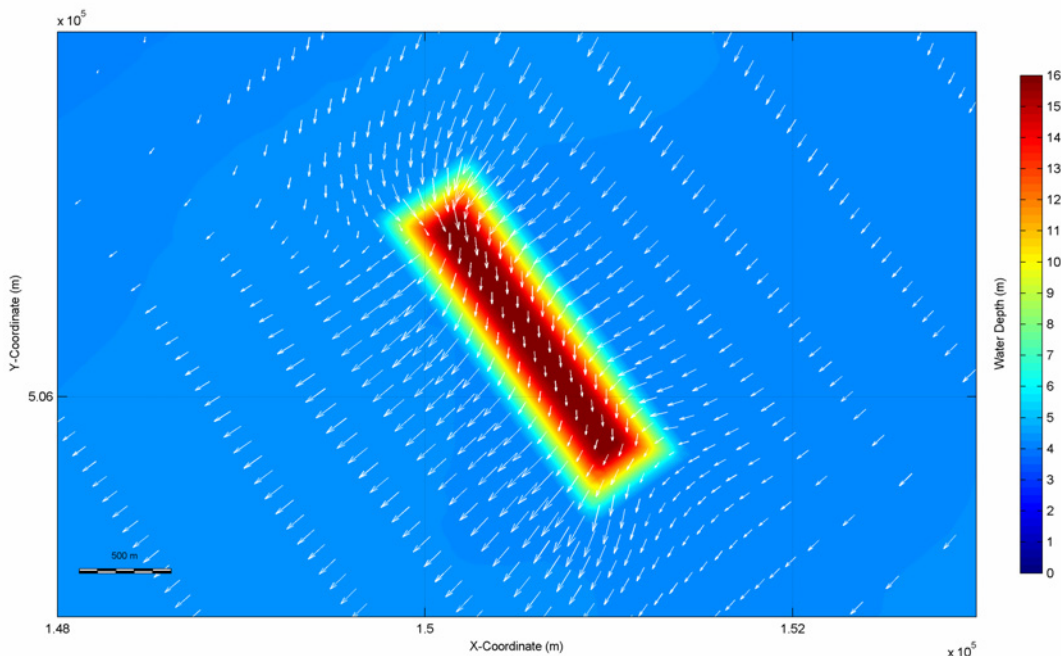


Figure C.7 : Depth average flow velocity situation trap perpendicular/oblique (simulation perpendicular 1). Time: 6th of December 6h00. The flow refracts on the slopes of the silt trap. Just upstream of the trap the flow is from the Northeast direction. Inside the trap the flow is refracted from the North. Just downstream of the trap the flow is again from the Northeast. Also this flow pattern corresponds to the theory.

Waves

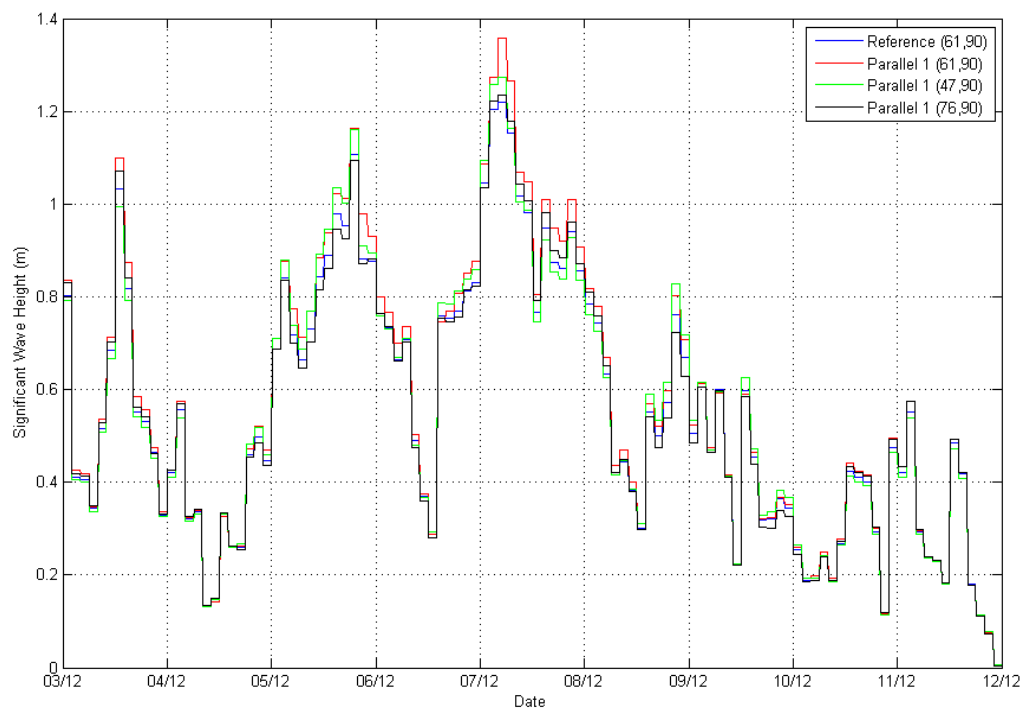


Figure C.8: Significant wave height (m) for 3 locations near and in the silt trap. The blue line is the reference case, without trap. The red line is the wave height in the middle of the trap. A slightly increase in wave height is observed above the trap.

Density Current

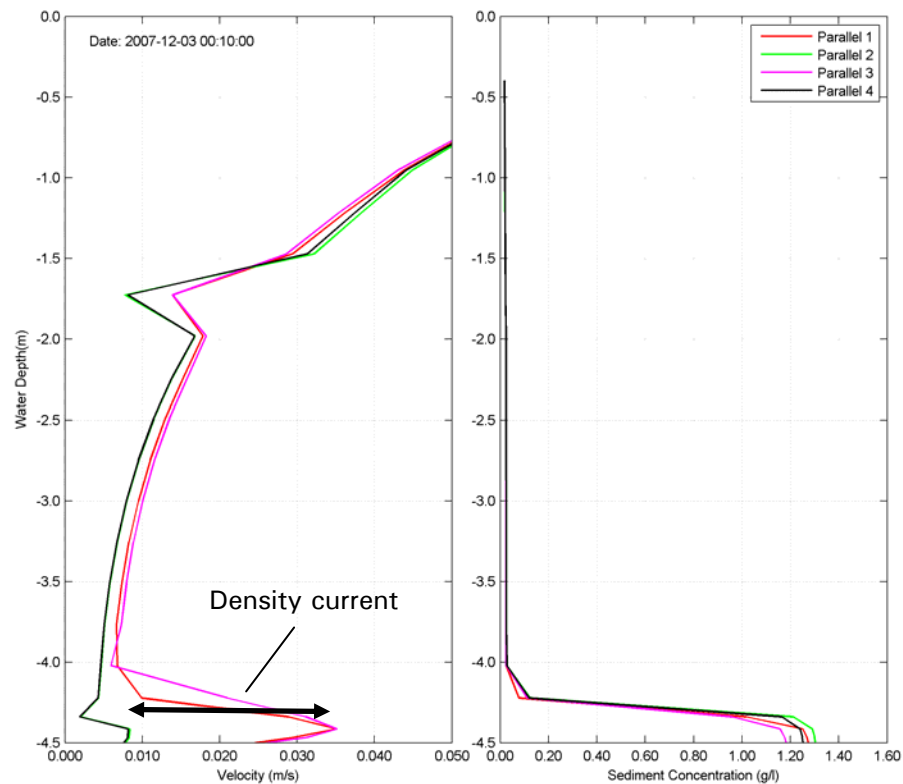


Figure C.9: Velocity (left) and Concentration profile (right) 3 December 0h10 (55,90). Simulation 1 and 3 (red and purple) are including density effect. Black and green show the result excluding density effect. The difference in velocity near the bed between red/purple and black/green is the magnitude of the density current (2 cm/s).

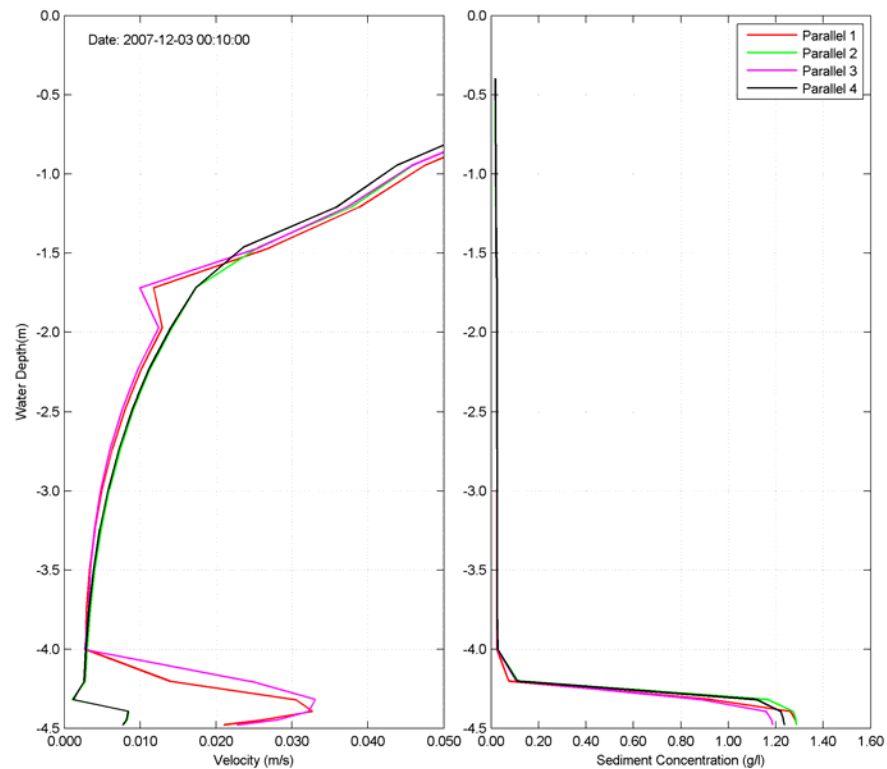


Figure C.10: Velocity and Concentration profile 3 December 0h10 (68,90).

Same figure as C.9, but on the other side of the silt trap. Also a density current of about 2 cm/s is generated. The discontinuity at a water depth of -1.7 m is an initial effect.

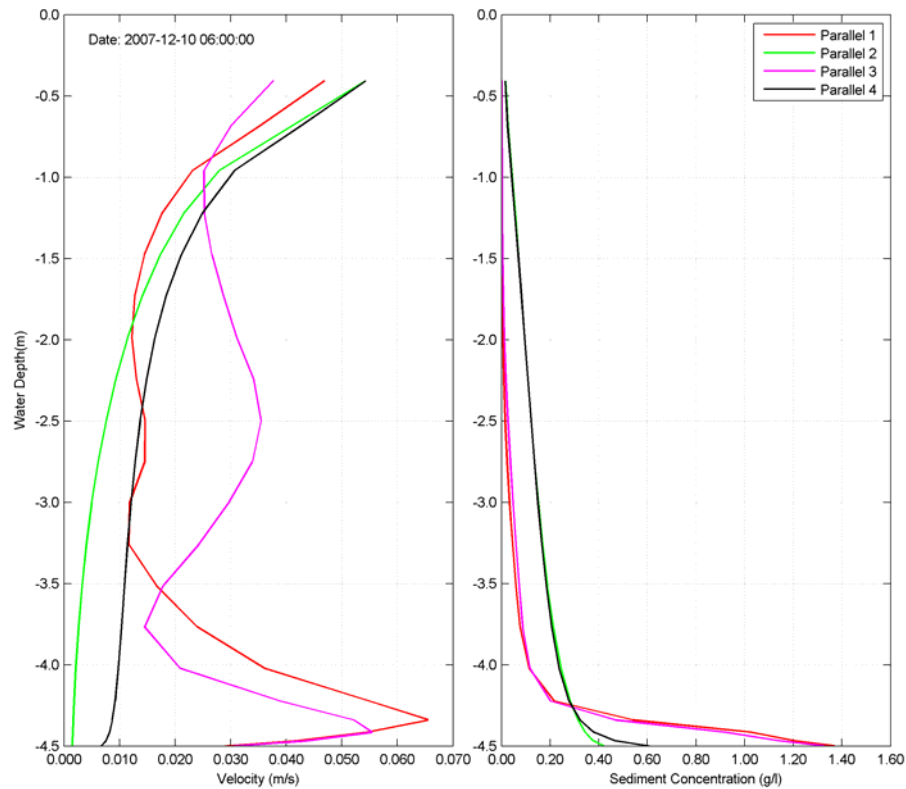


Figure C.11 : Velocity and Concentration profile 10 December 6h00 (55,90).

Same figure as C.9, but on a different time, just at the end of the period. The density current is about 4.5 cm/s.

C-4: Results

Density currents

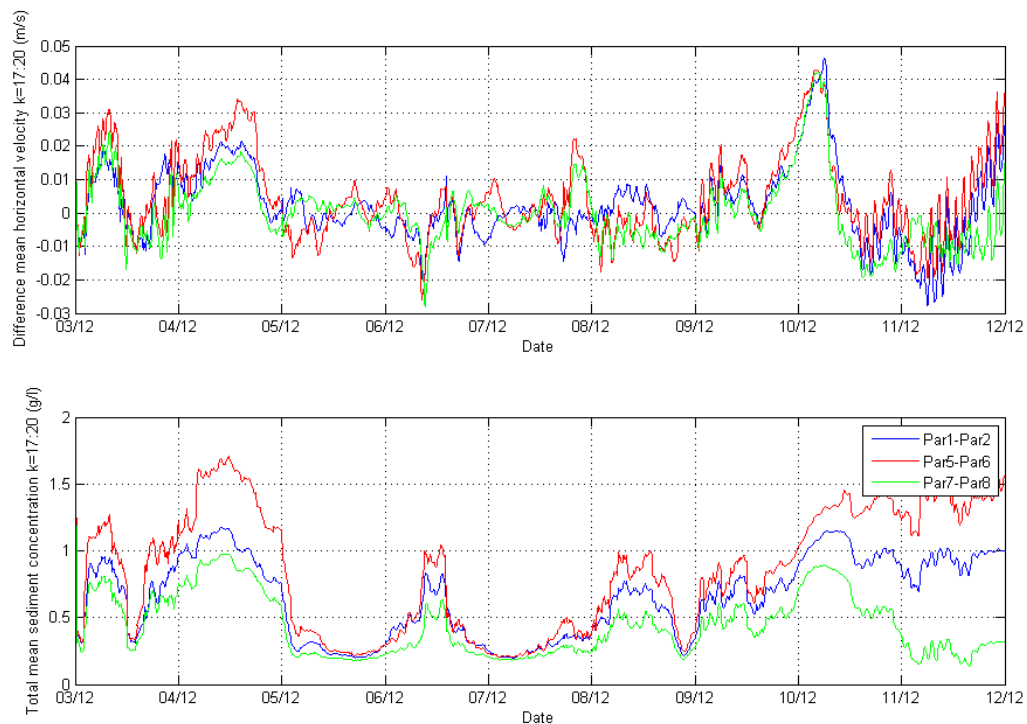


Figure C.12: Density current location (55,90), parallel simulation. First plot is the magnitude of the density current (averaged over the lowest 4 grid cells), second plot is the sediment concentration (also averaged). A density current is generated if the sediment concentration increases to about 1 g/l.



Figure C.13: Density current location (80,78), perpendicular simulation. Same figure as C.12, but in the perpendicular simulation. Results are the same.

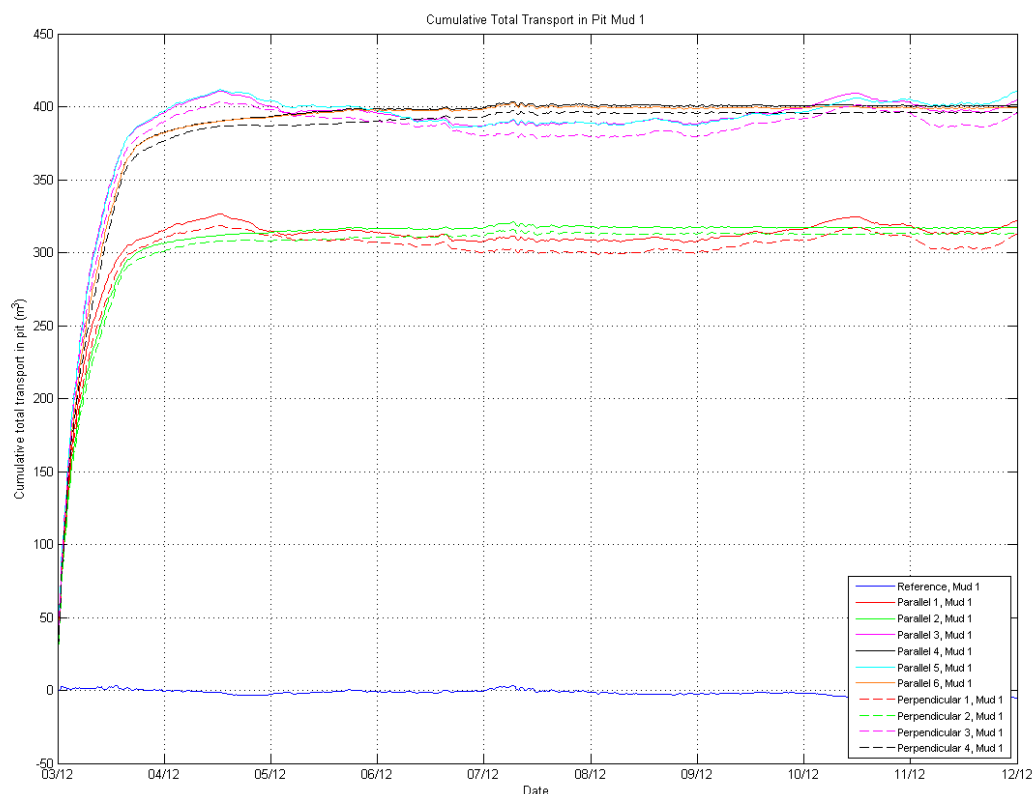


Figure C.14: Cumulative Total Transport in Trap Mud 1. All simulations without sedimentation effect in the trap. No sediment of fraction Mud 1 is accumulated in the trap. The strong increase in accumulation at the 3th of December is an initial effect.

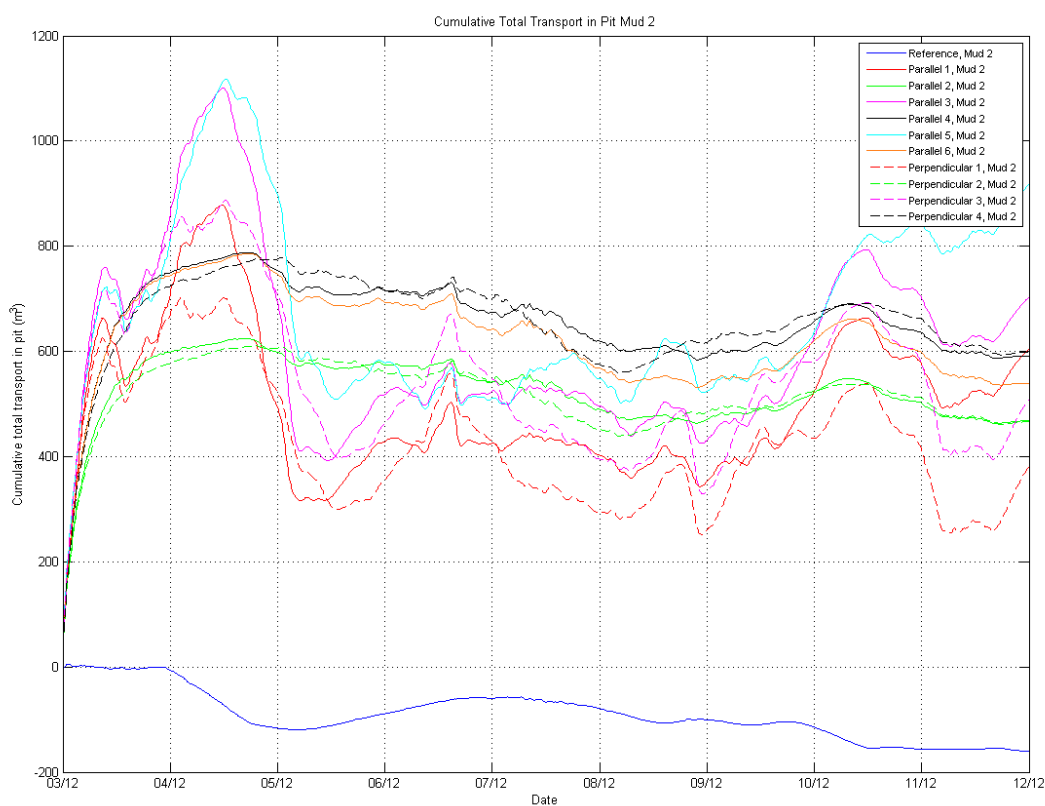


Figure C.15: Cumulative Total Transport in Trap Mud 2. Same figure as C.14, but with coarse fraction (Mud 2). Also for this fraction no clear accumulation of sediment is observed.

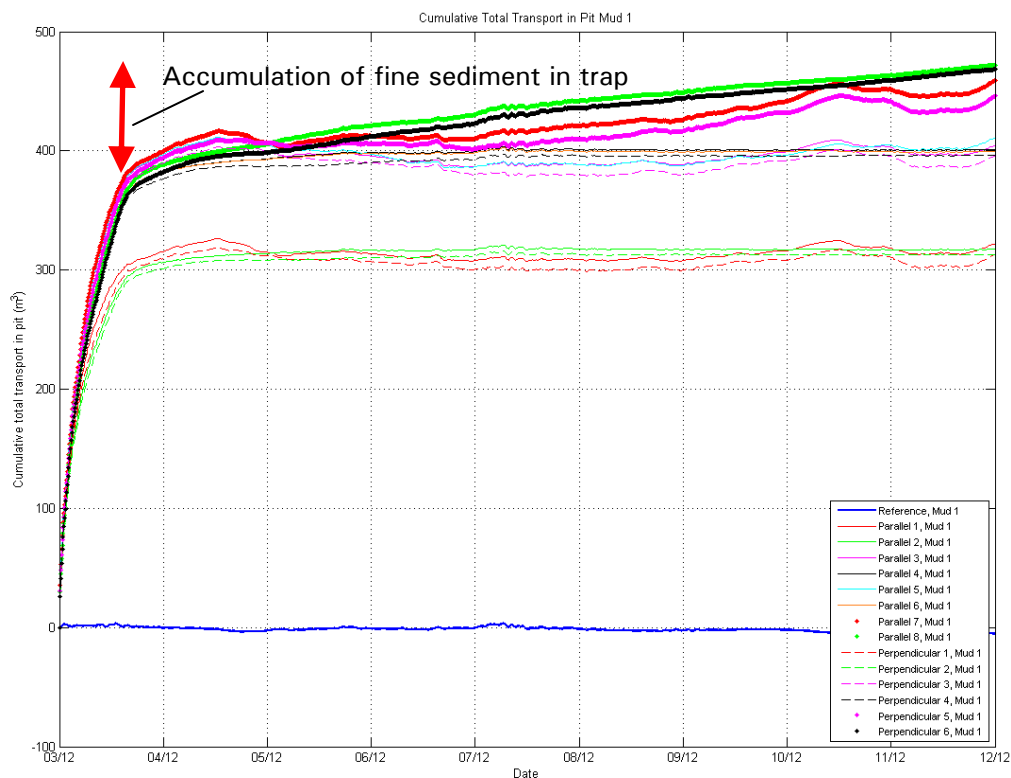


Figure C.16: Cumulative Total Transport in Trap Mud 1. Including simulations with full sedimentation inside the trap (thick line). Thick green/black: no density effect, thick red/purple: including density effect. No difference is observed between with and without density effect. Total accumulation of fine fraction is about 100 m³.

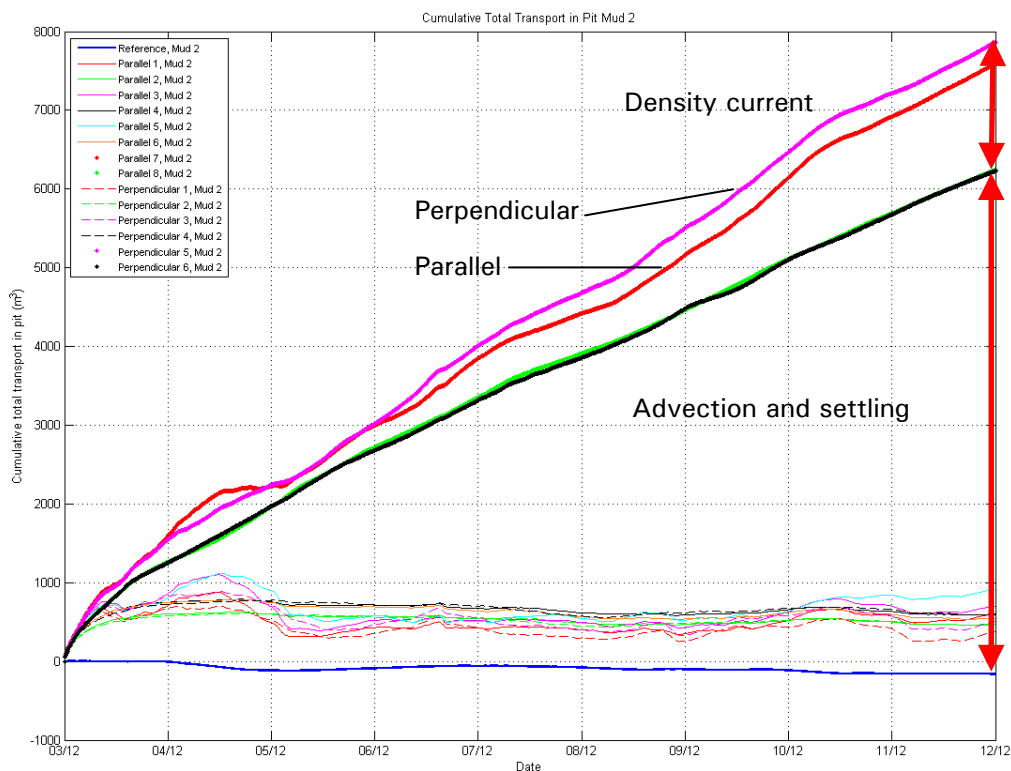


Figure C.17: Cumulative Total Transport in Trap Mud 2. Same figure as C.16, but with coarse fraction. Thick green/black: no density effect, thick red/purple: including density effect. The perpendicular trap has a larger accumulation than parallel trap. The density effect is larger. The density effect is about 20% of the filling of the trap, settling about 80 %.

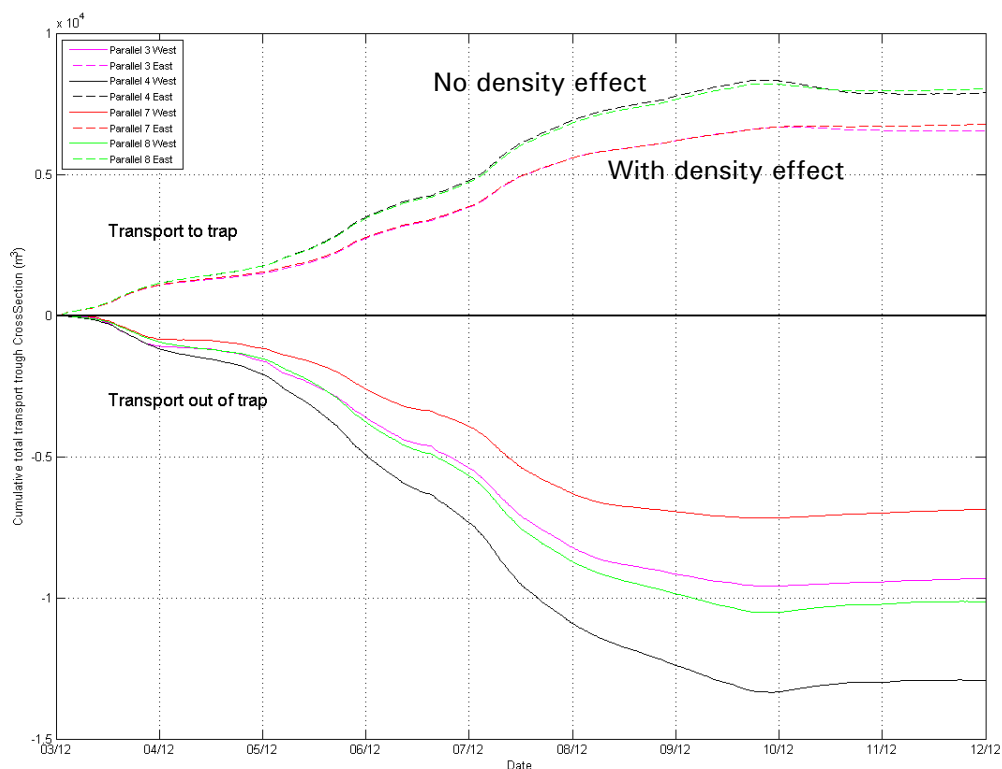


Figure C.18: Cumulative transport through each Cross section, parallel simulation. West (full line) and East (dashed line). Green/Black no density effect, red/purple with density effect. The transport without density effect is larger. Red: simulation with full sedimentation in trap, purple without sedimentation. Out transport is lower with full sedimentation.

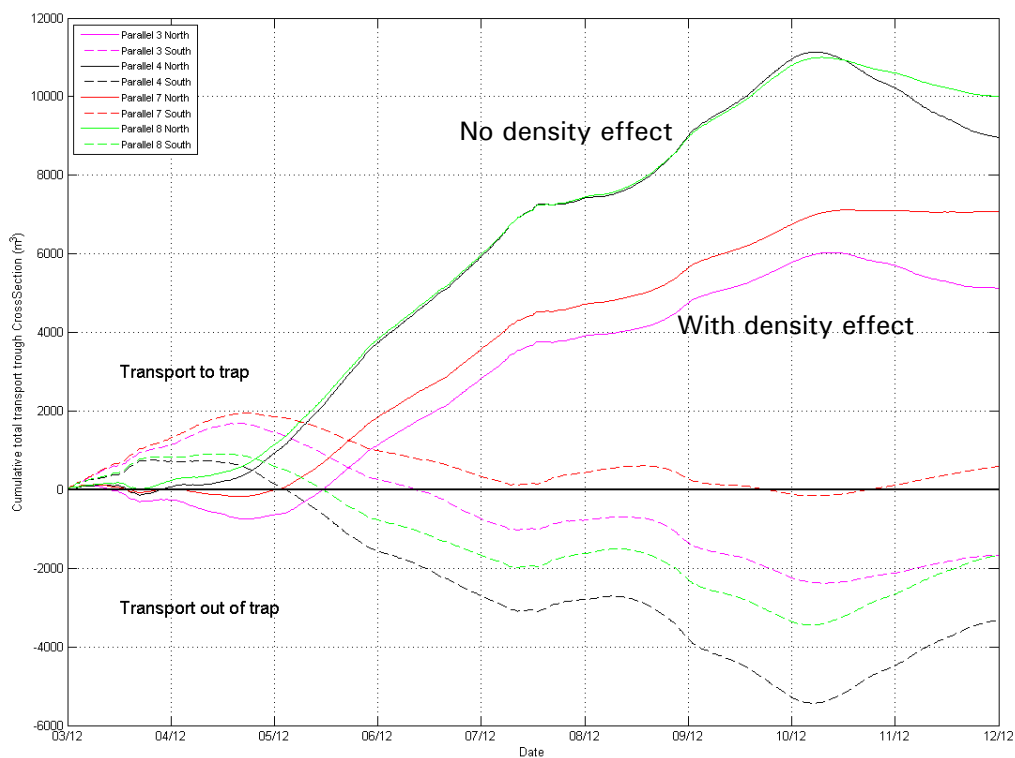


Figure C.19: Cumulative transport through each Cross section, parallel. North (full line) and South (Dashed line). The transport without density effect is larger.

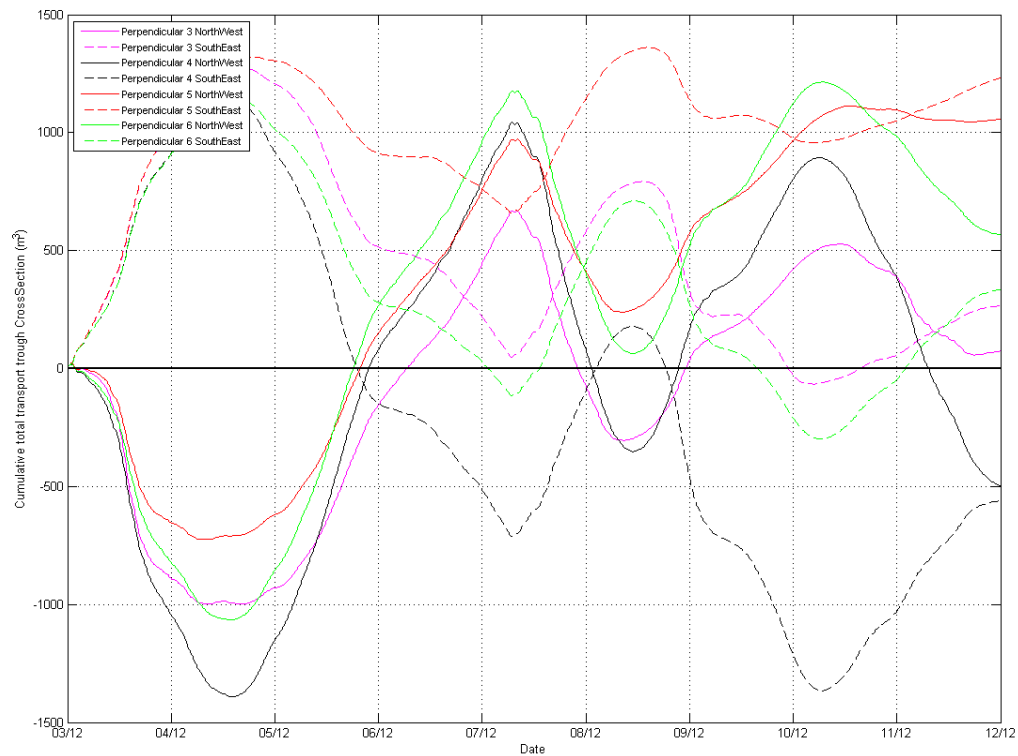


Figure C.20: Cumulative transport through each Cross section, perpendicular/ Northwest and Southeast. Transport through these small cross sections is much smaller than other cross sections.

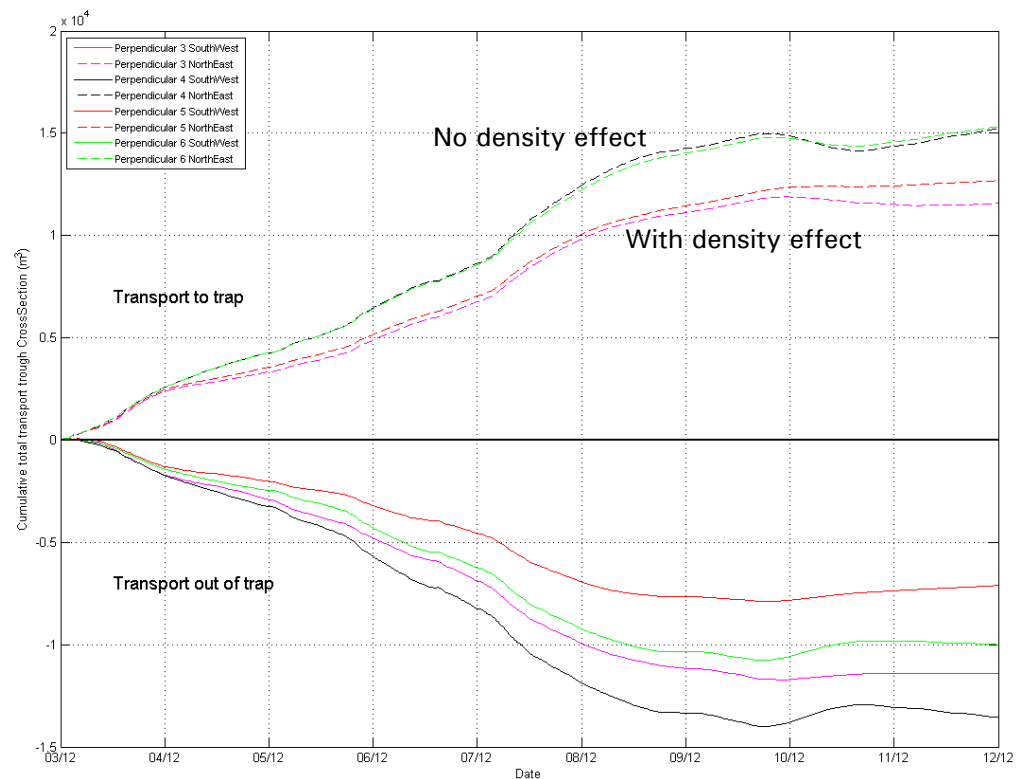


Figure C.21: Cumulative transport through each Cross section, perpendicular. Southwest (full line) and Northeast (dashed line). Green/Black no density effect, red/purple with density effect. The transport without density effect is larger. Red: simulation with full sedimentation in trap, purple without sedimentation. Out transport is lower with full sedimentation.

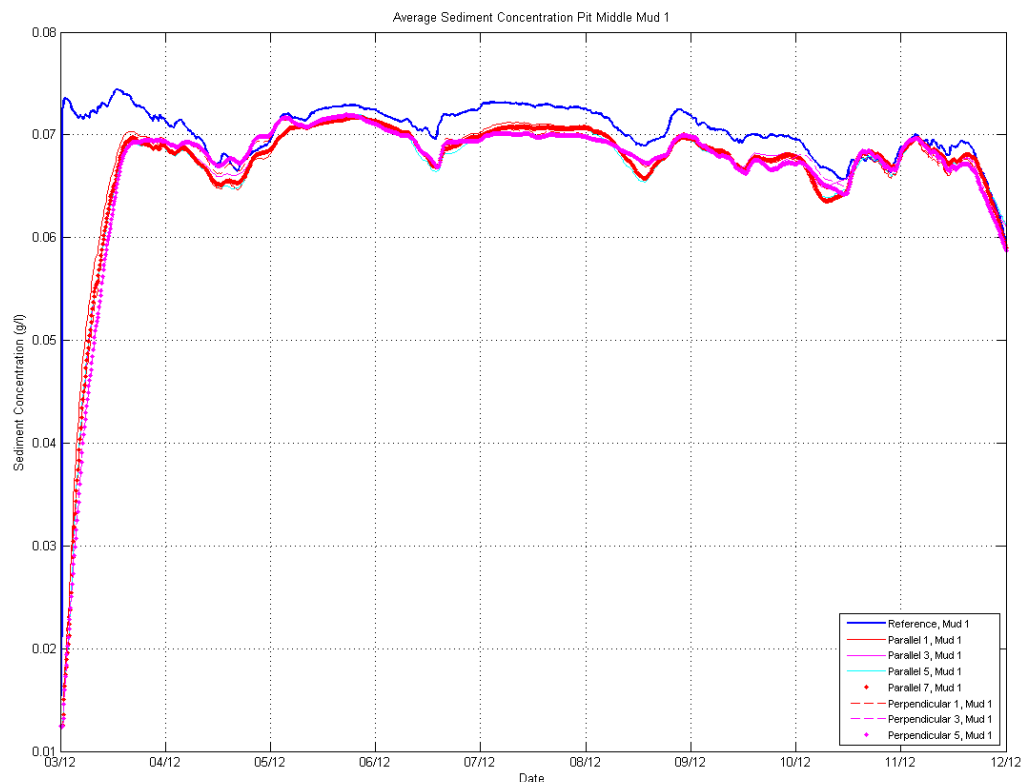


Figure C.22: Average Sediment Concentration fine fraction (Mud 1) centre of silt trap, averaged over first 3 m of the water column. Blue line (without trap), red/purple line (with trap). Decrease in sediment concentration is low (few %) for all simulations. Parallel and perpendicular same results.

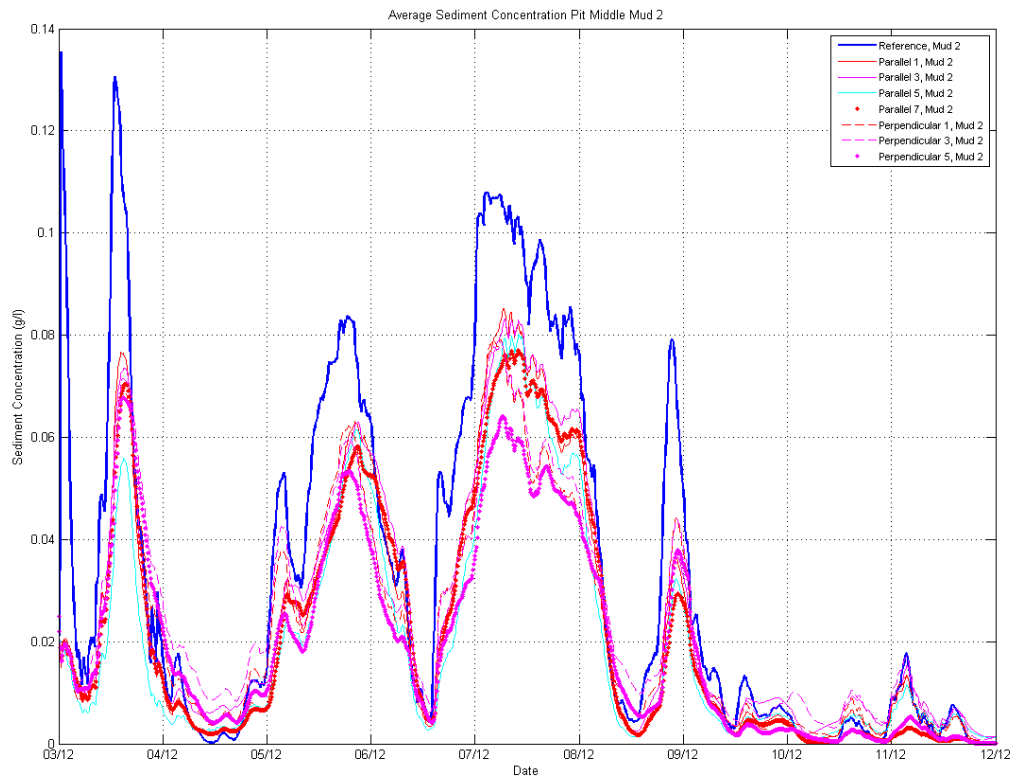


Figure C.23: Average Sediment Concentration coarse fraction (Mud 2). Same as in figure C.22. The blue line is the simulation without trap. Simulation perpendicular 5 (pointed purple line) gives highest reduction in sediment concentration., up to about 50 % (for example around 9th of December).

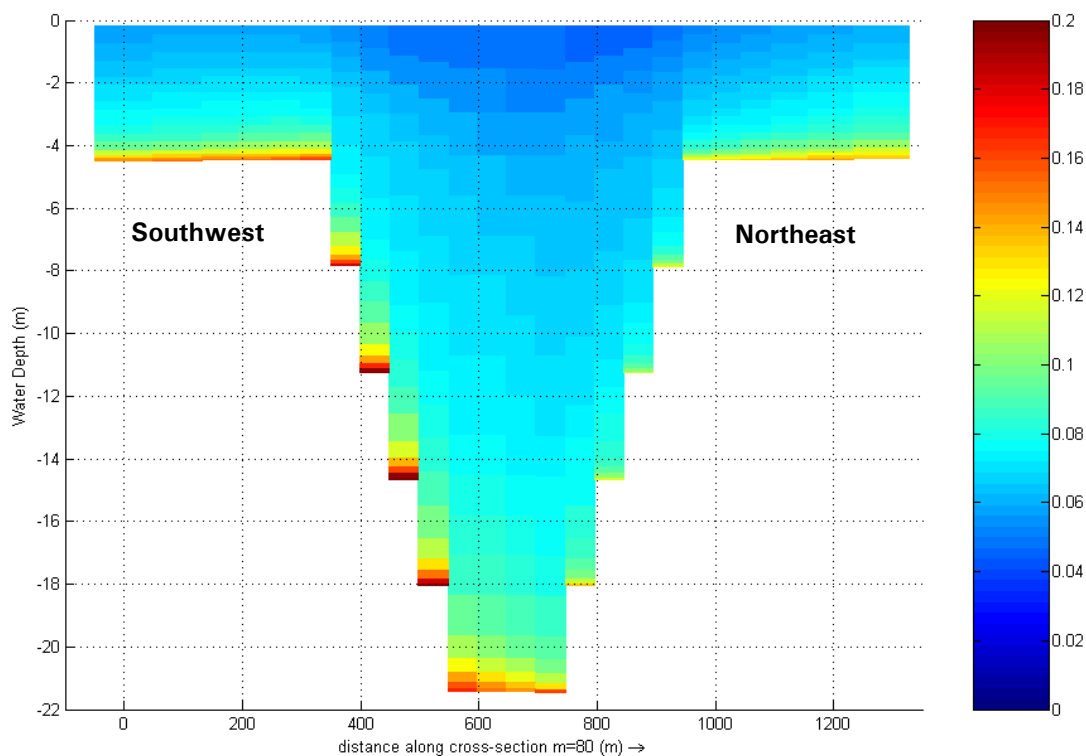


Figure C.24: Sediment concentration Mud 2 (kg/m^3), simulation Perpendicular 5, 5th of December 18h00. Cross section along line M=80, transverse section. Decrease in sediment concentration is only just in the upper part of the water column, above the silt trap and a few 100 m close to the trap.

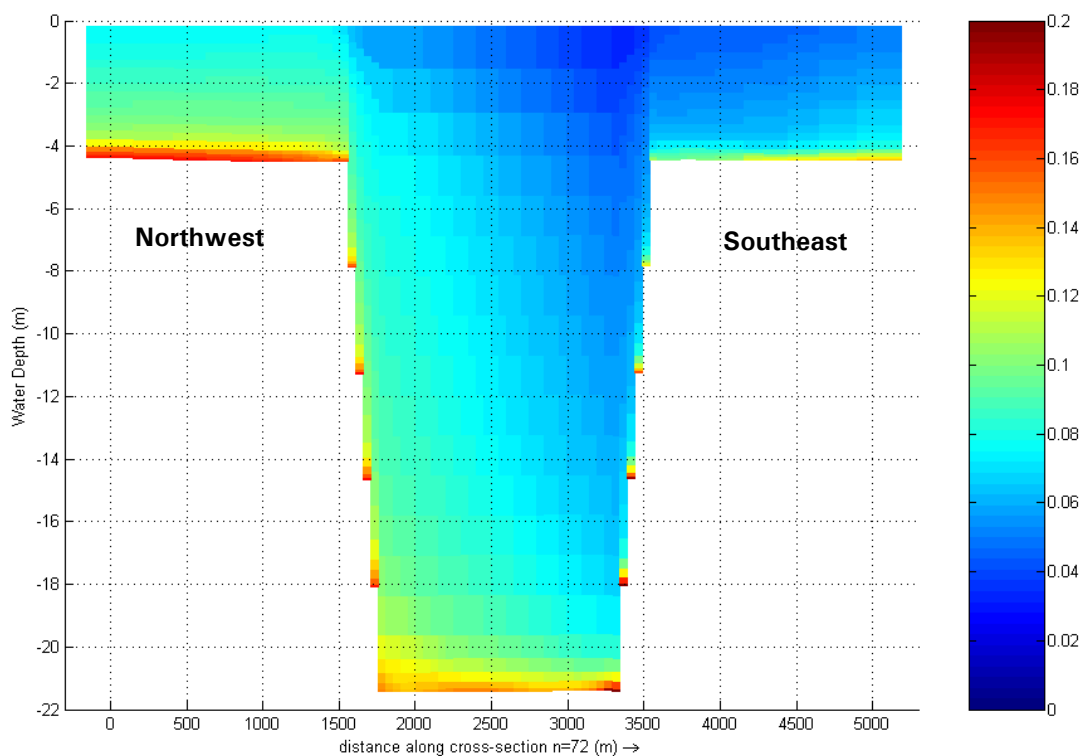


Figure C.25: Sediment concentration Mud 2 (kg/m^3), simulation Perpendicular 5, 5th of December 18h00. Cross section along line N=72, longitudinal section. Decrease in sediment concentration is only just in the upper part of the water column, above the silt trap and about 1.5 km to the Southeast.

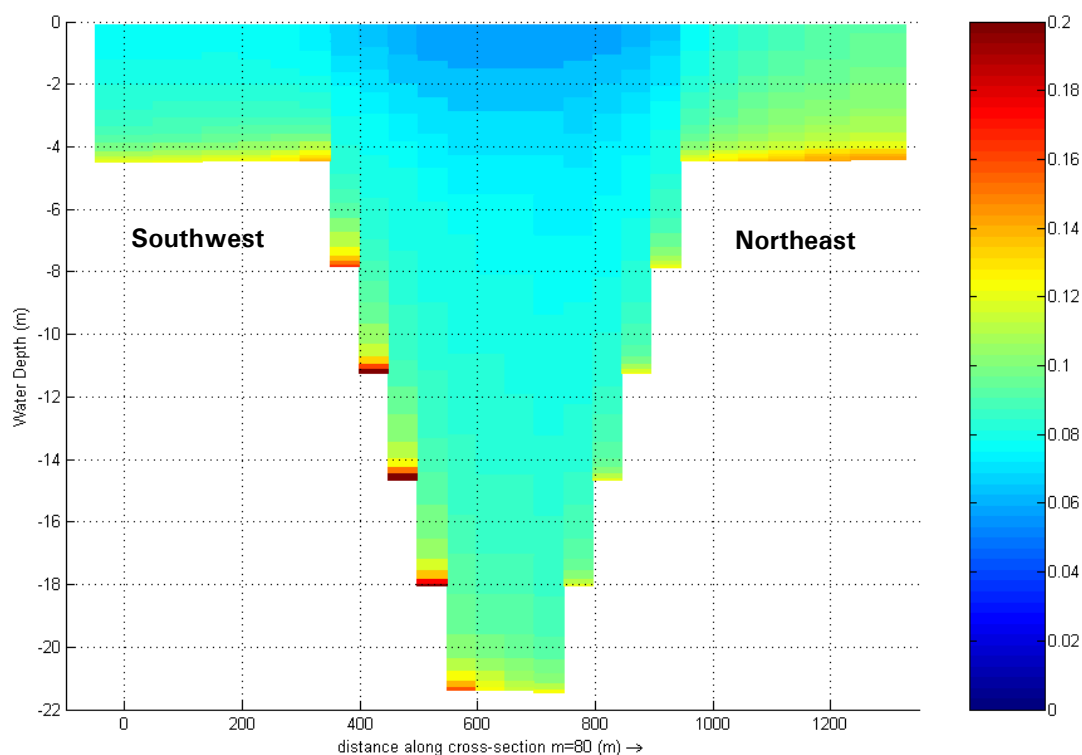


Figure C.26: Sediment concentration Mud 2 (kg/m^3), simulation Perpendicular 5, 7th of December 6h00. Cross section along line M=80, transverse section. Decrease in sediment concentration is only just in the upper part of the water column, above the silt trap and a few 100 m close to the trap.

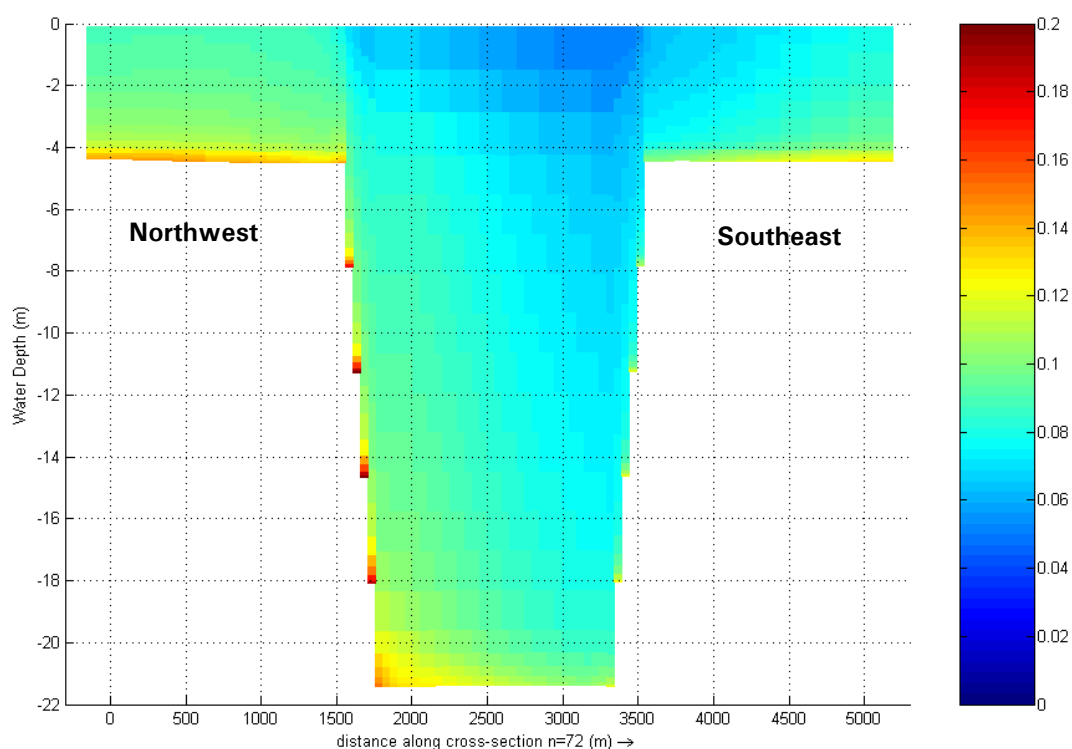


Figure C.27: Sediment concentration Mud 2 (kg/m^3), simulation Perpendicular 5, 7th of December 6h00. Cross section along line M=72, longitudinal section. Decrease in sediment concentration is only just in the upper part of the water column, above the silt trap and about 1.5 km to the Southeast.

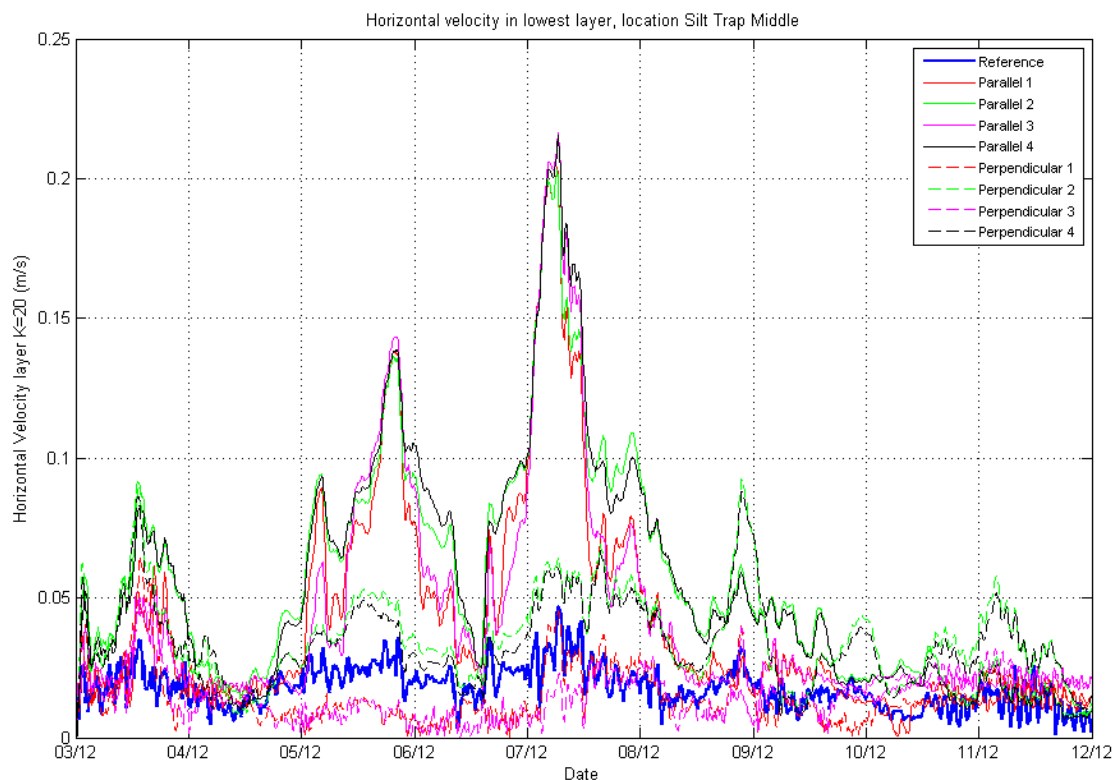


Figure C.28: Horizontal Velocity (m/s) in the lowest layer $K=20$ in the middle of the silt trap. Blue line the is the reference situation. All full lines are simulations with parallel orientation, dashed lines with perpendicular orientation. In case of parallel orientation an significant increase in horizontal velocity is observed in the lowest layer (up to 4 time higher).

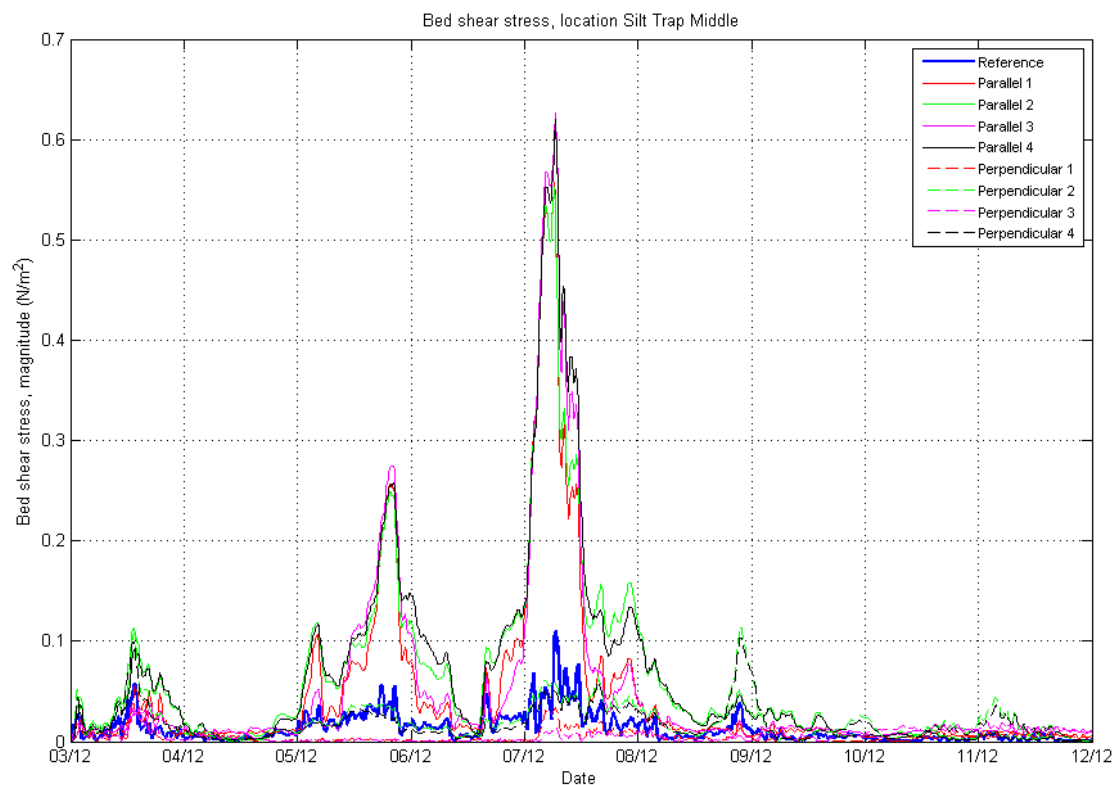


Figure C.29: Bed shear stress in the middle of the silt trap. Due to the increase in horizontal velocity (Figure C.28) an significant increase in bed shear stress is observed for the parallel case (up to about 6 times higher).

